SLAWOMIR KUMALA

FORMATION AND REPAIR OF DNA DOUBLE-STRAND BREAKS CAUSED BY IONIZING RADIATION IN THE EPSTEIN–BARR VIRUS MINICHROMOSOME

Thèse présentée
à la Faculté des études supérieures et postdoctorales
de l'Université Laval
dans le cadre du programme de doctorat en biologie cellulaire et moléculaire
pour l'obtention du grade de Philosophiae Doctor (Ph.D.)

DÉPARTEMENT DE BIOLOGIE MÉDICALE
FACULTÉ DE MÉDECINE
UNIVERSITÉ LAVAL
QUÉBEC

2012

© Slawomir Kumala, 2012

Résumé

L'ADN dans nos cellules est exposé continuellement à des agents génotoxiques. Parmi ceux-ci on retrouve les rayons ultraviolets, les agents mutagènes chimiques d'origine naturelle ou synthétique, les agents radiomimétiques, et les dérivés réactifs de l'oxygène produits par les radiations ionisantes ou par des processus tels que les cycles métaboliques redox. Parmi les dommages infligés par ces agents, les plus dangereux sont les cassures simples- et double-brin de l'ADN qui brisent son intégrité et doivent être réparées immédiatement et efficacement afin de préserver la stabilité et le fonctionnement du génome. Dans la cellule, ces cassures sont formées et réparées au niveau de la chromatine, où l'environnement moléculaire et les évènements impliqués sont plus complexes et les systèmes expérimentaux appropriés pour leur exploration sont peu développés.

L'objectif de ma recherche visait ainsi l'exploration de ces processus et le développement de nouveaux modèles qui nous permettraient d'étudier plus précisément la nature de la formation et de la réparation des cassures simple- et double-brin de l'ADN *in vivo*. J'ai utilisé comme modèle un minichromosome (l'episome du virus Epstein-Barr) d'environ 172 kb, qui possède toutes les caractéristiques de la chromatine génomique. Nous avons observé que la radiation gamma induit un changement conformationnel de l'ADN du minichromosome par la production d'une seule cassure double-brin (CDB) localisée de façon aléatoire. Une fois linéarisé, le minichromosome devient résistant à des clivages supplémentaires et par la radiation ionisante et par d'autres réactifs qui induisent des cassures, indiquant l'existence d'un nouveau mécanisme qui dépend de la structure chromatinienne et par lequel une première CSB dans le minichromosome confère une résistance à la formation d'autres cassures.

De plus, la reformation des molécules d'ADN du minichromosome surenroulées après l'irradiation indique que toutes les cassures simple-brin (CSB) et CDB sont réparées et les deux brins fermés de façon covalente. Nos découvertes indiquent que la réparation par ligature d'extrémités d'ADN non homologues est le principal mécanisme responsable de la réparation des CDB, alors que la réparation des CSB est indépendante de la polymérase poly-ADP ribose-1 (PARP-1). La modélisation mathématique de la cinétique de réparation et le calcul des vitesses de réparation a révélé que la réparation des CSB est indépendante

de la réparation des CDB, et représente l'étape limitante dans la réparation complète des minichromosomes.

Globalement, nous proposons que puisque ce minichromosome est comparable en longueur et en topologie aux boucles d'ADN sous contrainte de la chromatine génomique *in vivo*, ces observations pourraient fournir une vision plus détaillée de la cassure et de la réparation de la chromatine génomique.

General Abstract

DNA in our cells is exposed continually to DNA-damaging agents. These include ultraviolet light, natural and man-made mutagenic chemicals, and reactive oxygen species generated by ionizing radiation or processes such as redox cycling by heavy metal ions and radio-mimetic drugs. Of the various forms of damage that are inflicted by these mutagens, the most dangerous are the single- and double-strand breaks (SSBs and DSBs) which disrupt the integrity of DNA and have to be repaired immediately and efficiently in order to preserve the stability and functioning of the genome. In the cell, induction and repair of strand breaks takes place in the context of chromatin where the molecular environment and the events involved are more complex and suitable experimental systems to explore them are much less developed. A major focus of my research was therefore aimed towards exploring these processes and developing new models which will allow us to look more precisely into the nature of induction and repair of SSBs and DSBs in DNA *in vivo*.

We used as a model the naturally-occurring, ~172 kb long Epstein-Barr virus (EBV) minichromosome which posses all the characteristics of genomic chromatin and is maintained naturally in Raji cells. Gamma-irradiation of cells induces one, randomly-located DSB and several SSBs in the minichromosome DNA, producing the linear form. The minichromosome is then resistant to further cleavage either by ionizing radiation or by other break-inducing reagents, suggesting the existence of a novel mechanism in which a first SSBs or DSBs in the minichromosome DNA results in a conformational change of its chromatin which confers insensitivity to the induction of further breaks.

Supercoiled molecules of minichromosome DNA were reformed when cells were incubated after irradiation, implying that all SSBs and DSBs were repaired and both strands were covalently closed. Using specific inhibitors or siRNA depletion of repair enzymes, we found that Non Homologous End Joining was the predominant pathway responsible for DSB repair, whereas repair of SSBs was PARP-1 independent. We could also show clearly that topoisomerases I and II are not required for repair. Mathematical modeling of the kinetics of repair and calculation of rate constants revealed that repair of SSBs was independent of repair of DSBs and was the rate-limiting step in complete repair of minichromosomes.

Overall, we propose that since this minichromosome is analogous in length and topology to the constrained loops which genomic chromatin is believed to form *in vivo,* these observations could provide more detailed insights into DNA breakage and repair in genomic chromatin.

Avant-propos

Acknowledgements

Now that my thesis is finally written, I would like to express my gratitude to all those who made it possible. First of all, I would like to thank my supervisor, Dr. Ronald Hancock, whose patience, support and guidance contributed considerably to the success of this research project and to my scientific development. I really appreciated our scientific discussions, his stimulating suggestions, availability and encouragement which helped me during all the time of my research and writing of this thesis.

A very special thank you goes to my former mentor Dr. Joanna Rzeszowska, who supported me during my undergraduate years, aroused my interest in molecular biology, encouraged me to pursue a career in research, and provided me with assistance and technical support for the writing of my Master`s thesis and supported me to come to Quebec for my PhD studies. I owe her my eternal gratitude.

Furthermore, I would like to thank the members of my reading committee for taking the time to assess my work. Your advices for final corrections are greatly appreciated.

I also really appreciated working and discussing with Dr. Yasmina Hadj-Sahraoui. Her help and advice in developing techniques, analyzing and interpreting results and her encouragement are greatly acknowledged. I am also grateful to my friends in the Research Centre, especially Jasmin Mathew, Aleksander Mikryukow, Laurent Massip and Alain Bergeron for philosophical debates, exchanges of knowledge, releasing of frustration during PhD studies, and all the nice things we organized together.

Special thanks go to my parents for their support and love during my entire life. I am deeply grateful to my fiancée Joanna Jaworska, without whose love, encouragement and patience I would not have finished this thesis. This thesis is dedicated to her and to our wonderful daughter Zoë in eternal love.

A special thank you goes also to my friends Sly, the Barcz family, Piotr I., Piotr W., Nadia, the Pichavant family, and Lihn and Matteo for their kindness and support.

Table of contents

List of Figures

List of abbreviations

53BP1	p53-binding protein 1
8-oxoG	8-Oxoguanine
aa	Amino Acid
AOA1	Ataxia-oculomotor apraxia
AMP	Adenosine monophosphate
APE1	Apurinic–apyrimidinic endonuclease I
APTX	Aprataxin
ARS	Acute radiation syndrome
ASM	Acid sphingomyelinase
AT	Ataxia teleangiectasia
ATLD	Ataxia-telangiectasia-like-syndrome
ATM	Ataxia telangiectasia mutated
ATP	Adenosine-5'-triphosphate
ATR	Ataxia telangiectasia and rad3 related protein
ATRIP	ATM and Rad3-Related-Interacting Protein
BARD	BRCA1-associated RING domain 1
BER	Base excision repair
BIR	Break-induced replication
BLM	Blooms Syndrome
B-NHEJ	Back-up non homologous end joining pathway
BPV1	Bovine Papillomavirus Type 1
BRCA1	Breast cancer type 1 susceptibility protein
BRCA2	Breast cancer type 2 susceptibility protein
BRCT	BRCA1 C Terminus domain
BSA	Bovine serum albumin
CA	Chromosomal aberrations
CSA	Cockayne sundrome A protein
CtIP	C-Terminal Binding Protein Interacting Protein

DDR	DNA damage response
DNA	Deoxyribonucleic acid
DNA-PKcs	Catalytic subunit of DNA protein kinase
DSBs	Double-strand breaks
DSBR	Double-strand break repair
EBV	Epstein - Barr virus
FAR	Fraction of activity released
FCS	Fetal calf serum
FEN1	Flap endonuclease 1
FHA	ForkHead-Asociated
Gy	Gray
G1, G2	Gap 1, Gap2 phase
γH2AX	Histone variant H2AX phosphorylated at Ser139
H2A, H2B , H3 , H4	Histones
HJ	Holiday Junctions
H_2O_2	Hydrogen peroxide
HAT	Histone acetyltransferase
HR	Homologous recombination
i.e	id est
Ig	Immunoglobulin
IR	Ionizing radiation
IR-IF	Ionizing radiation-induced foci
kbp	Kilo base pair
LET	Linear energy transfer
LMDS	Locally multiple damaged sites
LOH	Loss of heterozygosity
LPR	Long patch repair
LTGC	Long track gene conversion
Mbp	Mega pase pair
MDA	Malondialdehyde
MDC1	Mediator of DNA damage checkpoint protein 1

Mdm2	Murine double minute
MOF	Males absent On the First
mRNA	Messenger RNA
miRNA	Micro ribonucleic acid
ncRNA	Non-coding ribonucleic acid
NAD	Nicotinamide adenine dinucleotide,
NBS	Njimegen breakage syndrome
NER	Nucleotide excision repair
NHEJ	Non homologous end joining
nm	Nanometer
NTP	Nucleoside triphosphate
$O_2^{-\bullet}$	Superoxide radical
OA	Okadaic acid
$OH^{\bullet}$	Hydroxy radical
P-ATM	Phosphorylated ATM
PAR	Poly(ADP) ribose
PARP	Poly(ADP-ribose) polymerase
PARG	Poly(ADP-ribose) glycohydrolase
PCNA	Proliferating Cell Nuclear Antigen,
PI3K	Phosphatidylinositol 3-kinase
PNK	Polynucleotide kinase
PP2A	Protein phosphatase 2A-like
PP5	Protein phosphatase 5
RB	Retinoblastoma
RBE	Relative biological effectiveness
RDS	Radioresistant DNA Synthesis
RMDS	Regional multiply-damaged sites
RNA	Ribonucleic acid
ROS	Reactive oxygen species
RPA	Replication protein A
RSC	Remodels the Structure of Chromatin

RS-SCID	Radiation-sensitive version of the SCID syndrome
S	S phase
SCAN1	Spinocerebellar ataxia with axonal neuropathy 1
SCID	Severe Combined Immuno Deficiency
SDSA	Synthesis-dependent strand annealing
SMC1	Structural Maintenance of Chromosome protein 1
SPR	Short path repair
SSA	Single-strand annealing
SSB	Single-strand break
SSBR	Single strand break repair
ssDNA	Single stranded DNA
STGC	Short track gene conversion
SV40	Simian virus 40
TB-SCID	T-B severe combined immunodeficiency
TdT	terminal deoxyribonucleotidyltransferase
TCR	T-cell receptors
UIM	ubiquitin-interaction motif
UV	Ultraviolet radiation
XRCC	X-ray repair cross complemention protein

1. Introduction

This Introductory section presents an overview of our current understanding of the different types of damage which occur in the DNA of eukaryotic cells exposed to ionizing radiation (IR) and of the molecular machines which repair this damage, especially strand breaks, and maintain the integrity of our genome.

1.1 Damage to DNA caused by ionizing radiation

DNA consists of two long backbone linear polymer chains made of sugar and phosphate groups joined by ester bonds. To each of the sugar moieties, one of the four bases adenine, guanine, thymine or cytosine is attached, forming two strands with an anti-parallel sequence of bases which encode the cell's genetic information. This information specifies the sequence of the amino acids (aa) in proteins and is essential for every process occurring in the cell. Although eukaryotic DNA is fairly stable in a chemical sense, many different agents have an effect on its structure and integrity and in consequence can lead to mutations that in some cases cause serious diseases in humans.

1.1.1 Types of DNA damage induced by radiation

Cellular DNA can be damaged by a plethora of different endo- and exo-genous agents. Spontaneous errors during replication, together with deamination, depurination and oxidation represent endogenous sources of damage, while UV radiation, ionizing radiation, chemical compounds, and genotoxic drugs are the best-known exogenous sources. Moreover, in addition to these known exogenous agents the constant industrial evolution over the last centuries has introduced millions of new exogenous pollutants into human enviroments, whose exact mechanism of action on living cells is unknown but of which many are believed to possess a carcinogenic and mutagenic capacity and can accumulate in cells during their life. It is believed that under normal circumstances DNA damage by endogenous factors predominates, but nevertheless mutations caused by exogenous sources are also of great importance and in highly-developed societies may be the cause of 75-80% of all cancer cases [2].

Ionizing radiation (IR) such as that created by radioactive decay or in cosmic rays is one of the best known and widely studied exogenous DNA damaging agents. It has long been known that it can induce a broad spectrum of DNA lesions including damage to nucleotides, bases, cross-linking, and single- and double-strand breaks [3]. From one side, at the cellular level DNA lesions caused by IR may hamper processes such as transcription or replication of DNA and result in cell cycle arrest and mutations as well as ultimately in cell death. At the organism level, DNA damage has been implicated in several inherited diseases such as cancers, genetic disorders, and aging. However, on the other hand since DNA-damaging agents such as IR, UV light or chemotherapeutic drugs are widely used in medicine and especially during cancer therapy an understanding of their action on cellular DNA is of great importance for every aspect of our life.

1.1.1.1 Modifications of DNA bases

In general, both direct and indirect modifications of purine and pyrimidine bases are the most frequently occurring types of DNA damage. They can undergo several different types of alteration such as oxidation, cross-linking, alkylation, deamination, or spontaneous hydrolysis of which the two first are the best known and characterized types of base damage induced by IR.

1.1.1.1.1 Oxidation

Under normal circumstances one of the most common processes by which DNA is damaged is oxidation of its components by very reactive molecules termed reactive oxygen species (ROS). On one hand, all kinds of ROS such as hydroxyl radicals, singlet oxygen, hydrogen peroxide, or peroxynitrite are formed as by-products of oxidative metabolism and are released during normal endogenous respiration processes, but on the other hand they are also known to be extensively generated by exposure to IR [3]. In aerobic conditions, cytochrome oxidase normally minimizes the level of ROS by catalyzing the metabolism of oxygen to water without the accumulation of reactive intermediates, but nevertheless some superoxide radicals ($O_2^{-\bullet}$) are formed and then metabolized to other forms of ROS [4]. On its own, the superoxide anion radical exhibits a very limited reactivity, but in the process

catalyzed by superoxide dismutase it is converted to hydrogen peroxide (H_2O_2) and subsequently to the very reactive hydroxyl radicals ($OH^{\bullet}$) and singlet oxygen ($^1O_2$) molecules (Fig. 1.1). The reactivity of $HO^{\bullet}$ is so great that it does not diffuse more than one or two molecular diameters before reacting with a cellular component [2]. In an average human cell it is estimated that approximately 1% of all molecules of oxygen are converted to a variety of ROS which produce around 10'000- 20'000 different oxidation–related DNA-damaging events per day [5, 6]. Moreover, in moments of additional environmental trauma such as exposure to IR the total level of ROS greatly exceeds the capacity of cellular antioxidant mechanisms and causes an "oxidative stress" which significantly accelerates DNA damage and contributes to cellular aging processes.

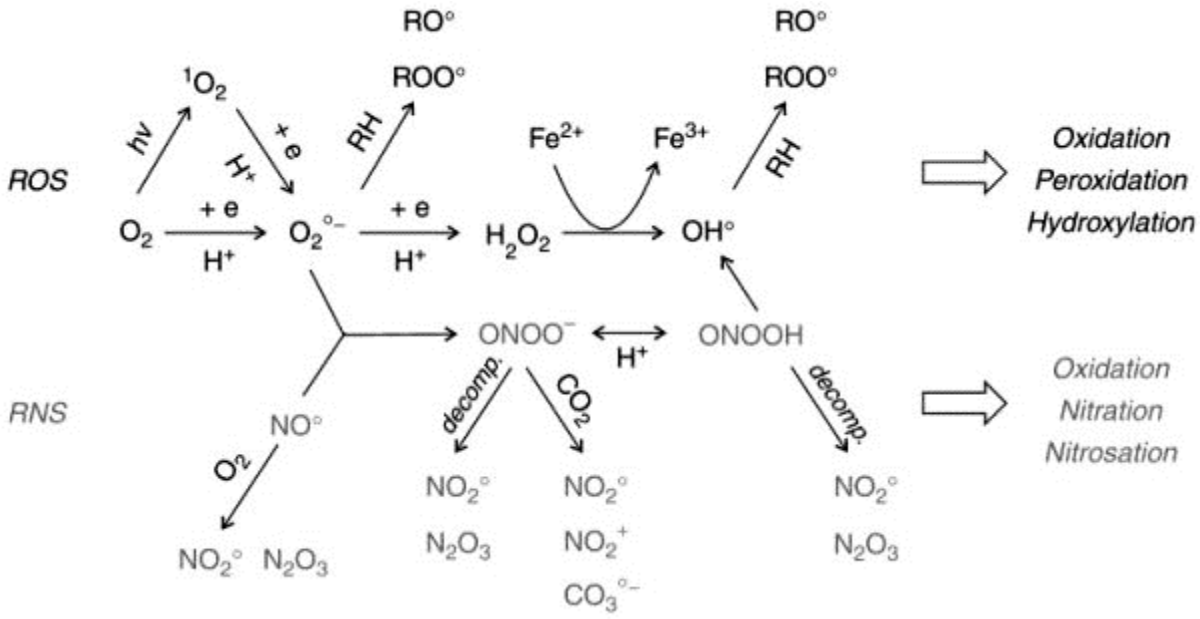

Fig. 1.1. The major reactive oxygen species (ROS) and reactive nitrogen species (RNS) derived from the biological conversion of oxygen into superoxide ion (O2°−) and nitric oxide (NO°) (adapted from [4]).

ROS formed in this way cause several types of DNA lesions, which although mainly affecting the DNA bases may also affect the integrity of the 2-deoxyribose moieties and cause formation of adducts as well as crosslinks. The most ROS produced by radiation,

hydroxyl radicals ($OH^{\bullet}$), react with guanine or adenine at positions 4, 5 or 8 and generate a variety of products (Fig. 1.2).

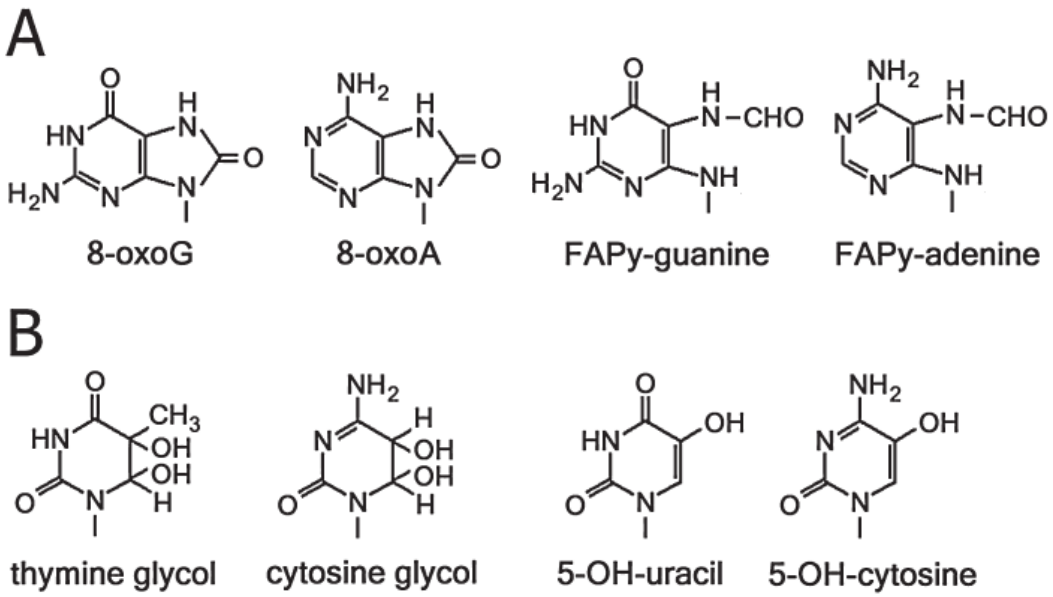

Fig. 1.2. Modified bases resulting from the attack of ROS on DNA. The structure of products formed by addition of a hydroxyl radical to position 8 of the purine ring (A) or position 5 or 6 of the pyrimidine ring (B). (Adapted from [7]).

Among these, the best studied and documented is 8-oxo-7,8-dihydroguanine (8-oxoG) which has a strong mutagenic potential and preferentially mispairs with adenine rather than cytosine during post-damage replication of DNA, generating GC→TA transversions. Another quite common oxidative modification of guanine results in formation of the OH-dG radical, which undergoes either oxidation or reduction shortly after its formation and also produces 8-oxoG or 2,6-diamino-4-hydroxy-5-formamidopyrimidine (FAPy-guanine, FAPy-dG), respectively. This latter modification can lead to GC→CG transversions and is caused especially by IR and other ROS-producing agents. Among the remaining types of oxidized bases, the most frequent are 4,6 diamino-5 formamidopyrimidine (Fapy-adenine), 5,6-dihydroxy-5,6-dihydrothymine (thymine

glycol), and 5,6-dihydroxy-5,6-dihydrocytosine (cytosine glycol). The latter two are often detected in human cells at levels similar to that of 8-oxoG, and if they remain unrepaired they can result in C→T transitions during the subsequent cycle of DNA replication [2, 7].

In addition to these oxidative modifications of DNA bases, ROS may also affect the stability of other components, i.e. the deoxyribose moieties. The most common example, abstraction of hydrogen from 2-deoxyribose and ribose by hydroxyl radicals, leads to the formation of carbon-centered radicals which in the presence of oxygen undergo different reactions giving rise to DNA strand breaks. On the other hand, oxidation of C1 and C4 of deoxyribose leads to either a strand break or to the formation of 2-deoxyribonolactone, respectively, whereas the C5 radical of 2-deoxyribose may react with the adjacent purine ring and among other effects form 8,5'-cyclo-2'deoxyguanosine which distorts the normal structure of DNA and is more difficult to repair than other base lesions [7].

At this point, it is worth mentioning that oxidation induced by IR may also cause damage to other important cellular components, phospholipids; these are major constituents of all cell membranes and their polyunsaturated fatty acid residues are very sensitive to oxidation by free radicals. The main oxidation products of phospholipids are short-lived hydroperoxides which are reduced to fatty acid alcohols, epoxides, aldehydes, and other products. The major aldehyde products are crotonaldehyde, acrolein and malondialdehyde (MDA). All of these are highly reactive substances and form very mutagenic exocyclic DNA adducts which block normal Watson-Crick base pairing [8].

Additionally, IR may also, both directly and indirectly, cause severe damage to RNA integrity. Strand breaks or oxidative damage to protein-coding RNAs or non-coding RNAs may cause errors in protein synthesis or dysregulation of gene expression [9]. The mechanism of mRNA damage and any resulting patho-physiological outcomes are poorly understood and the potential deleterious effects of RNA damage have not been widely appreciated. However, since a variety of RNA molecules have been found to have functions beyond the well-known roles of messenger, ribosomal and transfer RNA, damage cause by IR in these 'Non-coding RNAs' (ncRNAs) has recently become an interesting area of research. ncRNAs are formed in cells mainly from introns and transcripts from non-protein

coding genes, and play roles in the regulation of transcription, translation or localisation of RNA and protein [10]. Among the superfamilies of non-coding RNAs, micro-RNAs (miRNAs) have been the most investigated in regard to radiation damage. miRNAs are non-coding RNA species, 18-24 nucleotides in length, which in mammals are processed by the enzyme Dicer and function by base pairing imperfectly with a target mRNA to inhibit protein synthesis. The effect of radiation on miRNA expression appears to vary according to cell type, radiation dose, and post-irradiation time point [11]. Ilnyytskyy et al. [12] demonstrated that irradiation of hematopoietic tissues resulted in a significant deregulation of their microRNA expression and suggested that these changes may reflect a protective mechanisms counteracting radiation cytotoxicity. The observed significant increase in the expression of miR-34a was paralleled by a decrease in the expression of its target oncogenes NOTCH1, MYC, E2F3 and cyclin D1 whereas downregulation of miR-7 triggered upregulation of lymphoid-specific helicase LSH, a pivotal regulator of DNA methylation and genome stability [12]. Another example of radiation-regulated miRNA is miR-521, whose expression level changes significantly in irradiated prostate cancer cells. Interestingly, this radiation-dependent modulation of miR-521 expression was strictly correlated with the expression levels of its predicted target protein Cockayne syndrome protein A (CSA) which is a known DNA repair protein [13]. Furthermore, irradiation significantly altered the expression of microRNA 194 (miR-194) which putatively targets both DNA methyltransferases and thus regulates the epigenetic state of genes.

1.1.1.2 Formation of DNA-protein crosslinks

DNA-protein interactions are implicated in every aspect of gene expression, and because of this they are one of the most strictly regulated processes in cell metabolism. Under normal circumstances these interactions are reversible and only very few proteins, for example topoisomerases [14], bind covalently to DNA. However, regulatory proteins which are not covalently bound can become covalently cross-linked to chromatin or to already anchored protein-DNA complexes. In general, such crosslinks severely disrupt gene expression and may lead to arrest of ongoing replication and consequently to cell death if the damage is not repaired promptly [15]. It has been demonstrated that exposure of cells to IR increases the number of proteins which are covalently bound to DNA, reflecting the

formation of DNA-protein crosslinks. Treatment of irradiated cells with a protease, but not with a concentrated salt solution, completely removes the DNA-bound proteins which seem to be very similar to those seen after ultraviolet irradiation [15]. Formation of such DNA-protein crosslinks can be observed already after very small doses of radiation (0.5 Gy) and seems to be directly proportional to the irradiation dose [15, 16].

1.1.1.3 DNA strand breaks

Because of their crucial influence on genome stability, the formation and repair of single-strand breaks (SSBs) and double-strand breaks (DSBs) in DNA have been in the center of scientific interest for many years. Both of these are produced either during regular metabolic processes by topoisomerases [17], replication fork "collapse" [18] or by exogenous agents such as IR [19], topoisomerase inhibitors [17], or radiomimetic drugs [19]. Strand breaks pose a serious threat for genome stability, and if not repaired promptly may cause different types of DNA rearrangement and mutations with carcinogenic potential.

1.1.1.3.1 Single-strand breaks (SSBs)

SSBs, as the name indicates, are discontinues in one strand of the DNA double helix and under normal circumstances are believed to occur a few orders of magnitude more frequently than their double strand counterparts [20]. Under normal physiological conditions, SSBs are mainly formed by the DNA oxidation processes described above and are usually accompanied by loss of single nucleotides as well as by damaged termini at the site of the break. The first and direct cause of SSBs is disintegration of oxidized sugars, while the second, indirect cause is mainly related to base excision repair (BER) processes [21]. Moreover, some enzymes such as topoisomerase I which participates in changes of DNA topology during transcription and replication, introduce a transient SSB into DNA as an intermediate in their reaction (the “cleavable complex”). Chemical or physical deregulation of topoisomerase I activity, for example by the inhibitor camptothecin [17] or due to the close proximity of another DNA lesion, inhibits the resealing step of the enzyme's cleavage complex and converts it into a covalent topoisomerase I-linked SSB. It

has been demonstrated that formation of such complexes and defects in their repair may be a source of the serious genetic neurodegenerative disease spinocerebellar ataxia with axonal neuropathy 1 (SCAN1) [22]. At the molecular and cellular level, formation of SSBs and lack of efficient repair processes may results in several serious consequences. In proliferating cells formation of SSBs before or during the S phase and lack of their repair may cause blockage and collapse of ongoing replication forks, which subsequently can escalate the damage by giving rise to DSBs (described below) [23]. On the other hand, in non-proliferating cells SSBs affect transcription by blocking the progression of RNA polymerases; in the case of SSBs caused by topoisomerase I the site of this premature termination is located 10 base pairs upstream of the topoisomerase I-linked nucleotide on the coding strand [24]. Additionally, if many unrepaired SSBs accumulate the activity of their main sensor poly(ADP-ribose) polymerase 1 (PARP-1) leads to depletion of cellular NAD+ and ATP levels and in consequence the cell is condemned to apoptotic death [25].

1.1.1.3.2 Double-strand breaks (DSBs)

Among all the possible types of DNA lesions, DSBs symbolize the most serious and dangerous. DSBs represent the simultaneous interruption of both DNA strands such that base pairing and chromatin structure are unable to keep them juxtaposed. As a consequence, the two extremities of the DNA double helix are physically separated from one another causing disruption in continuity of the genetic information, and interestingly even one, single DSB may lead to cell death or carcinogenesis if not repaired promptly or repaired improperly [19].

DSBs are the primary source of the alterations of normal chromosome structure termed chromosomal aberration (CA) [19]. There are two main types of aberration, intra- and inter-chromosomal, the first comprising changes within a single chromosome, for example deletion or inversion, and the second rearrangements between two or more chromosomes such as translocation or formation of a dicentric chromosome. While certain types of CA are lethal, others may lead to oncogenic transformation and in fact their creation is a hallmark of cells of many tumours and of an ongoing carcinogenic process [19]. However, in spite of decades of research the molecular mechanisms of formation of CAs are still not entirely understood and three main hypotheses attempt to explain their

occurrence, namely the "breakage and reunion", the "exchange" and the "molecular" theories [19]. In all these models, the formation of a DSB is considered to be the primary lesion which initiates the subsequent steps in formation of a CA [26]. The current dogma is that DSBs are produced by both endogenous events including the action of topoisomerases, V(D)J recombination, replication, and meiosis as well as by exogenous agents including IR, topoisomerase inhibitors, and radiomimetic drugs [19].

1.1.1.3.2.1 Double-strand breaks formed during V(D)J recombination

V(D)J recombination occurs during the development of B- and T-lymphocytes and provides the basis for the antigen-binding diversity of immunoglobulins (Igs) and T-cell receptors (TCRs). This variety of possible protein structure combinations is necessary for the recognition of diverse antigens from bacterial, viral or parasitic invaders. Igs and TCRs are encoded by specific gene loci organized into sets of V gene segments, followed by D gene and J gene segments [27]. During V(D)J recombination, random parts of each of the segments are excised and joined together to form the antigen receptor variable domain exon that codes for specific Igs or TCRs. The V(D)J process is initiated by the proteins RAG1 and RAG2 that bind at specific recognition sequences (recombination signal sequences, RSSs) located directly next to the V, D or J gene segments. After binding, the RAG protein complex generates a DSB in the RSS region in two successive steps, forming a hairpin conformation at the terminus of each V, D or J segment and a blunt DNA end within the RSS region. Next, proteins of the non-homologous end joining (NHEJ) DNA repair pathway open the hairpins and join the resulting ends [27]. As a result, the antigen receptor gene segments are assembled next to one another and form a functional antigen receptor variable domain exon. Mutations in the genes responsible for coding the V(D)J pathway are often associated with cancers of lymphoid origin such as Burkitt's lymphoma, where the gene *c-myc* is often juxtaposed to the immunoglobulin heavy chain genes by rearrangement [28]. Under normal physiological conditions V(D)J recombination represents a very strictly regulated and harmonious process involving formation of DSBs.

1.1.1.3.2.2 Strand breaks produced by inhibitors of topoisomerases

Under normal conditions, topoisomerases are involved in relaxation of DNA in chromatin to relieve superhelical tension during DNA replication and transcription, as well as for recombinational processes and chromosome condensation and segregation. To date, four different topoisomerases have been reported in higher eukaryotes: topoisomerases I and III which belong to the type I topoisomerase family, and topoisomerases IIα and β that make up the topoisomerase II family. Both topoisomerase I and II have a somewhat similar DNA tension-relieving function in the cell, but whereas topoisomerase I is more active during transcription, toposiomserase IIα is essential in proliferating cells and assists in chromosome condensation, segregation and replication, whereas topo IIβ tends to be associated with DNA repair, transcription and development. The mechanism of action of the two types of topoisomerase differs significantly, since topoisomerase I allows DNA to swivel on its axis by creating a transient, enzyme-bound SSB while topoisomerase II causes formation of a transient enzyme-bound DSB through which another duplex is passed [17]. Mammalian topoisomerase II is the cellular target of many potent antitumour drugs such as VP-16 (etoposide), VM-26 (teniposide) or DNA-intercalating acridines (m-AMSA and o-AMSA), which are termed topoisomerase II poisons and interfere with the DNA rejoining reaction carried out by the enzyme, thus trapping it while covalently bound to DNA in what is termed the "cleavable complex" [17]. It is still not clear how these stalled topoisomerase II complexes are removed from DNA, but it has been demonstrated that their formation triggers the non-homologous end joining (NHEJ) system normally used for DSB repair (more details below) [29].

1.1.1.3.2.3 Strand breaks produced by ionizing radiation

In general, as mentioned above IR is a type of high-energy radiation capable of interacting with and removing one or more electrons from an atom or molecule through which it passes. IR includes X-rays, neutrons, and cosmic rays as well as radiation from radioactive materials such as alpha and beta particles or gamma rays. Because of their physical properties, different kinds of IR are widely used in many branches of today's medicine such as radiology or cancer therapy [30].

The damaging effects of IR on the human body became evident soon after the description of X-rays by Wilhelm Roentgen in 1895 [30]. Moreover, its "destructive" character was confirmed on a very wide scale after a series of accidental exposures during the 20th century and especially after the detonation of the atomic bombs in Japan. Radiation damage to humans can be classified in various ways, but one of the simplest and most important is related to the time it takes for the damage to be visible leading to a distinction between "prompt" and "delayed" effects. Prompt effects are those which become manifest within a year (or usually within days or weeks) following exposure and include visible skin damage and hair loss, as well as the classical symptoms of acute radiation poisoning termed radiation sickness or acute radiation syndrome (ARS). Delayed effects include cataracts, genetic damage, premature aging, or different types of cancer and leukemia and are not observed until years after the exposure to IR [31].

At the cellular level the effects of IR manifest themselves as damage to different cellular components including proteins, lipids, carbohydrates and, of particular significance, nucleic acids. In fact, DNA exemplifies the cellular component most sensitive to IR, and doses that efficiently induce DNA damage are substantially smaller that those which affect other cell components. Unlike chemical agents whose damaging potential are strongly dependent on diffusion processes and thus may be affected by cellular structures, IR is typically highly penetrating and damage induction is complete within a few microseconds after exposure. Random energy deposition by IR induces a wide variety of the kinds of DNA lesions described above such as SSBs and DSBs, oxidized bases, and apurinic/apyrimidinic sites. Of these, DSBs are known to be the most important for cell killing and as it has been estimated that 1 Gy of IR induces around 40-60 DSBs per diploid cell [6]. Moreover, in addition to the DNA breaks directly caused by irradiation, further breaks may be formed as a consequence of repair processes that eliminate closely-spaced base or sugar damage on opposite strands [6].

The damaging effect of IR is not limited to the induction of individual DNA lesions, but frequently leads to the production of clustered damage encompassing two or more DNA lesions of the same or different nature (DSBs, SSBs, oxidized bases, AP sites) in close proximity to each other [32]. In such a case, depending on the size of the region covered by damage one can distinguish local and regional multiply-damaged sites (LMDS and RMDS

respectively). The term LMDS applies mainly to a short damaged region of the DNA helix, while RMDS encompasses regions that spread over much larger distances of chromatin. It is believed that due to the high local concentration of DNA damage and the consequent challenging complications for repair, clustered damage at LMDS and RMDS are a primary source of post-radiation cell death [33].

In general, two main mechanisms by which IR can induce DNA damage can be distinguished. The first is a direct interaction of charged particles with DNA, whereas the second is mainly related to the radiolysis of water molecules and indirect DNA damage. In the direct mechanism the kinetic energy of photons directly affects the structure of the DNA helix and induces single and/or double strand breaks in the phosphodiester backbone. On the other hand, the indirect effect is strictly correlated with the production of the free radicals described above which cause oxidation-related DNA damage:

$$H_2O + IR \rightarrow e_{aq}^- + H_2O^+ \text{ (excited water)}$$
$$H_2O^+ + H_2O \rightarrow H_3O^+ + OH^\bullet \text{ (hydroxyl radical)}$$
$$H_2O + e^- \rightarrow OH^\bullet + H^\bullet \text{ (hydrogen radical)}$$
$$OH^\bullet + OH^\bullet \rightarrow H_2O_2 \text{ (peroxide)}$$

The radiolysis of water molecules is not the only source of free radicals produced by radiation, and in the presence of free metal cations additional ROS may be formed according to the Fenton reaction, for example:

$$H_2O_2 + Fe^{2+} \rightarrow OH^\bullet + OH^- + Fe^{3+}$$

A detailed molecular comparison revealed that indirect DNA damage induced by IR is essentially identical to that caused by ROS produced by metabolism. In both cases the resultant free radicals are highly reactive, and due to their very short life time ($\sim 10^{-10}$ sec) only those formed in a water layer of 2-3 nm around DNA are able to participate in DNA damaging processes. However, in the presence of dissolved oxygen additional more stable radicals can be formed which migrate for much larger distances and cause additional DNA damage:

$$H^{\bullet} + O_2 \rightarrow HO_2^{\bullet} \text{ (superoxide/hydroxy radical)}$$
$$OH^{\bullet} + O_2 \rightarrow HO_3^{\bullet} \text{ (hydrogen trioxy radical)}$$

The exact ratio of DNA damage produced by indirect and direct mechanisms varies between different types of radiation and is closely associated with their ionizing abilities as well as their relative biological effectiveness (RBE) [34]. RBE does not translate directly into physical units of exposure (Rads, Grays etc.) but allows two or more different kinds of radiation to be compared with respect to their efficacy in causing biological injury. One important consideration affecting RBE is the parameter termed the "quality" of the IR, and in general a given dose of alpha or neutron radiation is much more effective in causing biological damage than an equal dose of beta, gamma or x-radiation. This difference in effectiveness is related to a physical quantity called Linear Energy Transfer (LET) which describes the energy deposition pattern along the trajectory of radiation particles [35]. Sparsely IR such as beta, gamma or x-rays creates many ions, but their number created per unit of track length is relatively small and consequently they are termed "low-LET radiation". On the other hand, most of the protons or ions created by an alpha particle are quite close together, in fact confined to just a few cells, and are described as "high-LET radiation" [35, 36]. Because of its high ionization density it is believed that high-LET radiation damages DNA mainly by the direct pathway, while low-LET radiation induces a variety of lesions, representing up to 70% of all damaging events, by indirect, ROS-related mechanisms [36, 37]. This different mechanism is reflected in the relative RBE values, and experimental evidence indicates that the high-LET radiation always has a higher RBE than low-LET radiation [33, 36-38].

Apart from the radiation quality, the radiosensitivity of cells is influenced by many other factors such as their proliferation rate or stage in the cell cycle. It is generally believed that the most radiosensitive cells are these which are actively proliferating, for example in the blood-forming tissues or the reproductive organs. The blood-forming cells, located mainly in the bone marrow and both immature and rapidly-dividing, are highly susceptible to radiation injury whereas the most mature blood cells are relatively radioresistant. A curious exception to this rule is the lymphocyte, a particular kind of mature white blood cell which is extremely radiosensitive, but the reason for this

phenomenon is still unknown. In fact, since cancer cells proliferate more rapidly than healthy cells their preferential sensitivity to killing by IR is widely exploited during different kinds of radiation therapy. The sensitivity of cells to IR differs not only among different cell types but also between the same cells in different stages of the cell cycle, and in general they are most radiosensitive in the M and G_2 phases and most radioresistant in the S and late G_1 phases. This different sensitivity to IR is a very important factor in predicting the effects of radiotherapy; for example the lymphocytes of patients who showed no response to radiotherapy had a higher proportion of S-phase cells compared with those of partial or complete responders [39].

1.2 Cellular responses to DNA damage

Eukaryotic cells respond to DSBs and SSBs by activation of a complex cascade of events termed the DNA damage response (DDR). This sophisticated molecular circuitry involves sensing, amplification, and subsequent transmission of a signal that DNA has been damaged which leads to activation of several different mechanisms to repair of the breaks. The most important aim of DDR activation is the preservation of genomic integrity through the coupling of repair to other essential metabolic processes such as cell cycle progression, gene expression, or in extreme cases decisions leading to cell death.

1.2.1 Cell cycle regulation and cell cycle checkpoints

The cell cycle is the ordered series of events required for the faithful duplication of one eukaryotic cell into two genetically identical daughter cells, and has four distinct phases, gap 1 (G_1), synthesis (S), gap 2 (G_2) and mitosis (M) [40]. Additionally, cells that have temporarily or irreversibly stopped their division can enter a special quiescent state termed the G_0 phase, a characteristic of both neurons and mature muscle cells. G1, the longest phase, encompasses mainly transcription and translation processes where cells increase in size and prepare themselves for the subsequent S phase and DNA replication [41]. After completing DNA duplication, the cell passes on to the G_2 phase where it grows and produces extra proteins and microtubules required for the final division step. During

the M phase, which accounts for approximately 10% of the entire cycle, the cell divides into two daughter cells genetically identical to each other and to their parental cell. After mitosis, the whole cycle may start again or stop and remain in the G_0 phase for days, months, or even years. Under normal circumstances the passage from one phase to the next is a very precisely regulated process in which checkpoint systems play the pivotal roles [42]. In general, cell cycle checkpoints are a series of events that verify whether the processes at each phase of the cell cycle have been completed accurately before progression into the next phase. Consequently, after damage to DNA in the G_1 or G_2 phases checkpoint mechanisms arrest cell cycle progression, or in the S phase slow it down, to avoid incorrect genetic information from being passed to the progeny cells. During these pauses DNA damage is repaired, and if repair is successful the cell cycle is resumed. However, under circumstances when the DNA damage is too serious, the cell cycle is arrested permanently leading the cell to senescence or apoptosis. In eukaryotic cells three main checkpoints can be distinguished, located at the transition between G_1 and S, within S, and between the G_2 and M phases. The checkpoint signalling pathways are very complex mechanisms and require the cooperative activity of different factors classified as sensors, mediators, transducers, and effectors [40-42]. The sensor group involves MRN, Rad17, and 9-1-1 complexes which activate and recruit two principal signal transducers, the proteins ATM (Ataxia Telangiectasia Mutated) and ATR (ATM and Rad3-related) which initiate a cascade of phosphorylation events that transfer the DNA damage signal to the distal transducer checkpoint kinases, Chk1 and Chk2 respectively (Fig. 1.3). It is generally accepted that ATM acts as the primary mediator in the response to IR-induced damage, whereas ATR is activated mainly as a result of stalled replication forks and damage by UV radiation [43, 44]. Activated checkpoint kinases interact with and promote the degradation of the effector proteins A-, B- or C- Cdc25 phosphatases. Inactivated Cdc25 is unable to activate the cell cycle phase-specific cyclin-dependent kinases (CDK), which while inactive cannot promote entry into the next phase of the cycle [41]. Moreover, ATM and ATR may also phosphorylate a series of additional cell cycle mediators such as p53, BRCA1, MDC1, SMC1, FANCD2, H2AX, etc. Distinct from the “standard” Chk1/Chk2 mechanisms, these types of phosphorylations are strictly related to the cell cycle phase and/or the checkpoint arrest which is going to be induced. It is believed that these pathways functions mainly as a

back-up or support route which helps the normal Chk1/Chk2 mechanisms to arrest cell cycle progression [44].

1.2.1.1 The proteins ATM and ATR

The proteins Ataxia Telangiectasia Mutated (ATM) and its homolog ATM and Rad3-related (ATR) are the central components of signal transduction processes activated in the cell after formation of DSBs in DNA. ATM is the product of the gene mutated in the pleiotropic human disease Ataxia-Telangiectasia (AT) which is characterized by neuronal degeneration, immunodeficiency, hypogonadism, growth retardation, and cancer predisposition. Skin fibroblasts from A-T patients displays a high frequency of spontaneous chromosomal aberrations, a high rate of error-prone intra-chromosomal recombination, and acute radiation sensitivity. The complex clinical and cellular phenotypes of AT cells attest to the diversity of ATM kinase functions and suggest its importance for the maintenance of genome integrity. ATM is a large, ≈370 kDa nuclear phosphoprotein which is a member of the phosphatidylinositol 3-kinase (PI3Ks) super-family, a group of eukaryotic proteins known to have important functions in different regulatory pathways associated with DDR mechanisms [44].

For a long time it was believed that ATM might be, in fact, the primary sensor detecting DSBs, but more recent experiments have revealed that in some cases ATM may be activated at regions very distant from a break [45] or even in the absence of such damage [46]. These data suggest that distortion of chromatin structure may be an ample and sufficient signal for efficient ATM kinase activation and that there might to be an additional DSB-sensing protein that triggers ATM function. Indeed, recent studies have provided very convincing evidence that the main factor responsible for DNA damage-dependent ATM activation is the Mre11 complex [47] whose core contains the Mre11, Rad50 and Nbs1 proteins that play a pivotal function in the homologous repair (HR) pathway for DSBs (described in more detail in Chapter 1.4.3). Cells from patients with a hypomorphic mutation in the *NBS1* or *MRE11* gene (Nijmegen breakage syndrome and A-T like disease (ATLD), respectively) show severely defective ATM activation in response to DNA damage [47] which is closely related to a marked reduction of the expression of the

NBS1 protein. It is believed that NBS1 binds to and recruits inactive ATM kinase to sites of DNA damage, and that ATM then activates and in turn phosphorylates NBS1 as well as other cellular targets in the checkpoint signalling process. While Mre11/Rad50 may also recruit ATM to sites of DNA damage, only the complete Mre11 complex including NBS1 is capable of stimulating its kinase activity. All this evidence supports the model that the Mre11 complex acts both upstream and downstream of ATM kinase in the DNA damage response process and serves as a modulator/amplifier of its enzymatic activity [48].

Under normal circumstances, most of the ATM kinase exists as an inactive nuclear dimeric or multimer structure in which its kinase domain is folded back onto the region surrounding residue serine 1981. During activation of ATM this specific serine is autophosphorylated, causing dissociation of inactive multimers and formation of fully functional monomers that participate in the subsequent signalling events. It has been demonstrated that these changes related to phosphorylation of S1981 are among the earliest detectable responses to DNA damage and may be detected as early as 30 seconds after irradiation with 0.5 Gy [45]. Interestingly, in every ATM molecule at least two other autophosphorylation sites (S367 and S1893) are activated in response to DSBs. Mutations in either of these sites cause increased radiation sensitivity and defective cell cycle checkpoint activation compared to wild-type cells [49]. It is worth mentioning that all these residues are phosphorylated in a cell cycle-independent manner, suggesting that ATM autophosphorylation is a common event which, in contrast to the different ATM targets, does not change significantly during different phases of the cell cycle [50].

As well as being phosphorylated, ATM can also undergo dephosphorylation which also appears to control its kinase activity. Goodarzi et al. [51] demonstrated that the protein phosphatase inhibitor okadaic acid (OA) induces ATM autophosphorylation on residue S1981 in cells that had not been irradiated or treated with any DNA damaging agent. Neither DSBs nor visible γH2AX foci were observed, suggesting that OA induces ATM autophosphorylation mainly by inhibition of the protein phosphatase 2A-like (PP2A) rather than by DNA breakage. Moreover, under normal circumstances ATM coimmunoprecipitates with PP2A-like protein and interacts with its scaffolding subunit. Interestingly, after irradiation PP2A dissociates from ATM and loses its protein phosphatase activity, thereby facilitating ATM's damage-dependent autophosphorylation

and subsequent signal transducer activity [51]. Another protein reported to be involved in ATM dephosphorylation is the serine-threonine phosphatase 5 (PP5) which, in contrast to the PP2A-like phosphatase, interacts with ATM in a DNA-damage-inducible manner and whose decreased expression causes attenuation of ATM activity. Moreover, expression of a catalytically-inactive mutant of PP5 inhibited the IR- and neocarzinostatin-dependent autophosphorylation of Ser1981 of ATM as well as phosphorylation of other downstream ATM substrates such as p53 or Rad17 [52].

DNA damage-dependent ATM phosphorylation is also strictly related to the cellular acetylation network [53, 54] in which the main participant is the Tip60 complex known to be involved in a series of important processes such as DNA damage signalling, DNA repair, cell cycle control, and apoptosis. Overexpression of a dominant negative histone acetyltransferase (HAT)-deficient Tip60 complex greatly reduces both acetylation and autophosphorylation of ATM kinase and sensitizes cells to damage by IR. Moreover, this suppression of Tip60 activity reduces the ATM-dependent phosphorylation of p53 and Chk2 kinase to a level similar to that observed in cells stably expressing an ATM-silencing shRNA. Further data suggests that ATM forms a stable complex with Tip60 through the conserved FATC domain and while formation of this ATM-Tip60 cellular complex is not DNA damage-dependent, IR activates its HAT activity [53]. Another HAT shown to be involved in interaction with ATM is the human ortholog of the Drosophila protein Males absent On the First (MOF); specific blocking of hMOF-dependent acetylation of histone H4 induced by IR causes diminished ATM autophosphorylation and ATM kinase activity as well as decreased phosphorylation of ATM downstream effectors. Automatically, decreased hMOF activity is associated with loss of the cell cycle checkpoint response to DSBs and increased IR-dependent cell killing. At the same time, overexpression of a wild-type hMOF had the opposite effect and resulted in enhancement of cell survival and DNA damage repair after exposure to IR [54]. After activation, ATM monomers accumulate at sites of DNA damage and directly phosphorylate or mediate the phosphorylation and activation of numerous proteins, of which more than thirty have been identified to date and of which the majority are known to participate in DNA repair and cell cycle checkpoint processes [55].

As mentioned above, in mammalian cells ATM is thought to share its responsibilities as an apical cell cycle checkpoint protein with another important cellular kinase, ATR (ATM- and Rad3-related protein), which is mainly involved in responses to replication stress (stalled or broken replication forks) and damage caused by UV radiation. Like ATM, ATR belongs to the PIK3 family and exhibits phosphotransferase activity towards a variety of proteins containing Ser–Gln motifs which mainly participate in stress- and DNA damage-induced signalling. In contrast to ATM, ATR kinase is recruited to sites of DNA breakage by the ATR-interacting protein (ATRIP) and once recruited it phosphorylates Chk1 and thus, like ATM, induces cell cycle arrest [55].

1.2.1.2 The G1/S checkpoint

It is generally believed that the main mechanism responsible for activation of the G_1/S checkpoint is the accumulation and stabilization of the protein p53 [41]. This protein, known as "the guardian of the genome", is a very important transcriptional activator that plays a series of functions in regulation of genomic stability, the cellular response to DNA damage, and cell-cycle progression. Under normal circumstances the half-life of p53 in the cell is rather short (~30 min.) and greatly depends on the activity of the protein Murine double minute (Mdm2) that targets p53 for ubiquitination, nuclear export, and subsequent proteosomal degradation [56]. DSBs induce a rapid accumulation of p53 in the cell as well as its specific posttranslational modification. Interestingly, cells isolated from A-T patients and exposed to IR exhibit a reduced level of p53 accumulation, and moreover their G_1/S checkpoint activation is greatly delayed and inefficient [57, 58]. All of these changes in ATM-mutated cells are closely related to the status of ATM kinase, which under normal circumstances rapidly modifies the protein Chk2 which in turn phosphorylates p53 on residue S20 which greatly diminishes its interactions with Mdm2/p53 and stabilizes p53 in the nucleus. Additionally, ATM also exerts a second measure of control on p53 stability and directly phosphorylates Mdm2 on residue S395, which does not disrupt its interaction with /p53 but clearly impairs nuclear export and degradation of p53 which would normally occur [57]. Furthermore, ATM also directly phosphorylates residue S15 in the amino-terminal region of p53 and thus enhances its activity of activating transcription. In AT-

mutated cells, due to the normal activity of ATR this phosphorylation was not inhibited [58] suggesting that both of these regulatory kinases work in a quite coordinated manner in respect to p53 phosphorylation. All these data strongly suggest a model in which ATM represents the primary responder to IR-induced p53 phosphorylation, whereas ATR serves mainly as a back-up pathway and to maintain phosphorylation of S15. In this way, after DNA damage induction the hyper-activated and stabilized p53 protein up-regulates the cyclin-dependent kinase inhibitor p21 that in turn suppresses CyclinE/Cdk2 and CyclinA/Cdk2 activities, thereby preventing the G_1 to S phase cell cycle transition.

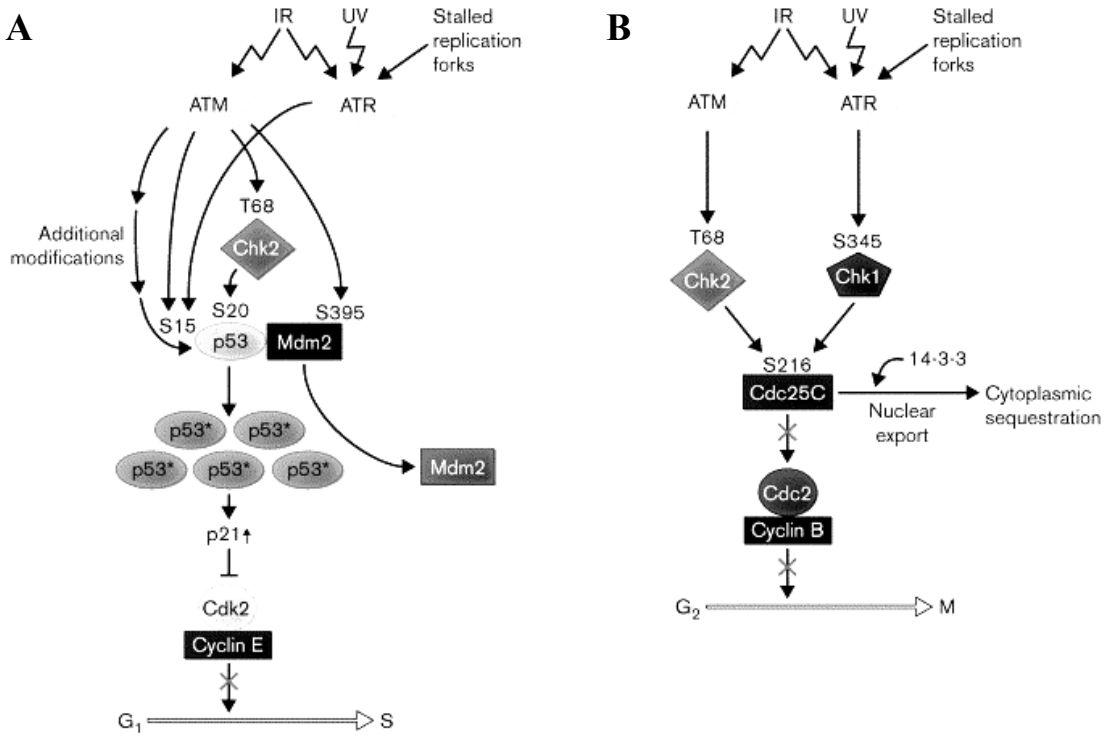

Fig. 1.3. Control of cell-cycle checkpoints by ATM and ATR during activation of the G_1/S (A) and the G_2/M checkpoints (B) (adapted from [59]).

1.2.1.3 The S-phase checkpoint

The main function of the S-phase checkpoint is to slow down ongoing DNA synthesis and promote DNA repair by the error-free HR pathway. Interestingly, due to the intrinsic risk of errors accompanying DNA replication the intra S-phase checkpoint is also

active in normal cells, and its activity is increased after DNA damage [57] The main hallmark of IR-induced S-phase checkpoint activation, decreased DNA replication, is the outcome of both inhibition of replication origin firing as well as slowing of replication fork progression. Given the many possible ways in which replication can be inhibited, it comes as no surprise that the intra-S phase checkpoint mechanism is quite complicated and still incompletely understood. Inability to activate the S-phase checkpoint results in "Radioresistant DNA Synthesis" (RDS) and is a common phenotype of all ATM and ATR mutated cells [57].

Recent experimental evidence suggests that there are at least two parallel mechanisms controlling the S-phase checkpoint, the ATM/ATR – Chk1/Chk2 – Cdc25A pathway and the ATM/Nbs1/FANCD2/Smc1 pathway, which are both believed to act simultaneously in response to DNA damage and to be required for efficient inhibition of intra-S phase replication. In the first pathway, activated ATM/ATR phosphorylates Chk2/Chk1 kinases which then target and inactivate the Cdc25A phosphatase and ubiquitin-dependent proteasomal degradation. Destabilization of Cdc25A phosphatase prevents dephosphorylation of Cdk2 and formation of the Cdk2/CyclinE and Cdk2/CyclinA complexes, which remain inactive and thus prevent DNA replication from continuing [57].

The second branch of the IR-induced S-phase checkpoint pathway is Cdc25A-independent and requires the activity of the protein NBS1 (Nijmegen Breakage Syndrome) (more details in Section 1.4.3). Cells mutated in NBS1 also display an IR-induced RDS-like phenotype and fail to slow down DNA replication. During NBS1–dependent intra-S phase checkpoint activation, ATM phosphorylates a number of downstream substrates including NBS1 on S343 and SMC1 (Structural Maintenance of Chromosome protein 1) on S957 and S966.

1.2.1.4 The G2/M checkpoint

The G2/M checkpoint is the final gatekeeper that blocks the entry of cells with damaged DNA into mitosis. Interestingly, in contrast to the two other checkpoint pathways that for G_2/M is essentially identical from fission yeasts to humans and probably represents the most ancient cell cycle arresting pathway. Experiments on AT-deficient cells revealed that activation of the G_2/M checkpoint is strictly related to the cell cycle phase in which

DNA damage was caused. Notably, when cells were exposed to IR during the G_1 or S phase any cells that reached the G_2 phase were effectively arrested before they initiated mitosis, but on the other hand if they were irradiated in the G_2 phase they failed to activate the G_2/M checkpoint and arrest of the cell cycle [60]. These data support the hypothesis that ATM may be dispensable for initiation of G_2 arrest and suggest that ATR plays a pivotal function in G_2/M checkpoint activation. Additional data confirm this theory and disclose that the crucial step in IR-induced G_2/M checkpoint arrest is resection of broken 5'-termini of DNA and formation of single-stranded DNA (ssDNA) fragments. These characteristic intermediate products formed during repair by HR (see Section 1.4.3 for more details) are recognized by two independent sensor proteins, the 9-1-1 complex (made up of the proteins Rad9, Rad1 and Hus1) and ATRIP (ATM and Rad3-Related-Interacting Protein). It is believed that the 9-1-1 complex directly recognizes and binds to ssDNA, whereas ATRIP recruits ATR kinase that, once bound to the DNA termini, starts to phosphorylate both its ATRIP partner as well as the 9-1-1 complex. This interaction initiates a cascade of events which leads to the phosphorylation of Chk1 kinase which in turn phosphorylates and deactivates Wee1 kinase and Cdc25C phosphatase. Phosphorylated Cdc25C interacts with 14-3-3 proteins and is either catalytically inhibited or sequestered in the cytoplasm. In either case, Cdc25C is unable to dephosphorylate and activate B-Cdc2 kinase and effectively blocks cells from entering mitosis. Additionally, the phosphorylated Wee1 kinase is transiently stabilized in the nucleus and inactivated during the period of cell cycle arrest. ATM kinase may also participate significantly in this process, and through Chk2 phosphorylation inactivates Cdc25 and creates an additional binding site for the 14-3-3 regulatory protein [59].

1.3 Repair of DNA single strand breaks

Of the different types of DNA damage, SSBs are the most common lesions induced by IR and moreover arise in cells at a frequency of tens of thousands per cell per day [36]. The majority of radiation-induced SSBs are the result of sugar damage and disintegration of the DNA backbone following absorption of IR energy, or of radiation-mediated formation of ROS [61]. Moreover, they can also be formed indirectly during BER of oxidised bases,

abasic sites, or bases that are damaged or altered in other ways by IR [62]. It is generally accepted that SSBs are far less toxic to cells than their double-stranded counterparts; however, this largely reflects the ability of cells to rapidly repair large numbers of SSBs, rather than an intrinsic lack of toxicity of these lesions. Given the frequency of 'spontaneous' SSBs (~20'000/cell/day) [20, 36], it is thus not surprising that cells have evolved highly efficient and diverse system for their repair termed Single Strand Break Repair (SSBR).

Typical SSBs induced by IR generally have blocked termini lacking the conventional 5′-phosphate and 3′-hydroxyl groups, and require further processing prior to ligation. The main enzymatic system used to deal with this kind of damage is very similar to that used in BER, and the initial step of the entire process depends on the structure of the termini, i.e. the blocking groups which residue on the 3' and 5' ends of the broken strand. The most common types of SSBs resulting from IR commonly have 3′-phosphate or 3′-phosphoglycolate groups that are substrates for polynucleotide kinase phosphatase (PNKP) and apurinic–apyrimidinic endonuclease I (APE1) respectively [61]. PNKP is an enzyme that catalyzes the transfer of a phosphate from ATP to the 5' end of DNA as well as dephosphorylate its 3'-phosphate termini, whereas APE1 3′-phosphoesterase activity removes 3′ blocking groups in DNA that are generated by DNA glycosylase/AP-lyases during removal of oxidized bases (BER pathway) or by direct IR damage due to the production of ROS. Moreover, SSBs generated as intermediates during BER typically harbour 5'-oxidized dRP termini which are removed by the AP lyase activity of DNA polymerase β or in special cases by flap endonuclease 1 (FEN1) [61, 63]. Additionally, in the case of an attempted ligation of abortive DNA intermediates with an adenylate group bound to the 5'-phosphate end the protein Aprataxin hydrolyase releases these groups and produces free 5′-phosphate termini [62].

After the broken DNA ends are restored to their proper, hydroxyl/phosphate configuration, in the next step the gap is re-filled and re-ligated. At this point, depending on the size of the gap which needs to be filled two alternative sub-pathways are used; the first, termed "Short Patch Repair" (SPR) is responsible for the repair of small, one-nucleotide gaps and the second termed "Long-Patch Repair" (LPR) carries out the replacement of 2-10 nucleotides surrounding the damaged site (Fig. 1.4) [63, 64]. Apart from the size of the

repair patch, these two sub-pathways differ in the enzymes involved. The protein Proliferating Cell Nuclear Antigen (PCNA) controls the LPR pathway and allows the replicative DNA polymerases δ/ε to be clamped in place [65]. Further, in the following step of repair PCNA also stimulates and recruits DNA ligase I (Lig I) which seals the break [62, 64, 66]. The major player in the SPR sub-pathway is XRCC1, a scaffold protein which has no catalytic activity itself but plays a central role as an assembly platform for different components involved in the repair of SSBs. XRCC1 contains 2 BRCA1 Carboxy Terminal (BRCT) modules (BRCA1 and BRCA2) through which it interacts with DNA polymerase β and DNA ligase IIIα (Lig IIIα) as well as with the poly(ADP-ribose) (PAR) chains formed by poly(ADP-ribose)polymerase-1 (PARP-1) during its automodification [64-66].

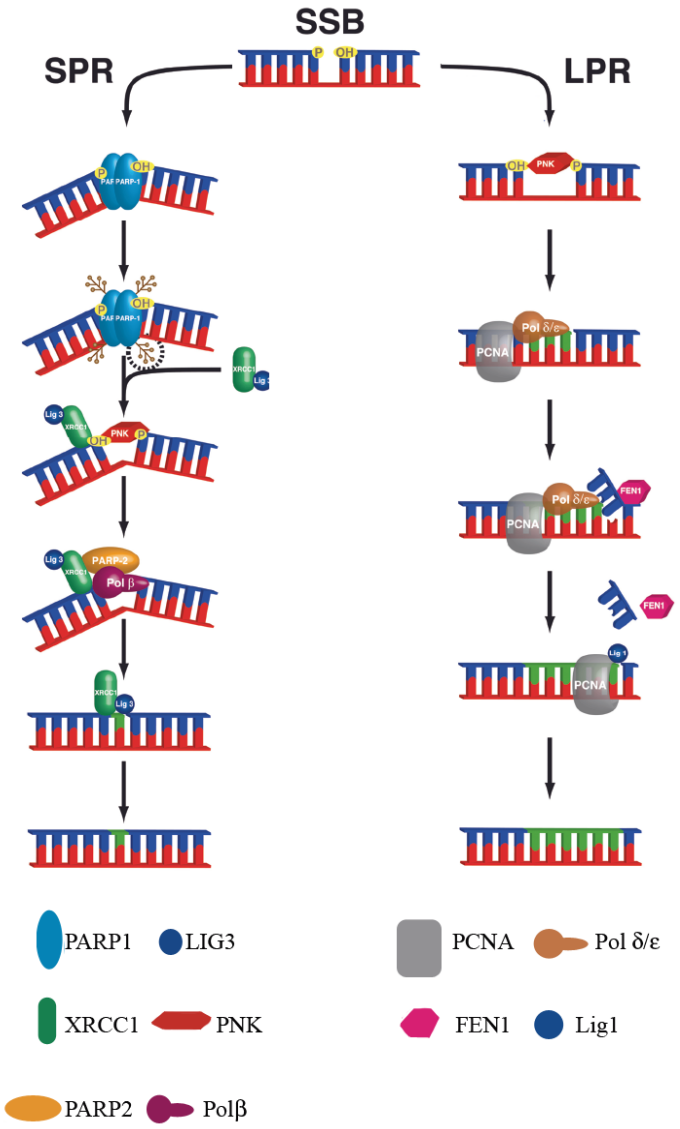

Fig. 1.4. Scheme summarizing the steps in repair of SSBs in mammalian cells caused by IR. SSBs arising directly from sugar damage or indirectly from base damage (via BER) may be repaired either by the short path repair (SPR) or long patch repair (LPR) pathway. In SPR, PARP-1 binds at the SSB and is activated, thereby sequestering the XRCC1-Ligase 3 complex. XRCC1 then replaces PARP on the concave side of the DNA at the SSB, establishing a molecular scaffold. After end-processing mediated by APE1 or PNK, DNA polymerase β binds to the break site and a single nucleotide is incorporated prior to DNA ligation mediated by DNA ligase 3. In LPR, APE1 or PNK process the damaged termini, PCNA recruits the DNA polymerases δ/ε, and the gap is filled (adapted from [67]).

1.3.1 Poly(ADP-ribose)polymerase (PARP-1)

PARP-1 is an abundant 116-kDa protein and a member of a large family of 17 enzymes which have an identical catalytic domain but rather distinct structures, functions, and localizations [68]. Interestingly, PARP-1 and PARP-2 are the sole members of this family whose catalytic activity is stimulated by DNA strand breaks [68]. The principal enzymatic activity of PARP-1 appears to be the early sensing of SSBs and covalent modification of carboxyl groups in a limited number of nuclear protein acceptors by poly(ADP-ribosyl)ation, whereas PARP-2, despite its low capacity to synthesize ADP-ribose polymers, seems to be an alternative to PARP-1 in BER pathway [69]. In addition to this activity, PARP-1 is also involved in many cellular processes including DNA replication [70], transcription [71], and chromatin remodeling [72]. It has been demonstrated that under normal physiological conditions, the major fraction of PARP-1 is associated with the nuclear matrix and physically interacts with lamin B whereas shortly after exposure of cells to IR it is re-localized to the proximity of SSBs and DSBs [64]. Binding of PARP-1 to damaged DNA triggers its poly(ADP-ribosyl)ation activity, resulting in attachment of long linear or branched homopolymers of ADP-ribose to itself (automodification; [73]) and to other target proteins (heteromodification; [64, 73]). These ADP-ribose chains are formed by cleavage of nicotinamide adenine dinucleotide (NAD^+) and range from a few to over 200 units joined by ribosyl-ribose glycosidic bonds [74]. In the automodification reaction the enzyme functions as a dimer, whereby 2 PARP-1 molecules interact for the mutual transfer of PAR-units to an acceptor site on the neighboring molecule [73]. During the first 5 min after exposure to H_2O_2, cells exhibit an increase of ~100-fold in their content of PAR which seems to be strongly correlated with the speed and efficiency of rejoining of DNA strand breaks, suggesting that formation of PAR is one of the earliest responses to DNA damage [75]. Under normal circumstances the DNA damage-dependent increase in PAR synthesis is associated with an accelerated catabolism of the polymer and a decrease in its cellular half-life time; after 15 min the level of PAR decreases gradually to that in untreated cells due to its degradation by the evolutionarily-conserved enzyme poly(ADP-ribose)glycohydrolase (PARG). The human *PARG* gene, mapped to the q11 region of chromosome 10, encodes an enzyme with endo-

and exo-glycosidic activities able to cleave polymers of PAR to ADP-ribose units [76]. It is believed that the PARP/PARG system represents a specific DNA strand break-signalling mechanism in which PARP-1 plays a dual role as a sensor and a signal transducer. The sensor function encompasses mainly binding, auto-modification and possibly stabilization of DNA and/or chromatin, whereas the more global transducer function signals the recruitment of downstream effectors such as cell cycle regulators or death effectors [25, 77].

1.4 Repair of double-strand breaks

As considered in Section 1.2, one of the main purposes of the activation of cell cycle checkpoints induced by IR is to facilitate the repair of DSBs in DNA. During evolution, eukaryotic cells have evolved complex and highly conserved systems to rapidly and efficiently detect different kinds of DNA damage and to execute their repair. To date, two major pathways for repair of DSBs have been identified in mammalian cells HR and NHEJ [1, 78]. Apart from these two pathways, there is increasing evidence for the existence of an alternative end-joining pathway termed back-up NHEJ (B-NHEJ) [79].

The HR pathway involves copying damaged and missing DNA sequence information from the undamaged homologous chromosome or sister chromatid, relying on sequence homology. This process is typically error-free and occurs only during the S and G_2 phases of the cell cycle in mammalian cells, and is mediated by proteins of the Rad52 epistasis group. In contrast, NHEJ effects repair by joining and ligating together two DNA termini with little (microhomology) or no homology. This pathway is usually predominant in higher eukaryotes and operates in most stages of the cell cycle, particularly in G_0 and G_1 [80].

1.4.1 Choice of pathway for repair of double-strand breaks

Within a few seconds after induction of a DSB, factors participating in NHEJ and HR are recruited independently to the DSB site and occupy the termini of the broken DNA together for a short period of time [81]. It is presumed that at this moment some of these proteins direct the choice of the pathway by which the DSB will be repaired. From the very beginning, HR and NHEJ factors appear to compete for the right to repair the break and the outcome of this rivalry may differ between species, between cell types in a single species, and even between different cells of the same type. It is believed that there is no single factor which decides the choice of repair pathway and that the final result is a combination of different factors such as cell cycle phase, cell proliferation rate, availability of a homologous repair template, and the expression level and accessibility of repair proteins.

It has been known for many years that whereas NHEJ-deficient vertebrate cells are hypersensitive to IR, yeast cells show increased sensitivity to IR only in the absence of HR. This suggests that yeast, in contrast to mammals, utilize a different preference for repair pathways to deal with DSBs and many hypotheses have been proposed to explain why NHEJ is so inefficient in yeast compared to mammals, but to date none of these seems to completely explain this phenomenon. One can argue that it may be due to the fact that the genomes of higher eukaryotes are too large and too complex to make homology searching as efficient as in yeast. Moreover, the larger genome of mammalian cells theoretically minimises the probability that errors during NHEJ will have deleterious consequences because random small-scale deletions and insertions have a lesser chance of affecting coding sequences, which form ~4% of the genome compared with ~80% in the yeast genome.

Interestingly, large differences exist between the relative use of NHEJ and HR not only between such distant organisms as yeast and human, but also between different cells of the same organism. For example, chicken B lymphocytes which utilize gene conversion to generate antibody diversity, and mice embryonic stem cells, both display enhanced capacity for HR [82] and a proposed, plausible explanation of this phenomenon is based on the p53 protein status of these cells which are genotypically $p53^{+}$ but functionally p53-

inactive [83]. Under normal circumstances, p53 may associate with Rad51 protein and suppress homologous recombination by inhibiting its DNA-joining activity, but functional inactivation of p53 completely abolishes this interaction and thus promotes the HR over the NHEJ pathway [84].

Additionally, recent experiments with cells from consecutive developmental stages of the mouse nervous system suggest that the HR/NHEJ ratio can be also modulated during the maturation process and that proliferating neural precursor cells have an enhanced HR activity in comparison to fully differentiated cells [85]. The most likely explanation of such fluctuations may be that the HR pathway is hyper-activated in rapidly-proliferating cells to promote fast restart of stalled or collapsed replication forks, while simultaneous suppression of NHEJ would ensure that the most error-free repair pathway is used and thus protect genome integrity during the critical developmental period [85].

As mentioned above, under normal circumstances the NHEJ pathway is predominant in the G_0 and G_1 phases of the cell cycle, whereas HR operates mainly in the late S and G_2 phases [80]. It is believed that this difference is closely related with the accessibility of a template and a close association of sister chromatids in the nucleus that greatly facilitate repair by the HR pathway. One of the key factors participating in this process is cohesin, the protein complex known to bind the sister chromatids together from the time they are formed in S phase until they segregate in anaphase [86]. Very shortly after formation of DSBs, cohesin colocalizes at the sites of DNA damage in a process which is strictly dependent on activity of the MRN complex. The peak of this MRN-cohesin interaction occurs in the S and G_2 cell cycle phases, and cells with mutations in cohesin which abolish interaction with MRN exhibit an increased sensitivity to DNA damaging agents, suggesting a deficiency in HR [87].

Fluctuation of the levels of different proteins during the cell cycle also seems to be a factor influencing the choice of DSB repair pathway. For example, the levels of two pivotal proteins in HR, Rad51 and Rad52, reach a maximum in the G_2/M phases and fall during S and G_1. One could speculate that since these changes are completely DNA damage-independent, this increased expression is an additional factor regulating the choice of DNA repair pathway [88]. Generally, Rad51 seems to be one of the most important proteins which modulate the ratio of repair by NHEJ and HR in the cell. Apart from the p53-

dependent mechanism described previously (Section 1.2), Rad51 also undergoes BRCA2-dependent phosphorylation which promotes the HR pathway and inhibits NHEJ while specific phosphorylation of BRCA2 blocks its interaction with Rad51 and thus inhibits HR (more details below); this particular type of regulation reaches a maximum in the M and early G_1 phases and therefore represents an additional mechanism to inhibit HR and promote the NHEJ pathway [89].

Another candidate protein that seems to regulate the choice of DNA repair pathway and which undergoes cell cycle-dependent fluctuations is DNA-dependent protein kinase, catalytic subunit (DNA-PKcs) the main kinase involved in NHEJ. As described in more detail below, after DSB formation DNA-PKcs undergoes a series of specific autophosphorylations that influence its activity and promote the NHEJ pathway. These modifications are strongly reduced in the S and G_2 phases and may function as a mechanism to down-regulate NHEJ activity [90, 91].

Finally, since several years there is increasing evidence suggesting that the crucial step in initiating the HR pathway and inhibiting NHEJ is the process of resection of DNA termini. Briefly (details are presented in Chapter 1.4.3), after formation of a DSB the 5' termini of the two DNA ends are resected and covered by the ssDNA-specific protein RPA. As described above, this process activates ATR kinase which in turn recruits RAD51 that nucleates on the resected DNA termini and initiates the subsequent steps of HR repair [92, 93]. Recent studies suggest that the pivotal protein responsible for the resection process in human cells is CtIP nuclease [94, 95]. Like Rad51, expression of CtIP is also cell cycle-dependent and whereas its level reaches a minimum in the G_1/M phase it increases significantly during S/G_2 [96].

1.4.2 The non-homologous end joining (NHEJ) pathway

The basics of the NHEJ mechanism are very simple: in the first step, a group of enzymes capture and secure both ends of the broken DNA molecule, in the second step other proteins form a bridge that keeps the two ends together, and finally in the third step the broken DNA molecule is re-joined by the enzymes responsible for ligation. This model of course oversimplifies the process, which in reality is rather complex and still not

completely understood. It is believed that in the first step (Fig. 1.5) the heterodimeric protein Ku forms two pseudo-symmetrical ring structures which embrace the DNA ends [97] and creates a scaffold for the catalytic subunit of DNA-PKcs. The subsequent intimate association of DNA-PKcs with the DNA termini triggers its kinase activity, resulting in phosphorylation of itself as well as other signalling and processing enzymes, and moreover the synaptic complex of DNA-PKcs with Ku stabilizes both the DNA ends and protects them from degradation by unspecific nucleases. In the following step the broken DNA termini are processed by polymerases, Artemis or PNKP and finally after formation of the correct 5'-phosphate and 3'-OH termini these are re-ligated by the complex of DNA ligase 4, X-ray repair cross complementing protein 4 (XRCC4), and Cernunnos (XLF) [98].

1.4.2.1 The holoenzyme of DNA-dependent protein kinase (DNA-PK)

DNA-PK is one of the most important and key factors involved in the NHEJ pathway [90, 91]. It is composed of a large catalytic subunit, DNA-PKcs, and two small heterodimeric proteins Ku70 and Ku80. DNA-PK knock-out cells are highly radiosensitive and show defects in processing of coding ends during V(D)J recombination [1], and moreover mutations of the DNA-PKcs gene in mice, dogs and horses causes SCID (Severe Combined Immuno Deficiency) syndrome [99, 100]. Surprisingly, although hundreds of SCID mutations have been characterized in humans during the last decade, only one of them results from a missense mutation (L3062R) which did not affect the kinase activity or DNA end-binding capacity of DNA-PKcs itself; rather, the presence of long P-nucleotide stretches in the immunoglobulin coding joints indicated that it caused insufficient Artemis activation, something that is dependent on Artemis interaction with autophosphorylated DNA-PKcs [101]. These data combined together with the great abundance of DNA-PKcs in cells suggests that residual DNA-PKcs kinase activity is indispensable in humans and that mutations on its components are lethal [102, 103].

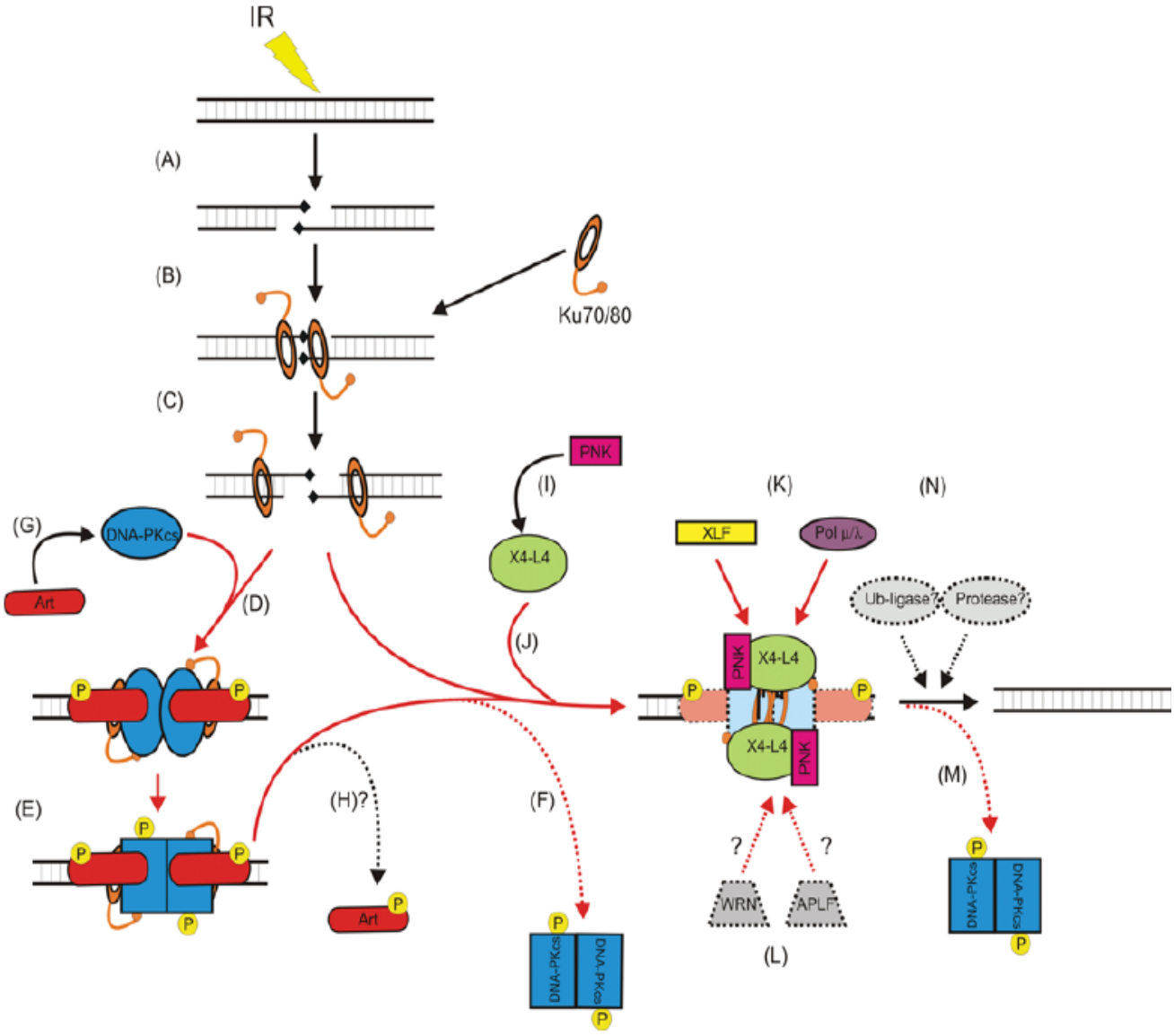

Fig. 1.5. Repair of a DSB by nonhomologous end-joining. (A) Formation of a non-religatable DSB by IR. (B) Binding of the Ku70/Ku80 heterodimer (orange) which translocates inwards on the DNA (C) and recruits DNA-PKcs (blue) which together form a "synaptic complex" (D). This process triggers phosphorylation of the DNA-PKcs (yellow circles) which undergoes a conformational change and releases the DNA ends (E); it is unclear whether DNA-PKcs is released from the complex prior to the binding of XRCC4/Lig4 (green) (F) or after repair is finished (M). (K) It is believed that the XRCC4/Lig4 complex recruits the associated protein factors XLF (yellow), PNK (pink) and DNA polymerases (violet). (G) A certain fraction of DNA-PKcs is associated with the protein Artemis (red), but so far there is no clear evidence as to when Artemis is released from the break (H). (adapted from [1]).

1.4.2.1.1 The protein Ku

The name Ku derives from the first two letters of the name of the patient in which this protein was first characterized as an autoantigen in polymyositis-scleroderma overlap syndrome [104]. The complex is composed of the two subunits Ku70 and Ku80 (70 and 82 kDa respectively) **(**Fig. 1.6**)** and represents one of the most abundant stably-expressed proteins in mammalian cells with ≈400'000 molecules per nucleus [105, 106]; both its subunits are present in almost every type of mammalian tissue and to date the only known cells which lack Ku are early spermatocytes until stage IV of pachytene [107]. It is believed that the main function of both Ku70 and Ku80 is their participation in the NHEJ repair pathway, especially in the detection of DSBs as well as contribution in telomere maintenance. The very high nuclear concentration of the Ku heterodimer means that any DSB is theoretically only 5 molecular diameters away from the nearest Ku molecule [64]. Consequently, it is believed that after formation of a DSB Ku is the first protein to recognize the break and dimerizes to binds and stabilizes the free DNA ends [108]. The Ku70/80 heterodimer binds DNA in a non-sequence-specific manner [109, 110] and the main regions responsible for binding are located in the central part of these two proteins [111, 112]. It is believed that upon binding to DNA, Ku undergoes a continuous dynamic exchange and that its three-dimensional structure sterically fits the DNA helix, but makes few direct contacts with the DNA backbone itself [108, 112]. After binding to DNA the Ku heterodimer attracts DNA-PKcs and strongly activates its kinase activity. The activated DNA-PKcs phosphorylates Ku70 and Ku80 and promotes their translocation by about one helical turn inward from the extremity of the DNA strand, producing space for binding of further DNA-PKcs which now has direct contact with ~10 bp of DNA at the end of the strand [113].

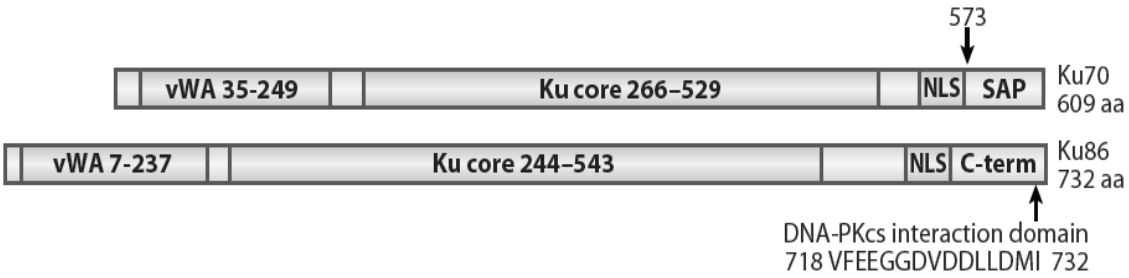

Fig. 1.6. Major domains in the Ku70/Ku80 heterodimer. On this scheme vWA designates the von Willebrand domain (aa 35-249 of Ku70 and 7-237 of Ku80), Ku designates the core (aa 266-529 and 244-543 for Ku70 and Ku80, respectively), and NLS indicates the location of putative nuclear localization sequences. SAP designates domains responsible for DNA binding. (adapted from [106])

At this point the Ku/DNA-PKcs complex starts to attract and recruit the other proteins which are necessary for repair by NHEJ. Interestingly, Ku is unable to form these complexes in the absence of DNA and interacts neither with DNA-PKcs nor with DNA polymerases and XRCC4/ligase IV complexes [114]. At the end of the repair process the ring-shaped Ku heterodimers are trapped on the religated DNA, and may be removed by a protease system [115]. Knock-out of either of the Ku subunits in human cells has been shown to result in increased radiosensitivity [79] and silencing of one subunit resulted in stable knock-down of the other, suggesting that under normal circumstances each subunit is required to stabilise the second [116, 117].

1.4.2.1.2 The catalytic subunit of DNA-dependent protein kinase (DNA-PKcs)

The catalytic subunit of DNA-PK (DNA-PKcs) is coded by a 30-kb segment of the *PRKDC* gene located in the q11 locus of the 8th human chromosome [118]. This ~470 kDa protein is one of the largest serine/threonine protein kinases stably expressed in mammalian cells [119]. Its ~500 long C-terminal region (Fig. 1.6**)** comprises a catalytic domain similar to that of the proteins ATM and ATR, which all fall into the phosphatidylinositol-3 kinase-like (PI3K/PIKK) family. According to recent studies of its 3-dimensional structure, DNA-

PKcs has three major domains, a "head", a "palm", and an "arm" [97, 120]; the N-terminal repeat regions comprise the palm which itself includes a distal N-terminal claw and a proximal DNA-binding claw [121, 122] while the "arm", probably containing regulatory autophosphorylation sites, connects the palm to the head which is composed of FAT (FRAP, ATM, TRRAP) as well as enzymatic (PI3 kinase) motifs [121]. As mentioned above, its very weak DNA binding and kinase activity are enhanced strongly in the presence of Ku heterodimer and ends of double stranded DNA [123, 124]. At the moment of DNA binding, DNA-PKcs undergoes a series of significant conformational changes which clamp the head and palm together and stabilize the protein–DNA interaction. In this so called "synapsis structure" its FATC domains protrude away and interact with the Ku heterodimer, whereas the rest of the molecule creates a channel which the DNA ends can reside in and pass through [125]. Observation of this complex by atomic force microscopy demonstrated that DNA-PKcs is present at the juxtaposed DNA ends and forms a "bridge" between the two termini, thus providing a platform for the enzymes required in subsequent steps of repair [126].

Apart from these structural characteristics, like other members of the PI3K family DNA-PKcs can phosphorylate many proteins on SQ/TQ motifs (Ser/Thr residues followed by a glutamine (Gln) residue) which seem to be particularly common in proteins involved in checkpoint signalling and DNA repair [127-129], providing a reasonable explanation for the requirement for DNA-PKcs kinase activity in the NHEJ repair pathway [130, 131]. There is a very long list of known proteins required for NHEJ which are excellent targets for DNA-PKcs *in vitro* and *in vivo* [113, 132-134], but at the same time there is unfortunately very limited knowledge if any of these interactions is actually required for NHEJ [135-137]. To date, the only relevant target seems to be DNA-PKcs itself [138, 139] and active DNA-PKcs can phosphorylate many of its own residues, such as Thr^{2609}, Ser^{2612}, Ser^{2624}, Thr^{2620}, Thr^{2638} and Thr^{2647}. All of these phosphorylation sites (termed the ABCDE cluster) represent one of the most extensively studied modification motifs in the entire molecule and encompass a 38-aa region which covers less than 5% of the total sequence **(**Fig. 1.7**)** [139]. Cui et al. defined a second major region of DNA-PKcs phosphorylation termed the PQR cluster which includes five conserved sites between Ser^{2023} and Ser^{2056} [140]. Interestingly, recent data revealed that complete inhibition of ABCDE

phosphorylation imparts a radiosensitive phenotype which is even more severe than complete lack of DNA-PKcs. In contrast, inhibition of PQR phosphorylation imparts only a modestly radiosensitive phenotype, suggesting that blocking of ABCDE phosphorylation strongly inhibits NHEJ which is only modestly impaired by blocking PQR phosphorylation [91]. Analysis of ABCDE and PQR mutants revealed that these two clusters function reciprocally to regulate access to DNA ends, and that whereas autophosphorylation of the ABCDE cluster promotes DNA end processing the same modification of the PQR cluster inhibits this process [140, 141]. It is believed that autophosphorylated DNA-PKcs dissociates from the break, looses its kinase activity, and is dephosphorylated by protein phosphatase 5 [142-144].

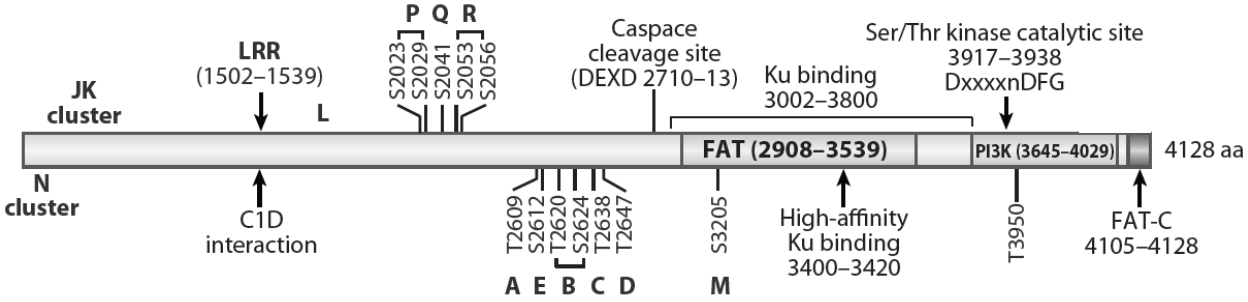

Fig. 1.7. Major structural features of DNA-PKcs. The N-terminal domain and the PIKK domain extend between aa 1-2908 and 3645-4029, respectively. LRR designates the leucine-rich region, PI3K the PI3 kinase domain, and FAT-C the FAT domain at the C terminus. ABCDE, PQR, LRR and M show clusters of sites which can be autophosphorylated (adapted from [106]).

1.4.2.2 Enzymes for processing damaged DNA termini

Since the only proper substrates for DNA ligase IV are 3'-hydroxyl and 5'-phosphate groups, all "dirty" termini produced by IR have to be processed and cleaned before the final religation step. This may encompass diverse reactions such as resection and modification of the 3' or 5' single-strand overhangs as well as the partial re-synthesis of

missing regions, and the main processing enzymes known to be involved are Artemis, PNKP, Aprataxin, and DNA polymerases of the X family.

1.4.2.2.1 Artemis

As far as the resection process is concerned, the best known factor involved in the NHEJ repair pathway is the protein Artemis (Snm1C), a nuclease which belongs to a large family of metallo-β-lactamase proteins, eukaryotic enzymes with a common 3-dimensional structure referred to as the αβ/βα sandwich conformation [145]. The human *Artemis* gene, whose mutation was first described as causing the TB severe combined immunodeficiency (TB-SCID) syndrome, is located in a 6.5 cM region of the short arm of chromosome 10 [146] and codes for a 692-aa protein with an N-terminal metallo-*β*-lactamase domain and a highly-phosphorylated C-terminal region of uncertain functions [145]. Inactivation of the Artemis protein results in accumulation of unopened DNA hairpins during V(D)J recombination and a radiation-sensitive version of the SCID syndrome (RS-SCID) [146]. Under normal circumstances Artemis is a 5'-3' exonuclease which is thought to be intrinsic and capable of degrading single- stranded DNA and RNA fragments however in the presence of DNA-PK and ATM kinases it acquires a 5' endonucleolytic activity towards regions of transition between double- and single-stranded DNA as well as towards unopened DNA hairpins [27, 132, 147, 148]. Generally, in the absence of DNA damage Artemis forms a large complex with the DNA-PKcs subunit in which its exonuclease activity is strongly suppressed [149]. The mechanism by which DNA-PKcs regulates this process is not fully understood, but is believed to be mainly by phosphorylation of the C-terminal part of the Artemis protein [147, 150]. Although Artemis-deficient cells are radiation-sensitive they do not show major defects in DSB repair, suggesting that *in vivo* Artemis is required for the repair of only a subset of breaks and that a further nuclease may be involved in NHEJ [151].

1.4.2.2.2 Polynucleotide kinase/phosphatase (PNKP) and aprataxin (APTX)

Human polynucleotide kinase/phosphatase (hPNKP) is a 57.1-kDa monomeric protein with dual activities, 5' DNA kinase and 3' phosphatase. Since breaks with 5'-hydroxyl or 3'-phosphate ends in DNA are hallmarks of many genotoxic agents including IR, PNK-dependent phosphorylation of 5'-DNA termini and dephosphorylation of 3'-DNA termini appear to be essential steps before they can be religated [152]. Knockdown of endogenous human PNK increases the frequency of spontaneous mutation as well as the sensitivity of cells to a broad range of genotoxic agents such as gamma-radiation, hydrogen peroxide (H_2O_2), or ultraviolet radiation (UV-C) [153]. *In vitro* experiments performed by Chappell at al. demonstrated that PNK promotes the exchange of phosphate at damaged termini but only in extracts from DNA-PKcs-deficient cells. Moreover, phosphorylation of terminal 5'-OH groups by PNK was blocked by depletion of XRCC4, suggesting that its DNA kinase activity is coupled to NHEJ processes [154]. The crystal structure of full-length mouse PNK reveals that it is folded into three compact domains, a C-terminal kinase domain, a central phosphatase domain, and an N-terminal FHA (ForkHead-Asociated) domain region [155]. Whereas the kinase and phosphate domains are responsible for enzymatic activity, the N-terminal region is crucial for interaction with XRCC4 and recruitment to sites of DNA damage [156].

The FHA domain of PNK is closely similar to that of another nuclear protein, Aprataxin (APTX). Mutations in the *APTX* gene destabilize the protein aprataxin and cause Ataxia-oculomotor apraxia (AOA1), a neurological disorder with symptoms that overlap those of ataxia-telangiectasia [157], and since cells from these patients are characterized by genome instability and an abnormal responses to DNA double-strand breaks ; it is possible that the APTX protein may be also involved in DNA repair. Aprataxin is a DNA-binding protein that catalyzes the deadenylation of AMP groups linked to 5' phosphate termini and interacts *in vitro* with Ku heterodimer and *in vivo* with XRCC4/Lig4 complexes [157-159].

1.4.2.2.3 DNA polymerases

DNA polymerases represent the second group of enzymes which prepare broken DNA termini for religation, and their main task is the re-synthesis of missing sequences near to the ends. It has been postulated that there are at least three members of the polymerase X family which participate in the NHEJ pathway, terminal deoxyribonucleotidyltransferase (TdT), polymerase μ, and polymerase λ , small (30-60 kDa) enzymes that are active on short gaps but lack editing exonuclease activity. All have a carboxy-terminal catalytic domain and an amino-terminal BRCT domain which probably participates in interactions with other NHEJ proteins [160]. TdT is a template-independent polymerase that mediates random addition of dNTPs to 3'-OH overhangs at DNA extremities, and is present only in cells actively undergoing V(D)J recombination [161]. In contrast, the two other members of the polymerase X family, pol μ and pol λ, are widely expressed in mammalian cells and have been shown to participate in rejoining of DSBs *in vitro* [162]. Both are prone to slippage on the polymerized strand which could generate sequence repeats [163] and have a different requirement as regards the DNA template. Pol μ is template-independent like TdT and is able to perform synthesis even without the existence of microhomology at the DNA terminus; it can polymerize across a discontinuous template strand, crossing from one DNA end to the other strand, and fold the polymerized strand onto itself generating inverted repeats units [164, 165]. In contrast, pol λ is mainly template-dependent and contains an 8 kDa domain with lyase activity which can remove a 5' deoxyribosephosphate group from the end of a polymerized strand [164, 166]. In the present state of knowledge it is difficult to describe precisely how and when these polymerases are recruited to sites of repair by NHEJ, but they co-immunoprecipitate with Ku as well as with the XRCC4-ligase IV complex and these interactions are believed to be crucial for their recruitment to sites of damage [160]. The levels of pol μ and TdT increase upon treatment of cells with IR or etoposide and both of them colocalize with γH2AX foci [167]. Depletion of either pol μ or pol λ from cell extracts reduces DNA end-joining activity *in vitro*, and cells expressing mutated form of pol λ are hypersensitive to IR [167-169]. On the other hand, cells isolated from animals with knock-out of pol μ or pol λ do not

show large differences in sensitivity to DNA-damaging agents [170, 171] suggesting that other DNA polymerases may be also involved in the DSB repair process.

1.4.2.3 XRCC4/Ligase 4 and Cernunnos/XLF)

After being processed, the broken DNA termini are ready to be rejoined by the XRCC4/Ligase 4/Cernunnos-XLF ligation complex. XRCC4$^{-/-}$ and Ligase 4$^{-/-}$ chicken DT40 cells are extremely sensitive to IR, and disruption of these genes in mice leads to early developmental defects and embryonic lethality [172-174]. So far, there is no information about the enzymatic activity of XRCC4; it is believed to act mainly as a scaffolding factor to facilitate the recruitment of other proteins involved in NHEJ by binding preferentially to nicked DNA or termini of broken DNA and, together with Ku and DNA-PKcs, holding them together during the entire repair process [114, 175]. The XRCC4 protein is composed of a globular head domain, a α helical stalk, and a C-terminal region that is responsible for its interaction with Ligase 4 [176, 177]. Under normal circumstances XRCC4 contains two identical subunits which can also form a tetramer and it is believed that the dimeric and tetrameric forms exist in an equilibrium state up to the moment when DNA Ligase 4 is bound [176].

DNA Ligase 4 (Lig4) is an ATP-dependent enzyme and one of the best characterized binding partners of the XRCC4 protein. It contains two C-terminal BRCT domains separated by a linker region which interacts with the extended coiled-coil α-helical region of XRCC4 [178]. It is believed that *in vivo* the amino-terminal heads of XRCC4 mediate an interaction with complexes of Ku bound to DNA, whereas Lig4 is responsible for the rejoining the broken DNA ends [177]. How the XRCC4/Lig4 complex is recruited to breakage sites remains a matter of controversy, but biochemical studies suggest that as in the case of other proteins involved in NHEJ, this may be a result of an intrinsic activity of DNA–PKcs [179]. However, laser-irradiated DNA-PKcs-deficient cells exhibit a normal accumulation of XRCC4 at sites of DSBs repair, which suggest the existence of an alternative, probably Ku70/80-dependent recruitment pathway. Additional data seems to support this hypothesis: in the presence of Ku the XRCC4/Lig4 complex can ligate several fully-incompatible DNA end configurations that do not have to share even 1 bp of terminal microhomology [180]. Interestingly, the XRCC4/Lig4 complex may act even across short

gaps and ligate one strand of the duplex even when the other strand is in a configuration that cannot be ligated [27]. Though the efficiency of this joining is rather low, an another very important partner of the XRCC4/Lig4 complex, the protein XLF (Cernunnos), can markedly stimulate this activity and enhance the ligation of incompatible DNA ends [181].

First described in 2006 by two independent research groups, Cernunnos/XLF is a 299 aa-long nuclear protein stably expressed in a wide range of eukaryotic cells [182, 183]. The human *Cernunnos/XLF* gene is located on chromosome 2q35 and its mutation causes a heritary variant of SCID. Patients suffering from this syndrome exhibit a variety of neuronal abnormalities, growth retardation, microcephaly, and problems of immunodeficiency [184] while their fibroblasts, like cells in which XLF has been depleted by siRNA, display an increased sensitivity to IR and to other DNA-damaging agents [183]. The XLF protein includes an N-terminal globular head domain followed by a coiled-coil region and C-terminal helices (Fig. 7) [185]. It is believed that the coiled-coil region provides a strong interaction between two Cernunnos/XLF monomers which, in the absence of DNA and other NHEJ proteins, may form a homodimer. These homodimers interact with homodimers of XRCC4 via their N-terminal globular domains, and mutations either at L115 of Cernunnos/XLF or K63 or K65 of the XRCC4 protein severely disrupt this interaction [185]. As demonstrated by co-immunoprecipitation studies, Cernunnos/XLF can also associate weakly with Lig4 [186, 187].

Our current knowledge suggests that the stoichiometry of the Cernunnos/XLF /XRCC4/Lig4 complex is 2:2:1 and that XLF interact via its globular domains with the head domains of XRCC4 (Fig. 7) [186-190]. The XRCC4 and Lig4 proteins are both needed to stabilize the recruitment of this multiprotein complex to the sites of DNA breaks, whereas Cernunnos/XLF is necessary to modulate the efficiency or specificity of the activity of XRCC4/Lig4 [186, 191]. In addition to these activities, Cernunnos/XLF responds to formation of a DSB in a Ku-dependent manner and starts to accumulate at a damaged site within a few seconds. Interestingly, XRCC4 is dispensable for this recruitment and stabilizes the binding of Cernunnos/XLF to DNA only during the later steps [192, 193], suggesting that Cernunnos/XLF contributes not only in the last phase of the NHEJ process but also forms a functional connection between DSB sensing and DNA ligation in the presence of Ku heterodimer.

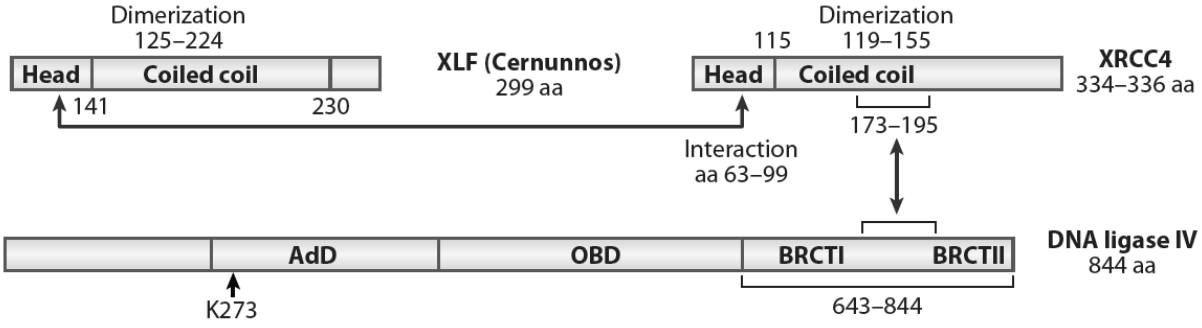

Fig. 1.8. Major features of the XRCC4/Ligase 4/Cernunnos/XLF complex. The arrows indicate the regions of physical interaction between these proteins. OBD designates the DNA binding domain and AdB the adenylaton domain of Ligase 4 (adapted from [106]).

1.4.3 The Homologous Recombination (HR) repair pathway

Homologous recombination (HR) is a type of repair in which nucleotide sequences are exchanged between two similar or identical DNA molecules, one damaged and the other intact. The classical HR process comprises three successive steps: initial resection of the 5'-extremity of DNA at the break site, strand invasion of a homologous DNA duplex by the 3' single-stranded DNA extremity, ligation, and finally separation of the recombinant intermediates and finalization of the repair process. Depending on the physical availability of both extremities at a DSB and the topology of the strand invasion intermediate, three major subtypes of HR have been identified: synthesis-dependent strand annealing (SDSA), classical double-strand break repair (DSBR), and break-induced replication (BIR) **(**Fig. 1.9**)**. Moreover, initial 5' resection of DSB termini may uncover repetitive DNA sequences and promote an additional type of HR termed the single-strand annealing (SSA) pathway. The majority of the data about HR obtained so far is derived from yeast, where HR plays a pivotal function in DSB repair. To date a plethora of different proteins have been implicated in regulation of the HR pathway; the most important encompass the Rad52 epistasis group (Rad50, Rad51, Rad52, etc.) as well as others such as nucleases, helicases

and polymerases. In addition, within the last few years significant progress has been made toward understanding the mechanism of HR in mammalian cells, and homologues of almost all the yeast repair genes have been described and characterized in human cells [194].

When compared to the NHEJ pathway, HR seems to be an almost error-free process with a relatively low mutagenic outcome. This high fidelity is the consequence of the duplication of an identical sequence from an intact homologous DNA molecule onto the DNA region carrying a DSB. There are two possible homologous donors available from which missing sequence information can be copied, the sister chromatid and the homologous chromosome, whose accessibility differs considerably during the cell cycle; whereas a homologous chromosome is present during the entire cycle, a sister chromatid is present only after it has been replicated. As discussed previously, the proximity of a copyable template is one of the key factors deciding the choice of DSB repair pathway. It is believed that post-replicative repair of a DSB by HR requires cohesion between sister chromatids to be mediated by the cohesin complex located along the chromosome arms [86] because in the absence of functional cohesin DSB repair in the G_2 phase is severely impaired in yeast mutants, although reintroduction of cohesin in post-replicative cells does not rescue this deficiency [195]. Cohesin components are recruited to the extended chromosome regions which surround a DSB caused by IR, but only when this is formed during the G_2 phase, and this accumulation is abolished and repair is defective in the absence of functional cohesin-loading proteins even though the sister chromatids are already connected by S phase-generated cohesin [196], demonstrating clearly that even if S-phase cohesion is fully functional, further cohesin has to be recruited to sites of damage to initiate efficient DNA repair. This DSB-dependent recruitment of cohesin seems to depend partially on the formation of foci which contain histone γH2AX, as well as on other proteins involved in HR such as Mre11 (part of the MRX complex) or Scc2p (a component of the cohesin loading machinery) [197].

Sister chromatids are believed to be the preferred and most efficient template for repair by HR and allow the damaged sequence to be restored to a state identical to that before breakage, and this is not surprising since sister chromatids are held in very close proximity. Moreover, repair by recombination with the homologous chromosome may lead

to loss of heterozygosity (LOH) in the repaired DNA region because sequence information from the undamaged chromosome is duplicated whereas that from the second broken chromosome is lost. Depending on the sub-type of recombination, this loss of heterozygosity may extend to several megabases of DNA and encompass multiple genetic loci or even whole chromosome arms (e.g. during repair by BIR), and analysis of markers and karyotypes in tumours suggest that loss of heterozygosity at specific tumour-suppressor loci is an important and quite frequent event during oncogenesis. The classic example is hereditary retinoblastoma, where inter-homologue recombination is estimated to lead to the loss of the wild-type chromosome in about 40% of all tumours [198]. Fortunately, the overall frequency of homologous chromosome-based repair seems to be very low and is estimated to represent around 1% of all HR repair events.

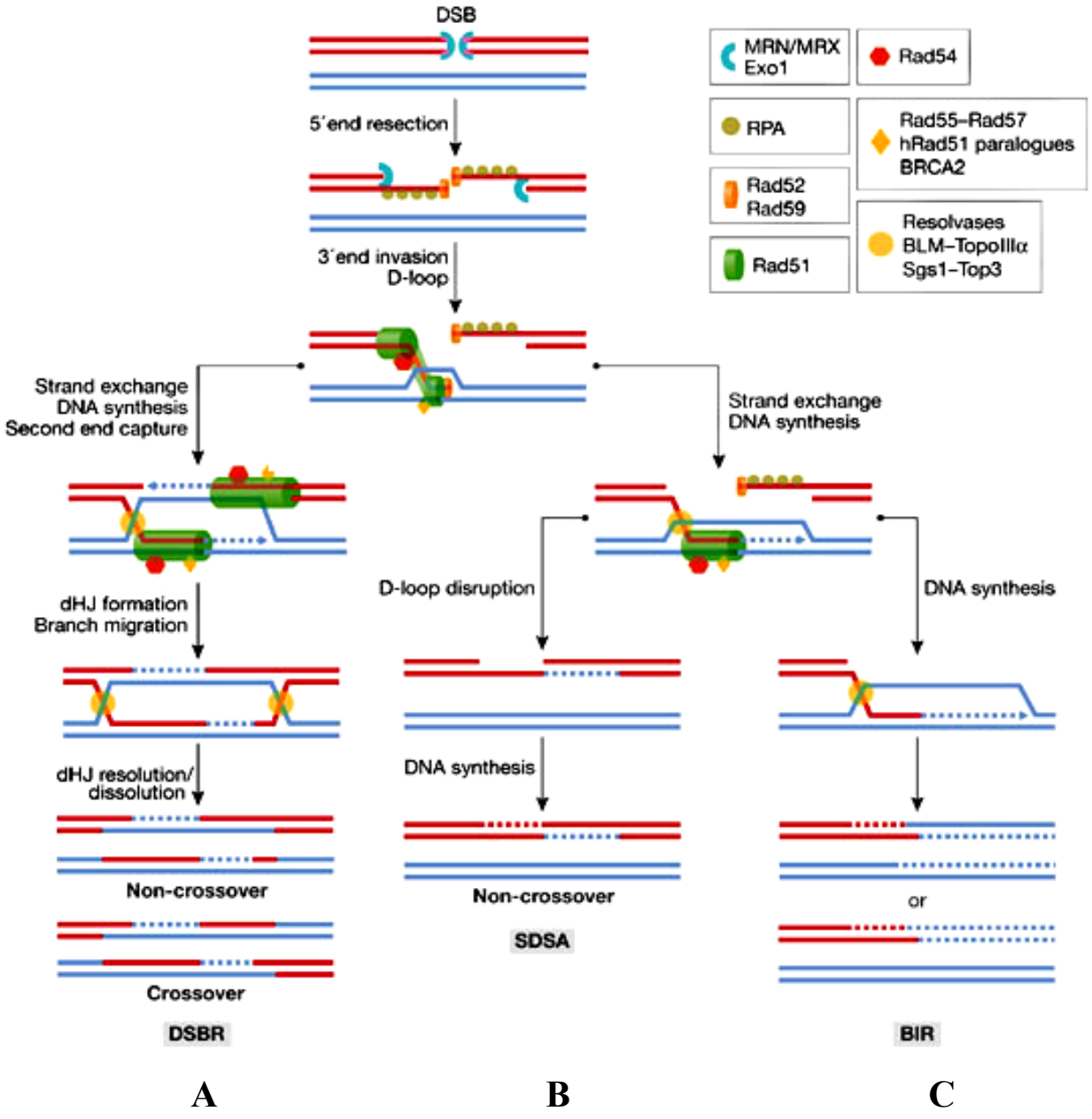

Fig. 1.9. Repair of a DSB by homologous recombination. Repair starts by the generation of 3' overhangs, which form complexes with the proteins RPA and Rad51 and invade the homologous chromosome or sister chromatid forming a displacement loop (D-loop). After this point, repair may continue by three different sub-pathways: A, double-strand break repair (DSBR); B, synthesis-dependent strand annealing (SDSA): or C, break-induced replication (BIR). A more detailed description is given in the text [adapted from [78]).

1.4.3.1 Recognition of DSBs for repair by HR

As for repair by NHEJ, the first step of HR repair is recognition of the break and the key player in this process is the MRE11/RAD50/NBS1 complex (MRN). It is believed that a few seconds after formation of a break, MRN binds to the DNA ends and forms oligomeric complexes which tether them together [199, 200]. Lack of any component of MRN leads to embryonic lethality in mammals, and mutations of the *NBS1* and *Mre11* genes cause Ataxia-teleangiectasia-like-syndrome (ATLD) and Njimegen Breakage Syndrome (NBS) respectively. MRN has also been implicated in several other crucial activities in eukaryotic cells such as telomere maintenance, checkpoint signalling, meiotic recombination, and DNA replication [201].

1.4.3.1.1. The Mre11/Rad50/Nbs1 complex

The *Mre11* gene is located on chromosome 11 and encodes a protein of 708 aa whose N-terminal part contains a long nuclease domain and the region of interaction with Nbs1, whereas the C-terminal portion contains two DNA-binding regions separated by a domain interacting with Rad50 [202, 203]. Under physiological conditions, two Mre11 molecules homodimerize through their N-terminal hydrophobic clusters and form a four-lobed U-shaped structure that is critical for proper assembly of the MRN complex and its DNA binding properties. *In vitro* studies have demonstrated that the N-terminal domains function as a single-strand DNA endonuclease, a 3'-5' single-strand DNA exonuclease, a double-strand DNA exonuclease, and a hairpin-opening enzyme. Under *in vivo* conditions and in the presence of DNA, Mre11 dimers are able to form two types of protein-DNA complexes termed "synaptic", formed with double-strand DNA with short 3' overhangs, or "branched" formed by binding an oligonucleotide containing both double- and single-stranded regions. In both cases a conformational change in Mre11 causes translocation of the DNA toward the nuclease site and thus provides endo- and exo-nuclease activities required for efficient repair by HR [201].

The human *Rad50* gene is located on the long arm of chromosome 5 and encodes a protein of 1312 aa containing two globular domains connected by a 50 nm-long coiled-coil

region with conserved Cys-X-X-Cys motifs located in the central hinge region of the molecule. These motifs are crucial for the proper functioning of Rad50 and form an interlocking hook that binds one Zn^{2+} ion **(**Fig. 1.10**)** [203, 204]. Under physiological conditions the N- and C- terminal globular domains of Rad50 interact with each other and form the so-called ABC transporter ATPase which is responsible for the regulation of DNA-dependent allosteric changes. This intra-molecular rearrangement results in the formation of a long, flexible coiled-coil arm that folds back on itself via the hinge region and forms a scaffold for a second molecule of Rad50. It is believed that under physiological conditions and in the presence of Zn^{2+} ions, the two Rad50 molecules are joined by hooks in their folded coiled-coil domains whereas their "heads" interact with and stabilize the DNA termini at a DSB [204] (FIG. 1.10 B).

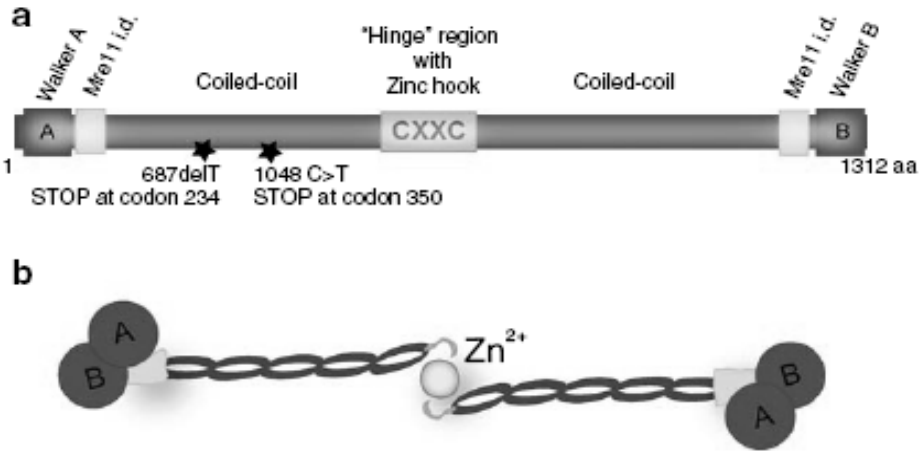

Fig. 1.10. Structure of the protein Rad50. (A) The Walker A and B motifs (the sequence GXXXXGKT/S), believed to be sites for binding nucleotides in many proteins, are located on the two opposite ends of the protein and responsible for its ATPase activity. The Mre11-binding domain is located next to these motifs and the center part corresponds to the hinge region that contains a zinc-hook motif. (B) Dimerisation of two Rad50 proteins through their hinge region in the presence of Zn^{2+} (adapted from [201]).

NBS1 (nibrin or p95) is a 95 kDa protein encoded by a 50 kb-long gene located on chromosome 8q21 [205]. As discussed above, mutations in the *Nbs1* gene cause a rare, autosomal-recessive human disease termed Nijmegen breakage syndrome (NBS)

characterized by severe immunodeficiency, chromosomal instability, microcephaly, growth retardation, radiosensitivity, and predisposition to lymphoid cancers [206]. The N-terminal part of human NBS1 contains a FHA (Forkhead-associated) domain and two adjacent BRCT motifs which often mediate phosphorylation-dependent protein-protein interactions and are characteristic for many other DNA-damage response proteins. Nbs1 is believed to play key functions in the majority of DNA-damage-checkpoint and DNA repair signalling processes. In NBS cells with truncating or nonsense mutations of the *NBS1* gene, Mre11 and Rad50 still complex with each other but do not translocate to the nucleus, suggesting that NBS1 is essential for the nuclear localisation of the complex [206]. Additionally, in the presence of NBS1 the DNA binding activity of Rad50 is stimulated strongly and the endonucleolytic activity of Mre11 increases [207]. The FHA domain of NBS1 promotes its interaction with the nuclease CtIP, thereby directly contributing to the resection step of HR repair (see below) [96].

The stoichiometry of the three proteins forming the MRN complex is still a matter of controversy. Sedimentation equilibrium analysis of the recombinant human complex indicates that an Mre11 dimer form a 1:1 complex with Nbs1, but both Mre11/Rad50 and Mre11/Rad50/Nbs1 complexes are large multimeric assemblies with a mass of ~1.2 MDa, significantly larger than the predicted size for 1:1:1 stoichiometry [207]. The stoichiometry ratio in the MRN complex seems to be 2:2:1, although this is not a constant value and may undergo slight changes depending on the availability and accessibility of its individual components. It is observed that in the presence of equal amounts of Mre11 and Nbs1 the MRN complex contains two or more Rad50 molecules, whereas in excess of Nbs1 the assembly reaction is shifted towards complexes containing multimers of Rad50. Additionally, it cannot be excluded that under physiological conditions MRN may also interact with itself and form higher order structures, which may explain the existence of the observed 1.2 MDa complexes [201]. Electron microscopy and structural studies seem to confirm this hypothesis and disclose that the "standard" MRN is a protein complex consisting of a heterotetrameric $(Mre11)_2/(Rad50)_2$ head and a double coiled-coil linker. In this conformation the Rad50 ATPase domain (head) and its adjacent coiled-coil regions undergo a series of conformational changes which influence and control Mre11 exonuclease activity [203]. Interestingly, whereas binding of NBS1 has no influence on the

basic structure of this complex the dynamic architecture of complete MRN is markedly affected when it binds to DNA. Binding of DNA by the MRN globular domain leads to a conformational change of the Rad50 coiled-coils regions, which protrude away from the DNA and become more rigid to efficiently keep the two DNA ends in close proximity. This change prevents intra-complex interactions and favours DNA tethering, thus facilitating subsequent steps of HR [203, 208].

1.4.3.2 The 5'-3' resection process

After recognition of a break, the next step of HR repair is resection of the 5' DNA termini by degradation of the 5' → 3' ends, producing a long 3' single-stranded overhang of ~100-200 nucleotides which is immediately covered by the RPA complex and used to prime the subsequent synthesis of DNA [92]. As already described briefly, it is believed that formation of these single-stranded DNA (ssDNA) tails is a crucial and decisive moment in the choice of repair pathway. In yeast, the complex of nucleases Sae2, Exo1, Sgs1 as well as MRX (the homolog of human MRN) works synergistically to resect the 5' strand and generate long 3' ssDNA tails for the subsequent "strand invasion" process [209]. This is a two-step process in which the initial attack is performed by Mre11 and Sae2 nucleases followed by long-range resection involving either Exo1 5'-3' nuclease or the Sgs1/Dna2 helicase-exonuclease complex; double mutants for Exo1 and Sgs1 are not able to perform efficient 5'-3' DNA degradation and generate only a small pool of single-stranded overhangs a few nucleotides long [210]. All these nucleases have their orthologues in mammalian cells termed Exo1, Bloom's syndrome protein (BLM), a homologue of yeast Sgs1 helicase, and C-terminal binding protein interacting protein (CtIP), and the yeast Sae2 homologue = CtIP, originally isolated, sequenced and characterized as a binding partner of C-terminal binding protein (CtBP), retinoblastoma (Rb), and BRCA1 [211] is believed to be the most important protein in DNA resection for DSB repair in mammals although recent studies revealed that it has other important functions in regulation of the cell cycle and checkpoint signalling. CtIP undergoes a series of ATM- and CDK-dependent modifications that regulate its activity. Inactivation of one CtIP allele predisposes mice to

multiple types of lymphomas, whereas homozygous inactivation leads to embryonic lethality [211].

The MRN complex activates ATM kinase, which in turn phosphorylates CtIP on S664 and S745 residues and promotes a conformational change and association with the FHA motif of the protein NBS1 [96], although localization of CtIP to sites of DNA damage is significantly delayed compared with that of the MRN complex agreeing with the hypothesis that recruitment of CtIP is Nbs1-dependent. It is not clear what could be the consequences of interaction between CtIP and MRN, but since purified human CtIP stimulates Mre11 nuclease activity *in vitro*, together they may cleave the 5' ssDNA and initiate the resection process. CtIP may serve also as a phosphorylation target for cyclin-dependent kinase 1 (Cdk1) [95, 212], which phosphorylates residues S327 and T847 and enhances its recruitment to DNA damage sites as well as binding to the C-terminal part of BRCA1. BRCA1 ubiquitinates CtIP and promotes its interaction with the proteins RAP80 and Abraxas (described below) which also appear to participate in its recruitment to sites of DNA damage. To summarize, in mammalian cells resection starts as a series of multiple ATP- and/or CDK-dependent regulations of CtIP, which binds to BRCA1 heterodimers (more details below), migrates to a DSB, and after reaching the broken extremity of the 5' strand performs 5'-3' end resection together with Exo1 and the MRN complex and produces a 3' ssDNA overhang ready for the next step of repair.

1.4.3.3 ssDNA invasion, strand exchange, and D-loop formation

Within a few seconds after resection, 3' ssDNA overhangs are bound by a high-affinity heterotrimeric complex of the ssDNA-binding protein Replication Protein A (RPA) [92], which not only protects them from nucleases but also melts the DNA and to some extent facilitates the subsequent formation of helical nucleoprotein filaments by Rad51 [213]. Rad51 is a eukaryotic ATPase able to bind to and modify the structure of ssDNA in a manner similarly to the bacterial RecA protein, forming filaments in which the DNA is shortened uniformly to ~50% of the length of normal B-form DNA and Watson-Crick pairing between the complementary invading and template strands is significantly accelerated [214]. The Rad51 protein does not show a strong preference for single-stranded DNA and has ATPase and strand exchange activities ~100 times smaller than its bacterial

orthologue [215]. For this reason it nucleates onto ssDNA rather slowly, thus rendering presynaptic filament assembly vulnerable to competing factors of which RPA, the first protein to bind to ssDNA termini, paradoxically competes with Rad51 for binding to the resected DNA as a consequence of its higher affinity and binding rate [216]. A number of accessory proteins, termed recombination mediators, help to facilitate nucleation of Rad51 onto ssDNA tails [217]. In yeast, the most important and best known of these are Rad52, Rad54, Rad55 and Rad57 which also form heterodimers that stabilize nucleofilaments and stimulate subsequent strand exchange, and there is a similar group of factors in mammalian cells including BRCA2 and BRCA1 as well as the less-known BARD1, PALB2 and DSS1 [217].

1.4.3.3.1 The proteins breast cancer 1 and breast cancer 2 (BRCA1 and BRCA2)

BRCA1 and *BRCA2* are two human genes which, when mutated, increase susceptibility to hereditary breast and ovarian cancer. The proteins BRCA1 and BRCA2 for which they code are involved in processes important for maintening genome integrity such as repair of DSBs, cell cycle control, and chromosome segregation. Because of these crucial functions, complete loss of either one of these proteins leads to a dramatic increase of genome instability and of the frequency of chromosome translocations.

The *BRCA1* gene is located on the long arm of chromosome 17 and codes for a phosphoprotein of 1863 aa that plays an important function in signal transduction and DNA repair processes. Mutations of *BRCA1* are responsible for approximately 40% of all inherited ovarian cancers and for more than 80% of inherited breast cancers. The N-terminal part of the BRCA1 protein contains a RING domain, a conserved pattern of eight Cys and His residues, that interacts with multiple cognate proteins and its C-terminal part contains a nuclear localization signal and two BRCT repeats responsible for interaction with other proteins involved in DNA repair, recombination and cell cycle control. BRCA1 interacts through its RING domain with the protein BRCA1-associated RING domain 1 (BARD1) and forms heterodimers that possess a ubiquitin ligase activity which is crucial for chromosome stability as well as cell proliferation and centrosome-independent mitotic spindle assembly [218]. BRCA1 may also interact with other BRCT-like proteins such as

the MRN complexes, CtIP nuclease, or histone H2AX through its carboxyl terminal domain which contains two BRCT repeats. Recently, several groups independently discovered other important factors which bind to BRCA1, Rap80 and Abraxa whose binding depends strictly on the ubiquitin ligase activity mentioned above. The function of these complexes is still uncertain, but Rap80 is believed to bind to polyubiquitinylated histone H2AX and thereby bring the BRCA1 complex to sites of DNA damage [219].

In view of the similar phenotypes of *BRCA1* and *BRCA2* patients and the spectrum of defects observed in cells deficient in these proteins, one would predict that the BRCA proteins might work in synchrony in processes essential for tumour suppression. Indeed, consistent with this notion interaction between them has been reported during recruitment of Rad51 to ssDNA overhangs and formation of nucleoprotein filaments [220]. It has been a longstanding question how these two proteins interact *in vivo*, and it is believed that the mediator protein PALB2 (FANC-N) plays an essential role in this process [221].

PALB2 and BRCA1 interact via their coiled-coil regions, and cells harbouring mutations that abrogate this interaction are defective in repair by HR. At the same time, the C-terminal part of PALB2 interacts with the N-terminal portion of BRCA2 and thus serves as the molecular scaffold for the formation of the entire BRCA1-PALB2-BRCA2 complex. The exact functions of these complexes are uncertain, but PALB2 is believed to modulate the loading of BRCA2-RAD51 heterodimers onto ssDNA termini [221, 222].

The *BRCA2* gene is located on the long arm of chromosome 13 and encodes a protein of 3418 aa. Heterozygous mutations of BRCA2, like those of BRCA1, predispose to an elevated risk (level) of female breast and ovarian cancers, whereas homozygous defects cause Fanconi anaemia. Interestingly, families with BRCA2 mutations also exhibit an increased risk of breast, pancreatic and prostate cancers in males [223, 224]. The central region of BRCA2 contains eight copies of a 70 aa BRC motif, each of which can interact with a Rad51 monomer as well as with ssDNA nucleoprotein filaments. It is therefore believed that BRCA2 participates in homology-directed repair, presumably in conjunction with the Rad51 recombinase, and this hypothesis is supported by a series of experiments on BRCA2 mutant cells which shows that cells harbouring mutations exhibit an up to 100-fold reduced level of HR [225]. More recent data demonstrate that interaction of BRCA2 with Rad51 causes a large movement of the flexible N-terminal domain of RAD51 and

facilitates its efficient nucleation on DNA tails and thereby stimulates the HR repair process. Moreover, after the formation of ssDNA-Rad51 complexes BRCA2 additionally stabilizes the resulting nucleoprotein filaments so that they cannot be dissociated or destroyed [226].

Rad51-coated ssDNA nucleoprotein filaments are the active intermediates in repair and their formation is crucial to initiate the onset of the strand invasion and displacement loop (D-loop) steps. During these two subsequent processes Rad51-coated 3'ssDNA termini capture a DNA template and search for sequence homology on the neighbouring DNA duplex. After the homologous region is found, the invading strand forms Watson-Crick base pairs with the intact template and sets up a D-loop intermediate. It has been estimated that in yeast, Rad51-dependent recombination requires a homologous region of at least 100 bp, and the formation of shorter regions strongly inhibits the whole mechanism [227]. It is unclear how the Rad51-ssDNA nucleofilament complex finds the homologous region of the DNA template, but this is believed to result from random collisions with continuous dissociation and association of Rad51 from the 3' ssDNA end of the nucleoprotein filament, as in the case of bacterial RecA protein [228]. Strand exchange and D-loop formation are the last common stages for all types of HR, and after this point the next steps of every sub-pathway differ significantly although all the final repair products contain the homologous replacement of the broken DNA sequence. In some cases, especially after repair by the DSBR pathway, the repaired region may contain extra sequences associated with a crossover exchange reaction (see below for more details) which increases the extent of loss of heterozygosity and may lead to modification of the entire chromosomal region. Nevertheless, as demonstrated in mouse embryonic stem cells non-crossover inter-sister homologue reactions predominate over the crossover type and their ratio is ~30 to 1 [229].

1.4.3.4 Synthesis-dependent strand annealing (SDSA) and sub-pathways for repair of double strand breaks

Double-strand break repair (DSBR) and synthesis-dependent strand annealing (SDSA) (Fig. 1.11 A and B, respectively) are two different types of homologous

recombination pathway which deal with the same type of DSB i.e. a typical two-ended DSB. In both cases, after generation of a D-loop intermediate the 3'-end of the invading strand primes DNA synthesis on the homologous duplex molecule as the template. There is still some controversy about the DNA polymerases involved, and so far the only substantial candidate able to perform this process both in *in vitro* and *in vivo* is DNA polymerase Eta (Pol η) [230, 231], an error-prone DNA polymerase which promotes translesion synthesis (TLS) through DNA lesions that may be also be formed spontaneously as well as by UV radiation. Interestingly, mutant cells that lack Polη activity demonstrate a significant decrease in the frequency of both Ig gene conversion and DSB repair by HR [230] as well as hypersensitivity to UV. Polη localizes mostly uniformly in the cell nucleus, and colocalizes with replication factories during S phase but following irradiation of cells with ^{60}Co photons it accumulates at stalled replication forks and partially colocalizes with foci containing Rad51 [232].

Most HR-dependent DNA synthesis events, either SDSA or DSBR, entail copying of only a short tract from the donor DNA molecule, a process called short track gene conversion (STGC) which predominates over that termed long track gene conversion (LTGC) [233]. The longest observed mammalian gene conversion process encompasses a distance of less than 10 kb, whereas in yeast it can extend up to hundreds of kb during Break Induced Repair [229] (see below for more details).

The annealing and resolution processes, the final steps of HR recombination, differ greatly between the SDSA and DSBR sub-pathways. In SDSA, after the successive DNA synthesis and small D-loop extension processes the invading ssDNA is displaced and base pairs (i.e. anneals) with the processed second end of the break followed by cleavage of sequences not involved in annealing and subsequent gap-filling synthesis and strand religation (Fig. 1.11 B). In contrast, during DSBR the initial 3'-end invasion and DNA synthesis are followed either by a "second end capture annealing" or "second end invasion" event. The most essential protein involved in these processes is Rad52, which possesses the unique capacity to anneal single-stranded DNA complexes with the cognate strand complexed with RPA. Interestingly, the simultaneous presence of Rad51 on ssDNA ends may be nonproductive for repair by HR because it blocks loading of Rad52, whose function may be taken over by Rad54 which works as a back-up pathway and partially catalyzes the

normal annealing process [234, 235]. Functional homologs of Rad52 protein can be found even in such distant organisms as bacteria and phage, suggesting that ssDNA annealing is an ancient and universal mechanism for "second-end capture". During the DSBR pathway this mechanism and the subsequent synthesis of the second DNA end generate two four-way structures composed of DNA strands base paired with their old and new partners simultaneously. These intermediate structures, termed double Holliday Junctions (dHJs) , have to be resolved and produce either cross-over or non-cross-over final products. The enzymes involved in "uncrossing" are termed Holliday Junction resolvases, but to date no single gene encoding a resolvase has been identified. It is believed that resolution of HJs is rather executed by several distinct enzyme complexes, and extracts from cells carrying mutations in the recombination/repair genes *RAD51C* or *XRCC3* have reduced levels of HJ cleavage. Double HJ intermediates can also be resolved by the action of Bloom's syndrome protein (a DNA helicase) and topoisomerase IIIα, which produce non-crossover products [236].

1.4.3.5 Break-induced DNA replication

Break-induced replication (BIR) is a special kind of HR which, in contrast to the previously-described processes of SDSA and DSBR, deals only with one-ended DSBs which arise when only one of the DSB ends shares homology with another region in the genome or when one end of a broken DNA molecule is lost. BIR was discovered initially as a specific mechanism which restarts DNA synthesis at collapsed replication forks in yeast, but it appears also to be one of the mechanisms responsible for alternative lengthening of mammalian and yeast telomeres [237]. The contribution of BIR to the repair of endogenous DSBs in wild-type cells is uncertain, but in Rad51 or Mre11 mutants it can makes a significant contribution to the repair of exogenously-induced breaks. In the absence of Rad51, BIR becomes a Rad52-dependent pathway and in the absence of Rad52 nearly 100% of broken chromosomes remain unrepaired [238, 239]. It has been shown that RAD51-independent recombination requires much less homology (~30 bp) for strand invasion to occur than that depending on RAD51 (~100 bp), and in fact the presence of Rad51 protein severely impairs the recombination of short homology motifs. It is believed

that in yeast these two pathways act as distinct systems to maintain correct telomere structure in the absence of telomerase [227].

The best illustration of the use of BIR is the repair of broken replication forks formed when DNA helicase encounters a nick on the DNA template, causing one arm of the replication fork to break (Fig. 1.11 A**)**. After initial formation of a D-loop structure, the 3'-single stranded overhang primes DNA synthesis and establishes a replication fork containing both leading and lagging strands. Migration of the Holliday Junction (HJ) separates the extended double-strand end from its templates so that the 5' end is resected once again and the 3' ssDNA re-invades the homologous region and repeats the entire process. After a few cycles of invasion, extension, and separation the more processive polymerase Pol ε continues replication to the end of the replicon or of the chromosome arm [240]. As easily imagined, the copying of such long DNA regions, often encompassing an entire arm of the template chromosome, could result in the loss of sequence information encoded on the distal region as well as loss of heterozygosity, as described above (Section 1.4.3).

1.4.3.6 Single-strand annealing (SSA)

Single-strand annealing (SSA) represents a special type of HR repair which does not involve the formation and resolution of HJ and whose activity is so far mainly characterized in yeast cells. SSA generally repairs DSBs between two repeated sequences oriented in the same direction, and since it does not involve strand exchange it is Rad51-independent. After the initial resection step the repeat sequences on the two 3' ssDNA overhangs are uncovered, aligned, and annealed together, the remaining un-annealed single stranded terminal sequences are removed, and the resulting gaps or nicks are filled in by successive synthesis and ligation (Fig. 1.11B**)**. SSA does not require a separate homologous DNA template and the resected region may extend up to several kb. In yeast, Rad52 complexed with RPA anneals the ssDNA overhangs whereas Rad1-Rad10 endonuclease cleaves non-homologous complexes after the annealing step [241]. Thus RAD52 plays a dual role in repair by HR, promoting the annealing of complementary single-stranded DNA

and stimulating the recombinase function of RAD51, but since Rad51 is not required for SSA, Rad52 probably takes over all its functions in this sub-pathway.

The last step of SSA repair is nucleolytic cleavage of non-homologous sequences, which is performed by the structure-specific endonuclease complex XPF/ERCC1 (the human counterpart of the yeast Rad1/Rad10 complex). In cell-free extracts XPF/ERCC1 is stably associated with Rad52 by interactions via the N-terminal domains of Rad52 and XPF, and formation of this complex stimulates the DNA structure-specific endonuclease activity of XPF/ERCC1 and attenuates the DNA strand annealing activity of Rad52 [242].

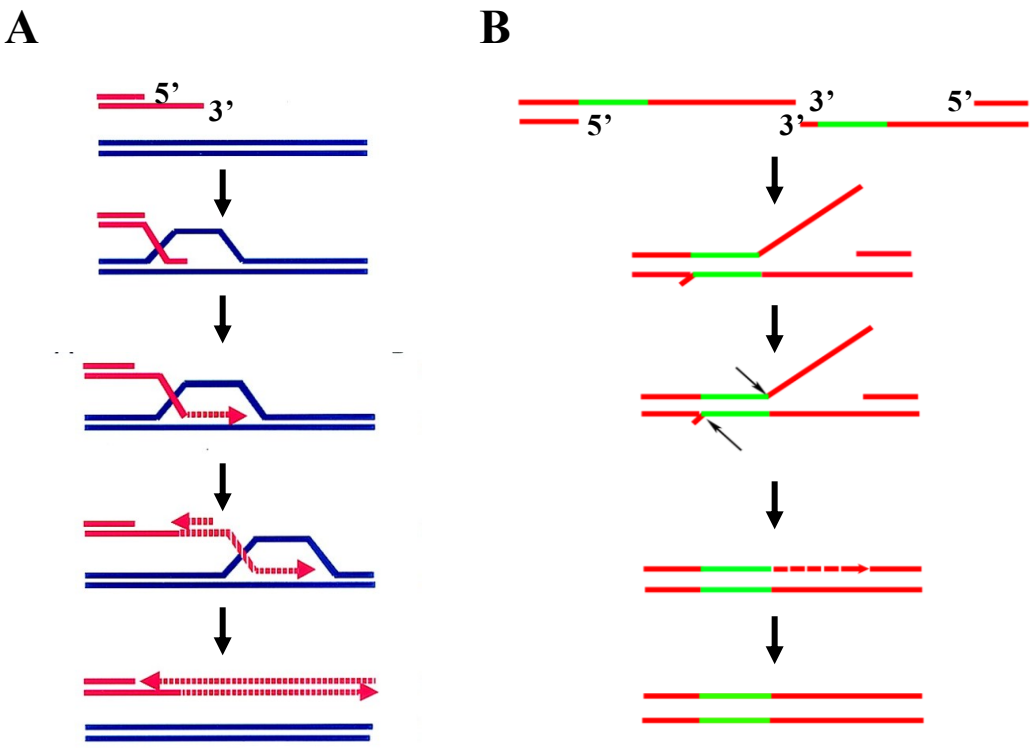

Fig. 1.11. Break-induced repair (BIR) and single-strand annealing (SSA). (A) In the BIR pathway, the end of a broken chromosome is resected and the 3′ terminus is used for subsequent strand invasion. This 3′ end initiates DNA replication leading to a migrating D-loop and formation of a newly-synthesized double stranded DNA. (B) In SSA, 5' DNA termini are resected and complementary DNA repeats (green) are annealed. Nonhomologous sequences are cleaved out (small arrow arrays), gaps are filled (dashed line), and the two strands are ligated (see the text for more details).

1.4.4 The backup-NHEJ pathway (B-NHEJ)

For several years, both *in vitro* and *in vivo* studies have suggested that there is another, alternative process which can participate in repair of DSBs apart from the HR and NHEJ mechanisms. Cells deficient in major components of the NHEJ or HR pathways are able to repair almost all DSBs after a sufficiently long incubation time, and the final level of damage is only slightly higher than that in their wild type counterparts [243-245]. One of the first proteins shown to be involved in this alternative repair pathway was PARP-1 which was known to participate in base excision and single strand break repair since many years, but its role in the repair of DSBs was a matter of controversy. Initial experiments performed by Hochegger et al. showed that PARP-$1^{-/-}$ DT40 cells exhibit increased sensitivity to various DSB-inducing agents and a decreased level of repair by HR. As it turned out, this specific phenotype was strictly related to the presence of Ku70 and double mutants for PARP-1 and Ku70 were not hypersensitive to IR and were normally proficient in HR repair [246]. Additional in-depth analysis revealed that PARP-1 interacts with Ku in both *in vitro* and *in vivo* conditions and its involvement in DSB repair is closely related to direct competition with Ku70. In irradiated wild type cells the higher affinity of Ku70 for DNA ends and the excessive number of other forms of DNA lesions limits the contribution which PARP-1 can make to repair of DSBs, but in cells with a Ku70 mutation it is recruited to DSBs slowly and initiates their repair [79]. It is postulated that in a manner analogous to its activity in repair of single strand breaks, PARP-1 heterodimers bind to DNA extremities at DSBs and activate XRCC1/DNA Ligase III which finalizes the repair process [247]. This mechanism, distinct from that previously described, is termed Back-Up Non-Homologous End Joining (B-NHEJ) to reflect its back-up and delayed function [79], and the hypothesis that it represents a new and potentially important mechanism for repair of DSBs has been confirmed by experiments on mouse embryo fibroblasts defective in HR and/or NHEJ [248]. B-NHEJ appears to be cell cycle-dependent and *in vivo* plasmid end-joining assays demonstrate that it is most active during the G2 phase.

1.5 Chromatin remodelling during DNA breakage and repair

During interphase, DNA is combined with proteins and organized into a precise, compact structure, a dense string-like fiber termed chromatin. A longstanding question in the study of the cellular response to IR is how such a complex structural environment of chromatin is influenced by lesions in DNA. The basic repeating unit of chromatin, the nucleosome, consists of DNA wrapped around an octamer of core histones composed of two molecules each of histones H2A, H2B, H3 and H4 forming a ~10 nm diameter fibre that is visible under the microscope as a "beads on a string" structure (Fig. 1.12). During interphase the string of nucleosomes is packed further into a denser structure known as a solenoid/30nm fibre that compacts the DNA by a factor of ~40 [249]. Moreover, when the cell enters metaphase the chromatin compaction state changes dramatically and condenses to an even greater degree into specialized structures for partioning the daughter genomes- the chromosomes. However, most of the time the cell is in interphase and its chromatin is less densely compacted than in chromosomes, and it is known to adopt two different levels of compaction. The predominant type of chromatin found in cells during interphase, euchromatin, is genetically active and more diffuse than the other kind of chromatin which is termed heterochromatin. The additional compression of heterochromatin is thought to involve various proteins in addition to the histones, and the DNA it contains is thought to be genetically inactive.

Chromatin, especially euchromatin regions, undergo constant remodelling processes whose frequency increases greatly after DNA damage and which are believed to play an important role in recognition and repair of DNA strand breaks [249-251]. As a result, the compact chromatin structure is believed to be relaxed to provide easier access and docking stations for the machinery which repairs damaged DNA [252].

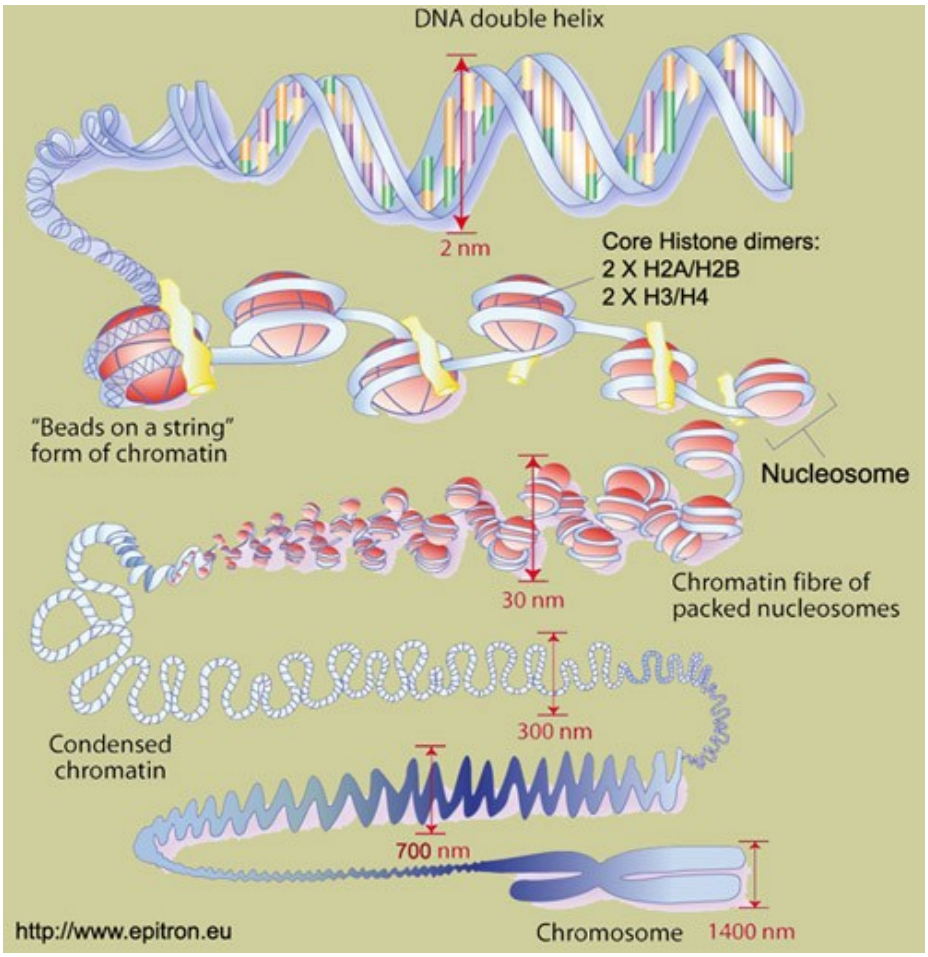

Fig. 1.12. Different levels of DNA condensation

1.5.1 Formation of foci containing repair proteins in the nucleus

As described above, recognition and repair of DSBs and SSBs involves the participation of several different groups of proteins with distinct but overlapping functions. Upon damage to DNA the majority of these proteins migrates rapidly to the sites of damage and accumulates in localized assemblies termed repair foci, whose formation in response to DNA damage is observed in many organisms ranging from yeasts to mammals. The first observation of DNA damage-dependent foci formation was made by Haaf et al., who

demonstrated that after irradiation the protein Rad51 becomes concentrated in multiple discrete regions whose number and size are significantly correlated with the level of DNA damage [253]. Since that time many other proteins have been shown to form DNA damage-dependent foci whose formation is predominantly a hallmark of SSB and DSB repair activity [254, 255]. It is believed that repair foci are formed in accordance with a hierarchical assembly model in which repair factors nucleate DSB in a synchronized, sequential manner and subsequently accumulate and occupy up to a few megabases from the break site. Thus in the case of DSB repair, for example, one can distinguish early foci containing ATM, MRN, MDC1 and γH2AX which form within seconds after damage, as well as late foci associated with the later steps of repair [256]. Interestingly, the protein components of repair foci do not appear to exist as pre-functional complexes and they interact only at the moment of DNA damage. Foci are intrinsically highly dynamic structures; the majority of their components undergo constant dynamic exchange between free and chromatin-bound states and their turnover depends on the type of damaging agent, the extent of DNA damage, and the type of DSB repair [257].

1.5.2 Changes in chromatin distribution in the nucleus

In the relaxed chromatin state, single chromosomes occupy defined nuclear volumes termed chromosomal territories [258]. The spatial distribution of these distinct territories within the nucleus appears to be dependent on the gene density of the respective chromosomes in spherical nuclei, and whereas heterochromatic and gene-poor regions are typically found at the periphery of the nucleus and around the nucleoli forming "sub-chromosomal foci" the euchromatic, gene-rich regions are located mainly in the center of the nucleus [259]. Interestingly, it is still a matter of controversy whether these two distinct regions of chromatin respond in the same way to IR-induced damage. Some early microscopic studies demonstrated that in mammalian cells no γH2AX damage signals could be observed within heterochromatic regions 1 h after sparsely-ionizing radiation, suggesting that DSBs are less frequent or are not processed in heterochromatin [260]. Additionally, as revealed by Soutoglou et al., breaks formed in euchromatin seem to be

strongly bound by Ku80 protein and thus positionally stable and unable to roam the cell nucleus [261].

In contrast, recent immunofluorescence analyses and quantitation studies revealed that in Drosophila cells there is almost identical and efficient formation of repair foci in both chromatin compartments, and the tight packaging of heterochromatin does not represent an obstacle to DSB recognition and processing. In fact, DSB repair foci were assembled very quickly in heterochromatin (many times faster than those in euchromatin) suggesting that features of heterochromatin may even amplify some aspects of the DSB response [262]. Moreover such breaks, like these observed in S. cerevisiae, show a clear movement of broken DNA termini to the exterior of the heterochromatin domain [262, 263]. Based on these facts, in the recent model suggested by Chiolo et al. [262] DSB formation and processing occur in both eu- and hetero-chromatin soon after damage is induced. However, breaks in heterochromatin require ATM-dependent phosphorylation of Kruppel-associated box-associated protein-1 (KAP-1), a heterochromatin-building protein. These findings suggest that DSBs formed in heterochromatin are repaired with much slower kinetics than those produced in euchromatin and that ATM functions to relieve compaction of heterochromatin via KAP-1 phosphorylation [264]. Additionally, there is dramatic expansion and dynamic protrusions of the heterochromatin domain in response to ionizing radiation (IR) in Drosophila cells, and moreover breaks in heterohromatic are repaired in majority by the HR pathway but with striking differences from euchromatin. Proteins involved in early HR events (resection) are rapidly recruited to DSBs within heterochromatin, in contrast to Rad51 which only associates with DSBs that relocalize outside of the domain. Heterochromatin expansion and relocalization of foci require checkpoint and resection proteins, especially the Smc5/6 complex which is enriched in heterochromatin and is required to exclude Rad51 from the domain and prevent abnormal recombination [265]. This model suggests that after damage to DNA, chromatin undergoes a series of global conformational changes that facilitate processes for its repair and that early steps during DSB processing occur within heterochromatin, whereas the later steps are excluded from this domain probably in order to prevent aberrant exchanges between DNA repeats regions which are know to be very frequent in heterochromatic regions.

1.5.3 Changes in chromatin architecture during repair

As mentioned above, during the last few years an increasing body of evidence suggests that chromatin remodelling plays a very important function in repair of strand breaks, especially DSBs. The pivotal steps in this process appear to be covalent modifications of the N-terminal tails of histones which protrude away from the nucleosomes core; the majority of these modifications reduce the affinity of the tails for adjacent nucleosomes and thereby decrease the compaction of the broken chromatin fiber. Two main classes of enzymes are involved in this post-traumatic regulation of chromatin accessibility, large, multi-utility complexes that use energy from ATP to weaken the interactions between histones and DNA in the region of a break, and a second group of enzymes which modify the N-terminal regions of the core histones by acetylation, phosphorylation, methylation, or ubiquitinylation.

1.5.3.1 Acetylation and ATP-dependent remodelling of chromatin

A series of studies suggest that acetylation and ATP-dependent remodelling mechanisms act together in the response to DNA damage, leading to a rapid local decompaction of chromatin to facilitate the access of repair proteins.

The main ATP-dependent proteins involved in chromatin remodelling belong to the SWI2/SNF2 protein superfamily which all contain a SNF2-like DEAD/H(SF2) ATPase subunit by which they catalyze remodelling processes. In yeast, two members of this family termed Remodels the Structure of Chromatin (RSC) and the Swi/Snf complex are directly recruited to sites of DSBs, and cells with mutations in these roteins are hypersensitive to DNA damaging agents [266, 267]. It is believed that these systems play distinct but overlapping roles during DSB repair, and that whereas RSC is necessary for the initial stages of assembly of repair proteins, Swi/Snf is required for the final steps of the process [266]. To date, it is unknown if the Swi/Snf complex plays the same functions in DSB repair in human cells, but mutations of its hSNF5 core subunit cause a highly lethal pediatric cancer, malignant rhabdoid tumour (MRT). Deletion of the *hSNF* gene in mouse

embryo fibroblasts results in increased sensitivity to agents inducing DSBs as well as increased chromosomal instability [268].

Another ATP-dependent enzyme involved in DSB repair in yeast is the INO80 complex, which *in vitro* remodels chromatin, facilitates transcription, and shows 3' to 5' DNA helicase activity. Cells with mutations in INO80 show severe defects in transcription as well as hypersensitivity to agents that cause DSBs [250]. Tsukuda et al. [252] demonstrated that INO80 is recruited to γH2AX foci 30 to 60 min after formation of a DSB and binds to the sequences next to the break, followed by eviction of nucleosomes in the vicinity. It is believed to also play some role in the recruitment of Rad51 and Rad52.

One of the best characterized acetylation processes involved in DSB repair is the above-mentioned modification of ATM kinase by the Tip60 and hMOF complexes [53, 54]. Tip60, a multiprotein histone acetyltransferase (HAT) complex, is also directly involved in chromatin remodelling processes and catalyzes the transfer of acetyl groups from acetyl coenzyme A to either the α-amino groups of N-terminal amino acids or to the ε-amino group of internal lysine residues. The best example of such activity is the acetylation of histone H4, which is believed to open up chromatin structure around the breakage site and thus facilitate accessibility to the factors required for repair [269].

As mentioned before, ATP-dependent chromatin remodelling and histone acetylation may cooperate in DSB repair, as demonstrated by examples from cells of D. melanogaster and yeast. In the first case, histone H2Av is rapidly acetylated and also phosphorylated by the dTIP60 complex after DNA damage, and after repair of the break the ATPase subunit (p400/domino) of TIP60 catalyses the exchange and replacement of the acetylated phospho-H2Av by unmodified H2Av [270]. An analogous process is observed in budding yeast, where dimers of phosphorylated histone H2A-H2B are replaced by fresh, unphosphorylated molecules by the NuA4-HAT complex [269].

1.5.3.2 Phosphorylation of histones

Phosphorylation probably represents one of the most-explored types of modification of histones that is observed during the formation and repair of DSBs. To date, the best known example is the phosphorylation of H2AX, an isoform of the core histone H2A,

which is believed to be one of the most conserved variants of H2A and whose quantity varies between 2% and 25% of the total H2A in the cell [271]. Upon DNA damage, H2AX is phosphorylated extensively on Ser139 to form gamma H2AX (γH2AX), which covers a large region of chromatin of up to 2 megabases adjacent to a break and may contain up to 2000 γH2AX molecules [272]. After a few minutes visible foci containing γH2AX form in the nucleus which are believed to represent sites of DSBs; their number correlates with that of DSBs in a 1:1 ratio and their disappearance correlates with the end of repair activity after IR doses ≤10 Gy. There is a difference in H2AX phosphorylation in different regions of chromatin, and after irradiation γH2AX foci form several times more efficiently in euchromatin than in heterochromatin, whereas inhibition of DNA synthesis in S-phase cells by hydroxyurea results in an approximately equal distribution. This suggests that phosphorylation of H2AX or formation of foci of γH2AX may be restricted in heterochromatin, probably due to its greater compaction and limited accessibility for phosphorylation, and that decompaction during DNA replication partially relieves this restriction [273].

In principle, H2AX may be phosphorylated by three transducer kinases, ATM, ATR and DNA-PK, but it is believed that under normal circumstances the principal role is played by ATM kinase. Calculations show that although formation of the majority of γH2AX foci induced by IR is ATM-dependent, ATR kinase is also require for ~10% suggesting that a small portion of ATR also could be involved in recognizing IR-induced DSBs [274]. It is not completely clear how phosphorylated H2AX is dephosphorylated, but data from yeast indicates that the HTP-C complex may play an essential function in this process; it contains the phosphatase Pph3 which is able to regulate phosphorylation of H2AX *in vivo* and dephosphorylates γH2AX efficiently *in vitro*. However, loss of γH2AX from chromatin surrounding DSBs is independent of the HTP-C complex, suggesting that γH2AX is first removed from chromatin and only then dephosphorylated [275]. In mammalian cells, one of the candidate for removing γH2AX from chromatin is the phosphatase 2A(PP2A) whose recruitment to DNA damage foci is γH2AX-dependent, but is not related to activity of ATM, ATR, or DNA-PK. Its catalytic subunit (PP2A(C)) coimmunoprecipitates with γH2AX and colocalizes in DNA damage foci, and when it is inhibited or silenced γH2AX

foci do not disappear and DNA repair is inefficient and cells are hypersensitive to DNA damaging agents [276].

Cells deficient in phosphorylation of histone H2AX show increased sensitivity to IR, elevated genomic instability, and defects in sister chromatid recombination during meiosis. Interestingly, H2AX seems to be not required for efficient NHEJ and its mutants show normal levels and fidelity of V(D)J recombination, although foci of BRCA1 or RAD51 induced by IR show a subtle decrease in size [277]. The main function of γH2AX thus appears to be the formation of a molecular platform that attracts and retains proteins involved in repair of DSBs, and in some cases to function as a recognition signal for repair and chromatin remodeling enzymes such as 53BP1, MDC1, INO80 or NuA4 [278].

Obviously the H2AX histone variant is not the only one which undergoes DNA damage-dependent phosphorylation, but in other cases the function of such modification in DSB repair processes is still not well documented. Ser14 in the N-terminal tail of histone H2B is phosphorylated at sites of DSBs, and the phosphorylated form accumulates in foci containing γH2AX [279]. Phosphorylation of histone H4 at ser1 has also been observed in response to DNA damage, and was shown to be dependent on casein kinase 2 and to inhibit the acetylation of histone H4 by the NuA4 acetyltransferase complex [280].

1.5.3.3 Ubiquitylation of histones

In eukaryotic cells ubiquitylation is commonly used as a signalling transduction mechanism that relies on covalent modification of target proteins by the attachment of the 76-aa ubiquitin to lysine residue(s). Several recent findings provide insight into the mechanism by which ubiquitylation regulates cellular responses to DSBs, and the major protein involved in this process seems to be the ubiquitin ligase RNF8 (ring finger protein 8) [281]. As mentioned previously, one of the first mechanisms activated in the cell after formation of DSBs is ATM-dependent phosphorylation of a variety of different proteins involved in the repair process. One of these proteins is MDC1, which in turn through its phosphorylated FHA domain rapidly recruits RNF8 to the sites of breakage [282]. Depletion of RNF8 by interfering RNA results in a failure of normal repair foci formation, suggesting that it may serve as a bridge connecting the recruitment of different DNA repair

factors [281]. Once recruited RNF8 ubiquitylates histones H2AX and H2A and additionally recruits several important regulatory proteins for repair such as the 53BP1 or BRCA1–BARD1 complexes. As described above, this last ubiquitin-mediated process is closely related to the adaptor protein Abraxas and the ubiquitin-interaction motif (UIM) of Rap80 protein [219]. Whether ubiquitylation of H2A or H2AX is necessary for the recruitment of all of these proteins, or their modification is merely a consequence of RNF8 recruitment, is still an open question and needs to be explored in the future. Another important ring finger protein which has been demonstrated to accumulate at DSBs sites and mediate chromatin ubiquitylation process is RNF168. RNF168 interacts with ubiquitylated H2A histones, assembles at DSBs in an RNF8-dependent manner, and, by targeting H2A and H2AX, amplifies local concentration of lysine 63-linked ubiquitin conjugates to the threshold required for retention of 53BP1 and BRCA1 [283]. In fact defects in RNF168 are the cause of Riddle syndrome (RIDDLES) which is characterized by increased radiosensitivity, immunodeficiency, mild motor control and learning difficulties, facial dysmorphism, and short stature. At the molecular level as is believed these defects are probably the consequences of impaired localization of TP53BP1 and BRCA1 at DNA lesions due to the mutations in RNF168 gene [284].

1.5.3.4 Methylation of histones

Methylation is another important post-translational modification whose exact role in the DNA damage response pathway is still largely unexplored. The majority of chromatin methylation events is carried out by histone methyltransferases (HMTs) which transfer methyl groups from *S*-adenosyl-L-methionine (SAMe) and covalently modify lysine and arginine residues in the amino terminal regions of histone tails [285]. One of the best characterized chromatin modification mechanisms activated after DNA damage is methylation of histones H3 and H4. The H3 histone methylation seems to be required for *in vivo* recruitment of mammalian 53BP1 to sites of DNA damage, and this process seems to be largely dependent on the Tudor domains of 53BP1 [285]. A similar mechanism exists in the case of histone H4 methylation and is mediated by the PR-SET7 methyltransferase. It is believed that in both of these processes the 53BP1 Tudor domains specifically interact with Lys20 residue of dimethylated H4 and cause the protein to attach to the modified histones

[286]. Apart from this direct modification of chromatin, methylation may also apply to proteins actively participating in DSB repair processes, and one of the best-documented examples is PRMT1-mediated methylation of the exonuclease MRE11. Mutation of the arginine responsible for this methylation severely impaired the exonuclease activity of Mre11, but surprisingly did not affect formation of the MRE11-RAD50-NBS1 complex. Moreover, cells containing un-methylated MRE11 displayed an intra-S-phase DNA damage checkpoint defect, suggesting that arginine methylation regulates the activity of the MRE11-RAD50-NBS1 complex during the intra-S-phase DNA damage checkpoint response [287]. All of these data suggest that methylation may play a function of a specific DSB "indicator" rather than a chromatin remodeller and might act in the recruitment of the different repair proteins to sites of DNA breakage.

1.6 Epstein-Barr virus (EBV) minichromosome

Because of the complex nature of genomic DNA, it is usefull to use model systems to investigate effects of genotoxic agents on DNA. Over recent years there have been an increasing number of data in which valuable paradigms have been discovered using plasmids – extrachromosomal DNAs in the cytoplasm of bacteria. Plasmids are small and therefore easier to analyze than complex human genomic DNA and moreover, because of their circular nature, topological form conversion assays can be used to detect DNA damage. However, since they are nonmammalian in origin and lack chromatin structure they do not completely resemble the structure of mammalian chromatin and therefore their utility as a model system is limited.

In mammalian cells there are several different analogs of bacterial plasmids which exist as physically separate DNAs termed extrachromosomal elements (EEs) [288]. These include episomes, minichromosomes, small polydispersed DNAs, or double minute chromosomes which are generated by genome rearrangements under physiological or pathological conditions. Some of those rearrangements occur randomly, but others are strictly non-random, highly regulated, and involve specific chromosomal locations (for example V(D)J-recombination, telomere maintenance mechanisms, *c-myc* deregulation)

[289]. All of the EEs are know to involve predominantly extrachromosomal amplification of an oncogene or a drug-resistance gene such as *mdr*1, and are often considered as precursors of expanded chromosomal regions that fail to display typical banding patterns after trypsin-Giemsa staining and known as "homogenously staining regions" (HSRs) [288, 289].

Minichromosomes are cytogenetically invisible large DNA molecules with the associated histone proteins that closely resemble the chromatin of the host cell's chromosomes. They are capable of containing whole genomic loci and being maintained as nonintegrating, replicating molecules in proliferating human somatic cells [288]. Minichromosomes assemble chromatin most efficiently in mammalian cells if they contain an origin of replication from a viral DNA. Minichromosomes are found in yeast cells, and also in eukaryotic cells in the case of DNA viruses which replicate through initiation of bidirectional replication from a chromosomal origin [290]. An example is the Epstein-Barr virus (human herpesvirus 4, HHV-4, EBV), a ubiquitous virus of the herpes family that preferentially infects B lymphocytes and is a primary cause of Mononucleosis [291]. EBV has been also associated with particular forms of cancer, particularly Hodgkin's lymphoma, Burkitt's lymphoma, nasopharyngeal carcinoma, and central nervous system lymphomas [291, 292]. The EBV genome codes for at least 30 polypeptides, has a molecular weight of ~10^8, and is 172-182 kbp in length depending on the strain of the virus. It is found in both integrated and episomal forms in various producer and nonproducer cell lines, respectively [292]. The nonproducer Raji cell line, propagated from a Burkitt's lymphoma patient, carries ~50-100 copies of the 172 kbp episomal form of EBV per nucleus which constitute about 0.1% of the total cell DNA [293]. In transformed Raji cells the EBV episome constitutively expresses a limited set of viral gene transcripts for so-called latent proteins: six nuclear antigens (EBNAs 1, 2, 3A, 3B, 3C and -LP), three latent membrane proteins (LMPs 1, 2A and 2B) (Fig. 1.13) as well as transcripts from the *Bam*HIA region of the viral genome (so-called BART transcripts). In addition to the latent proteins, Raji cells also show abundant expression of the small, non-polyadenylated (and therefore non-coding) RNAs, *EBER1* and *EBER2,* whose function is not clear but which are consistently expressed in all forms of latent EBV infection referred to as 'latency III' (Fig. 1.13) [291].

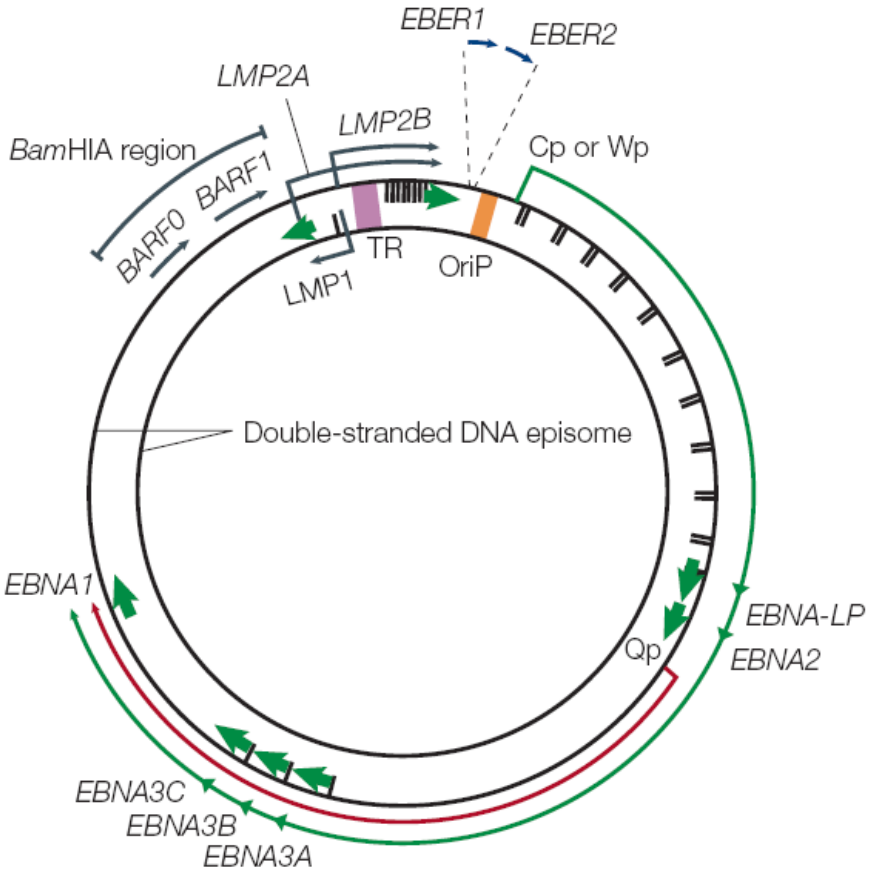

Fig. 1.13. Location and transcription of EBV latent genes on the double-stranded viral DNA episome. The origin of plasmid replication (OriP) is shown in orange. The large green solid arrows represent exons encoding each of the latent proteins, and the arrows indicate the direction in which the genes encoding these proteins are transcribed. The latent proteins include the six nuclear antigens (EBNAs 1, 2, 3A, 3B and 3C, and EBNA-LP) and the three latent membrane proteins (LMPs 1, 2A and 2B). Terminal repeat (TR) shows the region in which linear viral DNA is circularized producing the episome. The blue arrows at the top represent the highly transcribed nonpolyadenylated RNAs EBER1 and EBER2; The long outer green arrow represents transcription during a form of latency known as latency III [adapted from [291]].

1.7 Cell death

As described above, when mammalian cells are subjected to stress, for example IR, a range of gene products involved in the sensing and signalling of the stress are activated. This complicated cascade of events initiates pathways for the repair of DNA as well as cell cycle checkpoints which participate in the subsequent program for full biological recovery. However, if the damage is too extensive and impossible to repair or if repair is inefficient, cells may undergo a series of transformations that lead to their death. Commonly, lethality occurs because production of gross chromosomal changes, such as dicentric and acentric fragments, leads to loss of large amounts of genetic material when cells attempt to divide. In general, exposure to IR induces two different modes of cell death termed mitotic or clonogenic cell death, and apoptosis. DSBs are lethal lesions, and when unrepaired or misrepaired they lead to mitosis-associated cell death (also termed reproductive or postmitotic) or to P53-mediated apoptosis.

1.7.1 Mitotic (clonogenic) cell death

Mitotic (clonogenic) death is the characteristic form of death caused by irradiation of cells within solid tumors, and is their major response to anticancer drugs. The correlation between the frequency of mitotic cell death and the number of DNA lesions and chromosomal aberrations induced suggests that this pattern of death results from failure of cells to completely or accurately repair the resulting damage to DNA [294]. This unsuccessful repair leads to a series of aberrant mitoses that fail to produce correct segregation of chromosomes and lead to the formation of large nonviable cells with several micronuclei. The appearance of these giant multinucleated cells and, in consequence, mitotic death, has been characterized as the main mechanism of cell death by which the majority of solid tumours respond to clinical radiotherapy [294]. Notably, clonogenic cell death may occur after a variable number of cell cycles but the molecular mechanisms controlling its induction are still largely unknown. It is believed that the main function in induction of mitotic cell death is played by farnesylation of proteins, a posttranslationall

modification by the addition of a 15-carbon farnesyl group, as well as by the G_2 cell cycle checkpoint [295, 296].

1.7.2 Death by apoptosis

Apoptosis is an alternative mode of post-radiation cell death, and in contrast to mitotic cell death it is perceived as a process occurring during interphase which does not require cell division. Apoptosis is a genetically-regulated process that is a normal physiological method for removing cells that are irreversibly damaged. Unlike necrosis, it encompasses a series of programmed events involving distinct cellular changes such chromatin condensation, membrane blebbing, cell shrinkage, and production of fragments called apoptotic bodies that phagocytic cells are able to engulf and quickly remove before the contents of the cell can spill out onto surrounding cells and cause damage. Additionally, during the final steps of apoptosis a specific degradation of DNA occurs which results in a characteristic "ladder" of DNA fragments after agarose gel electrophoresis. There are two main distinct and independent signalling pathways which initiate radiation-induced apoptosis, the P53- and the Ceramide-dependent pathways (Fig. 1.14).

In the P53-mediated process one can distinguish two further categories, transcription-independent and transcription-dependent processes, and whereas the first is mainly based on interaction of P53 with BCL-XL and BCL-2 proteins to exert its direct apoptogenic function in mitochondria, the second depends on P53-dependent regulation of different genes with known proapoptotic activity [298]. All of these genes fall into three groups based on the subcellular location of their product; the first group encodes proteins that localize to the cell membrane (e.g., CD95, PERP), the second group proteins that localize to the cytoplasm (e.g., PIDD and PIGs), and the third group proteins that localize to the mitochondria (BAX, NOXA, PUMA) [299]. However, among all these genes none appears to be a principal mediator of the P53 apoptotic signal and further studies are necessary to clarify this problem.

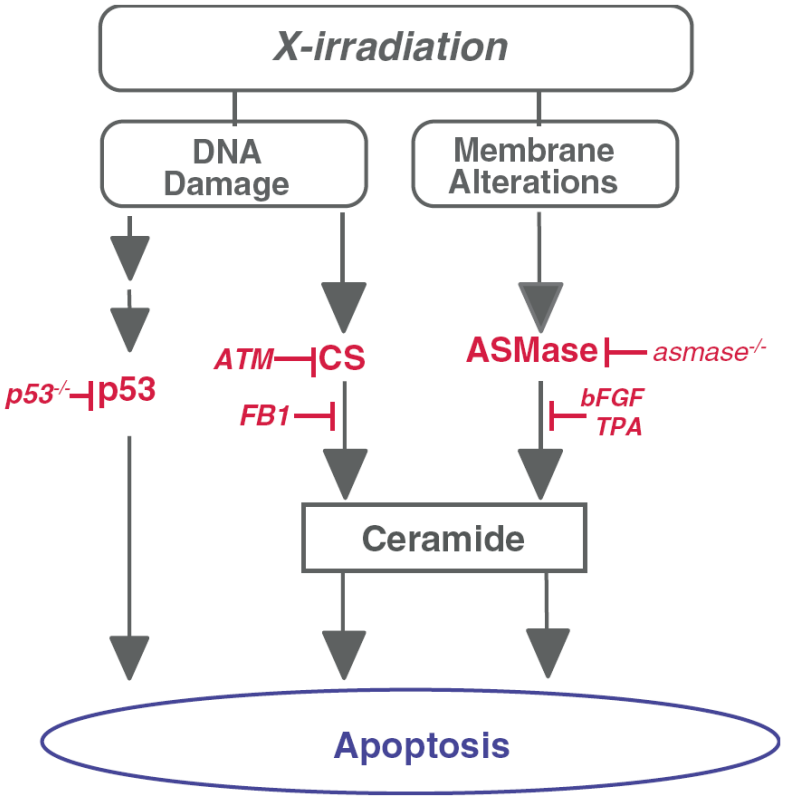

Fig. 1.14. Schematic representation of pathways of radiation-induced apoptosis (Adapted from [297])

The Ceramide–mediated pathway is believed to be the second possible mechanism of apoptosis induced by IR; radiation acts directly on the plasma membrane and activates acid sphingomyelinase (ASM) which generates ceramide by enzymatic hydrolysis of sphingomyelin. Ceramide then acts as a second messenger in initiating an apoptotic response via the mitochondrial system [300]. Additionally, radiation-induced DNA damage can also initiate a similar pathway by activation of mitochondrial ceramide synthase and *de novo* synthesis of ceramide. In some cells and tissues, BAX is activated downstream of ceramide, regulating commitment to the apoptotic process via release of mitochondrial cytochrome c. On the other hand, normal ceramide metabolism may produce metabolites, such as sphingosine 1-phosphate, which signal anti-apoptosis, thus controlling the intensity of the apoptotic response and constituting a mechanism for radiation sensitivity or resistance [297].

2. Work presented

Damage caused by IR in cells has been studied for many years due to its cytotoxic, mutagenic, and carcinogenic consequences. It seems likely that some or all of these effects can be attributed to damage to the genomic DNA which in eukaryotic cells exists as a complex and dynamic macromolecular structure, chromatin, in which the DNA is bound intimately to proteins. On one hand, this physical compaction of genomic DNA in chromatin protects DNA from damage and helps to overcome the problem of packing its ~2 m length into the ~500 μm^3 volume of the nucleus, but on the other hand it considerably complicates the detection and repair of damage. Although recently the induction and repair of different kinds of damage are becoming clearer at the molecular level, the precise mechanisms by which IR causes DNA breaks in chromatin and their nature remain elusive. A major focus of my research was therefore aimed towards understanding these important processes and developing a new model which will allow us to look more precisely into the nature of the induction and repair of strand breaks in chromatin *in vivo*. As the experimental system, I used the Epstein-Barr virus (EBV) minichromosome which contains a ~170 kb supercoiled closed circular DNA with a canonical nucleosomal structure [301] and nucleosome-free [302] and nuclear matrix attachment regions [303]. Its DNA has been entirely sequenced and functional features including promoters, replication origins, and transcription units have been mapped [292, 304]. Moreover, its length is in the same range as the topologically-closed loops which are believed to exist in genomic chromatin *in vivo* [305]. In the present context, the most crucial feature of this minichromosome is that the presence of ~50 copies in each cell nucleus allows the different topological forms of its DNA, and fragments which result from breakage by IR, to be detected and quantitated readily by hybridisation after separation of total cellular DNA by pulsed field gel electrophoresis (PFGE).

2.1 Objectives

My main objective was to obtain an overall and quantitative picture of the production and repair of DNA single- and double-strand breaks in the DNA of the EBV minichromosome in γ-irradiated cells. Knowledge of how IR-damaged sites are distributed and repaired in interphase chromosomes contributes not only to understanding biological effects of radiation, but may also provide useful information about the topography of chromosome territories within the nuclear space [306]. It is generally believed that the frequency of sites damaged by IR varies in different regions of the genome, and that single-strand breaks are more frequent in regions which are potentially or actively transcribed, for example the unexpressed beta-globin gene [307]. On the other hand, although the distribution of DSBs has been thought to be random [308], the observed profile of the lengths of double-stranded DNA fragments produced by IR does not correspond to the predictions of a scenario where breakage is completely random [34]. Additionally, recent studies based on formation of foci of γH2AX suggest that globally decondensed chromatin domains are much more susceptible to damage and more proficient in repair than condensed inactive domains [273, 309]. However, precise localisation and quantitation of radiation-induced strand breaks is not feasible by the commonly-used methods, and we describe experiments which allow these types of damage to be mapped and quantitated in a defined region of chromatin *in vivo* and their repair to be followed.

The particular aims of my research were:

1. to develop and characterize an experimental system to detect and quantify DNA double-strand breaks;
2. to localize and map DNA double-strand breaks and explore if there are any particular regions more sensitive to breakage by IR;
3. to explore the steps, mechanisms and enzymes which operate in the repair of radiation-induced DSBs.

3. DNA in a circular minichromosome linearised by restriction enzymes or other reagents is resistant to further cleavage: an influence of chromatin topology on the accessibility of DNA

Initially, the main objective of these studies was the formation of double-strand breaks in the DNA of a multicopy ~170 kb circular minichromosome in human cells exposed to γ-radiation. Hoverer, our initial observation that radiation causes only a single, randomly-located DSB in every minichromosome, which was clearly inconsistent with the theoretical expectation based on a Poisson distribution, led me to extend these studies to other DSB-inducing agents. Experiments using restriction enzymes, topoisomerase II inhibitors, and the radiomimetic agent; neocarzinostatin, which have different mechanisms of action and can potentially induce multiple DSBs, showed that the single cleavage caused by radiation is one example of a more general response of circular chromatin to formation of a DSB. Since this selective sensitivity was abolished after the minichromosomes were deproteinised, it is related to chromatin structure. The data suggest the existence of a novel mechanism in which a first DSB in the circular minichromosome DNA triggers a global change in its nucleosomal conformation which confers insensitivity to further breakage.

The results of these studies on DSB formation in DNA of the Epstein-Barr virus minichromosome are described in detail in Chapter 3. All the experimental work described in this manuscript was conceived and performed by myself, and I wrote the paper together with Dr. R. Hancock.

Nucleic Acids Research, accepted with revision

DNA in a circular minichromosome linearised by restriction enzymes or other reagents is resistant to further cleavage: an influence of chromatin topology on the accessibility of DNA

Sławomir Kumala[1], Yasmina Hadj-Sahraoui[1], Joanna Rzeszowska-Wolny[2] and Ronald Hancock[1,*]

[1] Laval University Cancer Research Centre, 9 rue MacMahon, Québec, QC G1R2J6, Canada

[2] Biosystems Group, Silesian University of Technology, Akademicka 16, Gliwice 44-100, Poland

* To whom correspondence should be addressed: Tel (1-418) 525-4444; FAX (1-418) 691-5439; e-mail ronald.hancock@crhdq.ulaval.ca

3.1 Abstract

The accessibility of DNA in chromatin is an essential factor in regulating its activities. We studied the accessibility of DNA in a ~170 kb circular minichromosome with a canonical nucleosomal structure to DNA-cleaving reagents with multiple potential cleavage sites, using pulsed-field gel electrophoresis and fibre-FISH on combed DNA molecules. Only one of several sites in the minichromosome DNA was accessible to restriction enzymes in permeabilised cells and only a single, essentially random site was accessible to neocarzinostatin, topoisomerase II poisons, and γ-radiation in growing cells; further sites were inaccessible in the linearised minichromosomes. Sequential exposure to combinations of these reagents also resulted in cleavage at a single site. Further sites became accessible when histone H1, ≥95% of histones H2A and H2B, and most nonhistone proteins were extracted. These observations, together with similar earlier findings on the accessibility of DNA in SV40 and bovine papilloma virus minichromosomes to probes, suggest that a global rearrangement of the three-dimensional packing of nucleosomes occurs when a circular minichromosome is linearised, and results in its DNA becoming inaccessible to probes. This influence of chromatin topology could have implications for the accessibility of DNA in loops of genomic chromatin.

3.2 Introduction

Understanding how the accessibility of DNA in chromatin is regulated is central to models of DNA transcription and replication and their control (1). Factors which influence accessibility in *vivo* include unrestrained superhelicity in DNA (2-5), nucleosomal structure (6-9), and compaction of chromatin (10), and have been studied using nucleases (4, 11-13), restriction enzymes (9, 14), methylases (15, 16), poisoned topoisomerase II (17-19), or chemical reagents (20-26) as probes. As a model system to explore these and other features of chromatin we are studying a minichromosome in human cells. This minichromosome, the Epstein-Barr virus (EBV) episome (27), contains a ~170 kb circular DNA (28) with a canonical nucleosomal structure (29, 30) and has characteristic features of genomic chromatin including a nucleosome-free region (31) and a putative nuclear matrix attachment region (32). Its length is in the range of those of the topologically-closed loops in genomic chromatin (2, 3, 33, 34).

The objective of the present study was to understand our unexpected observation that only full-length linear minichromosome DNA was produced when permeabilised cells were incubated with a restriction enzyme with multiple potential cutting sites, showing that accessibility of its DNA to the enzyme was limited to only a single site. Extending these experiments, we show here that several other reagents which potentially cause multiple strand breaks also cleave the minichromosome DNA at only one site. Somewhat similar observations, which may have the same mechanistic origin, have been reported in studies of SV40 (11) and bovine papilloma virus (15, 20) minichromosomes. These findings suggest the existence of a previously unidentified and novel mechanism by which the accessibility of DNA can be influenced by the topology of chromatin.

3.3 Materials and methods

3.3.1 Cells

Raji cells, which contain ~fifty copies of the EBV minichromosome (27), were maintained in exponential growth in RPMI-1640 medium with 2 mM L-glutamine and 10% heat-inactivated FBS. When indicated, the medium was supplemented for 18-24 h with BrdU (30 μM) (Sigma-Aldrich) to label DNA or with an [^{35}S] protein labelling mix (NEN; 4 MBq/litre). Growing cells at a density of ~5 x 10^5/ml were harvested for experiments.

3.3.2 Exposure of cells to DNA cleaving reagents

For incubation with a restriction enzyme, the nicking endonuclease Nb.BbvCI, or an exonuclease cells were washed in PBS, encapsulated in beads of 1% low melting-point (LMP) agarose (35), permeabilised in 10 mM Tris-HCl, 140 mM NaCl, 1 mM $MgCl_2$, pH 7.6 containing 0.5% v/v Triton X-100 (Sigma-Aldrich), and washed 3x 30 min in the same buffer without Triton X-100. Beads were equilibrated for 30 min on ice in the appropriate buffer, resuspended in fresh buffer, and the enzyme (New England Biolabs) was added followed by incubation as described in the Figure legends; control samples were incubated in buffer alone. To expose cells to neocarzinostatin or etoposide (Sigma-Aldrich), these reagents were dissolved in DMSO and added to growing cultures as detailed in the Figure legends; control cultures were incubated with DMSO alone at the same final concentration. The cells were washed 2x in PBS and embedded in blocks of 1% LMP agarose for PFGE by standard methods (~0.5-2 x 10^6 cells/block). For irradiation, cells in agarose blocks were immersed in growth medium in closed 2 ml microtubes on ice and irradiated with ^{60}Co γ

photons at 4.3 Gy/min in a Teratron (Atomic Energy of Canada) calibrated as described in (36); control samples were processed in parallel but not irradiated.

3.3.3 PFGE, probes, and in-gel hybridisation

Agarose beads or blocks were deproteinised in 1 ml of 0.2 M EDTA, 0.2% SDS, 1 mg/ml proteinase K (Invitrogen) for 48 h at ~18°C with rocking, and washed and stored in TE at 4°C. PFGE was in 1% agarose gels in 0.5X TBE at 14°C, using 190 v for 20 h with pulse time increasing linearly from 50 to 90 sec for most experiments, or alternatively conditions described in the Figure legends. For hybridisation gels were placed on 3MM paper, covered with Saran Wrap, and vacuum-dried at 60°C for 1 h. After incubation in 0.5 M NaOH, 1.5 M NaCl for 30 min, rinsing 3x in H_2O, neutralisation in 0.5 M Tris, pH 8.0, 1.5 M NaCl for 30 min, and rinsing with H_2O they were incubated in 6X SSC for 20 min, all at room temperature.

The hybridisation probe to detect minichromosome DNA was the DNA of EBV (GenBank AJ507799) isolated by PFGE in low melting-point (LMP) agarose from virus prepared from B95-8 cells stimulated by adding 12-O-tetradecanoyl-phorbol-13-acetate to the medium (37). Restriction fragments for probes were prepared by cutting this DNA with *Spe*I or *Swa*I (100 u/ml) for 18 h at 37°C or 25°C, respectively, and separating the fragments by PFGE in 1% LMP agarose using 190 V/cm for 7 h or 20 h and switch time ramped linearly from 0.4 to 6 s or from 0.3 to 3 s, respectively; fragments were extracted from gels and purified on Ultrafree spin columns (Millipore). Lanes containing length markers were hybridised with an appropriate specific probe. Probes were labeled with [α-

^{32}P]dCTP (111 TBq/mmol) using Megaprime kits (Amersham). Gels were prehybridised for 30 min and hybridised for 18 h in 6X SSC, 5X Denhardt's solution, 0.5% SDS, 0.5 μg/ml human Cot-1 DNA (Invitrogen) at 68°C, washed 3x 30 min in 0.1X SSC, 0.5% SDS at 68°C, sealed in Saran Wrap, and exposed to PhosphorImager screens. Signals were imaged, quantitated, and scanned using ImageQuant software (Molecular Dynamics).

3.3.4 Molecular combing and hybridisation of minichromosome DNA

DNA from cells grown with BrdU was separated by PFGE in LMP agarose and the region containing linear minichromosome DNA was excised. The agarose was incubated with YOYO-1 (5 μM) (Molecular Probes) for 30 min at room temperature, washed in TE, incubated in β-agarase buffer for 30 min on ice, melted in 50 mM MES, pH 5.7 at 65°C for 10 min, and solubilised by β-agarase (New England Biolabs) at 42°C for 4 h. The DNA was dissolved in the same buffer at 2 μg/ml and 4 μl was placed on a 3-aminopropyl-triethoxysilane-coated microscope slide (Sigma-Aldrich) and covered with a standard cover glass, which was pulled horizontally across the slide at a constant speed of ~300 μm/sec after 2 min. Slides were examined by fluorescence microscopy with a 60x objective (Nikon E800). For hybridisation, slides with well-spread DNA molecules were dried at room temperature for 5 min and then overnight at 60°C, incubated in 0.6X SSC, 70% formamide for 3 min at 95°C to denature DNA, and then in cold 70%, 85%, and 95% ethanol (2 min each). Hybridisation probes were an 8.1 kb BamHI-SalI fragment of cosmid cM301-99 and a 29 kb HindIII fragment from cosmid cMB-14 (38) (gifts from G. Bornkamm) excised from agarose gels, purified on a Microcon YM-100 (Qiagen), and labeled with biotin-11-

dUTP (Fermentas) by nick translation. Hybridisation was at 37°C in a humidified chamber for up to 48 h (39). The probes were detected with FITC-goat anti-biotin (Sigma-Aldrich) (1:50, 20 min) followed by Alexa 488-rabbit anti-goat antibody (Invitrogen) (1:50, 20 min), and DNA by subsequent incubation with rat anti-BrdU (Abcam) (1:30, 20 min) followed by Alexa 594-goat anti-rat antibody (Invitrogen) (1:50, 20 min). Antibody dilutions and washing were in PBS, 0.05% Tween-20 and slides were mounted in SlowFade Gold (Invitrogen). Minichromosome DNA molecules identified by hybridisation signals from both probes were imaged on a confocal microscope (Bio-Rad MRC1024). Images were aligned after minor adjustment to normalise the distance between the probes and lengths were calculated using the factor of 2.2 kb DNA/μm (39).

3.3.5 Extraction of proteins from chromatin

Cells encapsulated in beads of 1% LMP agarose and permeabilised as described above were washed 2x in 10 mM Tris-HCl, 140 mM NaCl, 1 mM $MgCl_2$, pH 7.6 containing protease inhibitor cocktail (Sigma-Aldrich; 1/200). Aliquots were incubated in the same buffer supplemented with NaCl at 0.14, 0.35, 0.6, 1.2, or 2 M for 1 h on ice with mild agitation, the buffer was replaced, and incubation was continued for 18 h at 4ºC. Beads were washed in cold PBS, mixed with 2X SDS-PAGE buffer, boiled for 5 min, and proteins were subjected to denaturing SDS-PAGE in a 12% gel together with size markers (Bio-Rad) and calf thymus histones (gift of W. T. Garrard). Gels were stained with Coomassie Blue.

3.4 Results

3.4.1 Minichromosome DNA and forms produced by cleavage.

The EBV minichromosome is formed by circularisation of the ~172 kb DNA of EBV through its cohesive termini (27). About fifty copies are present in the nuclei of Raji cells, and sites in its DNA which are accessible to nucleases or chemical probes can be detected and mapped by separating the topological forms and fragments of its DNA by pulsed field gel electrophoresis (PFGE) of total cell DNA and hybridisation with specific probes (in this paper the term site is used for simplicity, and does not imply a precise nucleotide position). For PFGE, total cell DNA was deproteinised at room temperature (~18°C) since certain types of DNA damage in irradiated cells are converted to extra double-strand breaks at temperatures >20°C (40) ; this procedure extracted >99% of the radioactivity precipitable by 10% TCA from cells containing ^{35}S-labelled proteins (data not shown). In-gel hybridisation was used because transfer of large DNA fragments by blotting is not quantitative (41, 42). The minichromosome DNA can also be detected readily by fibre-FISH and optical mapping (39) which we also used to map cleavage sites.

The supercoiled DNA of the minichromosome was detected readily by PFGE and hybridisation (Figure 3.1B, lane C), and the circular conformation of the DNA in this region was confirmed by its resistance to exonuclease III which digests duplex DNA from free 3'-OH termini (Figure 3.1B, lane Exo). In the gel shown in Figure 1B some hybridising material remained in or close to the sample well, as seen frequently in PFGE gels (for example 26, 43), but this was less evident (Figs. 3.2B, 7C) or was not seen (Figs. 3.2C, 3.3,

3.4, 3.8B) in other experiments and is believed to be due to overloading of gels (44). The linear form of minichromosome DNA was produced by incubating permeabilised cells with PacI, which has a single cutting site, and migrated with the same mobility as linear DNA from EBV (Figure 3.1B, lanes *Pac*I and Viral DNA); the linear conformation of minichromosome DNA from this region was confirmed by fibre-FISH (Figs. 3.2D, 3.5D). Because some of the reagents used here produce single- as well as double-strand breaks, we also identified the position of nicked circular minichromosome DNA. This form, produced by the nicking endonuclease Nb.BbvCI, migrated only a short distance from the sample well (Figure 3.1B, lane NbB), consistent with the slow migration of other nicked large circular DNAs in PFGE which is believed to be caused by impalement on agarose fibres (45, 46). Supporting evidence that nicked circular DNA migrate in this region was provided by molecular combing, which showed DNA molecules with the expected conformation (Figure 3.1C); these were not seen in gels of DNA from untreated cells, and they cannot be supercoiled DNA since this does not attach to slides in these conditions (data not shown; see also 47); further, they did not have the theta conformation characteristic of replicating minichromosome DNA (28).

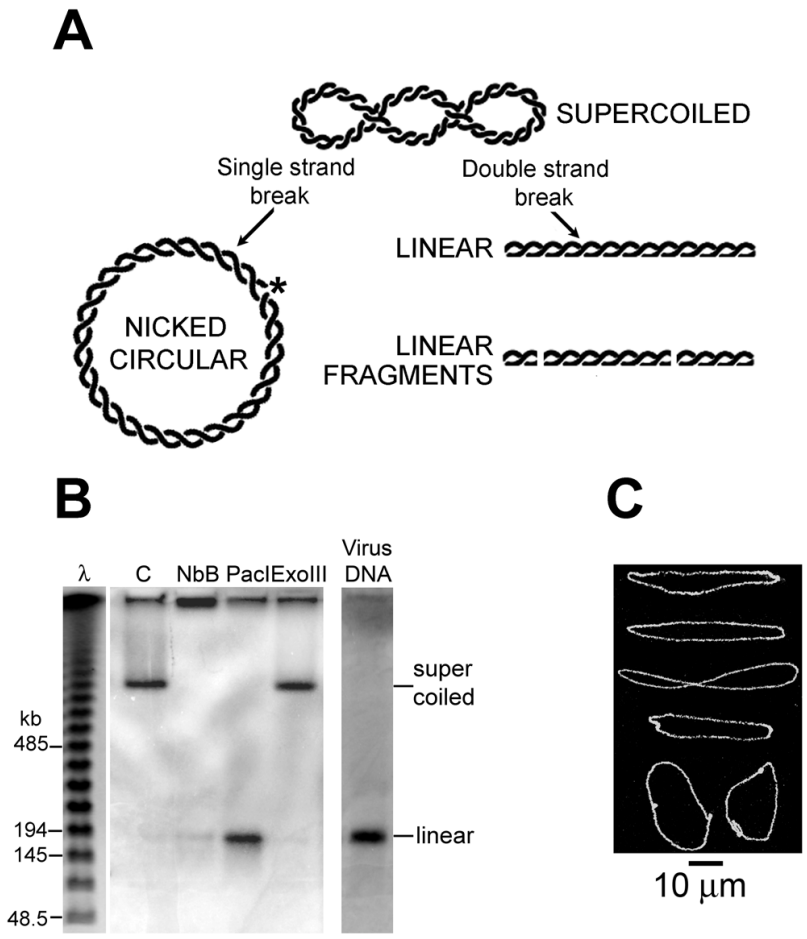

FIG. 3.1. A, forms of the minichromosome DNA considered in this study. **B**, migration of these forms in PFGE revealed by hybridising a PFGE gel of total cell DNA with a probe of EBV DNA. In this and the following images of gels the top is the position of the sample wells, each panel shows lanes from the same gel, and length markers were oligomers of λ DNA (48.5 kb) alone (λ) or together with HindIII fragments of λ DNA (M). Cells encapsulated in agarose beads and permeabilised were incubated with the appropriate enzyme and then deproteinised. Lanes show minichromosome DNA from cells incubated with: C, no addition (2 h); Exo, exonuclease III (400 u/ml, 18 h); *Pac*I (100 u/ml, 2 h) which cuts the minichromosome DNA at a single site; NbB, nicking endonuclease

Nb.BbvCI (100 u/ml, 1 h) which forms circular molecules containing single-strand breaks. Lane virus DNA: linear EBV DNA. **C**, Representative DNA molecules extracted from the hybridising region close to the gel origin (panel B, lane NbB), stained with YOYO-1 and spread by molecular combing. These are believed to be circular minichromosome DNA molecules which contain single-strand breaks (see text).

3.4.2 Restriction enzymes with multiple cutting sites produce only a single break in DNA in minichromosomes

Permeabilised cells were incubated with Spe1 or SwaI, which have seven and two cutting sites, respectively, in the minichromosome DNA (Figure 2A); these enzymes were used because they are not affected by common methylated sequences and some regions of the minichromosome DNA are highly methylated (48-50). Only full-length linear minichromosome DNA was produced (Figure 3.2B, C); further cutting was not limited by an insufficient amount of enzyme because a several-fold increase of enzyme concentration above that which linearised all of the minichromosome DNA did not result in more than one cut. The supercoiled minichromosome DNA remained intact in samples incubated in parallel without a restriction enzyme (Figure 3.2B lane C).

To distinguish if the minichromosome DNA was cut at only one particular site by these enzymes or at any one of their potential sites, we mapped the sites cut by SwaI whose fragments are fewer and therefore more easily identified. Minichromosome DNA linearised by incubating cells with SwaI was extracted from a PFGE gel and then digested with PacI, which has a single cutting site (Figure 3.2A); if SwaI had cut all the minichromosome DNA molecules at only one of its two sites, PacI would have produced a pair of fragments of

either 71.8 and 100.1 kb or 28.8 and 142.9 kb (Figure 3.2A). Instead, four fragments of ~140, 100, 72 and 28 kb were produced representing a mixture of these pairs (Figure 3.2C), showing that the initial single cut by SwaI had occured at either of its two sites in different minichromosomes.

This conclusion was confirmed by fibre-FISH and optical mapping of linear DNA combed on slides. Cells containing BrdU-labeled DNA were incubated with SwaI, linear minichromosome DNA was extracted from PFGE gels, combed, and the slides were hybridised with two EBV-specific probes labeled with biotin to identify minichromosome DNA molecules unambiguously and to orient their images. After immunolabelling all DNA with anti-BrdU antibodies, the length of these molecules was measured using the factor of 2.2 kb DNA/μm determined experimentally for combed linear minichromosome DNA (39). The length of the linear molecules is somewhat variable in this procedure (Figure 3.2D) due to variation of overall and local stretching during combing (39). The average length of the hybridising molecules was 167±10 kb (SEM from 100 molecules in 5 independent experiments), corresponding closely to the length of minichromosome DNA (~172 kb). The molecules fell into two classes; from a total of fifty which were imaged, twenty-eight had been cut by SwaI at the left site and twenty-two at the right site (Figure 3.2D), confirming that only one of the two SwaI sites was accessible to the enzyme in any particular minichromosome. As a control, DNA of minichromosomes cut by PacI had been cleaved at the expected position (Figure 3.2E).3

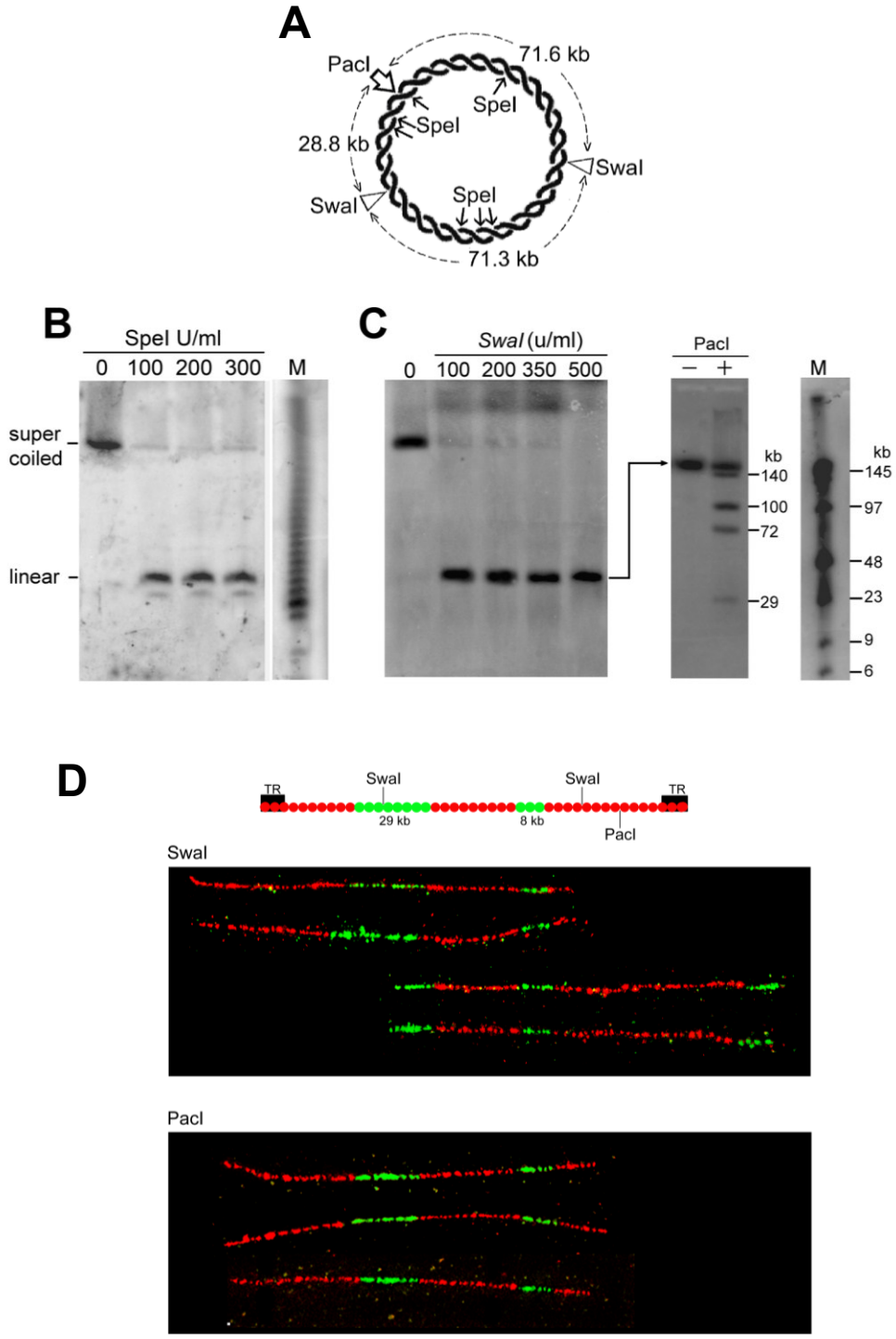

Fig. 3.2. DNA in minichromosomes is cut by SpeI or SwaI at only one of their potential cleavage sites. A, circular minichromosome DNA showing the cutting sites for

SpeI, SwaI, and PacI; the lengths of the SpeI fragments are not shown for clarity. **B**, minichromosome DNA from cells encapsulated in agarose beads, incubated with SpeI (100 u/ml, 3 h) which has seven potential cutting sites, and deproteinised. **C,** left panel, as B but incubated with SwaI (100 u/ml, 3 h) which has two potential cutting sites. Right panel, the position of SwaI cleavage mapped by gel hybridisation. Minichromosome DNA linearised by SwaI was isolated by PFGE in LMP agarose, cut by PacI (100 u/ml, 18 h), and the products were separated by PFGE. **D**, the position of SwaI cleavage mapped by fibre-FISH. The positions of the SwaI sites and of the two hybridisation probes (green) are shown on linear DNA; TR, terminal repeat sequences where EBV DNA is circularised in the minichromosome. Below are shown representative linear molecules from the two classes observed; these had been cut by SwaI at either the left (upper) or the right (lower) site on the map above. Linear molecules produced by cleavage at the single PacI site are shown for comparison below. Linear minichromosome DNA from BrdU-labelled cells was incubated with SwaI or PacI (200 u/ml, 2 h), extracted from a gel like that shown in C, combed, and hybridised with the two probes labeled with biotin. The probes were detected with anti-biotin antibodies (green) and DNA with anti-BrdU antibodies (red). The probe positions were aligned so that the extremities of the molecules indicate the site where they had been cut.

3.4.3 Neocarzinostatin and etoposide, reagents with multiple potential cutting sites, produce only a single break in DNA in minichromosomes

To explore if the inaccessibility of DNA in minichromosomes to restriction enzymes at all but one site was an example of a more general phenomenon, we examined the cleavage of this DNA when cells were incubated with neocarzinostatin (NCS) or etoposide, whose potential cleavage sites in DNA in chromatin are much more numerous. NCS is an enediyne chromophore bound to a small stabilising protein, and causes both single- and double-strand breaks in DNA *in vivo* and *in vitro* (22-26). The supercoiled form of minichromosome DNA was virtually eliminated after incubating cells with 300 μM NCS for 1 h (Figure 3.3A). The amount of linear DNA formed, quantitated by the hybridisation signal, was not significantly different from that formed by linearising the minichromosome DNA with *Pac*I (p= 0.94) (Figure 3.3C). The length of the linear molecules was 170±10 kb (n=5) measured by interpolation from adjacent markers in the same PFGE gel, consistent with cleavage at a single site. If NCS had caused breakage at all its preferred nucleotide sequences (22) a smear of smaller DNA fragments would have been produced.

Etoposide causes double-strand breaks in DNA by arresting the religation step of the reaction of topoisomerase II while it is covalently integrated into DNA, resulting in cleavage after deproteinisation, and is termed a topoisomerase II poison (17-20, 51). DNA in minichromosomes was linearised when cells were incubated with etoposide at the lowest concentration tested (50 μM) for 1 h (Figure 3.3C). After the maximum extent of cleavage (400 μM, 240 min) the amount of linear DNA formed was not significantly different from that when the minichromosome DNA was linearised with *Pac*I (p= 0.42) (Figure 3.3C).

NCS and etoposide thus cleaved DNA in all the minichromosomes only once, producing full-length linear DNA.

The position at which DNA was cleaved by these reagents was examined by cutting the linearised minichromosome DNA with *Swa*I; in both cases, a smear of fragments whose length extended down to ~10 kb was produced (Figure 3.3D) showing that the position of the initial cleavage varied in different minichromosomes.

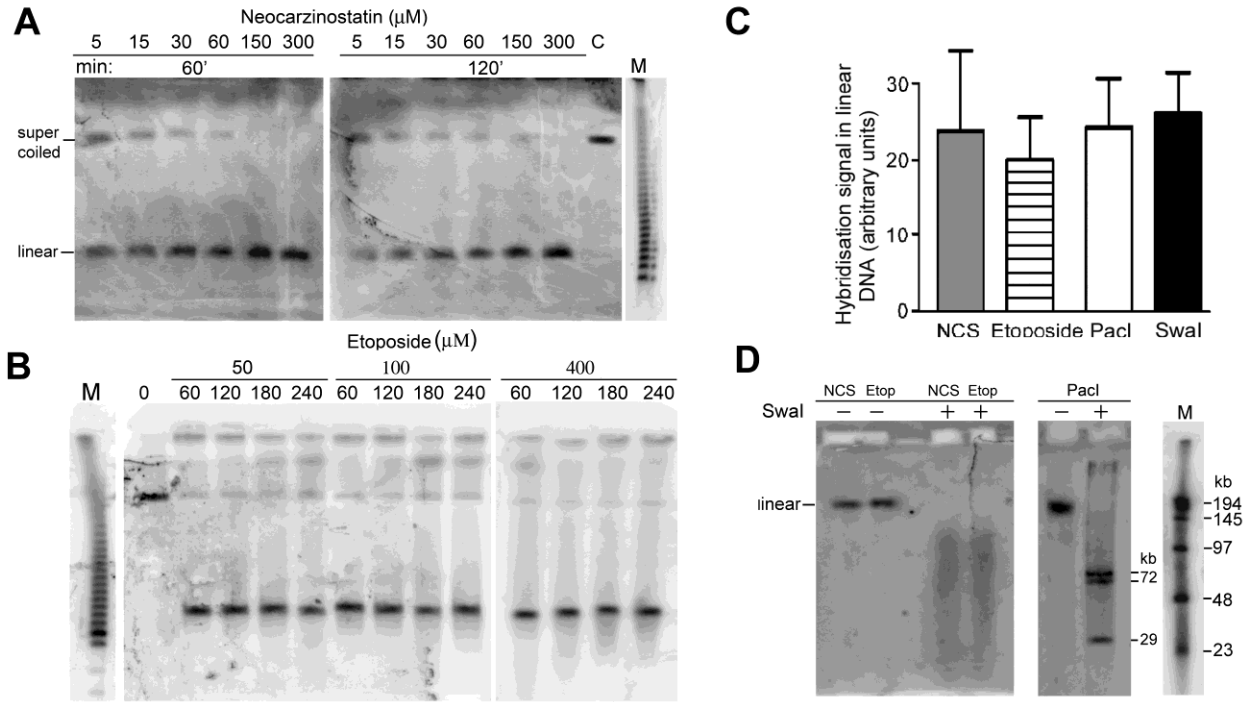

Fig. 3.3 DNA in minichromosomes is linearised by cleavage at a single site in cells incubated with neocarzinostatin (A) or etoposide (B), which have numerous potential cleavage sites. These reagents were dissolved in DMSO; lanes C show DNA from cells incubated with DMSO alone at the highest concentration used for 2 h. C, hybridisation signal from linear DNA after cleavage by neocarzinostatin (NCS) (300 nM, 120 min), etoposide (400 μM, 240 min), PacI (100 u/ml), or SwaI (100 u/ml); mean and SD from

three experiments. D, mapping the sites of cleavage by NCS, etoposide, or PacI. Cells were incubated with NCS (300 μM, 60 min), etoposide (Etop) (100 μM, 60 min), or PacI (100 u/ml, 3 h), linearised minichromosome DNA was separated by PFGE, digested with SwaI (100 u/ml, 18 h), and the products were separated by PFGE for 10 h with pulse time 10 to 70 sec. The smear of SwaI fragments from cells incubated with NCS or etoposide showed that the position of cleavage of minichromosome DNA by these reagents was not specific, while the three expected restriction fragments (Figure 3.2A) were produced from DNA which had been linearised by PacI.

3.4.4 DNA in minichromosomes is cleaved at a single site in γ-irradiated cells

As a further means to produce strand breaks in DNA *in vivo*, cells were exposed to γ-radiation which creates breaks mainly by producing OH radicals and other reactive oxygen species (52). The level of supercoiled minichromosome DNA decreased with increasing radiation dose, and it was undetectable after ≥100 Gy (Figure 3.4A). The length of the DNA formed was 170±10 kb (n=5) measured by interpolation from the λ markers, a value indistinguishable from that of full-length linear DNA. The linear conformation of this DNA was confirmed by its sensitivity to exonucleases (Figure 3.4B). No fragments shorter than full-length linear DNA were detected using PFGE conditions which separated fragments of length down to ~5 kb (Figure 3.4C), and the amount of linear DNA was not significantly different from that after cleavage at the single PacI site ($p = 0.45$) (Figure 3.4D). Together, these results show that the conversion of circular minichromosome DNA to the linear form was essentially quantitative.

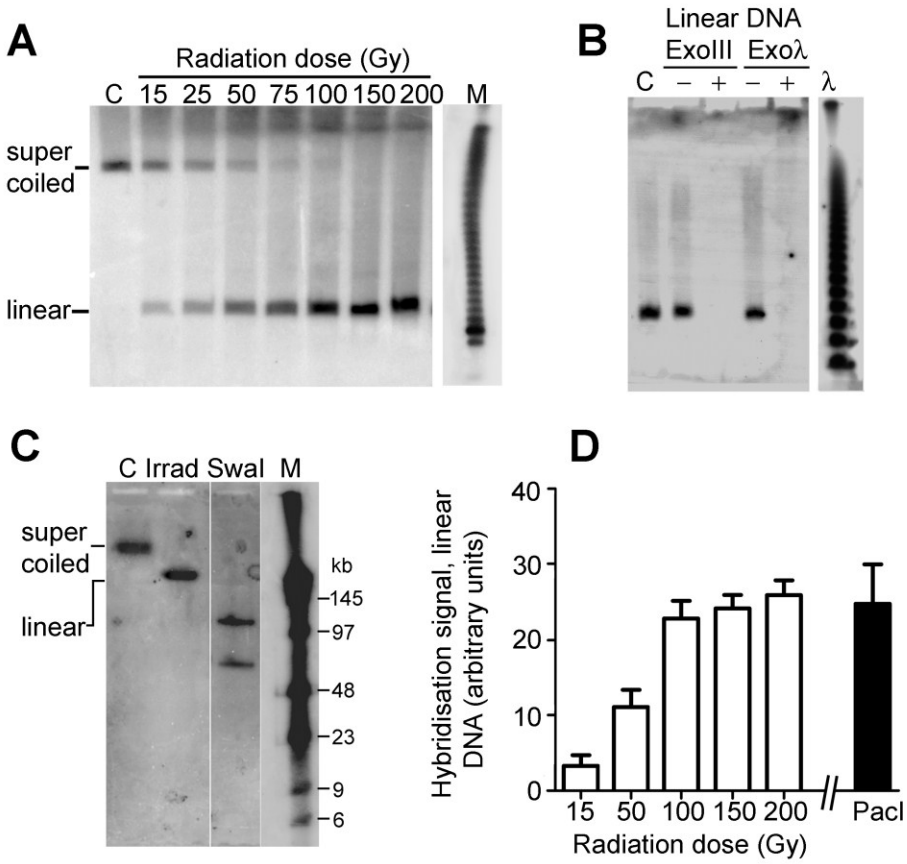

Fig. 3.4 Cleavage of DNA in minichromosomes at a single site in γ-irradiated cells. A, minichromosome DNA from cells irradiated with different radiation doses. **B**, complete digestion of minichromosome DNA from irradiated cells (100 Gy) by exonuclease III (ExoIII) or λ (Exo λ) (400 u/ml, 18 h) which digest duplex DNA containing free 3'-OH termini. **C** minichromosome DNA from irradiated cells (100 Gy) separated in PFGE conditions to detect fragments shorter than full length linear DNA. Lane C, unirradiated cells; lane SwaI, cells incubated with SwaI (100 u/ml, 18 h). **D**, comparison of the hybridisation signal from the linear DNA produced by irradiation with that produced by cleavage at the single PacI site (PacI 100 u/ml, 3 h); mean and SD from three experiments.

To map the sites of breakage of minichromosome DNA in irradiated cells, a procedure which was used to map cleavages in genomic DNA resulting from poisoning topoisomerase II was employed (18). DNA from control or irradiated cells was restricted and the fragments were separated by PFGE and hybridised with a probe which contained the same restriction fragments of linear EBV DNA. Breakage of minichromosome DNA at specific sites would cause truncation of the restriction fragments in which these sites occurred, and the site of cleavage could be deduced from their length. Two sets of overlapping probes were used to ensure that truncation sites close to fragment ends would not be overlooked (Figure 3.5A). In addition to the fragments predicted from the sequence of minichromosome DNA (53), some probes detected other less strong bands in DNA from both control and irradiated cells (Figure 3.5B); these may be caused by sequence polymorphisms in minichromosome DNA (54) and possibly, in the case of *Spe*I, by inhibition of cutting due to rare N^6-methyladenines (55), and they were not seen in restriction digests of the entire minichromosome DNA (Figure 3.2) because they represent only a minor fraction of the total DNA. For all the probes, the pattern of hybridising DNA fragments from irradiated cells was identical to that from unirradiated cells and no truncated fragments were detected (Figure 3.5B).

The random position of the single site of cleavage of minichromosome DNA in γ-irradiated cells was confirmed by fibre-FISH mapping, using the procedure and probes described in Figure 2. The two probes were in variable positions with respect to the extremities of the linear DNA molecules (Figure 3.5C), contrasting with their specific positions on molecules linearised by PacI (Figure 3.2D). The break was localised in any of the four quadrants in different minichromosome DNA molecules from irradiated cells (Figure 3.5D).

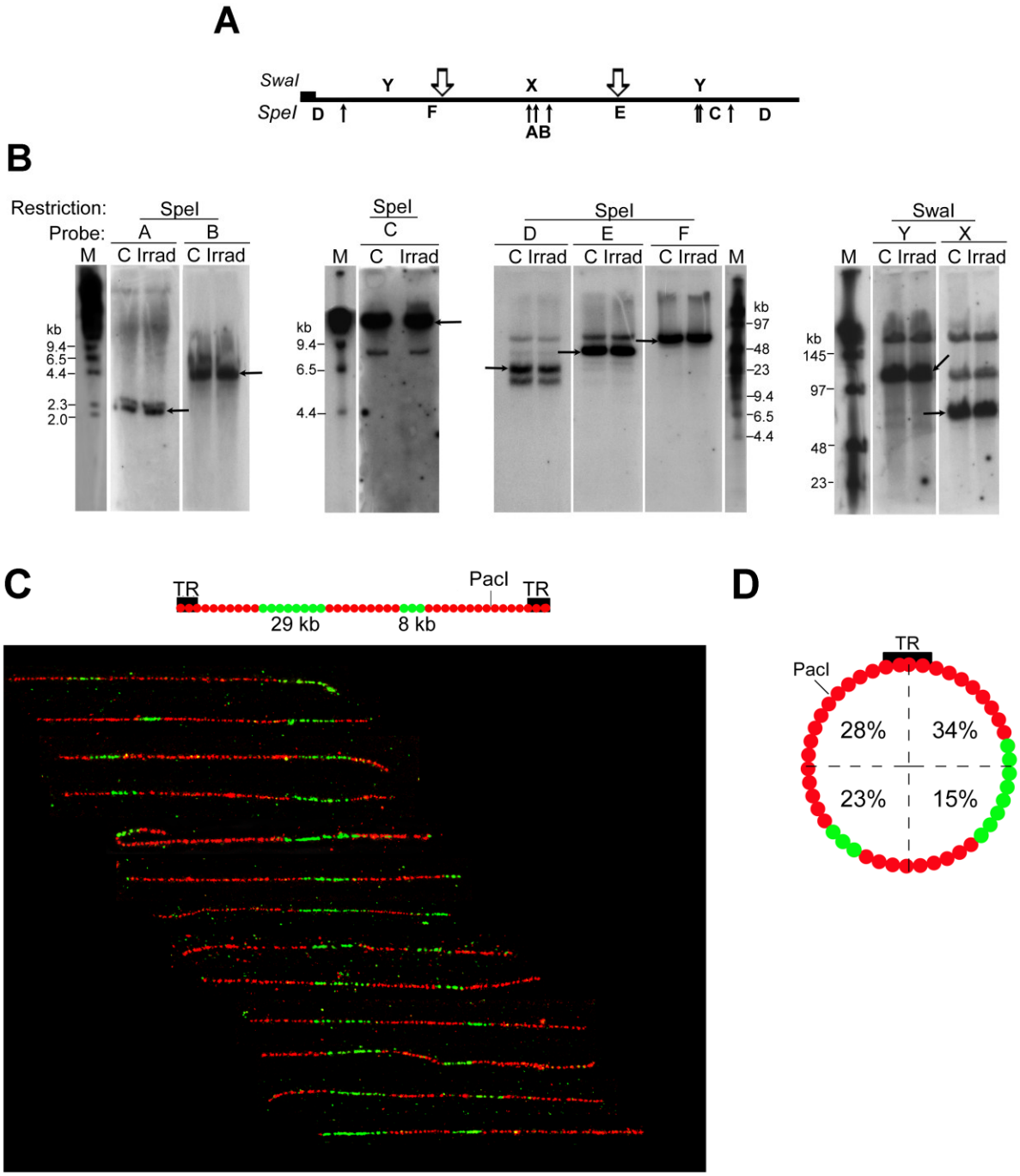

Fig. 3.5. Site of the single cleavage of minichromosome DNA in γ-irradiated cells. A, map showing the SpeI and SwaI restriction fragments of EBV used as probes for PFGE gels. **B**, hybridisation of these probes to DNA of control cells (C) or irradiated cells (100 Gy) (Irrad) restricted by the same enzyme. Arrows show the fragment predicted from the

sequence of minichromosome DNA in lanes where other hybridising fragments were seen whose origin is discussed in the text. Different PFGE conditions were used in each panel according to the length of the fragments to be detected. **C**, fibre-FISH: linear DNA showing the positions of the hybridisation probes and the PacI site, and representative signal arrays on linear DNA molecules from irradiated cells (100 Gy). The procedure was the same as that described in Figure 3.2; the probes are green and DNA is red. Molecules were aligned according to the probe positions so that their extremities represent the site of cleavage. **D**, distribution of the cleavage site in four equal sectors of minichromosome DNA from irradiated cells, shown as the % in each sector for fifty-five molecules measured.

3.4.5 Linearisation of DNA in minichromosomes confers resistance to further DNA cleavage by other reagents

To understand why only one site, which was not the same in all minichromosomes, was accessible to the reagents tested above we considered two possible mechanisms. In one model, all potential sites except one could be masked by nucleosomes or other proteins; this is perhaps plausible in the case of restriction enzymes whose sites may be masked when they are on the surface of nucleosomes (6-9, 14), but it appears improbable for NCS and for OH radicals formed by γ-radiation because these have many potential cleavage sites (24, 26, 56, 57). If this model was true, minichromosome DNA linearised by one agent could be still accessible at other positions to reagents with different cleavage sites. Alternatively, upon linearisation of the minichromosome a global rearrangement of its chromatin structure could occur which made DNA inaccessible to all the reagents; in this case, after linearisation by one reagent the DNA would not be cleaved further by any of them.

To distinguish between these scenarios, cells were exposed sequentially to two different conditions which caused DNA cleavage. For example, permeabilised cells were first incubated with SwaI to cut minichromosome DNA at one of its two potential sites (Figure 3.2) and then irradiated, which produces a single break at an approximately random site (Figure 3.5). Only linear DNA was produced (Figure 6B left panel, lane SwaI ⇒ Irrad, cells), showing that the circular minichromosome DNA had been cut at only one site. When this linear DNA was restricted by PacI, only the fragments characteristic of minichromosome DNA cleaved by SwaI were produced (also shown in Figure 3.2C), showing that after SwaI had cut at either of its two sites no further breaks had been made by radiation (Figure 3.6B right panel, lane PacI after SwaI ⇒ Irrad). Similarly, only linear DNA was produced when this sequence was reversed and cells were first irradiated and then incubated with SwaI, again showing that the circular DNA had been cut at only one site (Figure 3.6B left panel, lane Irrad ⇒ SwaI, cells). However, in this case restriction of the linearised DNA with PacI produced a smear of shorter fragments (Figure 3.6B right panel, lane PacI after Irrad ⇒ SwaI), confirming that the single break was located randomly and therefore must have been produced by the initial irradiation. In similar experiments, cells were incubated first with etoposide and then irradiated, which both result in a single break at an approximately random site when used alone (Figure 3.5) or this sequence was inversed. Only linear DNA minichromosome was produced in both cases, showing that the circular DNA had been cleaved at only only position (Figure 3.6D). Similarly, only linear DNA was produced after incubation with PacI followed by SwaI or the inverse sequence (Figure 3.6C) whereas three fragments would have been produced if these enzymes had access to all their potential sites.

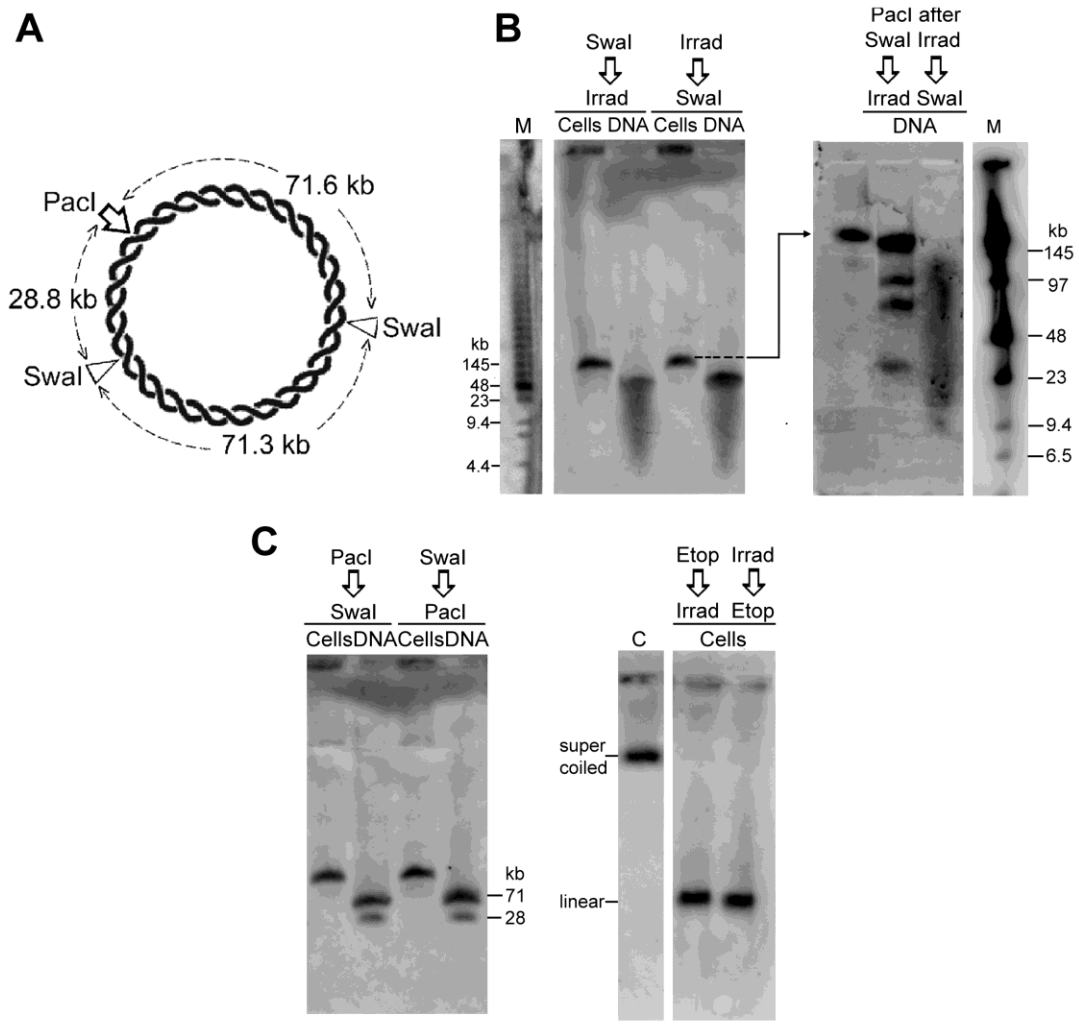

Fig. 3.6. Minichromosome DNA is cut at only a single site in cells exposed sequentially to two different cleavage reagents. A, circular minichromosome DNA showing the cutting sites for SwaI, and PacI. **B**, Left panel: cells (lanes cells) or deproteinised DNA (lanes DNA) were incubated with SwaI (100 u/ml, 2 h) and then irradiated (Irrad) or this sequence was reversed. Right panel: cleavage sites in the linearised DNA. Linear DNA was isolated and restricted with PacI; after the sequence SwaI ⇒ irradiation only the four predicted PacI fragments were produced (see also Figure 3.2C) showing that irradiation had produced no further breaks after the DNA had been linearised by SwaI. In contrast, a smear

of shorter fragments was seen after the sequence irradiation ⇒ SwaI, confirming that the single initial break caused by radiation had occurred at a random site. **C**, identical samples were incubated with PacI followed by SwaI (both 100 u/ml, 2 h) or this sequence was reversed. In deproteinised DNA either sequence resulted in fragments cut by both SwaI and PacI (the 71 kb band contains two fragments of similar length; see A). **D**, identical samples were incubated with etoposide (100 μM) (Etop) and then irradiated (200 Gy) (Irrad) which both cause a single break at a random position, or this sequence was reversed.

Quite different results were seen when deproteinised minichromosomes were exposed to the same conditions. After incubation with SwaI followed by irradiation, or the reverse sequence, a smear of fragments whose length extended down to at least ~6 kb was produced (Figure 3.6B, left panel lanes DNA). After incubation with SwaI, cutting by PacI showed that both of the potential SwaI sites had been cut (Figure 3.6C, lanes DNA) (note that the band at ~71 kb contains two fragments of very similar length, Figure 3.6A).

3.4.6 Proteins associated with inaccessibility of DNA in minichromosomes

The preceding experiments showed that DNA in minichromosomes was inaccessible for further cleavage after a single break had been produced by a restriction enzyme, NCS, etoposide, or radiation, but that further positions were accessible after it had been deproteinised (Figure 3.6B and C, compare lanes Cells and DNA). To identify the class of proteins responsible for this protection, permeabilised cells were extracted with solutions containing NaCl at different concentrations. Incubation with *Swa*I or irradiation after the

majority of non-histone proteins and histone H1 had been extracted by NaCl at concentrations up to 0.6 M (Figure 3.7A) still resulted in cleavage of minichromosome DNA at only a single position, producing linear DNA (Figure 3.7B, C). However, the DNA was cut by *Swa*I at both of its predicted sites to produce two fragments (Figure 7B) and was cleaved by radiation to produce a smear of fragments extending down to ~8 kb (Figure 3.7C, D) after histone H1, ≥95% of histones H2A and H2B, and most nonhistone proteins had been extracted with 1.2 M NaCl; we are aware that a minority (≤5%) of histones H2A and H2B may remain after this extraction and that H3-H4 tetramers which bear post-translational modifications could be bound more weakly and also extracted.

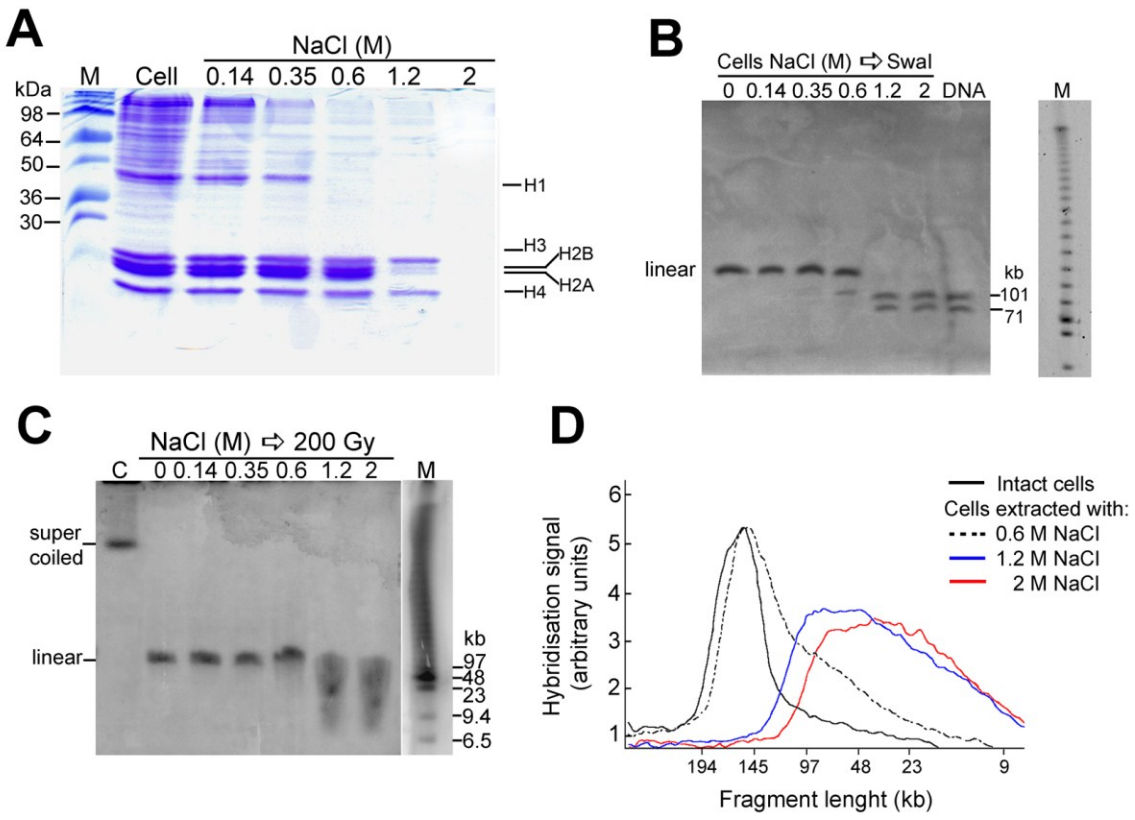

Fig. 3.7. Multiple sites in the DNA in minichromosomes can be cleaved by *Swa*I or γ-radiation after removing proteins. Agarose-encapsulated and permeabilised cells were

extracted with NaCl at the concentration shown, as described in Methods. **A**, proteins remaining in the cells, separated by denaturing SDS-PAGE; the positions of histones from calf thymus are shown. **B**, cutting of minichromosome DNA by SwaI (100 u/ml, 2 h) in cells extracted with NaCl or in deproteinised DNA (lane DNA). In unextracted cells (left lane) only one of the two SwaI sites was accessible producing linear DNA, but after extraction with NaCl at ≥1.2 M the two predicted restriction fragments (Figure 3.2A) were produced showing that both *Swa*I sites had become accessible. **C**, Cleavage of DNA in minichromosomes in irradiated cells (200 Gy) after extracting proteins; lane C, unirradiated cells. Linear DNA was produced in unextracted cells showing that only a single site was cleaved, while the smear of fragments after extraction with NaCl at ≥1.2 M shows that further sites had become accessible. **D**, lengths of the fragments of minichromosome DNA in irradiated cells without or after extraction with NaCl, calculated by scanning the signals in lanes in (**C**) and interpolation from the positions of the λ markers.

3.5 Discussion

These experiments are not the first in which DNA in a circular minichromosome has been observed to be accessible to probes at only one of several potential sites and to be inaccessible in the linear form. Restriction enzymes with multiple potential sites cut the circular ~5 kb DNA in purified SV40 minichromosomes predominantly at a single, but not unique, site and produce full-length linear molecules of which only ≤15% were cut further (11). The DNA-(cytosine-5)-methyltransferase HhaI could methylate the ~8 Kb circular DNA of bovine papilloma virus (BPV) minichromosomes in isolated cell nuclei, but DNA in linearised minichromosomes was not methylated in the same conditions (15), and in a chimeric variant of this minichromosome the DNA was cleaved to the full-length linear form in cells exposed to the topoisomerase II poison VM26 and shorter fragments were not observed (20).

In view of the variable position of the initial cut in different minichromosomes produced by NCS and γ -radiation, which do not have marked sequence preferences, it appears unlikely that this position can be related to particular features of the DNA sequence, for example the region which contains easily-unwound sequences (58) or the putative nuclear matrix attachment region (32) which lies in a region with a noncanonical nucleosomal structure (59) and contains preferred topoisomerase II cleavage sites (60), or the few regions which are transcribed in Raji cells (61). Cleavage of DNA in all the minichromosomes at only a single site was particularly unexpected in the case of ionising radiation, because in genomic DNA breaks caused by radiation are usually assumed to be distributed according to a Poisson distribution (for example 62-64). The quantitative

production of linear minichromosome DNA is clearly not consistent with this assumption, which predicts that random breakage would yield a maximum of only 38% (1/e) of the total molecules as full-length linear molecules (64).

Several hypotheses could be proposed to explain the acquisition of inaccessibility of minichromosome DNA to probes after it had been linearised by an initial cleavage. Rapid activation of a process involved in repair of strand breaks, for example phosphorylation of histone H2AX to form γ-H2AX (65), might influence nucleosomal structure in a manner which resulted in inaccessibility of DNA, but no formation of γ-H2AX was detected by immunofluorescence in permeabilised cells (data not shown). The strongest argument against a response of this type is that a similar loss of accessibility is seen when isolated circular SV40 minichromosomes (11) and BPV minichromosomes in isolated nuclei (15) are linearised.

The accessibility of only one of several potential sites for a restriction enzyme in a circular minichromosome could result from masking of the other sites by nucleosomes; restriction sites on the nucleosomal surface are less accessible than those in linker DNA, but can become available as transient fluctuations of nucleosome conformation occur (6-9, 14). Access of topoisomerase II to its preferred sites is also limited when they are on the surface of nucleosomes (17, 19). On the other hand, it is implausible that all the potential cleavage sites except one for neocarzinostatin (24, 26) and for OH radicals formed by γ-radiation (56, 57) could be inaccessible in view of their multiplicity and the accessibility of linker DNA to these reagents (68). This model could also be excluded experimentally, because minichromosome DNA linearised by one reagent was inaccessible to further cutting by other reagents with different cleavage sites.

Here we only monitored the conversion of circular to linear DNA, but by analogy

with the model proposed for SV40 minichromosomes (12) it could be argued that the event which results in inaccessibility of DNA is a single-strand and not a double-strand break, since NCS (26), γ-radiation (66), and possibly topoisomerase II poisons (67) cause breaks of both types; the weak signal in the region of nicked circular minichromosome DNA in cells exposed to NCS or radiation (Figures 3.3, 3.4) would be consistent with this model. Linear DNA could then be formed rapidly by a neighbouring single-strand break in the opposite DNA strand. When the DNA in isolated SV40 minichromosomes is relaxed by topoisomerase I, they become resistant to cleavage by micrococcal nuclease and nuclease S1 (12). It is not known if DNA in the minichromosome studied here contains unconstrained superhelicity, but this is plausible in view of the examples of SV40 (12) and BPV (15) minichromosomes; to explore this question, we incubated permeabilised cells with topoisomerase I before exposure to a DNA cleaving reagent but nicking by endogenous nucleases could not be supressed (data not shown).

In linear chromatin the three-dimensional packing of nucleosomes and the path of the polynucleosome chain have been studied extensively, and are influenced strongly by interactions between neighbouring nucleosomes (69-74); in circular chromatin the nucleosomal conformation is less well understoood, but experiments and modeling underline the influence of DNA superhelicity (75-78). Intuitively, it appears probable that the orientations and contacts of nucleosomes must differ in a circular (toroidal or plectonemic) and a linear polynucleosome chain. A distortion of nucleosome cores has been proposed to occur upon linearisation of a circular minichromosome whose DNA contains unrestrained superhelicity (76), accompanied by transfer of some linker DNA onto the nucleosome surface (11) which would reduce its accessibility. The increase which we observed in the accessibility of minichromosome DNA after removal of histones H2A

and H2B may be due to its partial dissociation from the remaining H3-H4 tetramers (79); in genomic chromatin, extraction of these histones results in a >10-fold increase of the frequency of double-strand breaks produced by γ-radiation (80).

Persuasive evidence suggests that chromatin forms topologically closed loops *in vivo* (2, 18, 33, 34, 81) which in at least some cases contain unrestrained supercoiling (2-5), and thus are formally analogous to a circular minichromosome. Whether the phenomenon studied here has implications for the accessibility of DNA in genomic chromatin is an interesting subject for further studies.

3.6 Acknowledgements

We are gratefull to L. Frappier for Raji cells, P. de Campos-Lima for B95-8 cells, G. Bornkamm for cosmids cM301-99 and cMB-14, W. T. Garrard for calf thymus histones, and J. St-Hilaire and N. Octave for advice and help with irradiation.

3.7 Funding

Supported partially by funds from the Medical Faculty and the Cancer Research Centre of Laval University. *Conflict of interest statement*. None declared.

3.7 References

1. Bell,O., Tiwari,V.K., Thomä,N.H. and Schübeler,D. (2011) Determinants and dynamics of genome accessibility. *Nat. Rev. Genet.*, **12**, 554-564.
2. Luchnik, A.N., Hisamutdinov,T.A. and Georgiev,G.P. (1988) Inhibition of

transcription in eukaryotic cells by X-irradiation: relation to the loss of topological constraint in closed DNA loops *Nucleic Acids Res.,* **16**, 5175-5190.

3. Rodi,C.P. and Sauerbier,W. (1989) Structure of Transcriptionally Active Chromatin: Radiological Evidence for Requirement of Torsionally Constrained DNA. *J. Cell Physiol.*, **141**, 346-352.
4. Villeponteau,B. and Martinson,H.G. (1987) Gamma Rays and Bleomycin Nick DNA and Reverse the DNase I Sensitivity of 3-Globin Gene Chromatin In Vivo. *Mol. Cell. Biol.*, **7**, 1917-1924.
5. Kramer,P.R. and Sinden,R.R. (1997) Measurement of Unrestrained Negative Supercoiling and Topological Domain Size in Living Human Cells. *Biochemistry*, **36**, 3151-3158
6. Morse,R.H. (1989) Nucleosomes inhibit both transcriptional initiation and elongation by RNA polymerase Ill in vitro. *EMBO J.*, **8**, 2343-2351.
7. Anderson, J.D., Thåström,A. and Widom,J. (2002) Spontaneous Access of Proteins to Buried Nucleosomal DNA Target Sites Occurs via a Mechanism That Is Distinct from Nucleosome Translocation. *Mol. Cell. Biol.*, **22**, 7147-7157.
8. Poirier,M.G., Bussiek,M., Langowski,J. and Widom,J. (2008) Spontaneous access to DNA target sites in folded chromatin fibers. *J. Mol. Biol.*, **379**, 772-786.
9. Prinsen,P. and Schiessel,H. (2010) Nucleosome stability and accessibility of its DNA to proteins. Biochimie, 92, 1722-1728.
10. van Steensel,B. (2011) Chromatin: constructing the big picture. (2011) *EMBO J .*, **30**, 1885-1895.
11. Liggins,G.L., English,M. and Goldstein,D.A. (1979) Structural Changes in Simian Virus 40 Chromatin as Probed by Restriction Endonucleases. *J. Virol.*, **31**, 718-732.

12. Barsoum,J, and Berg,P. (1985) Simian Virus 40 Minichromosomes Contain Torsionally Strained DNA Molecules. *Mol. Cell. Biol.*, **5**, 3048-3057.

13. Sundin,O.H, and Varshavsky,A. (1979) Staphylococcal nuclease makes a single non-random cut in the simian virus 40 viral minichromosome. *J. Mol. Biol.*, 132, 535-546.

14. Tims,H.S., Gurunathan,K., Levitus,M. and Widom,J. (2011) Dynamics of nucleosome invasion by DNA binding proteins. *J. Mol. Biol.*, **411**, 430-448.

15. Rösl,F. and Waldeck,W. (1991) Topological Properties of Bovine Papillomavirus Type 1 (BPV-1) DNA in Episomal Nucleoprotein Complexes: A Model System for Chromatin Organization in Higher Eukaryotes. *Mol. Carcinogen.*, **4**, 248-256.

16. Singh,J. and Klar,A.J. (1992) Active genes in budding yeast display enhanced in vivo accessibility to foreign DNA methylases: a novel in vivo probe for chromatin structure of yeast. *Genes Dev.*, **6**, 186-196.

17. Capranico,G., Jaxel,C., Roberge,M., Kohn,K.W. and Pommier,Y. (1990) Nucleosome positioning as a critical determinant for the DNA cleavage sites of mammalian DNA topoisomerase II in reconstituted simian virus 40 chromatin. *Nucleic Acids Res.,* **18**, 4553-4559.

18. Razin,S.V., Petrov,P. and Hancock,R. (1991) Precise localization of the β-globin gene cluster within one of the 20- to 300-kb DNA fragments released by cleavage of chicken chromosomal DNA at topoisomerase II sites in *vivo*: evidence that the fragments are DNA loops or domains. *Proc. Natl. Acad. Sci. USA.*, **88**, 8515-8519.

19. Udvardy,A. and Schedl,P. (1991) Chromatin Structure, Not DNA Sequence Specificity, Is the Primary Determinant of Topoisomerase II Sites of Action In *Vivo*. *Mol. Cell. Biol.*, 11, 4973-4984.

20. Cullinan,E.B. and Beerman,T.A. (1989) A Study of Drug-induced Topoisomerase II-

mediated DNA Lesions on Episomal Chromatin. *J. Biol. Chem.*, **264**, 16268-16275.

21. Komura,J. and Ono,T. (2003) Nucleosome Positioning in the Human c-FOS Promoter Analyzed by in *Vivo* Footprinting with Psoralen and Ionizing Radiation. *Biochemistry,* **42***,* 15084-15091.

22. D'Andrea,A.D. and Haseltine,W.A. (1978) Sequence specific cleavage of DNA by the antitumor antibiotics neocarzinos tatin and bleomycin. *Proc. Natl. Acad. Sci. USA*., **75**, 3608-3612,

23. Okamoto,A., Okabe,M. and Gomi,K. (1993) Analysis of DNA Fragmentation in Human Uterine Cervix Carcinoma HeLa S3 Cells Treated with Duocarmycins or Other Antitumor Reagents by Pulse Field Gel Electrophoresis. *Jpn. J. Cancer Res.*, **84**, 93-98.

24. Kuo,M.T. and Samy,T.S. (1978) Effects of neocarzinostatin on mammalian nuclei: release of nucleosomes. *Biochim. Biophys. Acta.*, **518**,186-190.

25. McHugh,M.M,, Woynarowski,J. and Beerman,T. (1982) Degradation of HeLa cell chromatin by neocarzinostatin and its chromophore. *Biochim. Biophys. Acta.*, **696**, 7-14.

26. Beerman,T.A., Mueller,G. and Grimmond,H. (1983) Effects of neocarzinostatin on chromatin in HeLa S3 nuclei. *Mol. Pharmacol.*, **23**, 493-499.

27. Sugden,B. and Leight,E.R. (2001) EBV's plasmid replicon: an enigma in cis and trans. *Curr. Top. Microbiol. Immunol.*, **258**, 3-11.

28. Gussander,E. and Adam,A. (1984) Electron microscopic evidence for replication of circular Epstein-Barr virus genomes in latently infected Raji cells. *J. Virol.*, **52**, 549-556.

29. Shaw,J.E., Levinger,L.F.C. and Carter,W. (1979) Nucleosomal structure of EB virus DNA in transformed cell lines. *J. Virol.*, **29**, 657-665.

30. Dyson,P.J. and Farrell, P.J. (1985) Chromatin structure of Epstein-Barr virus. *J. Gen. Virol.*, **66**, 1931-1940.

31. Sexton,J. and Pagano,J.S. (1989) Analysis of the EB virus origin of plasmid replication (oriP) reveals an area of nucleosome sparing that spans the 3' dyad. *J. Virol.*, **63**, 5505-5508.

32. Jankelevich,S., Kolman,J.L., Bodnar, J.W. and Miller,G. (1992) A nuclear matrix attachment region organizes the Epstein-Barr viral plasmid in Raji cells into a single DNA domain. *EMBO J.*, **11**, 1165-1176.

33. Benyajati,C. and Worcel,A. (1976) Isolation, characterization, and structure of the folded interphase genome of Drosophila melanogaster. *Cell*, **9**, 393-407.

34. Jackson,D.A., Dickinson,P. and Cook,P.R. (1990) The size of chromatin loops in HeLa cells *EMBO J.*. **9**, 567-571.

35. Jackson,D.A. and Cook,P.R. (1985) A general method for preparing chromatin containing intact DNA. *EMBO J.*, **4**, 913-918.

36. Almond,P.R., Biggs,P.J., Coursey,B.M., Hanson, W.F., Huq, M.S., Nath,R. and Rogers,D.W. (1999) AAPM's TG-51 protocol for clinical reference dosimetry of high-energy photon and electron beams. *Med. Phys.*, **26**, 1847-1870.

37. zur Hausen,H., Bornkamm,G.W., Schmidt,R. and Hecker,E. (1979) Tumor initiators and promoters in the induction of Epstein-Barr virus. *Proc. Natl. Acad. Sci. USA.*, **76**, 782-785.

38. Polack,A., Hartl,G., Zimber,U., Freese,U.K., Laux,G., Takaki,K., Hohn,B., Gissmann,L. and Bornkamm.G.W. (1984). A complete set of overlapping cosmid

clones of M-ABA virus derived from nasopharyngeal carcinoma and its similarity to other Epstein-Barr virus isolates. *Gene*, **27**, 279-288.

39. Norio,P. and Schildkraut,C.L. (2001) Visualization of DNA replication on individual Epstein-Barr virus episomes. *Science*, **294**, 2361-2364.

40. Stenerlöw,B., Karlsson,K.H., Cooper,B. and Rydberg,B. (2003) Measurement of prompt DNA double-strand breaks in mammalian cells without including heat-labile sites: results for cells deficient in nonhomologous end joining. *Radiat. Res.*, **159**, 502-510.

41. Wohl,T., Brecht,M., Lottspeich,F. and Ammer,H. (1995) The use of genomic DNA probes for in-gel hybridization. *Electrophoresis*, **16**, 739-741.

42. Leach,T.J. and Glaser,R. (1998) Quantitative hybridization to genomic DNA fractionated by pulsed-field gel electrophoresis. *Nucl. Acids Res.*, **26**, 4787-4789.

43. Little,R.D. and Schildkraut,C.L. (1995) Initiation of latent DNA replication in the Epstein-Barr virus genome can occur at sites other than the genetically defined origin. *Mol. Cell. Biol.*, **15**, 2893-2903.

44. Gurrieri,S., Smith,B. and Bustamente,C. (1999) Trapping of megabase-sized DNA molecules during agarose gel electrophoresis. *Proc. Natl. Acad. Sci. USA.*, **96**, 453-458.

45. Maleszka,R. (1993) Single-stranded regions in yeast mitochondrial DNA revealed by pulsed-field gel electrophoresis. *Appl. Theor. Electrophor.*, **3**, 259-263.

46. Beverley,S.M. (1989) Estimation of Circular DNA Size Using □-Irradiation and Pulsed-Field Gel Electrophoresis. *Anal. Biochem.*, **177**, 110-114.

47. Allemand,J,F., Bensimon,D., Jullien,L., Bensimon,A. and Croquette,V. (1997) pH-dependent specific binding and combing of DNA. *Biophys. J.*, **73**, 2064–2070.

48. Bhende,P.M,, Seaman,W.T., Delecluse,H.J. and Kenney,S.C. (2005) BZLF1 activation of the methylated form of the BRLF1 immediate-early promoter is regulated by BZLF1 residue 186. *J. Virol.*, **79**, 7338–7348.

49. Ernberg,I., Falk,K., Minarovits,J., Busson,P., Tursz,T., Masucci,M.G. and Klein,G. (1989) The role of methylation in the phenotype-dependent modulation of Epstein-Barr nuclear antigen 2 and latent membrane protein genes in cells latently infected with Epstein-Barr virus. *J. Gen. Virol.*, **70**, 2989–3002.

50. Minarovits,J., Minarovits-Kormuta,S., Ehlin-Henriksson,B., Falk,K., Klein,G. and Ernberg,I. (1991) Host cell phenotype-dependent methylation patterns of Epstein-Barr virus DNA. *J. Gen. Virol.*, **72**, 1591-1599.

51. D'Arpa,P. and Liu,L.F. (1989) Topoisomerase-targeting antitumor drugs. *Biochim. Biophys. Acta*, **989**, 163-177.

52. Halliwell,B. and Gutteridge,J.M. (1999) Free radicals in biology and medecine, Oxford University Press, Oxford.

53. de Jesus,O., Smith,P.R., Spender,L., Karstegl,C.E., Niller,H.H., Huang,D. and Farrell,P.J. (2003) Updated Epstein-Barr virus DNA sequence and analysis of a promoter for the BART (CST, BARF0) RNAs of Epstein-Barr virus. *J. Gen. Virol.*, **84**, 1443-1450.

54. Fruscalzo,A., Marsili,G., Busiello,V., Bertolini,L. and Frezza, D. (2001) DNA sequence heterogeneity within the Epstein–Barr virus family of repeats in the latent origin of replication, *Gene*, **265**, 165-173.

55. Hofer,B. (1988) The sensitivity of DNA cleavage by *Spe*I and *Apa*LI to methylation by M.EcoK. *Nucleic Acids Res.*, **16**, 5206.

56. Spotheim-Maurizot,M. and Charlier,M. (1997) Sequencing Gel Electrophoresis: A Tool for Studying Radiation Damage to DNA. *Radiat, Res*., **48**, 501-502.

57. Ward,J.F. (1988) DNA damage produced by ionizing radiation in mammalian cells: identities, mechanisms of formation, and reparability. *Prog. Nucleic Acid Res. Mol. Biol.,* **35**, 95-125.

58. Williams,D.L. and Kowalski,D. (1993) Easily unwound DNA sequences and hairpin structures in the EB virus origin of plasmid replication. *J. Virol*.. **67**, 2707-2715.

59. Wensing,B., Stuhler.A., Jenkins,P., Hollyoake,M., Karstegl,C.E. and Farrell,J. (2001) Variant Chromatin Structure of the oriP Region of Epstein-Barr Virus and Regulation of EBER1 Expression by Upstream Sequences and oriP. *J. Virol*., **75**, 6235-6241.

60. Mearini,G., Chichiarelli,S., Zampieri,M., Masciarelli,S., D'Erme,M., Ferraro,A. and Mattia,E. (2003) Interaction of EBV latent origin of replication with the nuclear matrix: identification of S/MAR sequences and protein components. *FEBS Lett.*, **547**, 119-124.

61. King,W., Van Santen,V. and Kieff,E. (1981) Epstein-Barr virus RNA. VI. Viral RNA in restringently and abortively infected Raji cells. *J. Virol.*, **38**, 649-360.

62. Sachs,R.K., Chen,P.L., Hahnfeldt,P.J. and Hlatky,L.R. (1992) DNA damage caused by ionizing radiation. *Math. Biosci.*, **112**, 271-303.

63. Löbrich,M., Ikpeme,S. and Kiefer,J. (1994) Measurement of DNA double-strand breaks in mammalian cells by pulsed-field gel electrophoresis: a new approach using rarely cutting restriction enzymes. *Radiat Res.*, **138**, 186-192.

64. Cedervall,B. and Radivoyevitch,T. (1996) Methods for analysis of DNA fragment distributions on pulsed field gel electrophoretic gels. *Electrophoresis*, **17**, 1080-1086.

65. Rogakou,E.P., Pilch,D.R., Orr, A.H. Ivanova, V.S. and Bonner,W.M. (1998) DNA

double-stranded breaks induce histone H2AX phosphorylation on serine 139. *J. Biol. Chem.*, **273**, 5858–5868.

66. Sharma,K.K., Milligan.J,R. and Bernhard.W,A. (2008) Multiplicity of DNA single-strand breaks produced in pUC18 exposed to the direct effects of ionizing radiation. *Radiat. Res.*, **170**, 156-162.

67. Muslimovic,A., Nyström,S., Gao,Y. and Hammarsten,O. (2009) Numerical analysis of etoposide induced DNA breaks. *PLoS One*, **4**, e5859.

68. Barone,F., Belli,M., Rongoni,E., Sapora,O. and Tabocchini,M. A. (1986) X-ray induced DNA double-strand breaks in polynucleosomes. In Bums,F.J., Upton,A.C., and Silini,G. (eds.), *Radiation Carcinogenesis and DNA Alterations*. Plenum, New York, pp. 293-296.

69. Engelhardt,M. (2007) Choreography for nucleosomes: the conformational freedom of the nucleosomal filament and its limitations. *Nucleic Acids Res.*, **35**, e106. Epub Aug 17.

70. Kepper,N., Foethke,D., Stehr,R., Wedemann,G. and Rippe,K. (2008) Nucleosome Geometry and Internucleosomal Interactions Control the Chromatin Fiber Conformation. *Biophys. J.*, **95**, 3692–3705.

71. Cinacchi,G., La Penna,G. and Perico,A. (2007) Anisotropic Internucleosome Interactions and Geometrical Constraints in the Organization of Chromatin. *Macromolecules*, **40**, 9603-9613.

72. Garner,M.M., Felsenfeld,G., O'Dea,M.H. and Gellert,M. (1987) Effects of DNA supercoiling on the topological properties of nucleosomes. *Proc. Natl. Acad. Sci. USA.,* **84**, 2620-2623,

73. Depken,M. and Schiessel,H. (2009) Nucleosome Shape Dictates Chromatin Fiber

Structure. *Biophys. J.*, **96**, 777–784.

74. Koslover,E.F., Fuller,C.J., Straight.A.F. and Spakowitz,A.J. (2010) Local Geometry and Elasticity in Compact Chromatin Structure. *Biophys. J.*, **99**, 3941-3950.

75. Thoma,F. and Zatchej,M. (1988) Chromatin Folding Modulates Nucleosome Positioning in Yeast Minichromosomes. *Cell*, **55**, 945-953.

76. White,J.H., Gallo,R. and Bauer,W.R. (1989) Dependence of the linking deficiency of supercoiled minichromosomes upon nucleosome distortion. *Nucleic Acids Res.*, **17**, 5827-5835.

77. Sivolob,A., Lavelle,C. and Prunell,A. (2009) Flexibility of nucleosomes on topologically constrained DNA. In Benham,C.J., Harvey,S. and Olson,W.K. (eds.), *Mathematics of DNA Structure, Function and Interactions*. Springer, New York, pp. 251-292.

78. Martino, J.A., Katritch,V. and Olson,W.K. (1999) Influence of nucleosome structure on the three-dimensional folding of idealized minichromosomes. *Structure*, **7**, 1009-1022.

79. Burlingame,R.W., Love,W.E., Wang,B.C., Hamlin,R., Xuong,N-H., and Moudrianakis,E.N. (1985) Crystallographic structure of the octameric histone core of the nucleosome at a resolution of 3.3 Å. *Science,* **228**, 546-553,

80. Elia,M.C. and Bradley,M.O. (1992) Influence of Chromatin Structure on the Induction of DNA Double-strand Breaks by Ionizing Radiation. *Cancer Res.*, **52**, 1580-1586.

81. Balbi,C., Sanna,P., Barboro,P., Alberti,I., Barbesino,M. and Patrone,E. (1999) Chromatin Condensation Is Confined to the Loop and Involves an All-or-None Structural Change. *Biophys J.*, **7**, 2725-2735.

4. Kinetics, pathways, and modeling of repair of DNA strand breaks in chromatin *in vivo*: lessons from a minichromosome

This work presents quantitative studies of the repair of single- and double-strand breaks produced in the minichromosome by IR and the consequences of inhibiting enzymes involved in their repair. We observed that after two hours of incubation of cells in which the minichromosome DNA had been linearized by irradiation, it was covalently reclosed without any detectable intermediate products, implying that the majority of the radiation-induced single- and double- strand breaks were repaired. The recircularization process was completely arrested by inhibitors of the catalytic subunit of DNA-dependent protein kinase (DNA-PKcs) but was only partially inhibited in cells incubated with inhibitors of the enzymes ataxia telangiectasia-mutated (ATM) or Mre11, or depleted in the protein Rad51. Moreover, overall repair was not detectably slowed by inhibitors of poly(ADP-ribose) polymerase (PARP) or by catalytic inhibitors of topoisomerases I and II. A mathematical model fitting the data provided rate constants for the repair of SSBs and DSBs, and revealed that repair of SSBs was the rate-limiting step in the overall repair of minichromosome DNA. We propose that repair of the minichromosome may offer analogies with repair in loops of genomic chromatin, which are of similar length and also topologically constrained.

The results of these studies are described in detail in Chapter 4. I planned all this work together with Dr. R. Hancock, based on preliminary work in our laboratory by D. Jayaraju, and I carried out essentially all these experiments. K. Fujarewicz contributed the mathematical modeling.

Repair of DNA strand breaks in a minichromosome in vivo: kinetics, modeling, and effects of inhibitors

Slawomir Kumala[a]. Krzysztof Fujarewicz[b], Dheekollu Jayaraju[a], Joanna Rzeszowska-Wolny[c], Ronald Hancock[a,*]

[a] Laval University Cancer Research Centre, Hôtel-Dieu Hospital, Québec, QC, Canada
[b] Bioinformatics Group, Institute of Automatic Control, Silesian University of Technology, Gliwice, Poland
[c] Biosystems Group, Institute of Automatic Control, Silesian University of Technology, Gliwice, Poland[3]

**Corresponding author at: Laval University Cancer Research Centre, Hôtel-Dieu Hospital, Québec, QC G1R2J6, Canada. Tel.: 1 418 525 4444; fax: 1 418 691 5439.*
E-mail address*: ronald.hancock@crhdq.ulaval.ca*

Running title: DNA repair in a minichromosome

Keywords:
DNA repair, minichromosome, topoisomerases, mathematical modeling

4.1 Abstract

To obtain an overall picture of the repair of DNA single and double strand breaks (SSBs and DSBs) in a defined region of chromatin *in vivo,* we studied their repair in a ~170 kb circular minichromosome whose length and topology are analogous to those of the closed loops in genomic chromatin. The rates of repair of SSBs after irradiating cells with γ photons were measured quantitatively by determining the sensitivity of the minichromosome DNA to nuclease S1, and of DSBs by assaying the reformation of supercoiled DNA by pulsed field electrophoresis. Reformation of supercoiled DNA, which requires that all SSBs have been repaired, was not slowed detectably by the inhibitors of poly(ADP-ribose) polymerase-1 NU1025 or 1,5-IQD. Repair of DSBs was slowed by 25-30% when homologous recombination was supressed by KU55933, caffeine, or siRNA-mediated depletion of Rad51, but was completely arrested by the inhibitors of nonhomologous end-joining wortmannin or NU7441, interpreted as reflecting competition between these DSB repair pathways similar to that seen in genomic DNA. The rate of reformation of supercoiled DNA was unaffected when topoisomerases I or II, whose participation in repair of SBs has been controversial, were inhibited by the catalytic inhibitors ICRF-193 or F11782. Modeling of the kinetics of repair provided rate constants and showed that repair of SSBs in minichromosome DNA proceeded independently of repair of DSBs. The simplicity of quantitating SBs in this minichromosome provides a usefull system for testing the efficiency of new inhibitors of repair of SBs, and since the sequence and structural features of its DNA and its transcription pattern have been studied extensively it offers a good model for examining other aspects of DNA breakage and repair.

4.2 Introduction

The molecular events which are implicated in repair of strand breaks (SBs) in DNA are becoming more clear [reviewed in 1-6], but an overall and quantitative picture of their repair *in vivo* is not yet available and would contribute to understanding the systems biology of repair and the effects of inhibitors. The repair of single strand breaks (SSBs) and double strand breaks (DSBs) cannot be quantitated simultaneously and precisely using current methodologies. Repair of DSBs, believed to be the crucial lesions leading to cell death [7], is commonly assayed by the restoration of the normal length of genomic DNA or of restriction fragments using pulsed-field gel electrophoresis (PFGE) [8-10], but repair of SSBs is not detected by this approach. Repair of SSBs, which may contribute to loss of viability by relaxing superhelical stress in genomic DNA loops and thus arresting transcription [11], cannot yet be quantitated specifically by methods with comparable precision.

As a model system to approach this question, we have studied the repair of SBs *in vivo* in a ~170 kb circular minichromosome. Two features of this minichromosome, the Epstein-Barr virus (EBV) episome which is maintained in the nuclei of Raji cells at 50-100 copies and localised at the periphery of interphase chromosomes [12-17], make it an attractive model for genomic chromatin: it can be considered as a defined region of chromatin in view of its canonical nucleosomal conformation [13] and the well-studied sequence and properties of its DNA, and its closed circular topology and length resemble those of the constrained loops which genomic chromatin forms *in vivo* [11,18-19]. We assayed the repair of SSBs in the minichromosome after irradiating cells with ^{60}Co photons by quantitating the loss of nuclease S1-sensitive sites, and the repair of DSBs by PFGE assays of the reformation of supercoiled DNA from molecules which had been linearised by a DSB. Circular molecules which contained SSBs could not be quantitated experimentally, and their levels were calculated using a mathematical model developed to fit the experimental data. We exploited the possibility of quantitating SB repair in this system to examine the implication of particular enzymes in repair of the minichromosome DNA, particularly topoisomerases I and II whose participation in repair has long been

controversial [20-24], poly(ADP-ribose) polymerase-1 (PARP-1) [25-32], Rad51 [33], the catalytic subunit of DNA-protein kinase (DNA-PKcs) [2-6,34], and ataxia telangiectasia mutated (ATM) kinase [2-6,35,36]. New features of the repair of SBs *in vivo* and of their kinetics were revealed by mathematical modeling.

4.3 Materials and methods

4.3.1 Cells, irradiation, and incubation for DNA repair

Raji cells were grown in RPMI-1640 with 2 mM L-glutamine and 10% heat-inactivated FBS. Growing cells (0.5-1 x 10^6) were washed in PBS, embedded in blocks of 1% low melting-point (LMP) agarose for PFGE, immersed in cold growth medium in closed 2 ml microtubes, and irradiated with ^{60}Co γ photons (Teratron) at 4.3 Gy/min on ice. To follow DNA repair, blocks were transferred immediately into microplate wells containing medium at 37°C and placed in a CO_2 incubator. Cells were encapsulated in beads of 1% LMP agarose [19] for incubation with restriction enzymes or the nicking endonuclease Nb.BbvCI (New England Biolabs) and then permeabilised in 10 mM Tris-HCl, 140 mM NaCl, 1 mM $MgCl_2$, pH 7.6, 0.5% v/v Triton X-100 (Sigma-Aldrich) and washed 3x 30 min in this buffer without Triton X-100.

4.3.2 Depletion of Rad51

Fifty µl of a preincubated mixture of 100 pmol siRNA for Rad51 (siGenome SMART pool, Dharmacon) and 0.8 µl Oligofectamine (Invitrogen) were added to wells of a 96-well dish containing ~2x10^5 cells in 50 µl serum- and antibiotic-free RPMI medium, followed by incubation overnight at 37°C. Transfection efficiency assayed in parallel using a fluorescein-labeled nonsilencing siRNA (Cell Signalling) was >85%. The cells were irradiated after 48 h and incubated for repair. Rad51 protein was quantitated by lysing cells in SDS/PAGE sample buffer, subjection to SDS/PAGE, and transfer to a nitrocellulose

membrane which was probed with anti-Rad51 antibody (H-92, Santa Crus) and with anti-actin (C2) (Jackson ImmunoResearch) as loading control.

4.3.3 Inhibition of enzymes involved in repair

Wortmannin and caffeine (Sigma-Aldrich), NU1025 and 1,5-IQD (Calbiochem), NU7441, KU55933, and Mirin (Tocris) were dissolved in DMSO. ICRF-193 (gift of J. Nitiss) and F11782 (gift of J-M. Barret) were dissolved in DMSO and H_2O, repectively. Inhibitors were present in the medium from 2 h before and during irradiation and were added freshly immediately after irradiation. Inhibition of topoisomerase II was assayed 1 h before incubation for repair by quantitating covalent enzyme-DNA reaction intermediates using a filter-binding assay [37] in lysates of cells grown for 48 h with [*methyl*-^{3}H]thymidine (37 kBq/ml). Inhibition of phosphorylation of DNA-PKcs or ATM was assayed by immunofluorescence using cells cytospun onto polylysine-coated slides, fixed in 4% formaldehyde in PBS for 15 min, permeabilised in PBS, 1% Triton X-100 (PBST) for 15 min, and incubated in blocking solution (Boehringer) for 1 h. Primary antibodies were mouse mAbs recognising DNA-PKcs phosphorylated on threonine-2609 (Abcam, 1:200) or ATM phosphorylated on serine-1981(Cell Signaling, 1:200), followed by Alexa 488-goat anti-mouse (1:400); DNA was labeled with DRAQ5 (20 □m, 10 min) (Invitrogen). Poly(ADP-ribose) (PAR) formation was assayed using a rabbit polyclonal antibody (Alexis) (1:50, overnight, 4°C) followed by Alexa 594-goat anti-rabbit IgG (1:200, 30 min, 37°C); DNA was stained with YOYO-1 (1 μM, 10 min). Antibody dilutions and washings were in PBST and slides were mounted in SlowFade Gold (Invitrogen). Cells were imaged on a Nikon E800 microscope with 40x objective and total pixel intensities and areas were measured in 200 nuclei using MetaMorph 4.60 (Molecular Devices).

4.3.4 PFGE, probes, and hybridisation

Agarose blocks were deproteinised in 1 ml 0.2 M EDTA, 1% SDS, 1 mg/ml Proteinase K (Roche) for 48 h with slow rocking at ~18°C; >99% of the 10% TCA-precipitable radioactivity in cells containing ^{35}S-labelled proteins was solubilised (data not

shown). PFGE was in 1% agarose in 0.5X TBE at 14°C using 190 v for 20 h with pulse time increased linearly from 50 to 90 sec. SSBs in linear minichromosome DNA were detected by excising the corresponding region from a gel, washing with S1 nuclease buffer, incubation with S1 nuclease (Invitrogen) for 15 h at 37°C, and PFGE. Hybridisation was performed on gels dried under vacuum at 60°C for 1 h on 3MM paper and covered with plastic film, incubated in 0.5 M NaOH, 1.5 M NaCl for 30 min, rinsed 3x in H_2O, neutralised in 0.5 M Tris, pH 8.0, 1.5 M NaCl for 30 min, rinsed with H_2O, and incubated in 6X SSC for 20 min, all at room temperature. Prehybridisation (30 min) and hybridisation (18 h) were in 6X SSC, 5X Denhardt's solution, 0.5% SDS, 0.5 μg/ml human Cot-1 DNA (Invitrogen) at 68°C. Gels were hybridised with DNA of EBV virus (GenBank accession number AJ507799) prepared from B95-8 cells [38] or a specific probe for marker lanes, labeled with [α-^{32}P]dCTP (3000 MBq/mM) using Megaprime kits (Amersham). Hybridised gels were washed 3x 30 min in 0.1X SSC, 0.5% SDS at 68°C, sealed in plastic film, and exposed to PhosphorImager screens. Signals were imaged and quantitated using ImageQuant (Molecular Dynamics) and are shown as (10^{-7} x arbitrary intensity units) in the region of interest after subtracting the mean background in identical areas below and above. Samples from the same cell population but without inhibitor were processed in parallel, separated in the same gel, and when a central marker lane was excised the remaining parts of the gel were hybridised together. Repair rates were quantitated in independent replicate experiments and inhibition was expressed as the difference in level of particular forms of minichromosome DNA between cells with and without an inhibitor after 120 min. p-values were calculated by the unpaired t-test.

4.3.5 Molecular combing and hybridisation of minichromosome DNA

Linear minichromosome DNA was excised from PFGE gels in LMP agarose of DNA from cells grown with BrdU. The agarose was incubated with YOYO-1 (5 μM) for 30 min, washed in TE, incubated in β-agarase buffer for 30 min on ice, melted in 50 mM MES, pH 5.7 at 65°C for 10 min, and solubilised by β-agarase (New England Biolabs) at 42°C for 4 h. Four μl of DNA dissolved in the same buffer at 2 μg/ml were placed on a 3-

aminopropyl-triethoxysilane-coated microscope slide (Sigma-Aldrich) and covered with a standard cover glass, which was pulled horizontally across the slide at ~300 μm/sec after 2 min. Slides with well-spread DNA molecules as seen by fluorescence microscopy (Nikon E800, 100x objective) were dried at room temperature for 5 min and overnight at 60°C, incubated in 0.6X SSC, 70% formamide for 3 min at 95°C, and then in cold 70%, 85%, and 95% ethanol (2 min each). Probes were an 8.1 kb BamHI-SalI fragment of cosmid cM301-99 and a 29 kb HindIII fragment of cosmid cMB-14 (gifts from G. Bornkamm) excised from an agarose gel, purified on a Microcon YM-100 (Qiagen), and labeled with biotin-11-dUTP (Fermentas) by nick translation. Hybridisation was in a humidified chamber for up to 48 h at 37°C. Probes were detected with FITC-goat anti-biotin (Sigma-Aldrich) (1:50, 20 min) followed by Alexa 488-rabbit anti-goat antibody (Invitrogen) (1:50, 20 min), and DNA by subsequent incubation with rat anti-BrdU (Abcam) (1:30, 20 min) followed by Alexa 594-goat anti-rat antibody (Invitrogen) (1:50, 20 min). Antibody dilutions and washing were in PBS, 0.05% Tween-20. Minichromosome DNA molecules identified by hybridisation signals from both probes were imaged by confocal microscopy (Bio-Rad MRC1024) and their lengths were calculated using the factor of 2.2 kb DNA/μm after minor adjustment of images to normalise the distance between the two probes, as described in [39].

4.3.6 Modeling repair kinetics

Four compartments each containing one form of minichromosome DNA were considered together with the four ordinary differential equations:

$$\begin{cases} \dfrac{d[S]}{dt} = k_s[CSSB] + s_{inh}k_d[L] \\ \dfrac{d[CSSB]}{dt} = s_{inh}k_{ds}[LSSB] - k_s[CSSB] \\ \dfrac{d[LSSB]}{dt} = -s_{inh}k_{ds}[LSSB] - k_{sd}[LSSB] \\ \dfrac{d[L]}{dt} = k_{sd}[LSSB] - s_{inh}k_d[L] \end{cases}$$

where:

$[X]$ = fraction of total amount (hybridisation signal) of DNA in form X (S=supercoiled, L=linear, LSSB=linear with SSBs, CSSB=circular with SSBs);

k_d = rate of repair of molecules containing only a DSB;

k_s = rate of repair of molecules containing only SSBs;

k_{ds} = rate of repair of the DSB in molecules containing both a DSB and SSBs;

k_{sd} = rate of repair of SSBs in molecules containing both SSBs and a DSB;

s_{inh} = switch reflecting inhibition of DSB repair: 1 for normal conditions, 0 when DSB repair was arrested by the DNA-PK inhibitor NU7441 (Fig. 7C).

The rationale for using first-order kinetics is considered in the Discussion. Fitting to the experimental data depended on estimating parameters and initial conditions in normal conditions or when DSB repair was inhibited, using a least squares approach to minimise the sum of squared residuals (differences between data and the model's output). Calculations were made in MATLAB.

4.4 Results

4.4.1 Strand breaks in the minichromosome in irradiated cells

The supercoiled minichromosome DNA in normal cells [12] and the linear DNA in irradiated cells resulting from a DSB were detected and quantitated by hybridising PFGE gels of total cell DNA with a probe of EBV DNA, the linear form of minichromosome DNA [14] (Fig. 4.1B). Circular minichromosome DNA containing SSBs, formed by incubating deproteinised cells with the nicking endonuclease Nb.BbvCI, migrated diffusely between the sample well and the supercoiled form (Fig. 4.1B) probably as a result of impalement on agarose fibres like other large nicked-circular DNAs [40-42]. Molecular combing of DNA from this region showed 181±11 kb long circular molecules (SEM from 30 molecules) with the expected conformation (Fig. 4.1F); these were not seen in gels of DNA from untreated cells and did not have the theta conformation characteristic of

replicating minichromosome DNA [43], while supercoiled DNA does not bind to slides in these conditions ([44] and data not shown). This region was diffuse and poorly separated from the sample well and may also contain replicating molecules [40], and therefore we did not attempt to quantitate nicked circular molecules directly and instead calculated their abundance by mathematical modeling (see Section 4.7).

In irradiated cells the minichromosome DNA had been converted to a form with the same mobility as linear molecules (Fig. 4.1B, lane 50 Gy). The length of these molecules was 170±10 kb (mean and SD from three independent experiments) measured by interpolation from markers, a value not significantly different from that of full-length linear DNA (~172 kb), and no shorter fragments were detected using a PFGE regime which separated DNA ≥2 kb in length (data not shown). The amount of this linear DNA was not significantly different from that produced by cutting minichromosome DNA at its single PacI site ($p=0.45$ from three replicate experiments) (Fig. 4.1E). FISH on combed linear minichromosome DNA from irradiated cells showed that the extremities of individual molecules were positioned differently with respect to specific probes (Fig. 4.1D and manuscript submitted). Together, these results show that in irradiated cells the minichromosome DNA was converted quantitatively to full-length linear DNA by a single DSB whose position was not specific.

Minichromosome DNA molecules which had been linearised by a DSB contained multiple SSBs, since they were cleaved to shorter fragments by the single strand-specific nuclease S1 which cuts the opposite DNA strand at SSBs caused by ionising radiation [45,46] (Fig. 4.1C). The mean length of the S1 nuclease fragments was ~48 kb with a minimum of ~15 kb (Fig. 4.1D), and did not decrease further when a higher concentration of nuclease was used (data not shown).

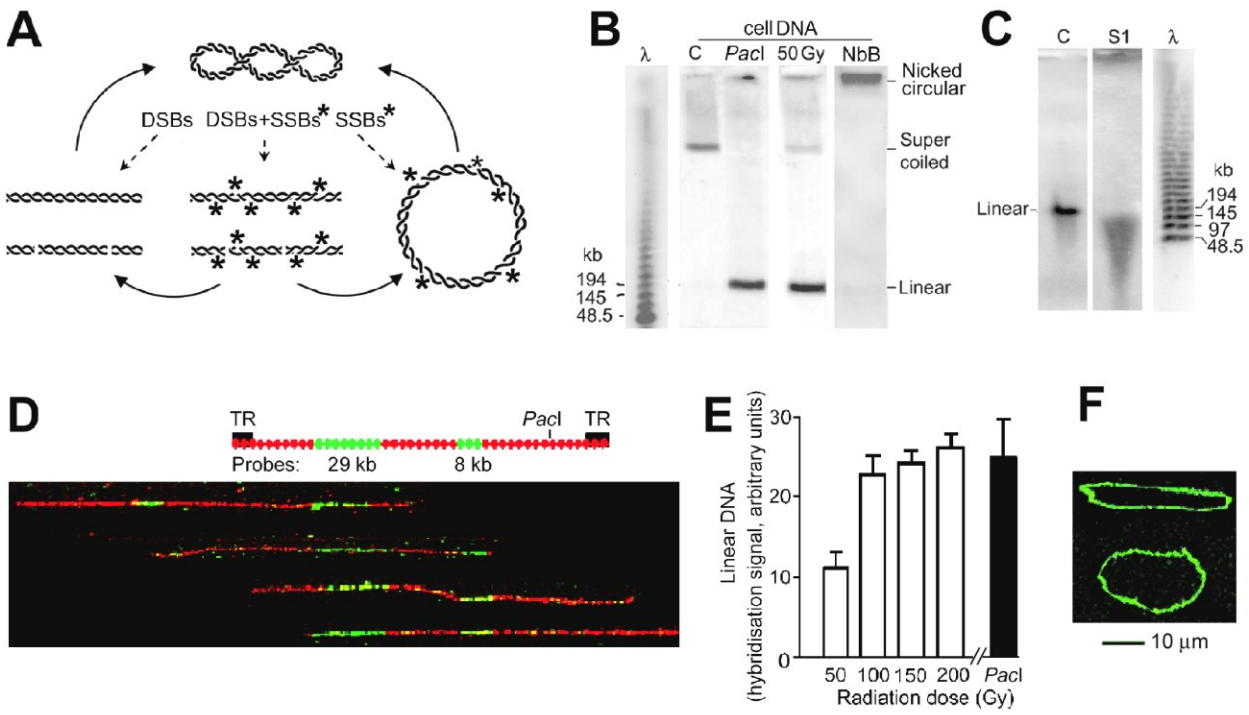

Fig. 4.1. Strand breaks in minichromosome DNA in irradiated cells. (A) The supercoiled minichromosome DNA and forms which result from DSBs and/or SSBs (*). (B) Minichromosome DNA separated by PFGE after incubating deproteinised cells with: lane C, no addition; lane PacI, PacI (100 u/ml, 3 h) which cuts minichromosome DNA at a single site; lane NbB, endonuclease Nb.BbvCI (100 u/ml, 1 h) which forms circular molecules containing SSBs. Lane 50 Gy, cells irradiated (50 Gy) before deproteinisation; lanes λ, oligomers of λ DNA. The gel was hybridised with a probe of EBV DNA; for the gel images in this and following Figures the top includes the sample well and panels were assembled from lanes of the same gel. (C) Linear minichromosome DNA from irradiated cells extracted from a gel, incubated without or with nuclease S1 (100 u/ml, 15 h), and subjected to PFGE. (D) Representative linear minichromosome DNA from irradiated cells spread by molecular combing and hybridised with two probes (upper map); TR are the terminal repeat sequences by which the minichromosome is circularised. The FISH probes were labeled with biotin and detected with anti-biotin antibodies (green), and DNA was labelled with BrdU and detected with anti-BrdU antibodies (red). The extremities of the molecules show the site of the DSB; the probe positions were aligned approximately considering the slightly variable stretching of DNA during combing. (E) Quantitation of

linear minichromosome DNA in irradiated cells compared with that after cleavage at its single *Pac*I site (100 u/ml, 3 h) in deproteinised cells; error bars show SEM from three independent experiments. (F) Representative DNA molecules believed to be relaxed circular minichromosome DNA containing single-strand breaks, extracted from the region close to the origin of a gel of DNA from cells incubated with endonuclease Nb.BbvCI (panel B, lane NbB), stained with YOYO-1, and combed (see text).

4.4.2 Repair of SBs

To quantitate repair rates precisely the maximum conversion of minichromosome DNA to the linear form was desirable, and cells were irradiated with 50 Gy, a dose similar to those commonly used to study repair of genomic DNA [for example 47,48] although above the lethal level. Cells were kept in agarose blocks for repair to minimise manipulations and time incubations precisely; nonspecific loss of DNA [47] did not occur during the 2 h repair period since 103±9% (n=9) of the initial quantity of minichromosome DNA was recovered in conditions where repair of DSBs was arrested (Fig. 4.7). The rate of repair of DSBs in minichromosome DNA was not significantly different from that in culture conditions (data not shown), as observed earlier for a double-minute chromosome [48].

The SSBs in linear minichromosome DNA were repaired progressively (Fig. 4.2B, C). Immediately after irradiation essentially all of these molecules were cut by nuclease S1 to fragments of average length ~48 kb, consistent with an average of ~3.6 SSBs in each ~172 kb molecule. After repair for 2 h, ~50% of the DNA had been converted to full-length linear molecules which were resistant to nuclease S1 and therefore contained no SSBs (Fig. 4.2C).

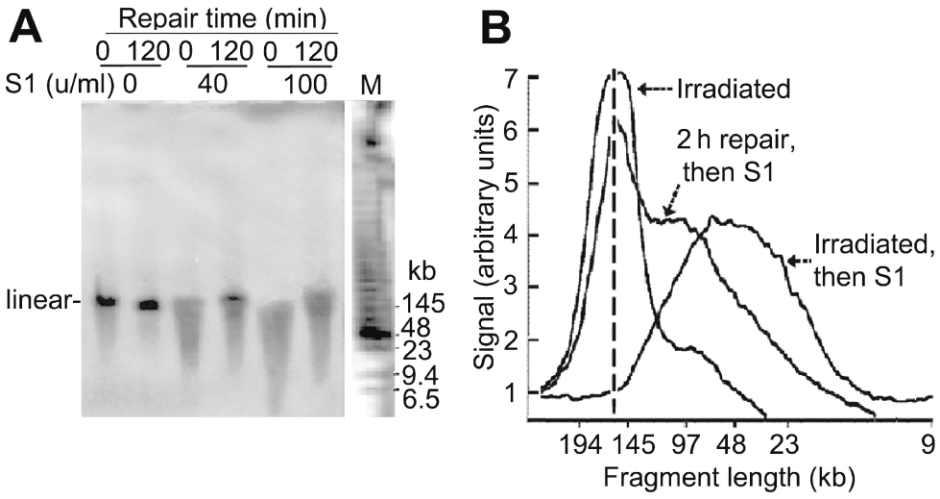

Fig. 4.2. Repair of SSBs in linear minichromosome DNA. (A) Fragmentation by nuclease S1 of linear minichromosome DNA isolated immediately after irradiation (50 Gy) or after repair for 2 h. Linear DNA isolated from a gel of total cell DNA was incubated without or with nuclease S1 for 15 h and the fragments produced were separated by PFGE. For these experiments, sufficient linear DNA could be conserved for 2 h only if repair of DSBs was arrested, and therefore the DNA-PK inhibitor NU7441 was included during the repair period (see Fig. 4.7). (B) Scans of the hybridisation signal from lanes in (A) (S1 100 u/ml); the position of full-length linear molecules is indicated by the vertical dashed line.

4.4.3 Repair of DSBs and recircularisation of minichromosome DNA

A progressive increase of the level of supercoiled DNA parallelled by a decrease of the linear form (Fig. 4.3B, white and black columns, respectively) during repair showed that the DSBs by which linear molecules had been produced were religated. The sum of the linear and supercoiled forms decreased progressively, reflecting an increase of the number of molecules which had been recircularized by repair of their DSB but still contained SSBs; nonspecific loss of minichromosome DNA during the repair period could be excluded (see Section 4.4.1). Linear dimers of minichromosome DNA which would have been produced if incorrect end-joining had occurred were not detected (Fig. 4.3A).

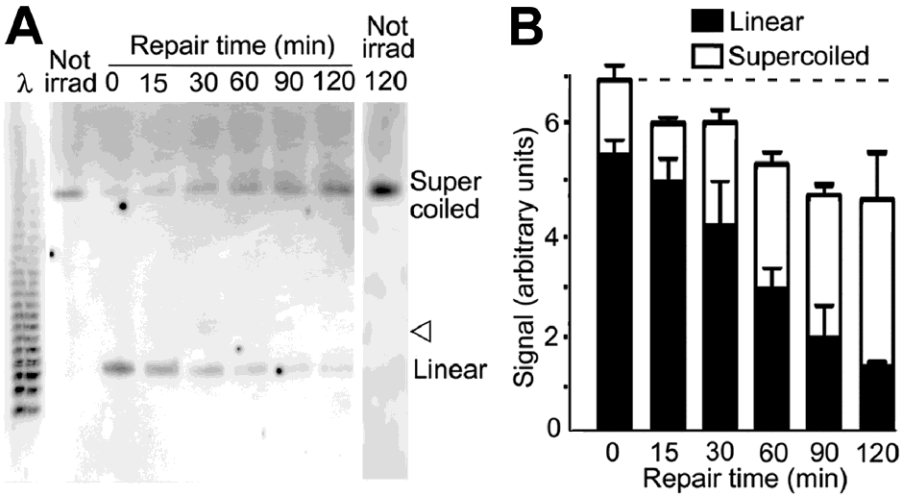

Fig. 4.3. Repair of DSBs shown by the conversion of linear to supercoiled minichromosome DNA. (A) Linear and supercoiled DNA during repair; the arrowhead shows the calculated position of linear dimers which would have been formed by incorrect end-joining. (B) Linear (black columns) and supercoiled (white columns) minichromosome DNA quantitated by hybridisation; error bars show SEM from three independent experiments. The total level of minichromosome DNA (linear plus supercoiled) before repair is shown by the horizontal dashed line.

4.4.4 Effect of inhibiting topoisomerases I and II on repair

To assess the contributions of particular enzymes to the repair of SBs in the minichromosome, we used chemical reagents which are widely accepted as appropriate and specific inhibitors because depletion of repair enzymes by siRNA methodology proved insufficient to provide unequivocal conclusions (see Discussion).

The question if topoisomerases I and/or II are implicated in the repair of SBs remains unresolved [20-24.49]. Noncatalytic inhibitors of these enzymes were used in previous studies [21,49], but these reagents themselves create SBs when DNA is deproteinised [50] and therefore cannot provide clear evidence for a role of topoisomerases in repair. Instead, we used inhibitors of the catalytic type which arrest the enzyme by trapping a noncovalent reaction intermediate whose deproteinisation does not cause DNA cleavage. To inhibit

topoisomerase II we employed ICRF-193 [51-53] (100 μM) which trapped intermediates of the enzyme-DNA reaction in cells [54] as efficiently as etoposide (Fig. 4.4A), which traps all cellular topoisomerase II at this concentration [55]. The epipodophylloid F11782 [56-58] was used to inhibit both topoisomerases I and II; since its efficiency in trapping enzyme-DNA reaction intermediates cannot be assayed [56] a concentration of 1 mM was used, which is >50-fold and >500-fold the IC_{50} for inhibition of human topoisomerases I and II, respectively, and >500-fold the IC_{50} for inhibition of growth of V79 cells [56].

Neither ICRF-193 or F11782 had a significant effect on the evolution of the levels of linear and supercoiled minichromosome DNA during repair (Fig. 4.4B, C). The p-values for the difference in the level of supercoiled DNA in the presence or absence of inhibitor after 2 h were 0.51 for ICRF-193 and 0.88 for F11782, and 0.71 and 0.51 respectively for the corresponding difference in linear DNA.

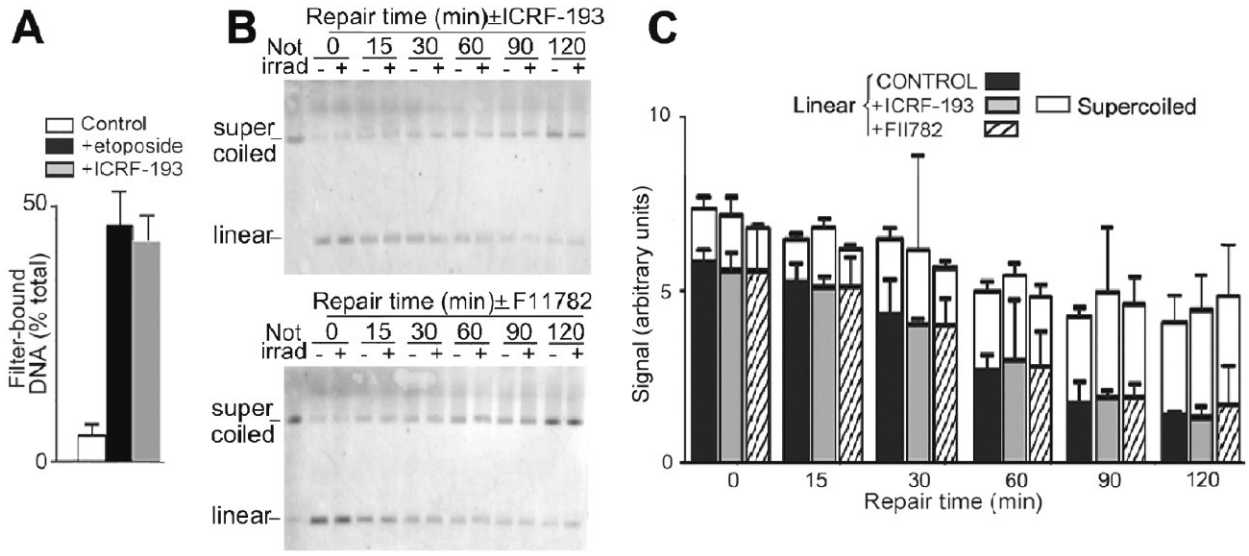

Fig. 4.4. Conversion of linear to supercoiled DNA is not affected when topoisomerase II or both topoisomerases I and II are inhibited. (A) Efficiency of ICRF-193 (100 μM) in inhibiting topoisomerase II compared with the noncatalytic inhibitor etoposide (100 μM), assayed by filter-binding of covalent enzyme-DNA reaction intermediates in lysates of [^{3}H]thymidine-labeled cells 1 h before incubating them for repair. (B) Effect of ICRF-193 (100 μM) or F11782 (1 mM) on the conversion of linear to supercoiled DNA during

repair. (C) Quantitation of linear and supercoiled DNA during repair. All error bars show SEM from three independent experiments.

4.4.5 Effect of inhibiting PARP-1 on repair

PARP-1 is implicated in sensing and repair of SSBs, although the precise step at which it intervenes has not been identified [25-32]. To inhibit PARP-1 we used NU1025 [59] or 1,5-IQD [60] at a concentration of 200 μM; their IC_{50} values for inhibition of PARP-1 are 0.4 μM [59,60]. The synthesis of PAR immediately after irradiation was reduced by >95% by these inhibitors (Fig. 4.5A). Repair of SSBs in linear molecules was not significantly affected and no detectable effect on repair of SSBs in circular molecules was seen because the reformation of supercoiled DNA, which can only occur when all SSBs have been repaired, was not slowed (Fig. 4.5B-D); the p-value for the difference in the level of supercoiled molecules at 120 min in the absence or presence of an inhibitor was 0.71 for NU1025 and 0.58 for 1,5-IQD.

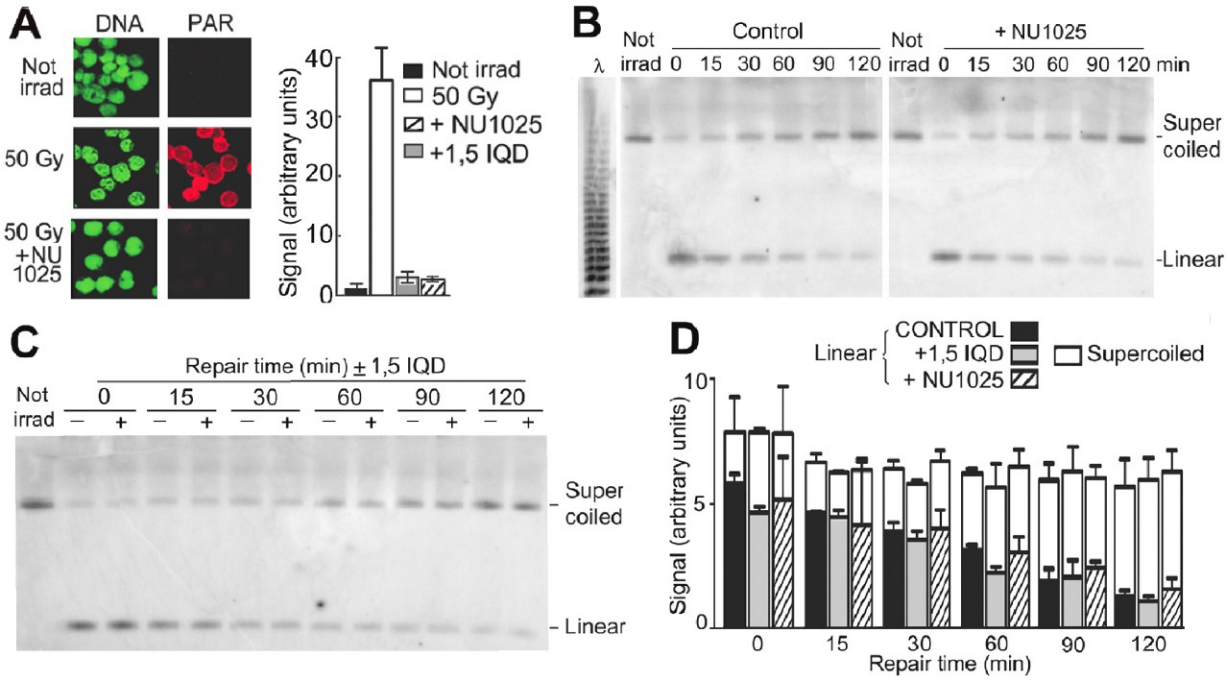

Fig. 4.5. Effect of inhibiting PARP-1 on repair of minichromosome DNA. (A) Inhibition of PAR synthesis immediately after irradiation in cells incubated without or with

NU1025 (200 μM) shown by immunofluorescence (red); DNA was labeled with YOYO-1 (green). Right panel: quantitation of PAR (red pixel intensity/nuclear area); error bars show SEM from 200 nuclei. (B) Conversion of linear to supercoiled DNA in cells incubated alone or with NU1025 (200 μM) or (C) with 1,5-IQD (200 μM). (D) Quantitation of linear and supercoiled DNA during repair; reformation of supercoiled DNA requires that all SSBs have been repaired. Error bars show SEM from four independent experiments.

4.4.6 Pathways for repair of DSBs

The contributions of the two major pathways for repair of DSBs in genomic DNA, homologous recombination (HR) and nonhomologous end-joining (NHEJ), to repair of DSBs in the minichromosome were examined. DSBs signal activation of ATM by autophosphorylation on serine 1981, which causes dissociation of dimers and initiates ATM kinase activity [2-6]. The inhibitor of ATM kinase KU55933 [61] reduced this phosphorylation in irradiated cells by ~95%, while the inhibitor caffeine [62] reduced it by ~80% (Fig. 4.6A). The rate of decrease in the level of linear DNA was reduced by ~30% in both cases (Fig. 4.6B) ($p<0.005$ for KU55933, $p<0.01$ for caffeine). This rate was reduced by ~26% in the presence of mirin (Fig. 4.6C) which inhibits the activation of ATM without affecting its kinase activity [63,64] and by ~20% in cells where Rad51, which participates uniquely in HR [33], had been depleted by ~90% by transfection of a specific siRNA (Fig. 4.6D). Together, these results are consistent in showing that 25-30% of the DSBs in the minichromosome were repaired by HR.

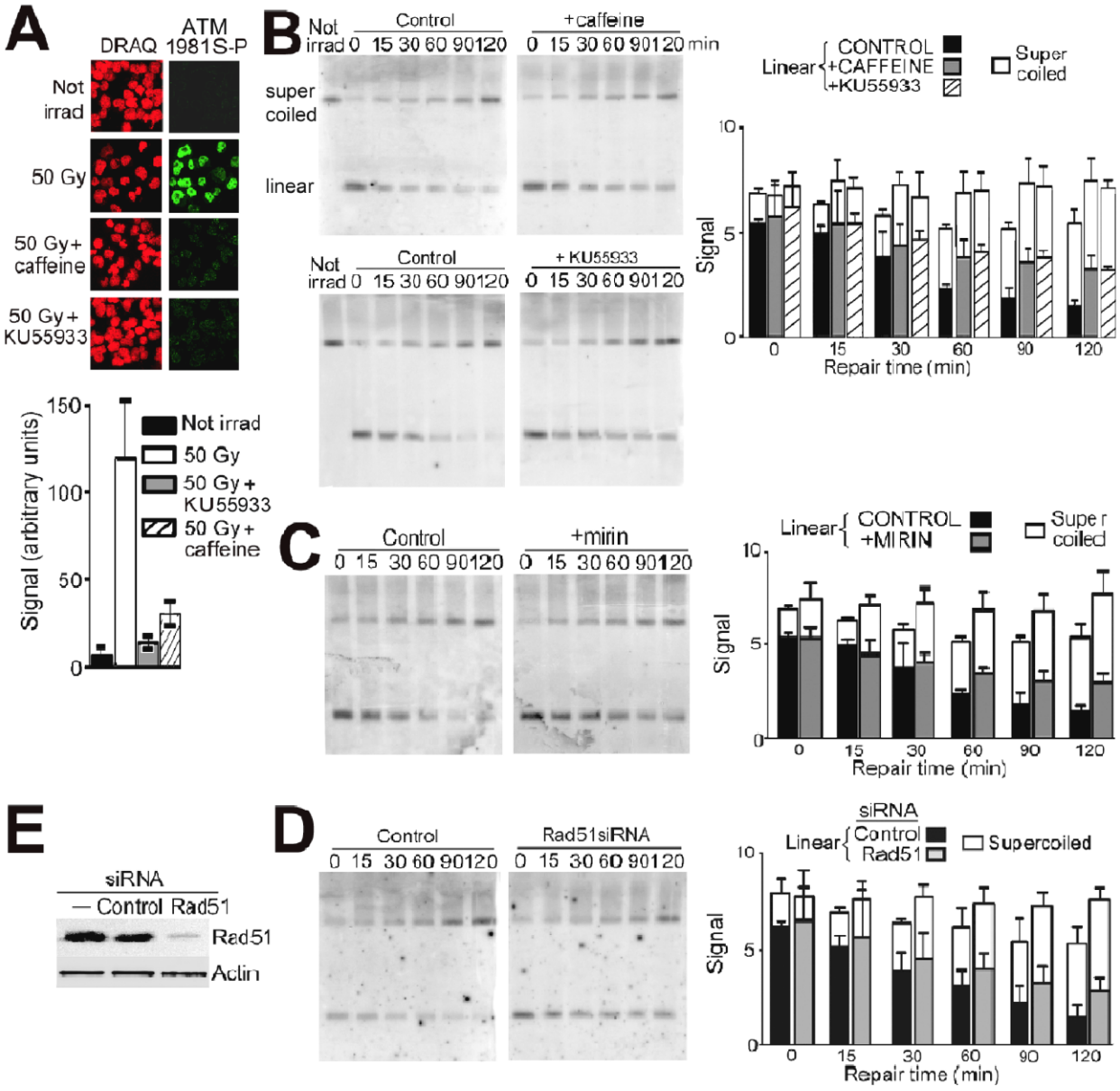

Fig. 4.6. **Effect of inhibiting DSB repair mediated by HR.** (A) ATM phosphorylated on Ser1981 in cells irradiated and incubated without or with caffeine (10 mM) or KU55933 (20 μM), detected by immunofluorescence (green); DNA was stained by DRAQ (red). Below, quantitation of the signal from ATM1981S-P (green pixel intensity/nuclear area). (B) Repair of minichromosome DNA in cells incubated without or with caffeine (10 mM) or KU55933 (20 μM), inhibitors of ATM kinase, or (C) with mirin (100 μM) which inhibits ATM activation without affecting its kinase activity. (D) Repair in cells transfected with siRNA to silence expression of Rad51 or with a control siRNA; cells were irradiated 48 h

later and incubated for repair. (E) Rad51 protein detected by Western blots in cell lysates; actin served as sample loading control. All error bars show SEM from three independent experiments.

Repair of DSBs by NHEJ is initiated by binding of Ku70/Ku80, followed by recruitment of DNA-PKcs which is then activated by phosphorylation on threonine-2609 [2-6]. This phosphorylation was inhibited by wortmannin [65] or NU7441 [66]; for wortmannin the level of DNA-PKcs2609Thr-P was not significantly greater than that in unirradiated cells ($p=0.104$ from two replicate experiments) while for NU7441 (10 μM) it was reduced by ~70% (Fig. 4.7A). The repair of DSBs in minichromosome DNA, shown by the decrease in the level of linear DNA, was arrested completely by both these inhibitors ($p=0.55$ for wortmannin, $p=0.88$ for NU7441) while the formation of supercoiled DNA continued, reflecting ongoing repair of SSBs in circular molecules (Fig. 4.7D). The relative contributions which HR and NHEJ make to repair are considered in the Discussion.

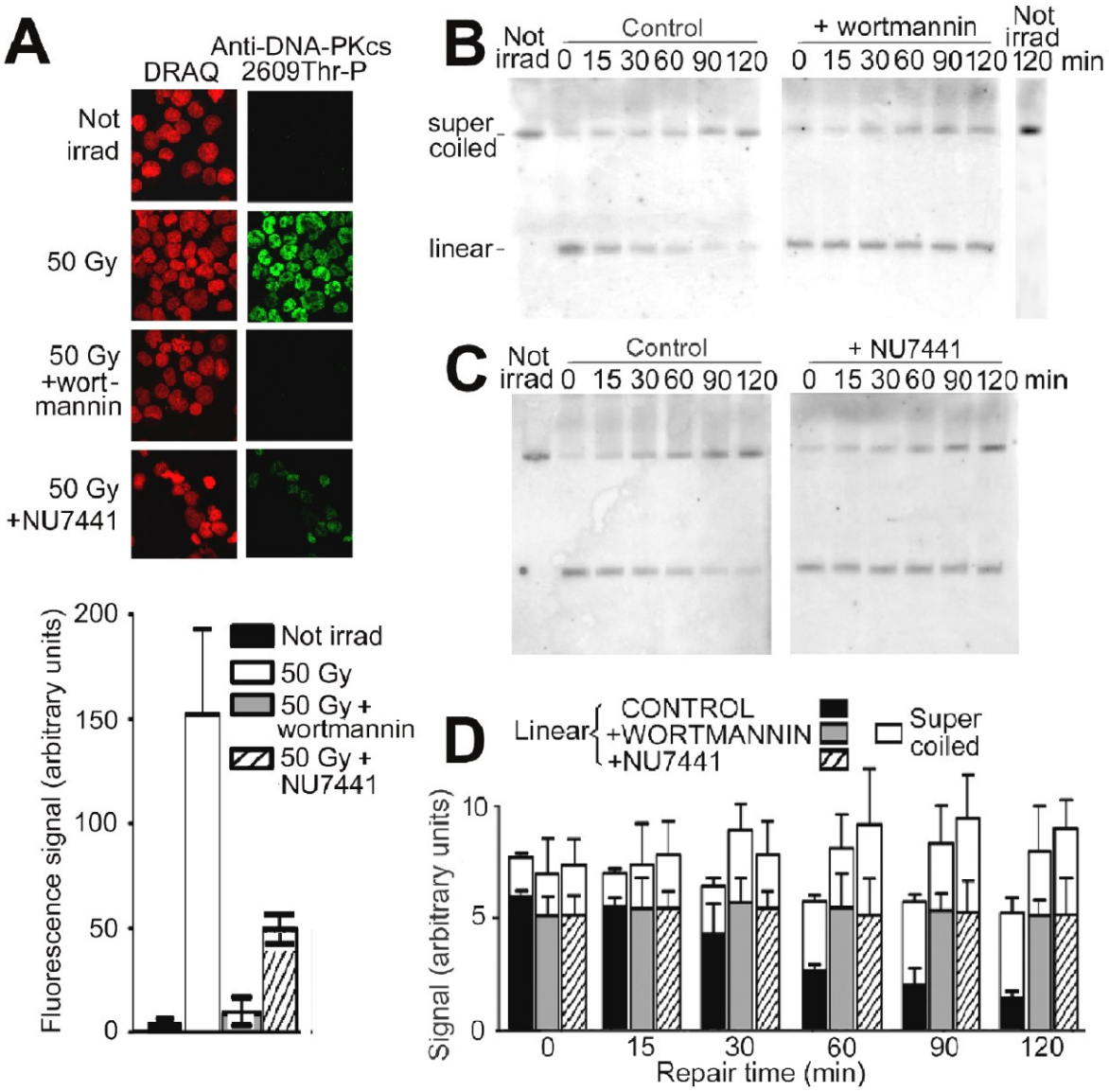

Fig. 4.7. Inhibitors of phosphorylation of DNA-PKcs arrest DSB repair. (A) Phosphorylation of DNA-PKcs on threonine-2609 in cells irradiated and incubated without or with wortmannin (100 μM) or (C) NU7441 (10 μM) detected by immunofluorescence (green); DNA was stained by DRAQ (red). Below, quantitation of the signal from DNA-PKcs2609Thr-P (green pixel intensity/nuclear area). (B) Repair in cells incubated with wortmannin (100 μM) or (C) NU7441 (10 μM). (D) Quantitation of linear and supercoiled DNA during repair. All error bars show SEM from three independent experiments.

4.4.7 Modeling the kinetics of SB repair

A model was developed to fit the experimental data for the kinetics of repair (Fig. 4.8A) with the primary objective of computing the abundance of circular minichromosome DNA molecules containing SSBs which were not measured experimentally, and offered the further advantage of providing rate constants for repair of SSBs and DSBs and a number of conclusions which were not directly evident from the experimental data (see Discussion). The interconversion of different forms of minichromosome DNA during repair was expressed by first-order kinetics, which require fewer parameters than Michaelis-Menten kinetics, because unique values of parameters cannot be estimated when too many are considered (the model is non-identifiable) and inferences are not reliable (see Discussion). The input data were the levels of linear and supercoiled DNA during repair in normal conditions and when repair of DSBs was arrested by NU7441 (Fig. 4.7 D). Initially, different values were assigned to the rate constants for repair of DSBs in molecules containing only a DSB or also containing SSBs (k_d and k_{ds}) and for repair of SSBs in molecules with only SSBs or also containing a DSB (k_s and k_{sd}), but the fit to the data was not better than using identical values and estimation of parameters was too sensitive to the choice of the starting point for optimisation. Identical values were therefore adopted for k_d and k_{ds} and for k_s and k_{sd}. For conditions where repair of DSB was arrested, k_d and k_{ds} were set at sero.

The calculated levels of the forms of minichromosome DNA and their fit to the experimental data are shown in Fig. 8B. The calculated rate constants were $k_s = k_{sd} = 0.212$ for repair of SSBs and $k_d = k_{ds} = 0.745$ for repair of DSBs; we note that these refer to the fraction of the total molecules transferred between compartments per hour and not to the number of SBs repaired per hour, and for molecules containing SSBs they are mean values because the number of SSBs per molecule varies (Fig. 4.2).

The levels of different forms of minichromosome DNA could be predicted for a longer period of repair if it was assumed that the rate constants during the first 2 h were maintained (Fig. 4.8C). The relative quantity of linear DNA without SSBs was predicted to increase transiently while that of linear DNA with SSBs decreased, reflecting ongoing

repair of these SSBs. When repair of DSBs was inhibited, linear DNA without SSBs was predicted to accumulate as expected if the repair of SSBs continued. The level of the circular form containing SSBs was predicted to increase transiently because linear molecules which contained SSBs were circularised before these SSBs were repaired; as expected, this increase was not seen when repair of DSBs was inhibited.

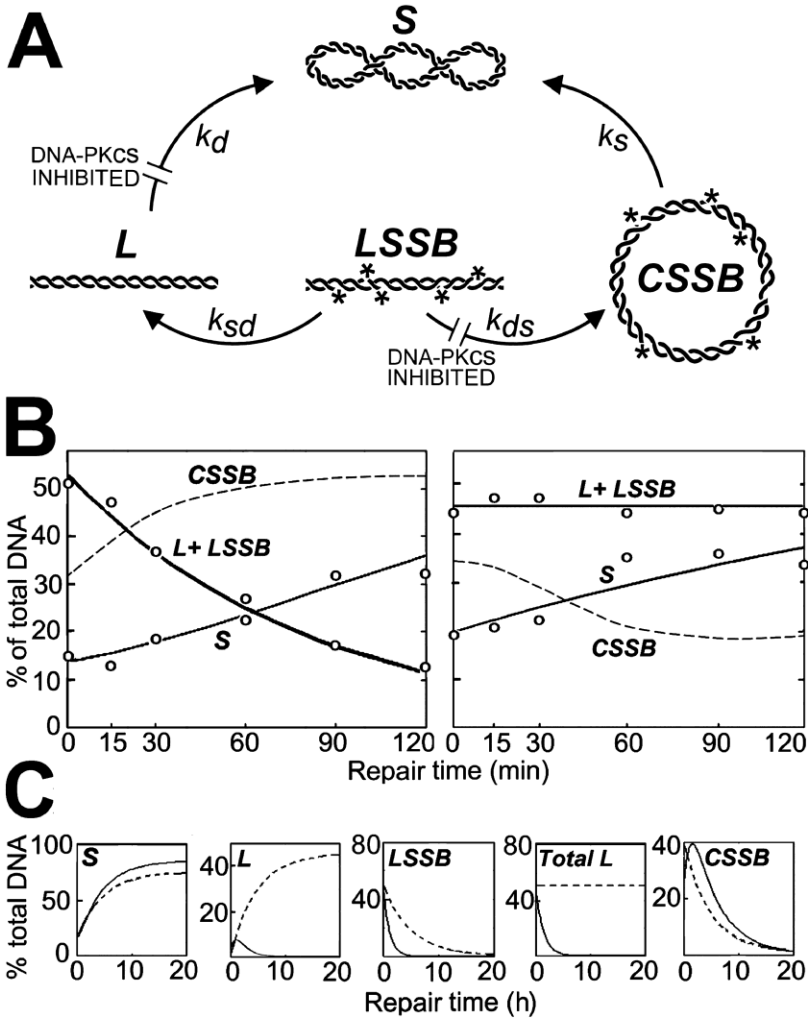

Fig. 4.8. Temporal evolution of the levels of the different forms of minichromosome DNA during repair calculated by modeling. (A) The model considered transfers of molecules between four compartments containing supercoiled molecules (S), linear molecules formed by a DSB (L), linear molecules also containng SSBs (*) (LSSB), and circular molecules containing SSBs (CSSB). k_s, k_{sd}, k_d, and k_{ds} are rate constants; k_d, and k_{ds} were set at zero when repair of DSBs was arrested by the inhibitor of DNA-PKcs NU7441.

(B) Calculated levels of the different forms of DNA (curves) compared with experimental data points (error bars omitted for clarity). Left panel, during normal repair; right panel, when repair of DSBs is arrested. (C) Calculated levels extrapolated for a period of 20 h in normal repair conditions (full lines) or when repair of DSBs is arrested (dashed lines).

4.5 Discussion

The simultaneous repair of SSBs and DSBs in a defined region of chromatin *in vivo* has not been studied previously using quantitative methods, to our knowledge. In earlier work SSBs were detected by filter elution or single-cell electrophoresis methods whose interpretation in terms of absolute numbers of breaks is not quantitative, and the measured relative rates of repair of SSBs and DSBs were variable [67,68]. To ensure accurate quantitation of SBs we used two conditions which are not always considered in studies of repair in genomic DNA: for PFGE, DNA was deproteinised at room temperature because at higher temperatures extra DSBs are created at radiation-damaged sites [69], and in-gel hybridisation was used because hybridisation to DNA blotted onto membranes [9,10] is not quantitative for large fragments [70]. In another study of repair of SBs in the EBV episome [71] published after this manuscript was completed, a significant amount of minichromosome DNA, interpreted as nicked circles, remained in the sample well of PFGE gels while here little or no DNA remained in the wells and nicked circular DNA migrated slowly into the gel, possibly reflecting methodological differences. The Poisson distribution of SBs assumed in [71] is not consistent with our finding that only a single DSB is formed in minichromosome DNA in irradiated cells (Fig. 4.1 and manuscript submitted).

We used chemical reagents to inhibit enzymes involved in repair of SBs because in most cases sufficient depletion could not be obtained by siRNA methodology (for example, 50-60% depletion for Ku70 and DNA-PKcs; data not shown). In other studies depletion of PARP-1 [72,73], DNA ligases [74], and topoisomerase II [75] was also less than complete and in some cases lethal [75]. The absence of effect of inhibitors of PARP-1 on the repair of minichromosome DNA is consistent with the current view that PARP-1 is not indispensable for, although it can accelerate, SSB repair in genomic DNA which is slowed

only modestly when PARP-1 is ablated or inhibited [25-32,76,77], and most inhibitors of PARP-1 showed no affect on repair of SBs in this minichromosome in another study [72]. Recent studies propose that its primary function is in base excision repair [30,78].

Between 25 and 30% of the DSBs in the minichromosome were repaired by HR according to the consequences of inhibiting activation or activity of ATM kinase or of depleting Rad51, but their repair was arrested completely by inhibitors of DNA-PKcs which operate in the NHEJ pathway. These findings can be interpreted by the model proposed to understand similar observations on the repair of DSBs in genomic DNA, where it is believed that the contribution of HR is obscured when DNA-PKcs is inhibited because factors involved in NHEJ are then trapped at DSB extremities and interfere with the access of factors required for HR [5,79-81]. We underline, however, that the quantitative outcomes of our model of repair kinetics are not influenced by the particular pathway of DSB repair which was arrested by inhibitors of DNA-PKcs.

A possible role for topoisomerases I or II in DNA repair has been discussed in numerous studies, but experimental evidence has been inconclusive [20-24]. A SB would relax any DNA superhelicity in the circular minichromosome which was not constrained by nucleosomes if the repair machinery did not prevent mutual rotation of the DNA strands; if rotation could occur, further negative supercoiling would be required after repair to normalise the superhelicity, but eukaryotic topoisomerases I and II do not possess this activity. Dissociation of nucleosomes in the neighbourhood of a SB would relax the negative superhelicity resulting from DNA wrapping on their surface, but this would be re-established when nucleosomes were reformed on the repaired region and no requirement for activity of a topoisomerase would be predicted. The continued conversion of linear to supercoiled minichromosome DNA at the normal rate when topoisomerases I and II were inhibited by catalytic inhibitors is therefore consistent with these topological considerations.

Kinetic models of SB repair could be constructed with different degrees of complexity; but theory shows that the least complex model is preferable in order to provide concrete predictions [82]. Our data were fitted well by using first-order kinetics (Fig. 4.8A), and we justified this strategy by considering that other datasets for DNA repair have been fitted satisfactorily by first-order kinetics [for example 8,83] which only deviate

significantly from higher-order models after two half-times (that is, after repair of 75% of the SBs) [83], and by theoretical arguments which show that "multiple processes (which are not neccessarily first-order) may combine to produce kinetic behavior indistinguishable from first-order and ... such combinations are more likely to exist when reactions occur in a complex environment" [84]. A number of conclusions which were not directly apparent from the experimental data illustrate the usefullness of modeling. First, when repair of DSBs was arrested the SSBs in linear molecules were still repaired and circular molecules containing SSBs were converted to supercoiled molecules at close to the normal rate (Fig. 8B), showing that operation of the systems for repair of SSBs was independent of those for DSB repair which has not been demonstrated previously as far as we are aware. Second, the calculated rate constants show that in an average linearised minichromosome the single DSB was repaired three to four times faster than all the SSBs, so that the rate-limiting step in complete repair of minichromosomes was the repair of SSBs. These repair rates cannot be compaired directly with those reported for genomic DNA where the methods used could not quantitate SBs directly, but comparisons can be made in terms of the half-time for repair which is reported to be independent of the radiation dose [85,86] and the length of the region considered [9]. In the minichromosome, the half-time for repair of the single DSB in each molecule calculated from the rate constant was ~40 min, which is within the same range (20 to 110 min) as that for genomic DNA [9,67,85]. For repair of SSBs the half-time of ~140 min was longer than that (~30 min) measured for genomic DNA by alkaline filter elution or comet assays [67,68,87,88]; the reasons for this difference remain to be understood but may include the detection of DSBs and damaged bases as well as SSBs by these methods. Supression of HR reduced the rate of decrease of linear minichromosome DNA by a statistically-significant factor of 25-30%, a value within the range of those for the contribution of HR to repair of genomic DNA which vary between rare [89] to predominant [90,91] in different cell types, but somewhat higher than that for human fibroblasts (~15%) [36]. This value is expected to depend on the compaction, topology, microenvironment, and accessibility to repair factors of different regions of chromatin [92] and in the minichromosome HR may be favoured by the proximity of daughter DNA molecules in catenated replicating forms [16] which would allow a region of homology to be found by searching a relatively limited volume. Linear oligomers of

minichromosome DNA were not detected during repair, as observed during repair of a 3 Mb double-minute chromosome [48] and transfected plasmids [22], reflecting juxtaposition of the DNA extremities by Ku [2-6] and the RMX complex [93]; we propose that a further important factor is the crowded macromolecular environment in the nucleus [94] because crowding strongly favours DNA circularisation and ligation by ligases IIIb and IV-XRCC4 which participate in NHEJ [95].

This minichromosome offers a simple system for quantitative testing of the efficiency of new potential inhibitors of the repair of SBs, and since the sequence and structural features of its DNA and its transcription pattern have been studied extensively [14] it provides a good model for examining other facets of DNA breakage and repair, for example mapping SBs and comparing repair in transcribed and nontranscribed regions. Such studies may be relevant to the repair of DNA in genomic chromatin in view of the topological similarity of the minichromosome to chromatin loops and its position in regions of lower chromatin density within the nucleus [15,17] where DSBs in genomic DNA and sites of their repair are predominantly localised [96,97].

Conflict of interest

The authors declare no conflicts of interest.

4.6 Acknowledgements

We thank L. Frappier for Raji cells, J. Nitiss and J-M. Barret for gifts of ICRF-193 and F11782 respectively, G. Bornkamm for cosmids, P. de Campos-Lima for B95-8 cells and discussions, J. St-Hilaire for irradiation, Y. Hadj-Sahraoui for assistance, and A. Swierniak for encouraging modeling. This work was supported partially by the Polish Ministry of Education and Science (Grant N N518 4976 39 to K.F. and J.R-W.).

4.7 References

[1] K.W. Caldecot, Chromosomal Single-Strand Break Repair, in: K.K. Khanna, Y.

Shiloh (Eds.), The DNA Damage Response: Implications on Cancer Formation and Treatment, Springer, Berlin, 2009, pp. 261-284.

[2] A.J. Hartlerode, R. Scully. Mechanisms of double-strand break repair in somatic mammalian cells. Biochem. J. 423 (2009) 157-168.

[3] M.R. Lieber. The mechanism of double-strand DNA break repair by the nonhomologous DNA end-joining pathway. Annu. Rev. Biochem. 79 (2010) 181-211.

[4] B.L. Mahaney, K. Meek, S.P. Lees-Miller. Repair of ionising radiation-induced DNA double-strand breaks by non-homologous end-joining. Biochem. J. 417 (2009) 639-650.

[5] M. Shrivastav, C.A. Miller, L.P. De Haro, S.T. Durant, B.P. Chen, D.J. Chen, J.A. Nickoloff. DNA-PKcs and ATM co-regulate DNA double-strand break repair. DNA Repair 8 (2009) 920-929.

[6] D.C. van Gent, M. van der Burg. Non-homologous end-joining, a sticky affair. Oncogene 26 (2007) 7731-7740.

[7] P.L. Olive. The role of DNA single- and double-strand breaks in cell killing by ionising radiation. Radiat. Res. 150 (1998) S42-51.

[8] S.Y. Ahn, B. Nevaldine, P.J. Hahn. Direct measurement by pulsed-field gel electrophoresis of induction and rejoining of X-ray-induced double-strand breaks in cultured mouse cells. Int. J. Radiat. Biol. 59 (1991) 661-675.

[9] M. Löbrich, B. Rydberg, P. Cooper. Repair of x-ray-induced DNA double-strand breaks in specific NotI restriction fragments in human fibroblasts: joining of correct and incorrect ends. Proc. Natl. Acad. Sci. U. S. A. 92 (1995) 12050-12054.

[10] B. Rydberg, M. Löbrich, P.K. Cooper. DNA Double-Strand Breaks Induced by High-Energy Neon and Iron Ions in Human Fibroblasts. I. Pulsed-Field Gel Electrophoresis Method. Radiat. Res. 139 (1994) 133-141.

[11] A.N. Luchnik, T.A. Hisamutdinov, G.P.Georgiev. Inhibition of transcription in eukaryotic cells by X-irradiation: relation to the loss of topological constraint in closed DNA loops. Nucleic Acids Res. 16 (1988) 5175-5190.

[12] E. Gussander, A. Adams. Electron microscopic evidence for replication of circular Epstein-Barr virus genomes in latently infected Raji cells. J. Virol. 52 (1984) 549-556.

[13] J.E. Shaw, L.F. Levinger, C.W. Carter. Nucleosomal structure of Epstein-Barr virus DNA in transformed cell lines. J. Virol. 29 (1979) 657-665.

[14] B. Sugden, E.R. Leight. EBV's plasmid replicon, an enigma in cis and trans. Curr. Top. Microbiol. Immunol. 258 (2001) 3-11.

[15] M.J. Deutsch, E. Ott, P. Papior, A. Schepers. The latent origin of replication of Epstein-Barr virus directs viral genomes to active regions of the nucleus. J. Virol. 84 (2010) 2533-2546.

[16] S. Ito, K. Yanagi. Epstein-Barr Virus (EBV) Nuclear Antigen 1 Colocalises with Cellular Replication Foci in the Absence of EBV Plasmids. J. Virol. 77 (2003) 3824-3831.

[17] T. Kanda, M. Kamiya, S. Maruo, D. Iwakiri, K. Takada. Symmetrical localisation of extrachromosomally replicating viral genomes on sister chromatids. J. Cell Sci. 120 (2007) 1529-1539.

[18] C. Benyajati, A. Worcel. Isolation, characterisation, and structure of the folded interphase genome of Drosophila melanogaster. Cell 9 (1976) 393-407.

[19] D.A. Jackson, P. Dickinson, P.R. Cook. The sise of chromatin loops in HeLa cells. EMBO J. 9 (1990) 567-571.

[20] D.K. Gaffney, M. Lundquist, R.L. Warters, R. Rosley. Effects of modifying topoisomerase II levels on cellular recovery from radiation damage. Radiat. Res. 154 (2000) 461-466.

[21] N. Giocanti, C. Hennequin, J. Balosso, M. Mahler, V. Favaudon. DNA Repair and Cell Cycle Interactions in Radiation Sensitisation by the Topoisomerase II Poison Etoposide. Cancer Res. 53 (1993) 2105-2111.

[22] S. Jacob, C. Miquel, A. Sarasin, F. Pras. Effects of camptothecin on double-strand break repair by non-homologous end-joining in DNA mismatch repair-deficient human colorectal cancer cell lines. Nucleic Acids Res. 33 (2005) 106-113.

[23] S. Mateos, N. Hajji, N. Pastor, F. Cortés. Modulation of radiation response by inhibiting topoisomerase II catalytic activity. Mutat. Res. 599 (2006) 105-115.

[24] S.Y. Terry, A.C. Riches, P.E. Bryant. Suppression of topoisomerase IIalpha expression and function in human cells decreases chromosomal radiosensitivity. Mutat. Res. 663 (2009) 40-45.

[25] S.L. Allinson, I.I. Dianova, G.L. Dionov. Poly(ADP-ribose) polymerase in base excision repair: always engaged, but not essential for DNA damage processing. Acta Biochim. Pol. 50 (2003) 169-179.

[26] A.E. Fisher, H. Hochegger, S. Takeda, K.W. Caldecott. Poly(ADP-ribose) polymerase 1 accelerates single-strand break repair in concert with poly(ADP-ribose) glycohydrolase. Mol. Cell. Biol. 27 (2007) 5597-5605.

[27] C. Flohr, A. Burkle, J.P. Radicella, B. Epe. Poly(ADP-ribosyl)ation accelerates DNA repair in a pathway dependent on Cockayne syndrome B protein. Nucleic Acids Res. 31 (2003) 5332-5337.

[28] C. Godon, F.P. Cordelières, D. Biard, N. Giocanti, F. Mégnin-Chanet, J. Hall, V. Favaudon. PARP inhibition versus PARP-1 silencing: different outcomes in terms of single-strand break repair and radiation susceptibility. Nucleic Acids Res. 36 (2008) 4454-4464.

[29] Noel, G., N. Giocanti, M. Fernet, F. Megnin-Chanet, and V. Favaudon. Poly(ADP-ribose) polymerase (PARP-1-1) is not involved in DNA double-strand break recovery. BMC Cell Biol. 4 (2003) 7.

[30] C.E. Ström, F. Johansson, M. Uhlén, C. Al-Khalili Ssigyarto, K. Erixon, T. Helleday. Poly(ADP-ribose)polymerase (PARP) is not involved in base excision repair but PARP inhibition traps a single-strand intermediate. Nucleic Acids Res. 39 (2011) 3166-3175.

[31] S.J. Veuger, N.J. Curtin, G.C. Smith, B.W. Durkacs. Effects of novel inhibitors of poly(ADP-ribose) polymerase-1 and the DNA-dependent protein kinase on enzyme activities and DNA repair. Oncogene 23 (2004) 7322-7329.

[32] B.C. Woodhouse, I.I. Dianova, J.L. Parsons, G.L. Dianov. Poly(ADP-ribose) polymerase-1 modulates DNA repair capacity and prevents formation of DNA double strand breaks. DNA Repair 7 (2008) 932-940.

[33] C.E. Tambini, K.G. Spink, C.J. Ross, M.A. Hill, J. Thacker. The importance of XRCC2 in RAD51-related DNA damage repair. DNA Repair 9 (2010) 517-525.

[34] J.A. Neal, V. Dang, P. Douglas, M.S. Wold, S.P. Lees-Miller, K. Meek. Inhibition of homologous recombination by DNA-dependent protein kinase requires kinase activity, is titratable, and is modulated by autophosphorylation. Mol. Cell. Biol. 31 (2011) 1719-1733.

[35] B.R. Adams, S.E. Golding, R.R. Rao, K.Valerie. Dynamic Dependence on ATR and ATM for Double-Strand Break Repair in Human Embryonic Stem Cells and Neural Descendants. PLoS ONE 5 (2010) e10001.

[36] A. Beucher, J. Birraux, L. Tchouandong, O. Barton, A. Shibata, S. Conrad, A.A. Goodarsi, A. Krempler, P.A. Jeggo, M. Löbrich. ATM and Artemis promote homologous recombination of radiation-induced DNA double-strand breaks in G2. EMBO J. 28 (2009) 3413-3427.

[37] C-G. Shin, J.M. Strayer, M.A. Wani, R.M. Snapka. Rapid Evaluation of Topoisomerase Inhibitors: Caffeine Inhibition of Topoisomerases In Vivo. Teratogenesis, Carcinogenesis, and Mutagenesis 10 (1990) 41-52.

[38] B.E. Griffin, E. Björck, G. Bjursell, T. Lindahl. Sequence complexity of circular Epstein-Bar virus DNA in transformed cells. J. Virol. 40 (1981) 11-19.

[39] P. Norio, C.L. Schildkraut. Visualization of DNA replication on individual Epstein-Barr virus episomes. Science 294 (2001) 2361-2364.

[40] S.M. Beverley. Characterisation of the 'unusual' mobility of large circular DNAs in pulsed field-gradient electrophoresis. Nucleic Acids Res. 16 (1988) 925-939.

[41] R. Maleszka. Single-stranded regions in yeast mitochondrial DNA revealed by pulsed-field gel electrophoresis. Appl. Theor. Electrophor. 3 (1993) 259-263.

[42] M. Wang, E. Lai. Pulsed field separation of large supercoiled and open-circular DNAs and its application to bacterial artificial chromosome cloning. Electrophoresis 16 (1995) 1-7.

[43] A. Adams. Replication of latent Epstein-Barr virus genomes in Raji cells. J. Virol. 61 (1987) 1743–1746.

[44] J,F. Allemand, D. Bensimon, L. Jullien, A. Bensimon, V.Croquette. pH-dependent specific binding and combing of DNA. Biophys. J. 73 (1997) 2064–2070.

[45] E.M. Geigl, F. Eckardt-Schupp. Chromosome-specific identification and quantification of S1 nuclease-sensitive sites in yeast chromatin by pulsed-field gel

electrophoresis. Mol. Microbiol. 4 (1990) 801-810.

[46] J. Legault, A. Tremblay, D. Ramotar, M-E. Mirault. Clusters of S1 nuclease-hypersensitive sites induced in vivo by DNA damage. Mol. Cell. Biol. 17 (1997) 5437-5452.

[47] B. Nevaldine, R. Riswana, P.J. Hahn. No detectable misrejoining in double-minute chromosomes. Radiat. Res. 152 (1999) 154-159.

[48] S.J. Whitaker, T.J. McMillan. Pulsed-Field Gel Electrophoresis in the Measurement of DNA Double-Strand Break Repair in xrs-6 and CHO Cell Lines: DNA Degradation under Some Conditions Interferes with the Assessment of Double-Strand Break Rejoining. Radiat. Res. 130 (1992) 389-392.

[49] C.E. Ng, A.M. Bussey, G.P. Raaphorst. Inhibition of potentially lethal and sublethal damage repair by camptothecin and etoposide in human melanoma cell lines. Int. J. Radiat. Biol. 66 (1994) 49-57.

[50] P. D'Arpa, L.F. Liu. Topoisomerase-targeting antitumor drugs. Biochim. Biophys. Acta 989 (1989) 163-177.

[51] R. Ishida, T. Miki, T. Narita, R. Yui, M. Sato, K.R. Utsumi, K. Tanabe, T. Andoh. Inhibition of intracellular topoisomerase II by antitumor bis(2,6-dioxopiperazine) derivatives: mode of cell growth inhibition distinct from that of cleavable complex-forming type inhibitors. Cancer Res. 51 (1991) 4909-4916.

[52] J. Roca, R. Ishida, J.M. Berger, T. Andoh, J.C. Wang. Antitumor bisdioxopiperazines inhibit yeast DNA topoisomerase II by trapping the enzyme in the form of a closed protein clamp. Proc. Natl. Acad. Sci. U. S. A. 91 (1994) 1781-1785.

[53] M. Sato, R. Ishida, T. Narita, J. Kato, H. Ikeda, H. Fukasawa, T. Andoh. Interaction of the DNA topoisomerase II catalytic inhibitor ICRF-193, a bisdioxopiperazine derivative, with the conserved region(s) of eukaryotic but not prokaryotic enzyme. Biochem. Pharmacol. 54 (1997) 545-550.

[54] H. Gao, E.F. Yamasaki, K.K. Chan, L.L. Shen, R.M. Snapka. Chloroquinoxaline sulfonamide (NSC 339004) is a topoisomerase IIalpha/beta poison. Cancer Res. 60 (2000) 5937-5940.

[55] Y. Hsiang, L.F. Liu. Evidence for the Reversibility of Cellular DNA Lesion Induced by Mammalian Topoisomerase II Poisons. J. Biol. Chem. 264 (1989) 9713-9715.

[56] C. Etiévant, A. Krucsynski, J.M. Barret, D. Perrin, B. van Hille, Y. Guminski, B.T. Hill. F11782, a dual inhibitor of topoisomerases I and II with an original mechanism of action in vitro, and markedly superior in vivo antitumour activity, relative to three other dual topoisomerase inhibitors, intoplicin, aclarubicin and TAS-103. Cancer Chemother. Pharmacol. 4 (2000) 101-113.

[57] L.H. Jensen, A. Renodon-Corniere, K.C. Nitiss, B.T. Hill, J.L. Nitiss, P.B. Jensen, M. Sehested. A dual mechanism of action of the anticancer agent F 11782 on human topoisomerase II alpha. Biochem. Pharmacol. 66 (2003) 623-631.

[58] D. Perrin, B. van Hille, J.M. Barret, A. Krucsynski, C. Etievant, T. Imbert, B.T. Hill. F11782, a novel epipodophylloid non-intercalating dual catalytic inhibitor of topoisomerases I and II with an original mechanism of action. Biochem. Pharmacol. 59 (2000) 807-819.

[59] R.J. Griffin, L.C. Pemberton, D. Rhodes, C. Bleasdale, K. Bowman, A.H. Calvert, N.J. Curtin, B.W. Durkacs, D.R. Newell, J.K. Porteous, B.T. Golding. Novel potent inhibitors of the DNA repair enzyme poly(ADP-ribose) polymerase (PARP-1). Anti-Cancer Drug Design 10 (1995) 507–514.

[60] M. Banasik, H. Komura, M. Shimoyama, K. Ueda. Specific Inhibitors of Poly(ADP-Ribose)synthetase and Mono(ADP-Ribosyl)transferase. J. Biol. Chem. 267 (1992) 1569-1575.

[61] I. Hickson, Y. Shao, C.J. Richardson, S.J. Green, N.M. Martin, A.I. Orr, P.M. Reaper, S.P. Jackson, N.J. Curtin, G.C. Smith. Identification and characterisation of a novel and specific inhibitor of the ataxia-telangiectasia mutated kinase ATM. Cancer Res. 64 (2004) 9152-9159.

[62] J.N. Sarkaria, E.C. Busby, R.S. Tibbetts, P. Roos, Y. Taya, L.M. Karnits, R.T. Abraham. Inhibition of ATM and ATR kinase activities by the radiosensitising agent, caffeine. Cancer Res. 59 (1999) 4375-4382.

[63] A. Dupré, L. Boyer-Chatenet, R.M. Sattler, A.P. Modi, J. Lee, M.L. Nicolette, L. Kopelovich, M. Jasin, R. Baer, T.T. Paull, J. Gautier. A forward chemical genetic screen reveals an inhibitor of the Mre11-Rad50-Nbs1 complex. Nature Chem. Biol. 4 (2008) 119-125.

[64] R.S. Williams, J.S. Williams, J.A. Tainer. Mre11-Rad50-Nbs1 is a keystone complex connecting DNA repair machinery, double-strand break signaling, and the chromatin template. Biochem. Cell Biol. 85 (2007) 509-520.

[65] J.N. Sarkaria, R.S. Tibbetts, E.C. Busby, A.P. Kennedy, D.E. Hill, R.T. Abraham. Inhibition of phosphoinositide 3-kinase related kinases by the radiosensitising agent wortmannin. Cancer Res. 58 (1998) 4375-4382.

[66] J.J. Leahy, B.T. Golding, R.J. Griffin, I.R. Hardcastle, C. Richardson, L. Rigoreau, G.C. Smith. Identification of a highly potent and selective DNA-dependent protein kinase (DNA-PK) inhibitor (NU7441) by screening of chromenone libraries. Bioorg. Med. Chem. Lett. 14 (2004) 6083-6087.

[67] P.J. Mayer, M.O. Bradley, W.W. Nichols. No Change in DNA Damage or Repair of Single- and Double-strand Breaks as Human Diploid Fibroblasts Age In Vitro. Exp. Cell Res. 166 (1986) 497-509.

[68] D. Wlodek, W.N. Hittelman. The Repair of Double-Strand DNA Breaks Correlates with Radiosensitivity of L5178Y-S and L5178Y-R Cells. Radiat. Res. 112 (1987) 146-155.

[69] B. Stenerlöw, K.H. Karlsson, B. Cooper, B. Rydberg. Measurement of prompt DNA double-strand breaks in mammalian cells without including heat-labile sites: results for cells deficient in nonhomologous end joining. Radiat. Res. 159 (2003) 502-510.

[70] T.J. Leach, R.L. Glaser. Quantitative hybridisation to genomic DNA fractionated by pulsed-field gel electrophoresis. Nucleic Acids Res. 26 (1998) 4787-4789.

[71] W. Ma, C.J. Halweg, D. Menendez, M.A. Resnick. Differential effects of poly(ADP-ribose) polymerase inhibition on DNA break repair in human cells are revealed with Epstein–Barr virus. Proc. Natl. Acad. Sci. U. S. A. (2012); published ahead of print April 9, 2012.

[72] R.K. Aneja, H. Sjodin, J.V. Gefter, B. Singarelli, R.L. Delude. Small interfering RNA mediated Poly (ADP-ribose) Polymerase-1 inhibition upregulates the heat shock response in a murine fibroblast cell line. J. Inflamm. 8 (2011) 3.

[73] M. Audebert, B. Salles, P. Calsou. Involvement of poly(ADP-ribose) polymerase-1 and XRCC1/DNA ligase III in an alternative route for DNA double-strand breaks rejoining. J. Biol. Chem. 279 (2004) 55117-55126.

[74] F. Windhofer, W. Wu, G. Iliakis. Low levels of DNA ligases III and IV sufficient for effective NHEJ. J. Cell. Physiol. 213 (2007) 475-483.

[75] M. Johnson, H.H. Phua, S.C. Bennett, J.M. Spence, C.J. Farr. Studying vertebrate topoisomerase 2 function using a conditional knockdown system in DT40 cells. Nucleic Acids Res. 37 (2009) e98.

[76] F. Dantser, G. de la Rubia, J. Ménisser-De Murcia, S. Hostomsky, G. de Murcia, V. Schreiber. Base excision repair is impaired in mammalian cells lacking Poly(ADP-ribose) polymerase-1. Biochemistry 39 (2000) 7559-7569.

[77] K.J. Bowman, A. White, B.T. Golding, R.J. Griffin, N.J. Curtin. Potentiation of anti-cancer agent cytotoxicity by the potent poly(ADP-ribose) polymerase inhibitors NU1025 and NU1064. Br. J. Cancer 78 (1998) 1269–1277.

[78] B.F. Pachkowski, K. Tano, V. Afonin, R.H. Elder, S. Takeda, M. Watanabe, J.A. Swenberg, J. Nakamura. Cells deficient in PARP1 show an accelerated accumulation of DNA single strand breaks, but not AP sites, over the PARP1-proficient cells exposed to MMS. Mutat Res. 671 (2009) 93–99.

[79] J.S. Kim, T.B. Krasieva, H. Kurumisaka, D.J. Chen, A.M. Taylor, K. Yokomori. Independent and sequential recruitment of NHEJ and HR factors to DNA damage sites in mammalian cells, J. Cell. Biol. 170 (2005) 341-347.

[80] E. Sonoda, H. Hochegger, A. Saberi, Y. Taniguchi, S. Takeda. Differential usage of non-homologous end-joining and homologous recombination in double strand break repair. DNA Repair 5 (2006) 1021-1029.

[81] L.S. Symington, J. Gautier. Double-strand break end resection and repair pathway choice. Annu. Rev. Genet. 45 (2011) 247-71. Epub 2011 Sep 12.

[82] S.J. Nelson. Models for DNA Damage Formation and Repair in Mammalian Cells Exposed to Ionising Radiation. Radiat. Res. 92 (1982) 120-145.

[83] J.E. Fowler. Is Repair of DNA Strand Break Damage from Ionising Radiation Second-Order Rather Than First-Order? A Simpler Explanation of Apparently Multiexponential Repair. Radiat. Res. 152 (1999) 124-136.

[84] J. S. Bandstra, P.G. Tratnyek. Central limit theorem for chemical kinetics in complex systems. J. Math. Chem. 37 (2005) 409-422.

[85] N. Foray, B. Fertil, M.G.A. Alsbeih, C. Badie N. Chavaudra, G. Iliakis, E.P. Malaise. Dose-rate effect on radiation-induced DNA double-strand breaks in the human fibroblast HF19 cell line. Int. J. Radiat. Biol. 69 (1996) 241-249.

[86] N. Foray, A-M. Charvet, D. Duchemin, V. Favaudon, D. Lavalette. The repair rate of radiation-induced DNA damage: A stochastic interpretation based on the Gamma function. J. Theoret. Biol. 236 (2005) 448-458.

[87] J. P. Banath, M. Fushiki, P.L. Olive. Rejoining of DNA single- and double-strand breaks in human white blood cells exposed to ionising radiation. Int. J. Radiat. Biol. 73 (1998) 649-660.

[88] A.R. Trseciak, J. Barnes, N. Ejiogu, K. Foster, L.J. Brant, A.B. Sonderman, M.K. Evans. Age, sex, and race influence single-strand break repair capacity in a human population. Free Radic. Biol. Med. 45 (2008) 1631-1641.

[89] O.D. Shahar, E.V. S.R. Ram, E. Shimshoni, S. Hareli, E. Meshorer, M. Goldberg. Live imaging of induced and controlled DNA double-strand break formation reveals extremely low repair by homologous recombination in human cells. Oncogene Nov 21 2011. doi: 10.1038/onc.2011.516. [Epub ahead of print]

[90] K.E. Orii, Y. Lee, N. Kondo, P.J. McKinnon. Selective utilisation of nonhomologous end-joining and homologous recombination DNA repair pathways during nervous system development. Proc. Natl. Acad. Sci. U. S. A. 103 (2006) 10017-10022.

[91] L. Serrano, L. Liang, Y. Chang, L. Deng, C. Maulion, S. Nguyen, J.A. Tischfield. Homologous Recombination Conserves DNA Sequence Integrity Throughout the Cell Cycle in Embryonic Stem Cells. Stem Cells Dev. 20 (2011) 363-374.

[92] H. Fung, D.M. Weinstock. Repair at Single Targeted DNA Double-Strand Breaks in Pluripotent and Differentiated Human Cells. PLoS ONE 6 (2011) e20514.

[93] K. Lobachev, E. Vitriol, J. Stemple, M.A. Resnick, K. Bloom. Chromosome fragmentation after induction of a double-strand break is an active process prevented by the RMX repair complex. Curr. Biol. 14 (2004) 2107-2112.

[94] R. Hancock, The crowded environment of the genome, in: K. Rippe (Ed.), Genome organisation and function in the cell nucleus, Wiley-VCH, Weinheim, 2012, pp. 169-184.

[95] L. Chen, K. Trujillo, P. Sung, A.E. Tomkinson. Interactions of the DNA ligase IV-XRCC4 complex with DNA ends and the DNA-dependent protein kinase. J. Biol. Chem. 275 (2000) 26196-26205.

[96] I.G. Cowell, N.J. Sunter, P.B. Singh, C.A. Austin, B.W. Durkacs, M.J. Tilby. γH2AX Foci Form Preferentially in Euchromatin after Ionising-Radiation. PLoS ONE 2 (2007) e1057.

[97] M. Falk, E. Lukasova, B. Gabrielova, V. Ondrej, S. Kosubek. Local changes of higher-order chromatin structure during DSB repair. J. Phys: Conference Series: 101 (2008) 012018.

5. Appendix

This Section shows some additional data obtained during the course of this work which was not included in the manuscripts submitted for publication.

5.1. Formation and repair of DSBs in genomic DNA

Exposure of Raji cells to γ-radiation also caused the formation of DSBs in genomic DNA in a dose-dependent manner (Figure 5.1 A). At higher doses of radiation, FAR assays of ^{14}C-labelled cellular DNA demonstrated extensive fragmentation of chromatin consistent with the production of multiple DSBs. Interestingly, the slope of the dose–FAR relationship became significantly shallower at higher doses, suggesting that the random breakage model fits the data reasonably well over the lower dose range (0-100 Gy) whereas at higher doses (100-200 Gy) it was approaching asymptotically to a constant value.

Incubation of irradiated cells for up to 2 h changed the size and distribution of the double-stranded fragments towards higher fragment sizes, indicating rejoining of radiation-induced DSBs (Figure 5.1 C). After 2 h the amount of genomic DNA migrating out of the well indicated that almost 80% of all DSBs were repaired (Figure 5.1.D) whereas phosphorylated H2AX histone (γ-H2AX) accumulated in nuclei to a level ~50-fold highter than that in nonnirradiated cells (Figure 5.1E).

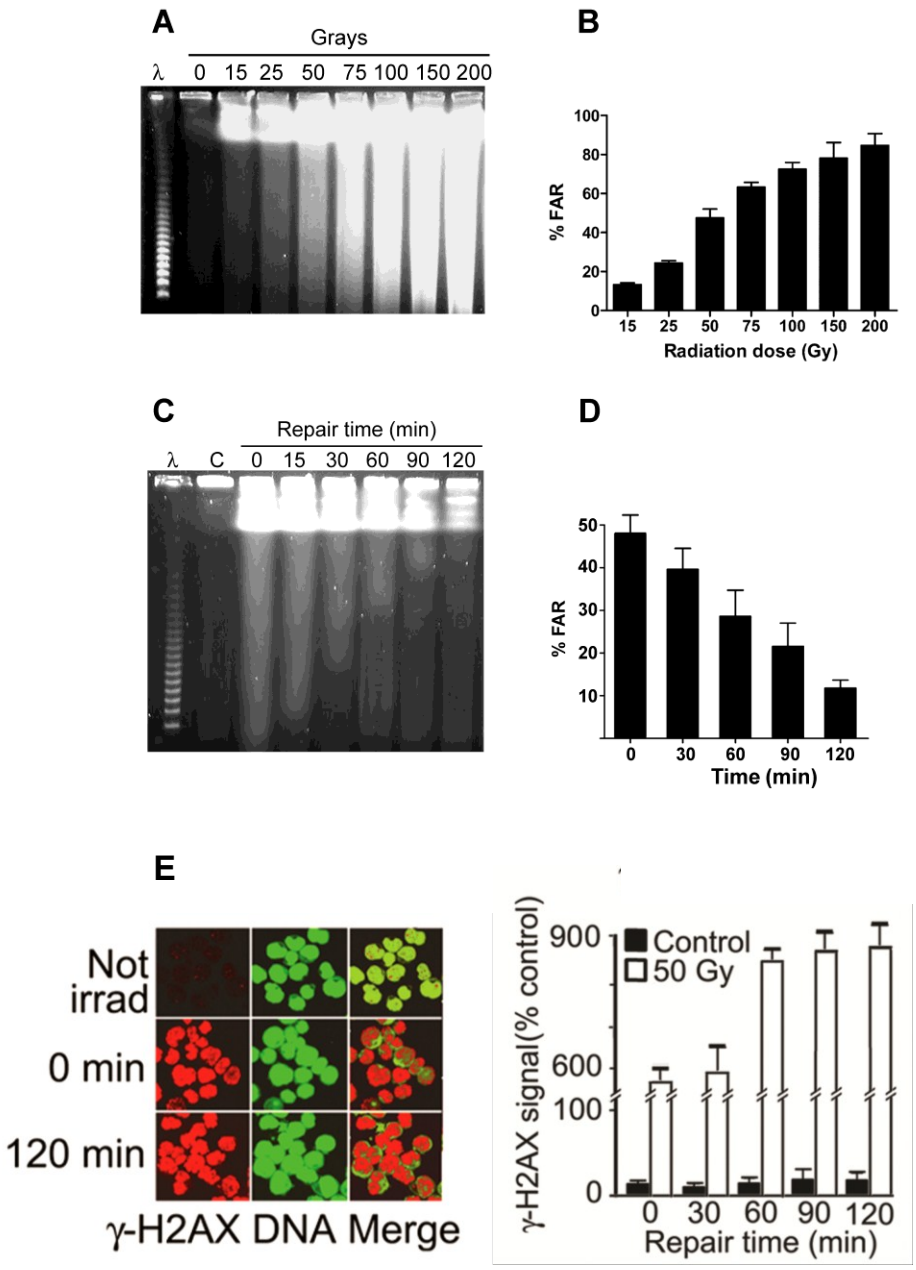

Figure 5.1 Induction and rejoining of DNA DSBs in γ-irradiated cells. Ethidium bromide-stained gels of DNA from Raji cells irradiated with different doses of radiation (**A**) or exposed to 50 Gy and incubated for different periods of time (**C**). Lambda/HindIII DNA served as size standards (lengths shown in kbp). **B** and **D,** FAR assays showing the percentage of ^{14}C-labelled genomic DNA released from the sample well as a function of dose (**B**) or of repair time (**D**). Error bars represent the SEM from three independent

experiments. **E** Formation of γ-H2AX in nuclei of irradiated cells (S2). Left, immunofluorescence (red), DNA stained by YOYO-1 (green). Right, red pixel intensity/ nuclear area relative to nonirradiated cells; error bars show SEM from 200 nuclei.

5.2 DNA polymerases required for recircularization of minichromosome DNA

The level of linear minichromosome DNA during repair decreased at 35% of the control rate in the presence of aphidicolin (Figure 5.2 A) and to an identical extent in the presence of ara-C (data not shown), specific inhibitors of DNA polymerases of the B family, at a concentration (100 μM) which inhibited genomic DNA synthesis by >97% and arrested growth in the G1 phase (Figure 5.2 C). This level decreased normally in the presence of an inhibitor of DNA polymerase β, prunasin (D-mandelonitrile-β-D-glucoside) (data not shown) and of acyclovir, a selective inhibitor of the specific EBV DNA polymerase which replicates EBV viral DNA during productive infection (Figure 5.2. A, B).

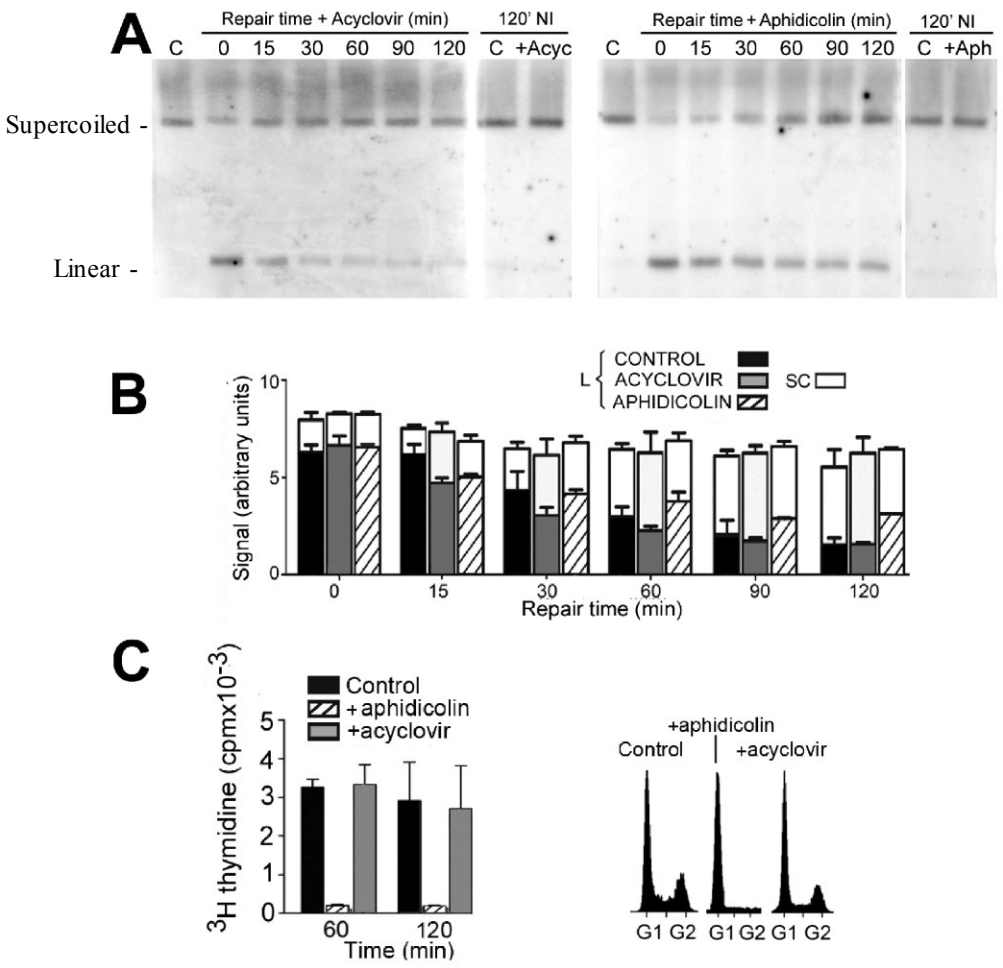

Figure 5.2 Effect of inhibitors of β family DNA polymerases on the repair of minichromosome DNA. (**A**) PFGE gel showing recircularization of the minichromosome in the presence of the DNA polymerase inhibitor aphidicolin (100 μM) or the selective inhibitor of EBV DNA polymerase, acyclovir (100 μM). NI, not irradiated, (**B**) Quantitation of linear and supercoiled forms during repair in the presence of acyclovir or aphidicolin. (**C**) Efficiency of DNA polymerase inhibitors in reducing incorporation of ^{3}H-thymidine into cell DNA (left) and blocking cell cycle traverse (right). Error bars represent the SEM from three independent experiments.

6. General discussion and conclusions

The main objectives of the studies described here focused on the formation and repair of single- and double-strand breaks (SSBs and DSBs) in DNA *in vivo* by ionizing radiation (IR). These types of damage are believed to play the major role in radiation-induced lethality and formation of chromosome deletions, and are therefore crucial to the response of cells to chemo- and radio-therapy [31, 38]. However, in spite of many years of research the precise nature and mechanisms of formation of DNA breaks in chromatin, and the exact mechanisms of their repair in the complex nuclear environment, still remain elusive. A major focus of my research was therefore aimed towards understanding these processes and developing a new model which would allow us to look more precisely into the nature of induction and repair of SSBs and DSBs *in vivo*. In my experiments I used a ~170 kb circular minichromosome which provides a topological analogy with the constrained loops which chromatin is believed to form in cells *in vivo*. This minichromosome, the Epstein-Barr virus (EBV) episome, has a canonical nucleosomal conformation [301] and its DNA sequence, transcription units, promoters, and localised structural features have been well explored and described [304]. These minichromosomes are maintained at ~50-100 copies in each nucleus of Raji (Burkitt lymphoma) cells where they are localized in the perichromatin region adjacent to chromosome territories, and may be tethered to chromatin via the EBNA-1 protein [304, 313].

6.1 DNA in the EBV minichromosomes is cleaved at only a single, randomly-located site in γ-irradiated Raji cells

Exposure of Raji cells to increasing doses of γ-radiation resulted in a decrease of the intensity of the band of supercoiled minichromosome DNA and the appearance of a linear band, while the genomic DNA was fragmented in a dose-dependent manner (Figs. 3.4 and

5.1A respectively). Interestingly, the fraction of supercoiled DNA converted to the linear form by induction of one double strand break reached a maximum at 100 Gy and further irradiation did not induce additional breakage. The production of such a single DSB or a cluster of close DSBs would be consistent with the similar clusters seen in genomic DNA of cells exposed to radiation, which are localised within a distance of 0.1-2 Kbp, and in line with models predicting interactions of radiation tracks with higher-order chromatin structure [34]. The measured frequency of DSBs in the supercoiled minichromosome DNA (~6 x 10^{-3} DSB/Mbp/Gy) was approximately ten times higher than that in genomic DNA in the same cells, as determined by FAR assays (Fig. 5.1B) using the relationships in [314]. To explain this discrepancy, it must be born in mind that values for genomic chromatin are means for the entire genome and that certain regions may be more sensitive to DSB induction than others, and thus the specific localization of minichromosome in the perichromatin region may reflect these variations. However, on the other hand the initial cleavage of the supercoiled minichromosome by radiation followed by its reduced sensitivity could be influenced by distinctive structural features of the native chromatin of the minichromosome, for example the region around oriP which is free of nucleosomes [302] and thus might be expected to be hypersensitive to damage.

In fact, the relationship between the yields of DSBs induced by IR and their distribution in different regions of chromatin has been an area of considerable controversy over the past several years. Starting with the first possibility, there is no consistent evidence indicating that radiation induces fewer DSBs in heterochromatin than in euchromatin, but as recently proposed genetically inactive condensed chromatin is much less susceptible to DSB induction than active euchromatin [273, 309]. However, since no intermediates other than free radicals are generated after energy deposition and their interaction with the DNA molecule are involved in creating strand breaks [315], it appears theoretically unlikely that because of this inactive heterochromatin would be very refractory to generation of DSBs by radiation. The most plausible explanation of this effect could be differences in free radical scavenging capacity between chromatin compartments results in different sensitivities to radiation. Falk et al postulated that lower sensitivity of heterochromatin to damage caused by IR is not a result of its greater condensation *per se* but plausibly the presence of a larger amount of proteins compared to genetically active and decondensed regions [309]. Notably,

it must also be taken into consideration that the majority of these results rely on measurements of numbers of γH2AX foci, and thus it is difficult to distinguish whether or not the observed effect is a result of reduced induction of DSBs *per se* or maybe rather reflects the changes in efficiency of DSB repair (discussed in more detail below).

On the other hand, a few years ago Sak et al. showed a non-random distribution of breaks formed by low LET radiation in the MYC gene locus. In particular, it appeared that DNA close to the matrix attachment regions was more resistant to breakage than the rest of the gene [316]. However other studies have observed no differences in DSB yields or their distributions in different parts of the genome [308]. For example, Rothkamm and Lobrich compared the DSB induction frequencies in the active housekeeping HPRT locus relative to other mostly inactive tissue-specific regions of chromatin and found no difference between them. Additionally, they also found no differences between these regions in normal human fibroblasts and cells of a human bladder carcinoma line and in Chinese Hamster Ovary (CHO) cells containing the dihydrofolate reductase gene [308]. Because the DSB or DSB cluster in minichromosome DNA induced by radiation shows no specific or preferential localisation, we have ruled out the hypothesis about the existence of hypersensitive sites and thus concluded that sensitivity of minichromosome to double-stranded cleavage is not influenced detectably by distinctive structural features of its chromatin.

6.2 A chromatin-dependent conformational change associated with linearization of a circular minichromosome results in resistance to induction of further double strand breaks

The limited cleavage of the minichromosome by restriction enzymes, neocarzinostatin, or etoposide which all potentially have multiple cleavage sites shows that while essentially all supercoiled molecules were linearized, they were not broken further

during the incubation of cells with either the same or another agent. In fact, several other studies of circular minichromosomes have described effects which may have a similar mechanistic origin. Liggins et al. demonstrated that relaxation of the topological constraints in circular SV40 chromatin altered its structure in such a way that the chromatin became highly resistant to the action of restriction nucleases [317]. Additionally, Rösl and Waldeck revealed that the DNA of the circular Bovine Papillomavirus Type 1 episome in its native chromatin state was susceptible to exogenously-added HhaI methyltransferase, but only when the episome was in the intact supercoiled conformation. Pre-treatment of nuclei with enzymes making a single cut in the viral DNA led to resistance of its nucleoprotein complexes to subsequently added HhaI methylase, demonstrating that a native chromatin conformation and DNA topology is crucial for access of the methylase [318].

At this point, we have no clear explanation of the "resistance" phenomenon, but since resistance was completely abolished after the minichromosomes were deproteinized we conclude that its activation must depend on a feature which is determined by proteins associated with the DNA. In fact, it is known that organization of nuclear DNA into both the basic nucleosome repeat structure and higher-order chromatin structure provide significant protection against DSB induction [319]. The measured yield of DSBs in deproteinized DNA was 70 times greater than that in DNA of intact CHO cells, and organization of DNA into the basic nucleosome repeat structure and condensation of the chromatin fibre into higher-order structure protected DNA from DSB induction by factors of 8.3 and 4.5, respectively [34]. Other researchers have found an additional 3- to 5-fold increase in the DSB yield for deproteinized DNA over DNA in chromatin fibres and demonstrated that at a dose of 20 Gy, removal of nonhistone proteins from nuclei results in a 3-fold increase in DSBs compared to intact cells [319]. Moreover, additional stripping of histone H1 results in a moderate increase in breakage whereas further removal of H2A-H2B dimers yields a greater than 10-fold increase in DSBs compared to intact cells, and the dose-response profile for this last sample becomes similar to that observed for purified DNA [319]. Our results seem to be in perfect agreement with the above data, because extraction of histones H1, H2A, H2B, and nonhistone proteins by different salt concentrations makes the linear form no longer resistant to further breakage either by radiation or restriction enzymes. Interestingly, even though histone H1 has been implicated

in stabilizing higher order chromatin folding we did not observe any difference in the sensitivity of minichromosomes after its removal. However, since chromatin fibres visibly compact even without histone H1 and moreover the yeast histone H1 gene homolog is not essential for cell viability [320] our findings still support the main hypothesis that changes in higher order folding of minichromosome chromatin after its linearization influence DNA sensitivity. Under physiological conditions chromatin is an intrinsically dynamic structure even when it seems to be visibly condensed and stable; *in vitro* studies on isolated nucleosome arrays demonstrated that they undergo spontaneous conformational transitions in which a stretch of DNA transiently unwraps off the histone surface and then rewraps. Notably, the rates of such processes are very rapid and nucleosomal DNA remains fully wrapped for only ~250 ms before spontaneous 10–50 ms-long cycles of unwrapping and rewrapping [321]. Thus it is believed that nucleosome positioning considerably influences the accessibility of target sites located on nucleosomes, while chromatin folding dramatically regulates access to target sites in linker DNA [320]. The existence of such a highly dynamic structure might explain the restricted accessibility of the circular DNA in minichromosomes to restriction enzymes and topoisomerase II, since all potential sites except one could be masked from all the cleavage agents by nucleosomes or other chromatin-bound proteins. However, this seems to be more improbable in the case of neocarzinostatin and γ-radiation since most of the damage induced by these agents is mediated indirectly by reactive radicals arising from radiolysis of water molecules, which have many potential cleavage sites and can break DNA on nucleosome cores as well as in linker regions. On the other hand, with their extremely short lifetime (10^{-10} to 10^{-5} s) [322] free radicals can harm DNA only within a radius of a few nanometres and thus more decondensed and hydrated chromatin may be more seriously affected by sparsely-ionizing radiation or neocarzinostatin [323, 324]. The ability of proteins to sequester free radicals and modify radiation damage to DNA is well documented; for instance, histones and inhibition of Fenton oxidation in anoxic conditions were shown to quench the oxidative damage to DNA about 50-fold [319, 325]. Thus more-condensed chromatin may be doubly protected from a harmful effect of sparsely-ionizing radiation or neocarzinostatin by a lower amount of water and a higher concentration of shielding proteins per unit of chromatin volume. This hypothesis seems to find a confirmation in the recent studies

demonstrating that chromatin fibres isolated from cells exposed to 30 Gy of γ-radiation are more regularly folded and have a more compact structure than those from non-irradiated cells [326]. Interestingly, since irradiation did not provoke any concomitant change in the sensitivity to micrococcal nuclease digestion it can be argued that although a repair response was elicited, this may encompass only the sites of damage and not affect the global nuclease accessibility. Therefore, it is reasonable that although DNA damage repair requires a localised decompaction of chromatin fibres, the repair process is accompanied by genome-wide compaction of bulk chromatin fibres which is believed to limit the effects of DNA damage and protect cells from further lesions whilst damaged regions are repaired [326].

In the light of these data, as the most plausible explanation of the observed minichromosome breakage phenomena we propose a model similar to that which was previously suggested for SV40 minichromosomes [317], namely that the initial cut which causes relaxation of topological constraint in the DNA imparts resistance to further breakage. Such a mechanism might involve either "winding" of the internucleosomal DNA into nucleosomes, or its successive right-hand rotation in such a way that linearized molecules would be more compact than the supercoiled form. It is not known if DNA in the EBV minichromosome studied here contains unconstrained superhelicity, but this appears plausible in view of the examples of SV40 and BPV minichromosomes [318, 327]. The principles of the three-dimensional packaging of nucleosomes in a circular minichromosome have not yet been elucidated, but it can be proposed that its conversion to the linear form requires subtle adjustments of their relative orientations and contacts when the axis of the chromatin fibre changes from a curved to a linear conformation. Since at least some regions of the genomic DNA of eukaryotes is negatively supercoiled and in a torsionally strained state [328] and although the influence of DNA supercoiling on basic biological processes has been investigated in some depth, its role in the susceptibility of DNA to damage by ionizing radiation remains poorly understood and, in the light of our results, opens completely new possibilities.

6.3 NHEJ is the major pathway for repair of DSBs in minichromosome DNA

Our initial observation that irradiated Raji cells are able to re-circularize up to 80% of minichromosome DNA during the first 2 h of incubation for repair (see Chapter 4) encouraged us to examine the relative contribution of each of the known repair pathways in this process. In theory, SSBs should be repaired by an error-free short- or long-patch mechanism, both based on the use of the undamaged strand as a template. On the other hand repair of DSBs can follow either of two pathways, the error-free homologous recombination (HR) route which repairs a break using the homologous chromatid or chromosome as template, or the error-prone nonhomologous end-joining (NHEJ) route that processes and ligates the DNA ends directly [1, 78]. To dissect which of these pathways is involved in the repair of minichromosome DNA in irradiated cells, we chemically inhibited known pathway-specific proteins and quantitated the recircularization of minichromosome DNA (Fig. 4.4 and 4.5). To arrest NHEJ, cells were incubated with wortmannin or NU7441, two well-studied and potent inhibitors of DNA-protein kinase (DNA-PKcs). On the other hand, due to the lack of specific inhibitors of HR we inhibited the proteins Mre11 and ATM, which have been postulated to participate in HR to a much larger extent than in NHEJ [201, 329]. Interestingly, the response of minichromosome DSBs repair to these inhibitors presents an obvious paradox: on the one hand inhibitors of DNA-PKcs completely arrest the repair of DSBs leading to the conclusion that religation and recircularization of minichromosome DNA are carried out exclusively by NHEJ, whereas on the other hand inhibitors of ATM or Mre11, which predominantly affect HR, arrest repair in ~30% of the molecules. To explain these contradictory results, we considered two types of possible scenarios. In the first, we took into consideration the possibility that arrest of HR by inhibition of ATM or Mre11 may not be as specific as previously reported and that ATM [330] as well as Mre11 [331] could be also partially involved in the NHEJ pathway. However, siRNA depletion of the Rad51 protein, which is involved uniquely in HR [215, 225], revealed that under these conditions recircularization of minichromosome DNA was reduced to an almost identical extent as when ATM and Mre11 were inhibited,

thus ruling out this hypothesis. Interestingly, in the complete absence of DNA-PKcs the majority of DSB repair is shunted toward HR, but when DNA-PKcs is present but catalytically inactive both the HR as well as the NHEJ pathway is blocked [332]. Moreover, Chan and Lees-Miller demonstrated in *in vitro* studies that autophosphorylation of DNA-PKcs is crucial for its dissociation from damaged DNA [142] and that inhibition of the kinase activity of DNA-PK by wortmannin completely abolishes this dissociation.

As the most plausible explanation of our observations, we propose a model similar to that already suggested [332] in which enzymatically-inactive DNA-PKcs holoenzyme immobilized on DNA ends leads to their physical inaccessibility to other repair proteins and thus arrests both DSB repair pathways. In this scenario, DNA-PKcs attaches to DNA ends earlier than other proteins involved in NHEJ and HR and becomes, in effect, a dominant negative inhibitor of both pathways. In contrast, when ATM and Mre11 are inhibited DNA-PKcs can still dissociate from the ends leaving them accessible for repair. To summarize, we propose that even though inhibitors of DNA-PKcs completely inhibit repair of DSBs in minichromosome DNA, plausibly by immobilizing the enzyme on the ends at DSBs, inhibition of ATM, Mre11 and especially depletion of Rad51 by siRNA indicates that the majority of repair of broken molecules takes place by the NHEJ pathway and only about 25% are religated by HR.

6.4 At high irradiation doses, disappearance of γH2AX foci does not necessarily reflect repair of DSBs

One of the first signalling processes triggered by DSBs is the phosphorylation of histone H2AX to form γH2AX, which accumulates at intranuclear foci [272]. This specific, ATM- and DNA-PK-dependent chromatin modification spreads over more than tens of kilobases around the DSB, and has been proposed to play numerous roles in the recognition of breaks and their repair. Formation and loss of γ-H2AX foci has been observed following exposure to radiation doses as low as 1 mGy, and the number of foci has been shown to

increase approximately linearly with the dose up to 100 Gy [333] In fact, after 100 Gy the fluorescence signal approaches saturation due to phosphorylation of almost all H2AX molecules, because the frequency of DSBs at this dose is approximately one in every 2 Mbp of DNA [333]. It is generally accepted that the initial number of γ-H2AX foci formed per nucleus agrees with the number of DSBs [272], and their disappearance over time follows rejoining of DSBs in repair-competent cells as well as in those where DSB repair is arrested by inhibition of key repair proteins [272]. In our studies, γH2AX foci accumulated in nuclei of irradiated Raji cells during the 2 h repair period to a level ~50-fold higher than that in non-irradiated cells (Fig. 5.1E). Interestingly, although the minichromosome DNA was recircularized and genomic chromatin was repaired as measured by FAR assays, we did not detect any decrease in the intensity or number of γH2AX foci. We speculate that in this case the formation and disappearance of γH2AX foci is not an exact reflection of the number of DSBs *per se,* but rather is only one part of a global signalling process that responds to alterations in chromatin. In fact, several studies have demonstrated that changes in chromatin structure are sufficient to elicit extensive formation of γ-H2AX foci in the relative absence of DNA strand breaks. For example, Clingen et al. demonstrated that γH2AX can act as a highly sensitive and general marker of DNA damage induced by the interstrand cross-linking agents mechlorethamine or Cisplatin [334], while Marti et al. observed that histone H2AX is also phosphorylated in response to UV irradiation in a process which depends strictly on nucleotide excision repair factors [335]. Thus in both of these cases the formation of γH2AX foci is not a response to DSBs specifically, but rather to changes in chromatin caused by different types of DNA damage. Further support for this hypothesis comes from recent studies demonstrating that expansion of chromatin in cells incubated in a hypotonic solution, which does not cause any detectable DSBs, is a sufficient signal to induce the formation of γH2AX foci to an extent equivalent to that seen after formation of 80–200 DSBs by ~5 Gy of γ-radiation [336]. These publications together with our data, suggests that γH2AX foci function primarily as a general sensor of alterations in chromatin structure resulting from effects of genotoxic conditions, rather than as a specific indicator of DSBs and their repair; one could speculate that selective pressure for its adaptation into a DSB-response niche may have been provided by exposure of cells to radiation early in evolution. Since the radiation dose used here was several-fold above

the lethal dose, it is plausible that the formation of foci reflects major alterations in chromatin structure rather than the number of DSBs and their repair

6.5 Repair of SSBs in minichromosome DNA is PARP-1-independent

Despite its central function in the Base Excision Repair pathway and in the metabolism of PAR, the relative importance of PARP-1 for repair of SSBs is still unclear. Although inhibitors of PARP cause an increase in radiosensitivity of cells, it is difficult to ascribe this effect totally to inhibition of SSB repair. Chemical inhibition of the catalytic activity of PARP-1 slows the rate of SSBR and prevents complete rejoining of the breaks, but does not arrest the overall process completely [337]. On the other hand, Vodenicharov et al. demonstrated that repair of SSBs is very efficient in X irradiated mouse fibroblasts lacking PARP-1, and moreover removal or depletion of PARP-1 from chicken as well as human cells did not ablate SSB repair but rather reduced its global rate [338]. Since the same effect was observe in cells lacking XRCC1, a known scaffold protein for repair of SSBs, it is possible that the residual SSB repair in cells lacking PARP-1 or XRCC1 reflects the presence of partially redundant systems [339]. Alternatively, it is possible that XRCC1 and PARP-1 serve only to accelerate SSB repair by increasing the rate at which other repair proteins access chromosomal SSBs. In fact, as recently proposed there is a peculiar switch between the long- (LPR) and short- (SPR) patch sub-pathways of SSB repair that depends on the presence and/or activity of PARP-1 [67]. According to this model, although chemical inhibition of poly(ADP-ribosyl)ation in PARP-1 proficient cells results in accumulation of PARP-1 in the vicinity of sites of DNA damage and initially reduces the global rate of SSB repair, it does not impact the radiosensitivity of cells probably because they have enough time to perform repair via the LPR sub-pathway. Although the exact role of PARP-1 in LPR is still unclear, it seems not to be as essential as it is for SPR. The lack of effect of inhibitors of PARP on rejoining of SSBs in minichromosome DNA is consistent with the evidence that its enzymatic activity accelerates, but is not essential for,

the repair of this kind of DNA lesion [67, 339], and we propose that SSBs in minichromosome DNA are repaired by a PARP-1-independent pathway.

6.6 DNA topoisomerases are not involved in the repair of DSBs in minichromosome DNA or in its recircularization

DNA topoisomerases I and II are key enzymes involved in carrying out high-precision checkups of chromatin conformation inside the cell nucleus. They have unique functions of co-ordinated cleaving, manipulating, and religating DNA strands, thereby regulating DNA superhelicity and disentangling regions of chromosomes [17]. It has been unclear if the activity of either of these enzymes is essential during the repair of strand breaks [340], and theoretical arguments suggest that this would depend on the dynamics of the neighbouring nucleosomes. In genomic DNA, only a few nucleosomes at the most appear to migrate, dissociate, or be disrupted during repair of a strand break [251]. It could be speculated that if all nucleosomes remain associated with minichromosome DNA after the formation and repair of a break, the DNA's negative superhelicity will remain unchanged and the activity of topoisomerases would not be required during its recircularization. On the other hand it can be hypothesized that if some nucleosomes dissociate during these processes, the negative superhelicity of the circular molecules formed by religation would be reduced and topoisomerase activity, probably topoisomerase II [341], would be essential to normalize the superhelicity before or during final reassembly with nucleosomes.

Previously published studies of requirements for topoisomerases for DSB repair [340] are difficult to interpret because non-catalytic ("poisoning") inhibitors of topoisomerases II (etoposide) and I (camptothecin) were employed which themselves cause strand breaks when DNA is purified, thus masking any effects on repair. Additionally, recent studies which suggest the possible involvement of topoisomerase II in post-radiation repair of DSBs are quite elusive due to the low specificity of the inhibitors tested and their possible influence on the cellular repair process as a whole, independently of the suppression of

topoisomerase activity [340, 342, 343]. As reported by Mateos et al. these inhibitors increase cell killing caused by x-radiation, suggesting that in fact topoisomerases may participate directly or indirectly in the repair of radiation-induced DNA damage [343]. In our experiments we used the very specific catalytic inhibitors ICRF-193 for topoisomerase II and F11782 for both topoisomerase I and II, which in contrast to etoposide and camptothecin completely arrest the enzyme's catalytic activity without formation of a "cleavable complex". We demonstrated unambiguously that the inhibition of topoisomerase I or II activity does not change the rate of recircularization of minichromosome DNA, suggesting that the radiosensitizing effect observed by Mateos et al. was not a result of inhibition of DSB repair. At this point it is difficult to evaluate what role, if any, topoisomerases might play in slowing recovery from radiation damage, but one could speculate that this could be a result of restarting cell replication while the catalytic activity of topoisomerases is inhibited; since topoisomerases are known to participate in DNA replication [17] a reduction of the number of active molecules could lead to DNA lesions caused by the impossibility of resolving the topological problems arising during replication fork progression, and accumulation of such lesions could decrease clonogenic survival and thereby sensitize the cells to radiation.

6.7 Involvement of DNA polymerases in repair of DSBs

As mentioned in the Introduction, the extremities of DNA at radiation-induced DSBs are frequently called "dirty" ends because they are characterized by additional complex nucleotide damage that forms gaps and overhangs on the broken termini [344]. Because the only proper substrate for DNA ligases are correct 3'-OH and 5'-phosphate termini, such modifications have to be cleaned and the resultant gaps re-filled before the subsequent religation process. It is still a matter of controversy which DNA polymerases are involved in the re-synthesis of missing sequences near to the broken ends. Cells with a knock-out of polymerase μ or λ, the main candidates for participation in DSB repair, do not show an increased sensitivity to DNA-damaging agents [170, 171] suggesting that other

polymerases may be involved in the DSB repair process. Because successful depletion of DNA polymerases other than polymerase β [345] has not been reported to our knowledge, we used specific and potent chemical inhibitors to assess which polymerases may be involved in repair of minichromosome DNA. The slower repair of linear DNA in the presence of aphidicolin or cytosine arabinoside shows that a DNA polymerase of the B family, which includes the replicative DNA polymerase α, is needed to replace damaged components of DNA. In genomic DNA, repair of ~40% of the DSBs produced by ionizing radiation is inhibited by aphidicolin and other polymerases mediate the repair of more complex lesions [346]. Further, from the kinetics of repair of the linear form of minichromosome DNA in the presence of aphidicolin or Ara-C it can be observed that inhibition is not detectable during the first hour but becomes evident after this time (Fig. 5.2). This later effect may reflect the greater complexity of repair of "dirty" DNA ends which requires the participation of polymerases and takes a longer time than the repair of "clean" ends which can be ligated rapidly.

6.8 Mathematical modelling of the repair of single- and double-strand breaks in minichromosome DNA reveals a novel dynamic aspect of the global strand break repair process

DNA damage and repair can be modelled mathematically in several possible ways, and a detailed description should take mechanistic relationships into account. In our case an essential element in quantitative modelling of the dynamics of operation of the pathways was the observed arrest of the conversion of linear minichromosome DNA to other conformations when repair of DSBs was completely blocked by inhibitors of DNA-PKcs (Fig. 4.7). The simplified model which we developed considered the different forms of minichromosome DNA as four compartments, and allowed calculation of the amount of circular EBV form containing SSBs which could not have been deduced directly from the

experimental data (Fig. 4.8A). Moreover, by using this approach we were also able to calculate exact rate constants for the repair of SSBs and DSBs in the same cells as well as in the same region of chromatin *in vivo*.

The first main conclusion which could be drawn from modelling is that repair of SSBs and DSBs appears to operate independently, since when repair of DSBs was arrested the SSBs in both linear and circular molecules were still repaired and the rate of conversion of circular molecules containing SSBs to supercoiled molecules was almost identical to that in normal conditions. Additionally, based on these calculations (and confirmed by nuclease S1 digestion experiments (Fig. 4.2)) SSBs were more frequent than DSBs in minichromosome DNA immediately after irradiation because ~30% of the total molecules were calculated to contain SSBs but to remain circular (Fig. 8A, CSSB), consistent with the higher frequency of SSBs than DSBs in genomic DNA [347] and in the DNA of SV40 minichromosomes in the nuclei of irradiated cells [348]. In terms of complete repair, ~50% of the minichromosome DNA molecules were predicted to regain a supercoiled conformation after repair for 4 h and more than 80% after 20 h (Fig. 4.8C). These results are consistent with the putative biphasic repair of SSBs, with a fast component rejoining most of the damage in the first few hours after irradiation and a slow component that repairs residual breaks within 24 h [349]. Finally, it follows from the calculated rate constants, which we recall do not refer to the repair of individual strand breaks but to the complete repair of all the breaks in a minichromosome, that in the average molecule of linear minichromosome DNA the single DSB was repaired ~3.5 times faster than all the SSBs. This suggests that in a single minichromosome molecule the rate-limiting step in complete repair was the repair of the SSBs, which on the average were 5 times more abundant than DSBs.

Additionally, as mentioned above one of the greatest advantages of our model system was the ability to quantitate simultaneously both SSBs and DSBs and to follow and model their rejoining in a defined region of chromatin *in vivo*. For example, an approximate rate for the repair of DSBs in minichromosome DNA could be derived from the changes in the abundance of linear (L+LSSB) molecules during repair. After 60 min these molecules had decreased from around 55% to 38% of the total signal (Fig. 4.8B), implying that around 30% of the linear molecules had been circularised, i.e. their single DSB had been repaired. If we assume that each cell contained roughly ~100 copies of minichromosome DNA each

of length 172 kb, the total number of repaired DSBs was therefore ~16 in 5.16 Mb (172 kb x 30) of DNA in 60 min, or ~3 DSBs repaired/Mb DNA/h. For genomic DNA, the average of published rates is ~1-2 DSBs repaired /Mb/h [350] and considering the different technical approaches and the uncertainties in the values used for these calculations the rate of repair of DSBs in the minichromosome does not appear to differ widely from that in genomic chromatin. This small difference could be an effect of the localization of minichromosomes in perichromatin regions of the nucleus. As discussed above, there are two distinct nuclear chromatin compartments, hetero- and eu-chromatin, and whereas the first is a gene-poor region which remains condensed during interphase, the second is less compact and rich in genes and comprises the most active portion of the genome. It is a still of matter of controversy how these two different compartments of chromatin respond to the induction of DSBs, but since a few years there is emerging evidence suggesting that the susceptibility to formation of DSBs and especially their repair differs greatly between these two nuclear environments; open chromatin is believed to be much more sensitive to radiation damage than compact chromatin [273, 309], but this is not a consequence of the reduced chromatin condensation *per se* but rather of its functional properties because its radiosensitivity and the frequency of DSBs measured by γH2AX foci are not influenced when its condensation is increased in hypertonic media [309]. Additionally, since theoretical considerations suggest an essentially random distribution of DSBs induced by X-radiation, the observed difference in formation of γH2AX foci may be related to specific characteristics of the processing and repair of breaks in eu- and hetero-chromatin rather than to a different frequency of breaks. Since γH2AX is regarded as a platform for the recruitment or retention of other DNA repair and signalling molecules [272] its preferential localization in euchromatic regions following X-irradiation [273] implies that the processing of DSBs in heterochromatin differs from that in euchromatin. At the same time, it could be speculated that the specific localization of minichromosome in perichromatin regions may allow its faster and more adequate repair.

6.9 General conclusion

The results presented here provide insights into the formation and the kinetics of repair of SSBs and DSBs produced by IR in a chromatin context *in vivo*. As a model, we used a multicopy ~170 kb circular minichromosome which has all the characteristics of genomic chromatin and is maintained at ~50 copies per nucleus of Raji cells, so that its different topological forms and fragments resulting from breakage can be readily separated and quantitated.

Our results demonstrate that at the higher radiation doses, all the supercoiled circular minichromosome DNA molecules were converted to the linear form due to the formation of one, randomly located DSB. Moreover, extended studies with other DSB-inducing reagents which all potentially can cause multiple DNA strand breaks revealed that all of these cleave the minichromosome DNA only at one random site (with the predicted exception of restriction enzymes). In view of these data we propose that after an initial cut, the minichromosome chromatin undergoes a conformational change, possibly associated with loss of unrestrained superhelicity in its DNA, which results in inaccessibility of the linear form to OH radicals produced by IR and to the other probes used.

After irradiation, the single DSB was repaired, mostly by the non homologous end joining pathway, and supercoiled minichromosome DNA was reformed without any erroneous end-joining which would have formed linear oligomers. By using this approach we demonstrated that the process of recircularization was unaffected by inhibitors of poly(ADP-ribose) polymerase, or by catalytic inhibitors of topoisomerases I and II whose implication in DSBs repair has been controversial. Additionally, a mathematical model fitting the experimental data provided rate constants for the repair of SSBs and DSBs, and showed that minichromosomes containing only a DSB were recircularised ~3.5 times more rapidly than those which also contained SSBs so that the rate-limiting step in complete repair was the repair of the SSBs, plausibly reflecting the several-fold greater abundance of SSBs than DSBs.

As far as we are aware, these are the first experiments that quantitate the formation and repair of single- and double-strand breaks in a specific region of chromatin at the same

time *in vivo*. In view of the analogies of this minichromosome to a closed loop of chromatin, this data may provide useful insights into the formation and kinetics of repair of strand breaks in genomic chromatin.

7. References

1. Mahaney, B.L., K. Meek, and S.P. Lees-Miller, *Repair of ionizing radiation-induced DNA double-strand breaks by non-homologous end-joining.* Biochem J, 2009. **417**(3): p. 639-50.
2. De Bont, R. and N. van Larebeke, *Endogenous DNA damage in humans: a review of quantitative data.* Mutagenesis, 2004. **19**(3): p. 169-85.
3. Goodhead, D.T., *Initial events in the cellular effects of ionizing radiations: clustered damage in DNA.* Int J Radiat Biol, 1994. **65**: p. 7-17.
4. Arbault, C.A.a.S., *Oxidative Stress at the Single Cell Level*, in *Electrochemical Methods for Neuroscience*, A.C.M.a.L.M. Borland, Editor. 2007, CRC Press: University of Pittsburgh, Pennsylvania.
5. Ames, B.N., *Endogenous DNA damage as related to cancer and aging.* Mutat Res, 1989. **214**(1): p. 41-6.
6. Pfeiffer, P., W. Goedecke, and G. Obe, *Mechanisms of DNA double-strand break repair and their potential to induce chromosomal aberrations.* Mutagenesis, 2000. **15**(4): p. 289-302.
7. Altieri, F., et al., *DNA damage and repair: from molecular mechanisms to health implications.* Antioxid Redox Signal, 2008. **10**(5): p. 891-937.
8. Esterbauer, H., P. Eckl, and A. Ortner, *Possible mutagens derived from lipids and lipid precursors.* Mutat Res, 1990. **238**(3): p. 223-33.
9. Newton, D.L., et al., *RNA damage and inhibition of neoplastic endothelial cell growth: effects of human and amphibian ribonucleases.* Radiat Res, 2001. **155**: p. 171-174.
10. Szymanski, M. and J. Barciszewski, *Beyond the proteome: non-coding regulatory RNAs.* Genome Biol, 2002. **3**: p. reviews0005.
11. Ma, S., et al., *Low-dose radiation-induced responses: focusing on epigenetic regulation.* Int J Radiat Biol, 2010. **86**: p. 517-28.
12. Ilnytskyy, Y., et al., *Altered microRNA expression patterns in irradiated hematopoietic tissues suggest a sex-specific protective mechanism.* Biochem Biophys Res Commun, 2008. **377**: p. 41-5.

13. Josson, S., et al., *Radiation modulation of microRNA in prostate cancer cell lines.* Prostate, 2008. **68**: p. 1599-606.
14. Tse, Y.C., K. Kirkegaard, and J.C. Wang, *Covalent bonds between protein and DNA. Formation of phosphotyrosine linkage between certain DNA topoisomerases and DNA*. J Biol Chem, 1980. **255**: p. 5560-5.
15. Cress, A.E. and G.T. Bowden, *Covalent DNA-protein crosslinking occurs after hyperthermia and radiation.* Radiat Res, 1983. **95**: p. 610-9.
16. Fornace, A.J., Jr. and J.B. Little, *DNA crosslinking induced by x-rays and chemical agents.* Biochim Biophys Acta, 1977. **477**: p. 343-55.
17. Corbett, K.D. and J.M. Berger, *Structure, molecular mechanisms, and evolutionary relationships in DNA topoisomerases.* Annu Rev Biophys Biomol Struct, 2004. **33**: p. 95-118.
18. Kuzminov, A., *Single-strand interruptions in replicating chromosomes cause double-strand breaks.* Proc Natl Acad Sci U S A, 2001. **98**: p. 8241-6.
19. Pfeiffer, P., W. Goedecke, and G. Obe, *Mechanisms of DNA double-strand break repair and their potential to induce chromosomal aberrations.* Mutagenesis, 2000. **15**: p. 289-302.
20. Roots, R., G. Kraft, and E. Gosschalk, *The formation of radiation-induced DNA breaks: the ratio of double-strand breaks to single-strand breaks.* Int J Radiat Oncol Biol Phys, 1985. **11**: p. 259-65.
21. Hegde, M.L., T.K. Hazra, and S. Mitra, *Early steps in the DNA base excision/single-strand interruption repair pathway in mammalian cells.* Cell Res, 2008. **18**(1): p. 27-47.
22. El-Khamisy, S.F., et al., *Defective DNA single-strand break repair in spinocerebellar ataxia with axonal neuropathy-1.* Nature, 2005. **434**(7029): p. 108-13.
23. Kuzminov, A., *Single-strand interruptions in replicating chromosomes cause double-strand breaks.* Proc Natl Acad Sci U S A, 2001. **98**(15): p. 8241-6.
24. Bendixen, C., et al., *Camptothecin-stabilized topoisomerase I-DNA adducts cause premature termination of transcription.* Biochemistry, 1990. **29**(23): p. 5613-9.

25. Heeres, J.T. and P.J. Hergenrother, *Poly(ADP-ribose) makes a date with death.* Curr Opin Chem Biol, 2007. **11**(6): p. 644-53.
26. Bryant, P.E., L.J. Gray, and N. Peresse, *Progress towards understanding the nature of chromatid breakage.* Cytogenet Genome Res, 2004. **104**(1-4): p. 65-71.
27. Ma, Y., et al., *Hairpin opening and overhang processing by an Artemis/DNA-dependent protein kinase complex in nonhomologous end joining and V(D)J recombination.* Cell, 2002. **108**(6): p. 781-94.
28. Jackson, S.P., *Sensing and repairing DNA double-strand breaks.* Carcinogenesis, 2002. **23**(5): p. 687-96.
29. Kantidze, O.L., O.V. Iarovaia, and S.V. Razin, *Assembly of nuclear matrix-bound protein complexes involved in non-homologous end joining is induced by inhibition of DNA topoisomerase II.* J Cell Physiol, 2006. **207**(3): p. 660-7.
30. Podgorsak, E.B., *Radiation oncology physics: a handbook for teachers and students*. 2006, Viena: International Atomic Energy Agency,.
31. Jeggo, P. and M.F. Lavin, *Cellular radiosensitivity: how much better do we understand it?* Int J Radiat Biol, 2009. **85**(12): p. 1061-81.
32. Gollapalle, E., et al., *Detection of oxidative clustered DNA lesions in X-irradiated mouse skin tissues and human MCF-7 breast cancer cells.* Radiat Res, 2007. **167**(2): p. 207-16.
33. Ward, J.F., *Biochemistry of DNA lesions.* Radiat Res Suppl, 1985. **8**: p. S103-11.
34. Prise, K.M., et al., *A review of studies of ionizing radiation-induced double-strand break clustering.* Radiat Res, 2001. **156**(5 Pt 2): p. 572-6.
35. Kawata, T., et al., *G2 chromatid damage and repair kinetics in normal human fibroblast cells exposed to low- or high-LET radiation.* Cytogenet Genome Res, 2004. **104**: p. 211-5.
36. Ward, J.F., *DNA damage produced by ionizing radiation in mammalian cells: identities, mechanisms of formation, and reparability.* Prog Nucleic Acid Res Mol Biol, 1988. **35**: p. 95-125.
37. Ward, J.F., *The complexity of DNA damage: relevance to biological consequences.* Int J Radiat Biol, 1994. **66**: p. 427-32.

38. Kadhim, M.A., M.A. Hill, and S.R. Moore, *Genomic instability and the role of radiation quality*. Radiat Prot Dosimetry, 2006. **122**(1-4): p. 221-7.
39. Tell, R., et al., *Comparison between radiation-induced cell cycle delay in lymphocytes and radiotherapy response in head and neck cancer.* Br J Cancer, 1998. **77**(4): p. 643-9.
40. Schafer, K.A., *The cell cycle: a review*. Vet Pathol, 1998. **35**: p. 461-78.
41. Vermeulen, K., D.R. Van Bockstaele, and Z.N. Berneman, *The cell cycle: a review of regulation, deregulation and therapeutic targets in cancer.* Cell Prolif, 2003. **36**: p. 131-49.
42. Jeggo, P.A. and M. Lobrich, *Contribution of DNA repair and cell cycle checkpoint arrest to the maintenance of genomic stability.* DNA Repair (Amst), 2006. **5**: p. 1192-8.
43. Shiloh, Y., *ATM and related protein kinases: safeguarding genome integrity.* Nat Rev Cancer, 2003. **3**(3): p. 155-68.
44. Shiloh, Y. and M.B. Kastan, *ATM: genome stability, neuronal development, and cancer cross paths.* Adv Cancer Res, 2001. **83**: p. 209-54.
45. Bakkenist, C.J. and M.B. Kastan, *DNA damage activates ATM through intermolecular autophosphorylation and dimer dissociation.* Nature, 2003. **421**(6922): p. 499-506.
46. Krajewski, W.A., *Alterations in the internucleosomal DNA helical twist in chromatin of human erythroleukemia cells in vivo influences the chromatin higher-order folding*. FEBS Lett, 1995. **361**(2-3): p. 149-52.
47. Uziel, T., et al., *Requirement of the MRN complex for ATM activation by DNA damage*. Embo J, 2003. **22**(20): p. 5612-21.
48. Difilippantonio, S. and A. Nussenzweig, *The NBS1-ATM connection revisited.* Cell Cycle, 2007. **6**(19): p. 2366-70.
49. Kozlov, S.V., et al., *Involvement of novel autophosphorylation sites in ATM activation*. Embo J, 2006. **25**(15): p. 3504-14.
50. Pandita, T.K., et al., *Ionizing radiation activates the ATM kinase throughout the cell cycle*. Oncogene, 2000. **19**(11): p. 1386-91.

51. Goodarzi, A.A., et al., *Autophosphorylation of ataxia-telangiectasia mutated is regulated by protein phosphatase 2A.* Embo J, 2004. **23**(22): p. 4451-61.
52. Ali, A., et al., *Requirement of protein phosphatase 5 in DNA-damage-induced ATM activation.* Genes Dev, 2004. **18**(3): p. 249-54.
53. Sun, Y., et al., *A role for the Tip60 histone acetyltransferase in the acetylation and activation of ATM.* Proc Natl Acad Sci U S A, 2005. **102**(37): p. 13182-7.
54. Gupta, A., et al., *Involvement of human MOF in ATM function.* Mol Cell Biol, 2005. **25**(12): p. 5292-305.
55. Matsuoka, S., et al., *ATM and ATR substrate analysis reveals extensive protein networks responsive to DNA damage.* Science, 2007. **316**(5828): p. 1160-6.
56. Unger, T., et al., *Critical role for Ser20 of human p53 in the negative regulation of p53 by Mdm2.* Embo J, 1999. **18**(7): p. 1805-14.
57. Shackelford, R.E., W.K. Kaufmann, and R.S. Paules, *Cell cycle control, checkpoint mechanisms, and genotoxic stress.* Environ Health Perspect, 1999. **107 Suppl 1**: p. 5-24.
58. Khanna, K.K., et al., *Nature of G1/S cell cycle checkpoint defect in ataxia-telangiectasia.* Oncogene, 1995. **11**(4): p. 609-18.
59. Shiloh, Y., *ATM and ATR: networking cellular responses to DNA damage.* Curr Opin Genet Dev, 2001. **11**(1): p. 71-7.
60. Beamish, H. and M.F. Lavin, *Radiosensitivity in ataxia-telangiectasia: anomalies in radiation-induced cell cycle delay.* Int J Radiat Biol, 1994. **65**(2): p. 175-84.
61. Horton, J.K., et al., *XRCC1 and DNA polymerase beta in cellular protection against cytotoxic DNA single-strand breaks.* Cell Res, 2008. **18**: p. 48-63.
62. Dianov, G.L. and J.L. Parsons, *Co-ordination of DNA single strand break repair.* DNA Repair (Amst), 2007. **6**: p. 454-60.
63. Caldecott, K.W., *Mammalian DNA single-strand break repair: an X-ra(y)ted affair.* Bioessays, 2001. **23**: p. 447-55.
64. Vidakovic, M., G. Poznanovic, and J. Bode, *DNA break repair: refined rules of an already complicated game.* Biochem Cell Biol, 2005. **83**(3): p. 365-73.
65. Fortini, P., et al., *Different DNA polymerases are involved in the short- and long-patch base excision repair in mammalian cells.* Biochemistry, 1998. **37**: p. 3575-80.

66. Mortusewicz, O. and H. Leonhardt, *XRCC1 and PCNA are loading platforms with distinct kinetic properties and different capacities to respond to multiple DNA lesions.* BMC Mol Biol, 2007. **8**: p. 81.

67. Godon, C., et al., *PARP inhibition versus PARP-1 silencing: different outcomes in terms of single-strand break repair and radiation susceptibility.* Nucleic Acids Res, 2008. **36**(13): p. 4454-64.

68. Ame, J.C., C. Spenlehauer, and G. de Murcia, *The PARP superfamily.* Bioessays, 2004. **26**(8): p. 882-93.

69. Schreiber, V., et al., *Poly(ADP-ribose) polymerase-2 (PARP-2) is required for efficient base excision DNA repair in association with PARP-1 and XRCC1.* J Biol Chem, 2002. **277**: p. 23028-36.

70. Sugimura, K., et al., *PARP-1 ensures regulation of replication fork progression by homologous recombination on damaged DNA.* J Cell Biol, 2008. **183**: p. 1203-12.

71. Aguilar-Quesada, R., et al., *Modulation of transcription by PARP-1: consequences in carcinogenesis and inflammation.* Curr Med Chem, 2007. **14**: p. 1179-87.

72. Ahel, D., et al., *Poly(ADP-ribose)-dependent regulation of DNA repair by the chromatin remodeling enzyme ALC1.* Science, 2009. **325**: p. 1240-3.

73. Desmarais, Y., et al., *Enzymological properties of poly(ADP-ribose)polymerase: characterization of automodification sites and NADase activity.* Biochim Biophys Acta, 1991. **1078**: p. 179-86.

74. Masson, M., et al., *Poly(ADP-ribose) polymerase: structure-function relationship.* Biochimie, 1995. **77**(6): p. 456-61.

75. Ryabokon, N.I., et al., *Changes in poly(ADP-ribose) level modulate the kinetics of DNA strand break rejoining.* Mutat Res, 2008. **637**(1-2): p. 173-81.

76. Meyer, R.G., et al., *Human poly(ADP-ribose) glycohydrolase (PARG) gene and the common promoter sequence it shares with inner mitochondrial membrane translocase 23 (TIM23).* Gene, 2003. **314**: p. 181-90.

77. Rancourt, A. and M.S. Satoh, *Delocalization of nucleolar poly(ADP-ribose) polymerase-1 to the nucleoplasm and its novel link to cellular sensitivity to DNA damage.* DNA Repair (Amst), 2009. **8**(3): p. 286-97.

78. Aguilera, A. and S.J. Boulton, *How to exchange your partner. Workshop on recombination mechanisms and the maintenance of genomic stability.* EMBO Rep, 2007. **8**(1): p. 28-33.
79. Wang, M., et al., *PARP-1 and Ku compete for repair of DNA double strand breaks by distinct NHEJ pathways.* Nucleic Acids Res, 2006. **34**(21): p. 6170-82.
80. Rothkamm, K., et al., *Pathways of DNA double-strand break repair during the mammalian cell cycle.* Mol Cell Biol, 2003. **23**(16): p. 5706-15.
81. Kim, J.S., et al., *Independent and sequential recruitment of NHEJ and HR factors to DNA damage sites in mammalian cells.* J Cell Biol, 2005. **170**(3): p. 341-7.
82. Yamazoe, M., et al., *Reverse genetic studies of the DNA damage response in the chicken B lymphocyte line DT40.* DNA Repair (Amst), 2004. **3**(8-9): p. 1175-85.
83. Aladjem, M.I., et al., *ES cells do not activate p53-dependent stress responses and undergo p53-independent apoptosis in response to DNA damage.* Curr Biol, 1998. **8**(3): p. 145-55.
84. Mekeel, K.L., et al., *Inactivation of p53 results in high rates of homologous recombination.* Oncogene, 1997. **14**(15): p. 1847-57.
85. Orii, K.E., et al., *Selective utilization of nonhomologous end-joining and homologous recombination DNA repair pathways during nervous system development.* Proc Natl Acad Sci U S A, 2006. **103**(26): p. 10017-22.
86. Cortes-Ledesma, F. and A. Aguilera, *Double-strand breaks arising by replication through a nick are repaired by cohesin-dependent sister-chromatid exchange.* EMBO Rep, 2006. **7**(9): p. 919-26.
87. Kim, J.S., et al., *Specific recruitment of human cohesin to laser-induced DNA damage.* J Biol Chem, 2002. **277**(47): p. 45149-53.
88. Chen, F., et al., *Cell cycle-dependent protein expression of mammalian homologs of yeast DNA double-strand break repair genes Rad51 and Rad52.* Mutat Res, 1997. **384**(3): p. 205-11.
89. Esashi, F., et al., *CDK-dependent phosphorylation of BRCA2 as a regulatory mechanism for recombinational repair.* Nature, 2005. **434**(7033): p. 598-604.

90. Chen, B.P., et al., *Cell cycle dependence of DNA-dependent protein kinase phosphorylation in response to DNA double strand breaks.* J Biol Chem, 2005. **280**(15): p. 14709-15.

91. Meek, K., V. Dang, and S.P. Lees-Miller, *DNA-PK: the means to justify the ends?* Adv Immunol, 2008. **99**: p. 33-58.

92. Zou, L. and S.J. Elledge, *Sensing DNA damage through ATRIP recognition of RPA-ssDNA complexes.* Science, 2003. **300**(5625): p. 1542-8.

93. Sung, P. and H. Klein, *Mechanism of homologous recombination: mediators and helicases take on regulatory functions.* Nat Rev Mol Cell Biol, 2006. **7**(10): p. 739-50.

94. Huertas, P. and S.P. Jackson, *Human CtIP mediates cell cycle control of DNA end resection and double strand break repair.* J Biol Chem, 2009. **284**(14): p. 9558-65.

95. Sartori, A.A., et al., *Human CtIP promotes DNA end resection.* Nature, 2007. **450**(7169): p. 509-14.

96. Chen, L., et al., *Cell cycle-dependent complex formation of BRCA1.CtIP.MRN is important for DNA double-strand break repair.* J Biol Chem, 2008. **283**(12): p. 7713-20.

97. Rivera-Calzada, A., et al., *Three-dimensional structure and regulation of the DNA-dependent protein kinase catalytic subunit (DNA-PKcs).* Structure, 2005. **13**(2): p. 243-55.

98. Weterings, E. and D.J. Chen, *The endless tale of non-homologous end-joining.* Cell Res, 2008. **18**(1): p. 114-24.

99. Blunt, T., et al., *Identification of a nonsense mutation in the carboxyl-terminal region of DNA-dependent protein kinase catalytic subunit in the scid mouse.* Proc Natl Acad Sci U S A, 1996. **93**(19): p. 10285-90.

100. Ding, Q., et al., *DNA-PKcs mutations in dogs and horses: allele frequency and association with neoplasia.* Gene, 2002. **283**(1-2): p. 263-9.

101. van der Burg, M., et al., *A DNA-PKcs mutation in a radiosensitive T-B- SCID patient inhibits Artemis activation and nonhomologous end-joining.* J Clin Invest, 2009. **119**(1): p. 91-8.

102. Fattah, K.R., B.L. Ruis, and E.A. Hendrickson, *Mutations to Ku reveal differences in human somatic cell lines.* DNA Repair (Amst), 2008. **7**(5): p. 762-74.
103. Ruis, B.L., K.R. Fattah, and E.A. Hendrickson, *The catalytic subunit of DNA-dependent protein kinase regulates proliferation, telomere length, and genomic stability in human somatic cells.* Mol Cell Biol, 2008. **28**(20): p. 6182-95.
104. Mimori, T., et al., *Characterization of a high molecular weight acidic nuclear protein recognized by autoantibodies in sera from patients with polymyositis-scleroderma overlap.* J Clin Invest, 1981. **68**(3): p. 611-20.
105. Woodgett, J.R., *A kinase with Ku-dos.* Curr Biol, 1993. **3**(7): p. 449-50.
106. Lieber, M.R., *The Mechanism of Double-Strand DNA Break Repair by the Nonhomologous DNA End-Joining Pathway.* Annu Rev Biochem, 2009.
107. Hamer, G., et al., *Function of DNA-protein kinase catalytic subunit during the early meiotic prophase without Ku70 and Ku86.* Biol Reprod, 2003. **68**(3): p. 717-21.
108. Mari, P.O., et al., *Dynamic assembly of end-joining complexes requires interaction between Ku70/80 and XRCC4.* Proc Natl Acad Sci U S A, 2006. **103**(49): p. 18597-602.
109. Mimori, T., J.A. Hardin, and J.A. Steitz, *Characterization of the DNA-binding protein antigen Ku recognized by autoantibodies from patients with rheumatic disorders.* J Biol Chem, 1986. **261**(5): p. 2274-8.
110. Mimori, T. and J.A. Hardin, *Mechanism of interaction between Ku protein and DNA.* J Biol Chem, 1986. **261**(22): p. 10375-9.
111. Cary, R.B., et al., *A central region of Ku80 mediates interaction with Ku70 in vivo.* Nucleic Acids Res, 1998. **26**(4): p. 974-9.
112. Walker, J.R., R.A. Corpina, and J. Goldberg, *Structure of the Ku heterodimer bound to DNA and its implications for double-strand break repair.* Nature, 2001. **412**(6847): p. 607-14.
113. Chan, D.W., et al., *DNA-dependent protein kinase phosphorylation sites in Ku 70/80 heterodimer.* Biochemistry, 1999. **38**(6): p. 1819-28.
114. Nick McElhinny, S.A., et al., *Ku recruits the XRCC4-ligase IV complex to DNA ends.* Mol Cell Biol, 2000. **20**(9): p. 2996-3003.

115. Gullo, C.A., et al., *Ku86 exists as both a full-length and a protease-sensitive natural variant in multiple myeloma cells.* Cancer Cell Int, 2008. **8**: p. 4.

116. Downs, J.A. and S.P. Jackson, *A means to a DNA end: the many roles of Ku.* Nat Rev Mol Cell Biol, 2004. **5**(5): p. 367-78.

117. Vandersickel, V., et al., *Lentivirus-mediated RNA interference of Ku70 to enhance radiosensitivity of human mammary epithelial cells.* Int J Radiat Biol. **86**(2): p. 114-24.

118. Connelly, M.A., et al., *The promoters for human DNA-PKcs (PRKDC) and MCM4: divergently transcribed genes located at chromosome 8 band q11.* Genomics, 1998. **47**(1): p. 71-83.

119. Karran, P., *DNA double strand break repair in mammalian cells.* Curr Opin Genet Dev, 2000. **10**(2): p. 144-50.

120. Boskovic, J., et al., *Visualization of DNA-induced conformational changes in the DNA repair kinase DNA-PKcs.* EMBO J, 2003. **22**(21): p. 5875-82.

121. Dobbs, T.A., J.A. Tainer, and S.P. Lees-Miller, *A structural model for regulation of NHEJ by DNA-PKcs autophosphorylation.* DNA Repair (Amst), 2010. **9**(12): p. 1307-14.

122. Gupta, S. and K. Meek, *The leucine rich region of DNA-PKcs contributes to its innate DNA affinity.* Nucleic Acids Res, 2005. **33**(22): p. 6972-81.

123. Carter, T., et al., *A DNA-activated protein kinase from HeLa cell nuclei.* Mol Cell Biol, 1990. **10**(12): p. 6460-71.

124. Gottlieb, T.M. and S.P. Jackson, *The DNA-dependent protein kinase: requirement for DNA ends and association with Ku antigen.* Cell, 1993. **72**(1): p. 131-42.

125. Spagnolo, L., et al., *Three-dimensional structure of the human DNA-PKcs/Ku70/Ku80 complex assembled on DNA and its implications for DNA DSB repair.* Mol Cell, 2006. **22**(4): p. 511-9.

126. Yaneva, M., T. Kowalewski, and M.R. Lieber, *Interaction of DNA-dependent protein kinase with DNA and with Ku: biochemical and atomic-force microscopy studies.* EMBO J, 1997. **16**(16): p. 5098-112.

127. Matsuoka, S., et al., *Ataxia telangiectasia-mutated phosphorylates Chk2 in vivo and in vitro.* Proc Natl Acad Sci U S A, 2000. **97**(19): p. 10389-94.

128. Cortez, D., et al., *Requirement of ATM-dependent phosphorylation of brca1 in the DNA damage response to double-strand breaks.* Science, 1999. **286**(5442): p. 1162-6.

129. Stewart, G.S., et al., *MDC1 is a mediator of the mammalian DNA damage checkpoint*. Nature, 2003. **421**(6926): p. 961-6.

130. Kurimasa, A., et al., *Requirement for the kinase activity of human DNA-dependent protein kinase catalytic subunit in DNA strand break rejoining.* Mol Cell Biol, 1999. **19**(5): p. 3877-84.

131. Kienker, L.J., E.K. Shin, and K. Meek, *Both V(D)J recombination and radioresistance require DNA-PK kinase activity, though minimal levels suffice for V(D)J recombination*. Nucleic Acids Res, 2000. **28**(14): p. 2752-61.

132. Goodarzi, A.A., et al., *DNA-PK autophosphorylation facilitates Artemis endonuclease activity*. EMBO J, 2006. **25**(16): p. 3880-9.

133. Leber, R., et al., *The XRCC4 gene product is a target for and interacts with the DNA-dependent protein kinase.* J Biol Chem, 1998. **273**(3): p. 1794-801.

134. Costantini, S., et al., *Interaction of the Ku heterodimer with the DNA ligase IV/Xrcc4 complex and its regulation by DNA-PK*. DNA Repair (Amst), 2007. **6**(6): p. 712-22.

135. Yu, Y., et al., *DNA-PK phosphorylation sites in XRCC4 are not required for survival after radiation or for V(D)J recombination.* DNA Repair (Amst), 2003. **2**(11): p. 1239-52.

136. Yu, Y., et al., *DNA-PK and ATM phosphorylation sites in XLF/Cernunnos are not required for repair of DNA double strand breaks.* DNA Repair (Amst), 2008. **7**(10): p. 1680-92.

137. Douglas, P., et al., *DNA-PK-dependent phosphorylation of Ku70/80 is not required for non-homologous end joining.* DNA Repair (Amst), 2005. **4**(9): p. 1006-18.

138. Soubeyrand, S., et al., *Threonines 2638/2647 in DNA-PK are essential for cellular resistance to ionizing radiation.* Cancer Res, 2003. **63**(6): p. 1198-201.

139. Ding, Q., et al., *Autophosphorylation of the catalytic subunit of the DNA-dependent protein kinase is required for efficient end processing during DNA double-strand break repair*. Mol Cell Biol, 2003. **23**(16): p. 5836-48.

140. Cui, X., et al., *Autophosphorylation of DNA-dependent protein kinase regulates DNA end processing and may also alter double-strand break repair pathway choice.* Mol Cell Biol, 2005. **25**(24): p. 10842-52.

141. Meek, K., et al., *trans Autophosphorylation at DNA-dependent protein kinase's two major autophosphorylation site clusters facilitates end processing but not end joining.* Mol Cell Biol, 2007. **27**(10): p. 3881-90.

142. Chan, D.W. and S.P. Lees-Miller, *The DNA-dependent protein kinase is inactivated by autophosphorylation of the catalytic subunit.* J Biol Chem, 1996. **271**(15): p. 8936-41.

143. Merkle, D., et al., *The DNA-dependent protein kinase interacts with DNA to form a protein-DNA complex that is disrupted by phosphorylation.* Biochemistry, 2002. **41**(42): p. 12706-14.

144. Wechsler, T., et al., *DNA-PKcs function regulated specifically by protein phosphatase 5.* Proc Natl Acad Sci U S A, 2004. **101**(5): p. 1247-52.

145. Dominski, Z., *Nucleases of the metallo-beta-lactamase family and their role in DNA and RNA metabolism.* Crit Rev Biochem Mol Biol, 2007. **42**(2): p. 67-93.

146. Moshous, D., et al., *Artemis, a novel DNA double-strand break repair/V(D)J recombination protein, is mutated in human severe combined immune deficiency.* Cell, 2001. **105**(2): p. 177-86.

147. Ma, Y., et al., *The DNA-dependent protein kinase catalytic subunit phosphorylation sites in human Artemis.* J Biol Chem, 2005. **280**(40): p. 33839-46.

148. Pawelczak, K.S. and J.J. Turchi, *Purification and characterization of exonuclease-free Artemis: Implications for DNA-PK-dependent processing of DNA termini in NHEJ-catalyzed DSB repair.* DNA Repair (Amst), 2010. **9**(6): p. 670-7.

149. Yannone, S.M., et al., *Coordinate 5' and 3' endonucleolytic trimming of terminally blocked blunt DNA double-strand break ends by Artemis nuclease and DNA-dependent protein kinase.* Nucleic Acids Res, 2008. **36**(10): p. 3354-65.

150. Soubeyrand, S., et al., *Artemis phosphorylated by DNA-dependent protein kinase associates preferentially with discrete regions of chromatin.* J Mol Biol, 2006. **358**(5): p. 1200-11.

151. Wang, J., et al., *Artemis deficiency confers a DNA double-strand break repair defect and Artemis phosphorylation status is altered by DNA damage and cell cycle progression.* DNA Repair (Amst), 2005. **4**(5): p. 556-70.

152. Bernstein, N.K., et al., *Polynucleotide kinase as a potential target for enhancing cytotoxicity by ionizing radiation and topoisomerase I inhibitors.* Anticancer Agents Med Chem, 2008. **8**(4): p. 358-67.

153. Rasouli-Nia, A., F. Karimi-Busheri, and M. Weinfeld, *Stable down-regulation of human polynucleotide kinase enhances spontaneous mutation frequency and sensitizes cells to genotoxic agents.* Proc Natl Acad Sci U S A, 2004. **101**(18): p. 6905-10.

154. Chappell, C., et al., *Involvement of human polynucleotide kinase in double-strand break repair by non-homologous end joining.* EMBO J, 2002. **21**(11): p. 2827-32.

155. Bernstein, N.K., et al., *The molecular architecture of the mammalian DNA repair enzyme, polynucleotide kinase.* Mol Cell, 2005. **17**(5): p. 657-70.

156. Koch, C.A., et al., *Xrcc4 physically links DNA end processing by polynucleotide kinase to DNA ligation by DNA ligase IV.* EMBO J, 2004. **23**(19): p. 3874-85.

157. Rass, U., I. Ahel, and S.C. West, *Actions of aprataxin in multiple DNA repair pathways.* J Biol Chem, 2007. **282**(13): p. 9469-74.

158. Macrae, C.J., et al., *APLF (C2orf13) facilitates nonhomologous end-joining and undergoes ATM-dependent hyperphosphorylation following ionizing radiation.* DNA Repair (Amst), 2008. **7**(2): p. 292-302.

159. Clements, P.M., et al., *The ataxia-oculomotor apraxia 1 gene product has a role distinct from ATM and interacts with the DNA strand break repair proteins XRCC1 and XRCC4.* DNA Repair (Amst), 2004. **3**(11): p. 1493-502.

160. Nick McElhinny, S.A. and D.A. Ramsden, *Sibling rivalry: competition between Pol X family members in V(D)J recombination and general double strand break repair.* Immunol Rev, 2004. **200**: p. 156-64.

161. Chang, L.M. and F.J. Bollum, *Molecular biology of terminal transferase.* CRC Crit Rev Biochem, 1986. **21**(1): p. 27-52.

162. Nick McElhinny, S.A., et al., *A gradient of template dependence defines distinct biological roles for family X polymerases in nonhomologous end joining.* Mol Cell, 2005. **19**(3): p. 357-66.

163. Bebenek, K., et al., *The frameshift infidelity of human DNA polymerase lambda. Implications for function.* J Biol Chem, 2003. **278**(36): p. 34685-90.

164. Ramadan, K., et al., *De novo DNA synthesis by human DNA polymerase lambda, DNA polymerase mu and terminal deoxyribonucleotidyl transferase.* J Mol Biol, 2004. **339**(2): p. 395-404.

165. Davis, B.J., J.M. Havener, and D.A. Ramsden, *End-bridging is required for pol mu to efficiently promote repair of noncomplementary ends by nonhomologous end joining.* Nucleic Acids Res, 2008. **36**(9): p. 3085-94.

166. Garcia-Diaz, M., et al., *Identification of an intrinsic 5'-deoxyribose-5-phosphate lyase activity in human DNA polymerase lambda: a possible role in base excision repair.* J Biol Chem, 2001. **276**(37): p. 34659-63.

167. Mahajan, K.N., et al., *Association of DNA polymerase mu (pol mu) with Ku and ligase IV: role for pol mu in end-joining double-strand break repair.* Mol Cell Biol, 2002. **22**(14): p. 5194-202.

168. Capp, J.P., et al., *The DNA polymerase lambda is required for the repair of non-compatible DNA double strand breaks by NHEJ in mammalian cells.* Nucleic Acids Res, 2006. **34**(10): p. 2998-3007.

169. Lee, J.W., et al., *Implication of DNA polymerase lambda in alignment-based gap filling for nonhomologous DNA end joining in human nuclear extracts.* J Biol Chem, 2004. **279**(1): p. 805-11.

170. Bertocci, B., et al., *Nonoverlapping functions of DNA polymerases mu, lambda, and terminal deoxynucleotidyltransferase during immunoglobulin V(D)J recombination in vivo.* Immunity, 2006. **25**(1): p. 31-41.

171. Kobayashi, Y., et al., *Hydrocephalus, situs inversus, chronic sinusitis, and male infertility in DNA polymerase lambda-deficient mice: possible implication for the pathogenesis of immotile cilia syndrome.* Mol Cell Biol, 2002. **22**(8): p. 2769-76.

172. Ferguson, D.O. and F.W. Alt, *DNA double strand break repair and chromosomal translocation: lessons from animal models.* Oncogene, 2001. **20**(40): p. 5572-9.

173. Barnes, D.E., et al., *Targeted disruption of the gene encoding DNA ligase IV leads to lethality in embryonic mice.* Curr Biol, 1998. **8**(25): p. 1395-8.

174. Gao, Y., et al., *A critical role for DNA end-joining proteins in both lymphogenesis and neurogenesis.* Cell, 1998. **95**(7): p. 891-902.

175. Modesti, M., J.E. Hesse, and M. Gellert, *DNA binding of Xrcc4 protein is associated with V(D)J recombination but not with stimulation of DNA ligase IV activity.* EMBO J, 1999. **18**(7): p. 2008-18.

176. Junop, M.S., et al., *Crystal structure of the Xrcc4 DNA repair protein and implications for end joining.* EMBO J, 2000. **19**(22): p. 5962-70.

177. Wu, P.Y., et al., *Structural and functional interaction between the human DNA repair proteins DNA ligase IV and XRCC4.* Mol Cell Biol, 2009. **29**(11): p. 3163-72.

178. Grawunder, U., D. Zimmer, and M.R. Leiber, *DNA ligase IV binds to XRCC4 via a motif located between rather than within its BRCT domains.* Curr Biol, 1998. **8**(15): p. 873-6.

179. Drouet, J., et al., *DNA-dependent protein kinase and XRCC4-DNA ligase IV mobilization in the cell in response to DNA double strand breaks.* J Biol Chem, 2005. **280**(8): p. 7060-9.

180. Gu, J., et al., *XRCC4:DNA ligase IV can ligate incompatible DNA ends and can ligate across gaps.* EMBO J, 2007. **26**(4): p. 1010-23.

181. Gu, J., et al., *Single-stranded DNA ligation and XLF-stimulated incompatible DNA end ligation by the XRCC4-DNA ligase IV complex: influence of terminal DNA sequence.* Nucleic Acids Res, 2007. **35**(17): p. 5755-62.

182. Ahnesorg, P., P. Smith, and S.P. Jackson, *XLF interacts with the XRCC4-DNA ligase IV complex to promote DNA nonhomologous end-joining.* Cell, 2006. **124**(2): p. 301-13.

183. Buck, D., et al., *Cernunnos, a novel nonhomologous end-joining factor, is mutated in human immunodeficiency with microcephaly.* Cell, 2006. **124**(2): p. 287-99.

184. Dai, Y., et al., *Nonhomologous end joining and V(D)J recombination require an additional factor.* Proc Natl Acad Sci U S A, 2003. **100**(5): p. 2462-7.

185. Andres, S.N., et al., *Crystal structure of human XLF: a twist in nonhomologous DNA end-joining.* Mol Cell, 2007. **28**(6): p. 1093-101.

186. Wu, P.Y., et al., *Interplay between Cernunnos-XLF and nonhomologous end-joining proteins at DNA ends in the cell.* J Biol Chem, 2007. **282**(44): p. 31937-43.

187. Lu, H., et al., *Length-dependent binding of human XLF to DNA and stimulation of XRCC4.DNA ligase IV activity.* J Biol Chem, 2007. **282**(15): p. 11155-62.

188. Ropars, V., et al., *Structural characterization of filaments formed by human Xrcc4-Cernunnos/XLF complex involved in nonhomologous DNA end-joining.* Proc Natl Acad Sci U S A, 2011. **108**(31): p. 12663-8.

189. Li, Y., et al., *Crystal structure of human XLF/Cernunnos reveals unexpected differences from XRCC4 with implications for NHEJ.* EMBO J, 2008. **27**(1): p. 290-300.

190. Hammel, M., et al., *XRCC4 protein interactions with XRCC4-like factor (XLF) create an extended grooved scaffold for DNA ligation and double strand break repair.* J Biol Chem, 2011. **286**(37): p. 32638-50.

191. Hentges, P., et al., *Evolutionary and functional conservation of the DNA non-homologous end-joining protein, XLF/Cernunnos.* J Biol Chem, 2006. **281**(49): p. 37517-26.

192. Yano, K. and D.J. Chen, *Live cell imaging of XLF and XRCC4 reveals a novel view of protein assembly in the non-homologous end-joining pathway.* Cell Cycle, 2008. **7**(10): p. 1321-5.

193. Yano, K., et al., *Ku recruits XLF to DNA double-strand breaks.* EMBO Rep, 2008. **9**(1): p. 91-6.

194. Wood, R.D., et al., *Human DNA repair genes.* Science, 2001. **291**(5507): p. 1284-9.

195. Sjogren, C. and K. Nasmyth, *Sister chromatid cohesion is required for postreplicative double-strand break repair in Saccharomyces cerevisiae.* Curr Biol, 2001. **11**(12): p. 991-5.

196. Strom, L., et al., *Postreplicative recruitment of cohesin to double-strand breaks is required for DNA repair.* Mol Cell, 2004. **16**(6): p. 1003-15.

197. Unal, E., et al., *DNA damage response pathway uses histone modification to assemble a double-strand break-specific cohesin domain.* Mol Cell, 2004. **16**(6): p. 991-1002.

198. Hagstrom, S.A. and T.P. Dryja, *Mitotic recombination map of 13cen-13q14 derived from an investigation of loss of heterozygosity in retinoblastomas.* Proc Natl Acad Sci U S A, 1999. **96**(6): p. 2952-7.

199. Lisby, M., et al., *Choreography of the DNA damage response: spatiotemporal relationships among checkpoint and repair proteins.* Cell, 2004. **118**(6): p. 699-713.

200. de Jager, M., et al., *Human Rad50/Mre11 is a flexible complex that can tether DNA ends.* Mol Cell, 2001. **8**(5): p. 1129-35.

201. Rupnik, A., N.F. Lowndes, and M. Grenon, *MRN and the race to the break.* Chromosoma, 2010. **119**(2): p. 115-35.

202. Williams, R.S., et al., *Mre11 dimers coordinate DNA end bridging and nuclease processing in double-strand-break repair.* Cell, 2008. **135**(1): p. 97-109.

203. Hopfner, K.P., et al., *Structural biochemistry and interaction architecture of the DNA double-strand break repair Mre11 nuclease and Rad50-ATPase.* Cell, 2001. **105**(4): p. 473-85.

204. Hopfner, K.P., et al., *The Rad50 zinc-hook is a structure joining Mre11 complexes in DNA recombination and repair.* Nature, 2002. **418**(6897): p. 562-6.

205. Matsuura, S., et al., *Positional cloning of the gene for Nijmegen breakage syndrome.* Nat Genet, 1998. **19**(2): p. 179-81.

206. Carney, J.P., et al., *The hMre11/hRad50 protein complex and Nijmegen breakage syndrome: linkage of double-strand break repair to the cellular DNA damage response.* Cell, 1998. **93**(3): p. 477-86.

207. Lee, J.H., et al., *Regulation of Mre11/Rad50 by Nbs1: effects on nucleotide-dependent DNA binding and association with ataxia-telangiectasia-like disorder mutant complexes.* J Biol Chem, 2003. **278**(46): p. 45171-81.

208. Moreno-Herrero, F., et al., *Mesoscale conformational changes in the DNA-repair complex Rad50/Mre11/Nbs1 upon binding DNA.* Nature, 2005. **437**(7057): p. 440-3.

209. Mimitou, E.P. and L.S. Symington, *Sae2, Exo1 and Sgs1 collaborate in DNA double-strand break processing.* Nature, 2008. **455**(7214): p. 770-4.

210. Zhu, Z., et al., *Sgs1 helicase and two nucleases Dna2 and Exo1 resect DNA double-strand break ends.* Cell, 2008. **134**(6): p. 981-94.

211. You, Z. and J.M. Bailis, *DNA damage and decisions: CtIP coordinates DNA repair and cell cycle checkpoints.* Trends Cell Biol, 2010. **20**(7): p. 402-9.

212. Limbo, O., et al., *Ctp1 is a cell-cycle-regulated protein that functions with Mre11 complex to control double-strand break repair by homologous recombination.* Mol Cell, 2007. **28**(1): p. 134-46.

213. Alani, E., et al., *Characterization of DNA-binding and strand-exchange stimulation properties of y-RPA, a yeast single-strand-DNA-binding protein.* J Mol Biol, 1992. **227**(1): p. 54-71.

214. Moynahan, M.E. and M. Jasin, *Mitotic homologous recombination maintains genomic stability and suppresses tumorigenesis.* Nat Rev Mol Cell Biol. **11**(3): p. 196-207.

215. Bianco, P.R., R.B. Tracy, and S.C. Kowalczykowski, *DNA strand exchange proteins: a biochemical and physical comparison.* Front Biosci, 1998. **3**: p. D570-603.

216. Sung, P., *Yeast Rad55 and Rad57 proteins form a heterodimer that functions with replication protein A to promote DNA strand exchange by Rad51 recombinase.* Genes Dev, 1997. **11**(9): p. 1111-21.

217. Sung, P., et al., *Rad51 recombinase and recombination mediators.* J Biol Chem, 2003. **278**(44): p. 42729-32.

218. Joukov, V., et al., *The BRCA1/BARD1 heterodimer modulates ran-dependent mitotic spindle assembly.* Cell, 2006. **127**(3): p. 539-52.

219. Sobhian, B., et al., *RAP80 targets BRCA1 to specific ubiquitin structures at DNA damage sites.* Science, 2007. **316**(5828): p. 1198-202.

220. O'Donovan, P.J. and D.M. Livingston, *BRCA1 and BRCA2: breast/ovarian cancer susceptibility gene products and participants in DNA double-strand break repair.* Carcinogenesis. **31**(6): p. 961-7.

221. Sy, S.M., M.S. Huen, and J. Chen, *PALB2 is an integral component of the BRCA complex required for homologous recombination repair.* Proc Natl Acad Sci U S A, 2009. **106**(17): p. 7155-60.

222. Oliver, A.W., et al., *Structural basis for recruitment of BRCA2 by PALB2.* EMBO Rep, 2009. **10**(9): p. 990-6.

223. *Cancer risks in BRCA2 mutation carriers. The Breast Cancer Linkage Consortium.* J Natl Cancer Inst, 1999. **91**(15): p. 1310-6.

224. Howlett, N.G., et al., *Biallelic inactivation of BRCA2 in Fanconi anemia.* Science, 2002. **297**(5581): p. 606-9.

225. Moynahan, M.E., A.J. Pierce, and M. Jasin, *BRCA2 is required for homology-directed repair of chromosomal breaks.* Mol Cell, 2001. **7**(2): p. 263-72.

226. Esashi, F., et al., *Stabilization of RAD51 nucleoprotein filaments by the C-terminal region of BRCA2.* Nat Struct Mol Biol, 2007. **14**(6): p. 468-74.

227. Ira, G. and J.E. Haber, *Characterization of RAD51-independent break-induced replication that acts preferentially with short homologous sequences.* Mol Cell Biol, 2002. **22**(18): p. 6384-92.

228. Ristic, D., et al., *Human Rad51 filaments on double- and single-stranded DNA: correlating regular and irregular forms with recombination function.* Nucleic Acids Res, 2005. **33**(10): p. 3292-302.

229. Stark, J.M. and M. Jasin, *Extensive loss of heterozygosity is suppressed during homologous repair of chromosomal breaks.* Mol Cell Biol, 2003. **23**(2): p. 733-43.

230. Kawamoto, T., et al., *Dual roles for DNA polymerase eta in homologous DNA recombination and translesion DNA synthesis.* Mol Cell, 2005. **20**(5): p. 793-9.

231. McIlwraith, M.J., et al., *Human DNA polymerase eta promotes DNA synthesis from strand invasion intermediates of homologous recombination.* Mol Cell, 2005. **20**(5): p. 783-92.

232. Kannouche, P., et al., *Domain structure, localization, and function of DNA polymerase eta, defective in xeroderma pigmentosum variant cells.* Genes Dev, 2001. **15**(2): p. 158-72.

233. Johnson, R.D. and M. Jasin, *Sister chromatid gene conversion is a prominent double-strand break repair pathway in mammalian cells.* EMBO J, 2000. **19**(13): p. 3398-407.

234. Wu, Y., et al., *Rad51 protein controls Rad52-mediated DNA annealing.* J Biol Chem, 2008. **283**(21): p. 14883-92.

235. Sugiyama, T., J.H. New, and S.C. Kowalczykowski, *DNA annealing by RAD52 protein is stimulated by specific interaction with the complex of replication protein A and single-stranded DNA*. Proc Natl Acad Sci U S A, 1998. **95**(11): p. 6049-54.
236. Wu, L., et al., *BLAP75/RMI1 promotes the BLM-dependent dissolution of homologous recombination intermediates.* Proc Natl Acad Sci U S A, 2006. **103**(11): p. 4068-73.
237. Lundblad, V. and E.H. Blackburn, *An alternative pathway for yeast telomere maintenance rescues est1- senescence.* Cell, 1993. **73**(2): p. 347-60.
238. Kang, L.E. and L.S. Symington, *Aberrant double-strand break repair in rad51 mutants of Saccharomyces cerevisiae.* Mol Cell Biol, 2000. **20**(24): p. 9162-72.
239. Malkova, A., E.L. Ivanov, and J.E. Haber, *Double-strand break repair in the absence of RAD51 in yeast: a possible role for break-induced DNA replication.* Proc Natl Acad Sci U S A, 1996. **93**(14): p. 7131-6.
240. Lydeard, J.R., et al., *Break-induced replication and telomerase-independent telomere maintenance require Pol32.* Nature, 2007. **448**(7155): p. 820-3.
241. Kantake, N., et al., *The recombination-deficient mutant RPA (rfa1-t11) is displaced slowly from single-stranded DNA by Rad51 protein.* J Biol Chem, 2003. **278**(26): p. 23410-7.
242. Motycka, T.A., et al., *Physical and functional interaction between the XPF/ERCC1 endonuclease and hRad52.* J Biol Chem, 2004. **279**(14): p. 13634-9.
243. DiBiase, S.J., et al., *DNA-dependent protein kinase stimulates an independently active, nonhomologous, end-joining apparatus.* Cancer Res, 2000. **60**(5): p. 1245-53.
244. Wang, H., et al., *Genetic evidence for the involvement of DNA ligase IV in the DNA-PK-dependent pathway of non-homologous end joining in mammalian cells.* Nucleic Acids Res, 2001. **29**(8): p. 1653-60.
245. Wang, H., et al., *Efficient rejoining of radiation-induced DNA double-strand breaks in vertebrate cells deficient in genes of the RAD52 epistasis group.* Oncogene, 2001. **20**(18): p. 2212-24.
246. Hochegger, H., et al., *Parp-1 protects homologous recombination from interference by Ku and Ligase IV in vertebrate cells.* EMBO J, 2006. **25**(6): p. 1305-14.

247. Audebert, M., B. Salles, and P. Calsou, *Involvement of poly(ADP-ribose) polymerase-1 and XRCC1/DNA ligase III in an alternative route for DNA double-strand breaks rejoining.* J Biol Chem, 2004. **279**(53): p. 55117-26.

248. Wu, W., et al., *Repair of radiation induced DNA double strand breaks by backup NHEJ is enhanced in G2.* DNA Repair (Amst), 2008. **7**(2): p. 329-38.

249. Korolev, N., et al., *Modelling chromatin structure and dynamics: status and prospects.* Curr Opin Struct Biol, 2012. **22**(2): p. 151-9.

250. Shen, X., et al., *A chromatin remodelling complex involved in transcription and DNA processing.* Nature, 2000. **406**(6795): p. 541-4.

251. Sinha, M. and C.L. Peterson, *Chromatin dynamics during repair of chromosomal DNA double-strand breaks.* Epigenomics, 2009. **1**(2): p. 371-385.

252. Tsukuda, T., et al., *Chromatin remodelling at a DNA double-strand break site in Saccharomyces cerevisiae.* Nature, 2005. **438**(7066): p. 379-83.

253. Haaf, T., et al., *Nuclear foci of mammalian Rad51 recombination protein in somatic cells after DNA damage and its localization in synaptonemal complexes.* Proc Natl Acad Sci U S A, 1995. **92**(6): p. 2298-302.

254. Au, W.W. and B.R. Henderson, *Identification of sequences that target BRCA1 to nuclear foci following alkylative DNA damage.* Cell Signal, 2007. **19**: p. 1879-92.

255. Raderschall, E., E.I. Golub, and T. Haaf, *Nuclear foci of mammalian recombination proteins are located at single-stranded DNA regions formed after DNA damage.* Proc Natl Acad Sci U S A, 1999. **96**(5): p. 1921-6.

256. Bekker-Jensen, S., et al., *Spatial organization of the mammalian genome surveillance machinery in response to DNA strand breaks.* J Cell Biol, 2006. **173**(2): p. 195-206.

257. Essers, J., et al., *Nuclear dynamics of RAD52 group homologous recombination proteins in response to DNA damage.* Embo J, 2002. **21**(8): p. 2030-7.

258. Cremer, T. and C. Cremer, *Chromosome territories, nuclear architecture and gene regulation in mammalian cells.* Nat Rev Genet, 2001. **2**: p. 292-301.

259. Zink, D. and T. Cremer, *Cell nucleus: chromosome dynamics in nuclei of living cells.* Curr Biol, 1998. **8**: p. R321-4.

260. Cowell, I.G., et al., *gammaH2AX foci form preferentially in euchromatin after ionising-radiation.* PLoS One, 2007. **2**: p. e1057.

261. Soutoglou, E., et al., *Positional stability of single double-strand breaks in mammalian cells.* Nat Cell Biol, 2007. **9**: p. 675-82.

262. Chiolo, I., et al., *Double-strand breaks in heterochromatin move outside of a dynamic HP1a domain to complete recombinational repair.* Cell, 2011. **144**: p. 732-44.

263. Lisby, M., U.H. Mortensen, and R. Rothstein, *Colocalization of multiple DNA double-strand breaks at a single Rad52 repair centre.* Nat Cell Biol, 2003. **5**: p. 572-7.

264. Shibata, A., et al., *Factors determining DNA double-strand break repair pathway choice in G2 phase.* EMBO J, 2011. **30**(6): p. 1079-92.

265. Chiolo, I., et al., *Double-strand breaks in heterochromatin move outside of a dynamic HP1a domain to complete recombinational repair.* Cell, 2011. **144**(5): p. 732-44.

266. Chai, B., et al., *Distinct roles for the RSC and Swi/Snf ATP-dependent chromatin remodelers in DNA double-strand break repair.* Genes Dev, 2005. **19**(14): p. 1656-61.

267. Shim, E.Y., et al., *The yeast chromatin remodeler RSC complex facilitates end joining repair of DNA double-strand breaks.* Mol Cell Biol, 2005. **25**(10): p. 3934-44.

268. Klochendler-Yeivin, A., E. Picarsky, and M. Yaniv, *Increased DNA damage sensitivity and apoptosis in cells lacking the Snf5/Ini1 subunit of the SWI/SNF chromatin remodeling complex*. Mol Cell Biol, 2006. **26**(7): p. 2661-74.

269. Sapountzi, V., I.R. Logan, and C.N. Robson, *Cellular functions of TIP60.* Int J Biochem Cell Biol, 2006. **38**(9): p. 1496-509.

270. Kusch, T., et al., *Acetylation by Tip60 is required for selective histone variant exchange at DNA lesions.* Science, 2004. **306**(5704): p. 2084-7.

271. Redon, C., et al., *Histone H2A variants H2AX and H2AZ.* Curr Opin Genet Dev, 2002. **12**(2): p. 162-9.

272. Kinner, A., et al., *Gamma-H2AX in recognition and signaling of DNA double-strand breaks in the context of chromatin.* Nucleic Acids Res, 2008. **36**(17): p. 5678-94.

273. Cowell, I.G., et al., *gammaH2AX foci form preferentially in euchromatin after ionising-radiation.* PLoS One, 2007. **2**(10): p. e1057.

274. Friesner, J.D., et al., *Ionizing radiation-dependent gamma-H2AX focus formation requires ataxia telangiectasia mutated and ataxia telangiectasia mutated and Rad3-related.* Mol Biol Cell, 2005. **16**(5): p. 2566-76.

275. Keogh, M.C., et al., *A phosphatase complex that dephosphorylates gammaH2AX regulates DNA damage checkpoint recovery.* Nature, 2006. **439**(7075): p. 497-501.

276. Chowdhury, D., et al., *gamma-H2AX dephosphorylation by protein phosphatase 2A facilitates DNA double-strand break repair.* Mol Cell, 2005. **20**(5): p. 801-9.

277. Bassing, C.H., et al., *Increased ionizing radiation sensitivity and genomic instability in the absence of histone H2AX.* Proc Natl Acad Sci U S A, 2002. **99**(12): p. 8173-8.

278. Misteli, T. and E. Soutoglou, *The emerging role of nuclear architecture in DNA repair and genome maintenance.* Nat Rev Mol Cell Biol, 2009. **10**(4): p. 243-54.

279. Fernandez-Capetillo, O., C.D. Allis, and A. Nussenzweig, *Phosphorylation of histone H2B at DNA double-strand breaks.* J Exp Med, 2004. **199**(12): p. 1671-7.

280. Utley, R.T., et al., *Regulation of NuA4 histone acetyltransferase activity in transcription and DNA repair by phosphorylation of histone H4.* Mol Cell Biol, 2005. **25**(18): p. 8179-90.

281. Huen, M.S., et al., *RNF8 transduces the DNA-damage signal via histone ubiquitylation and checkpoint protein assembly.* Cell, 2007. **131**(5): p. 901-14.

282. Mailand, N., et al., *RNF8 ubiquitylates histones at DNA double-strand breaks and promotes assembly of repair proteins.* Cell, 2007. **131**(5): p. 887-900.

283. Doil, C., et al., *RNF168 binds and amplifies ubiquitin conjugates on damaged chromosomes to allow accumulation of repair proteins.* Cell, 2009. **136**(3): p. 435-46.

284. Stewart, G.S., et al., *The RIDDLE syndrome protein mediates a ubiquitin-dependent signaling cascade at sites of DNA damage.* Cell, 2009. **136**(3): p. 420-34.

285. Huyen, Y., et al., *Methylated lysine 79 of histone H3 targets 53BP1 to DNA double-strand breaks.* Nature, 2004. **432**(7015): p. 406-11.

286. Botuyan, M.V., et al., *Structural basis for the methylation state-specific recognition of histone H4-K20 by 53BP1 and Crb2 in DNA repair.* Cell, 2006. **127**(7): p. 1361-73.

287. Boisvert, F.M., et al., *Arginine methylation of MRE11 by PRMT1 is required for DNA damage checkpoint control.* Genes Dev, 2005. **19**(6): p. 671-6.

288. Kuttler, F. and S. Mai, *Formation of non-random extrachromosomal elements during development, differentiation and oncogenesis.* Semin Cancer Biol, 2007. **17**(1): p. 56-64.

289. Gaubatz, J.W., *Extrachromosomal circular DNAs and genomic sequence plasticity in eukaryotic cells.* Mutat Res, 1990. **237**(5-6): p. 271-92.

290. Huberman, J.A., *DNA replication, the cell cycle and genome stability.* Mutat Res, 2003. **532**(1-2): p. 1-4.

291. Young, L.S. and A.B. Rickinson, *Epstein-Barr virus: 40 years on.* Nat Rev Cancer, 2004. **4**(10): p. 757-68.

292. Young, L.S. and P.G. Murray, *Epstein-Barr virus and oncogenesis: from latent genes to tumours.* Oncogene, 2003. **22**(33): p. 5108-21.

293. Johnson, P.G. and T.A. Beerman, *Damage induced in episomal EBV DNA in Raji cells by antitumor drugs as measured by pulsed field gel electrophoresis.* Anal Biochem, 1994. **220**(1): p. 103-14.

294. Gewirtz, D.A., S.E. Holt, and L.W. Elmore, *Accelerated senescence: an emerging role in tumor cell response to chemotherapy and radiation.* Biochem Pharmacol, 2008. **76**(8): p. 947-57.

295. Milia, J., et al., *Farnesylated RhoB inhibits radiation-induced mitotic cell death and controls radiation-induced centrosome overduplication.* Cell Death Differ, 2005. **12**(5): p. 492-501.

296. Roninson, I.B., E.V. Broude, and B.D. Chang, *If not apoptosis, then what? Treatment-induced senescence and mitotic catastrophe in tumor cells.* Drug Resist Updat, 2001. **4**(5): p. 303-13.

297. Kolesnick, R. and Z. Fuks, *Radiation and ceramide-induced apoptosis.* Oncogene, 2003. **22**: p. 5897-906.

298. Fei, P. and W.S. El-Deiry, *P53 and radiation responses.* Oncogene, 2003. **22**: p. 5774-83.

299. Benchimol, S., *p53-dependent pathways of apoptosis.* Cell Death Differ, 2001. **8**: p. 1049-51.

300. Dewey, W.C., C.C. Ling, and R.E. Meyn, *Radiation-induced apoptosis: relevance to radiotherapy.* Int J Radiat Oncol Biol Phys, 1995. **33**: p. 781-96.

301. Shaw, J.E., L.F. Levinger, and C.W. Carter, Jr., *Nucleosomal structure of Epstein-Barr virus DNA in transformed cell lines.* J Virol, 1979. **29**(2): p. 657-65.

302. Sexton, C.J. and J.S. Pagano, *Analysis of the Epstein-Barr virus origin of plasmid replication (oriP) reveals an area of nucleosome sparing that spans the 3' dyad.* J Virol, 1989. **63**(12): p. 5505-8.

303. Mearini, G., et al., *Interaction of EBV latent origin of replication with the nuclear matrix: identification of S/MAR sequences and protein components.* FEBS Lett, 2003. **547**(1-3): p. 119-24.

304. Sugden, B. and E.R. Leight, *EBV's plasmid replicon: an enigma in cis and trans.* Curr Top Microbiol Immunol, 2001. **258**: p. 3-11.

305. Jackson, D.A., P. Dickinson, and P.R. Cook, *The size of chromatin loops in HeLa cells.* EMBO J, 1990. **9**(2): p. 567-71.

306. Kreth, G., J. Finsterle, and C. Cremer, *Virtual radiation biophysics: implications of nuclear structure.* Cytogenet Genome Res, 2004. **104**(1-4): p. 157-61.

307. Bunch, R.T., D.A. Gewirtz, and L.F. Povirk, *Ionizing radiation-induced DNA strand breakage and rejoining in specific genomic regions as determined by an alkaline unwinding/Southern blotting method.* Int J Radiat Biol, 1995. **68**(5): p. 553-62.

308. Rothkamm, K. and M. Lobrich, *Misrejoining of DNA double-strand breaks in primary and transformed human and rodent cells: a comparison between the HPRT region and other genomic locations.* Mutat Res, 1999. **433**(3): p. 193-205.

309. Falk, M., E. Lukasova, and S. Kozubek, *Chromatin structure influences the sensitivity of DNA to gamma-radiation.* Biochim Biophys Acta, 2008. **1783**(12): p. 2398-414.

310. Lett, J.T., *Damage to DNA and chromatin structure from ionizing radiations, and the radiation sensitivities of mammalian cells.* Prog Nucleic Acid Res Mol Biol, 1990. **39**: p. 305-52.

311. Olive, P.L., *The role of DNA single- and double-strand breaks in cell killing by ionizing radiation.* Radiat Res, 1998. **150**(5 Suppl): p. S42-51.

312. Rothkamm, K. and M. Lobrich, *Evidence for a lack of DNA double-strand break repair in human cells exposed to very low x-ray doses.* Proc Natl Acad Sci U S A, 2003. **100**: p. 5057-62.

313. Deutsch, M.J., et al., *The latent origin of replication of Epstein-Barr virus directs viral genomes to active regions of the nucleus.* J Virol, 2010. **84**(5): p. 2533-46.

314. Newman, H.C., et al., *DNA double-strand break distributions in X-ray and alpha-particle irradiated V79 cells: evidence for non-random breakage.* Int J Radiat Biol, 1997. **71**(4): p. 347-63.

315. Ward, J.F., *The complexity of DNA damage: relevance to biological consequences.* Int J Radiat Biol, 1994. **66**(5): p. 427-32.

316. Sak, A., et al., *Induction of DNA double-strand breaks by ionizing radiation at the c-myc locus compared with the whole genome: a study using pulsed-field gel electrophoresis and gene probing.* Int J Radiat Biol, 1996. **69**(6): p. 679-85.

317. Liggins, G.L., M. English, and D.A. Goldstein, *Structural changes in simian virus 40 chromatin as probed by restriction endonucleases.* J Virol, 1979. **31**(3): p. 718-32.

318. Rosl, F. and W. Waldeck, *Topological properties of bovine papillomavirus type 1 (BPV-1) DNA in episomal nucleoprotein complexes: a model system for chromatin organization in higher eukaryotes.* Mol Carcinog, 1991. **4**(3): p. 249-56.

319. Elia, M.C. and M.O. Bradley, *Influence of chromatin structure on the induction of DNA double strand breaks by ionizing radiation.* Cancer Res, 1992. **52**(6): p. 1580-6.

320. Poirier, M.G., et al., *Spontaneous access to DNA target sites in folded chromatin fibers.* J Mol Biol, 2008. **379**(4): p. 772-86.

321. Li, G., et al., *Rapid spontaneous accessibility of nucleosomal DNA.* Nat Struct Mol Biol, 2005. **12**(1): p. 46-53.

322. Sies, H., *Strategies of antioxidant defense.* Eur J Biochem, 1993. **215**(2): p. 213-9.

323. Stepan, V. and M. Davidkova, *Theoretical modelling of radiolytic damage of free DNA bases and within DNA macromolecule.* Radiat Prot Dosimetry, 2006. **122**(1-4): p. 110-2.

324. Radiation, U.N.S.C.o.t.E.o.A., *Sources and Effects of Ionizing Radiation. ANNEX F: DNA REPAIR AND MUTAGENESIS.*, in *UNSCEAR 2000 Report to the General Assembly, with scientific annexes Vol. II*. 2006, United Nations Scientific Committee on the Effects of Atomic Radiation.

325. Joenje, H., *Genetic toxicology of oxygen.* Mutat Res, 1989. **219**(4): p. 193-208.

326. Hamilton, C., R.L. Hayward, and N. Gilbert, *Global chromatin fibre compaction in response to DNA damage.* Biochem Biophys Res Commun, 2011. **414**(4): p. 820-5.

327. Barsoum, J. and P. Berg, *Simian virus 40 minichromosomes contain torsionally strained DNA molecules.* Mol Cell Biol, 1985. **5**(11): p. 3048-57.

328. Rodi, C.P. and W. Sauerbier, *Structure of transcriptionally active chromatin: radiological evidence for requirement of torsionally constrained DNA.* J Cell Physiol, 1989. **141**(2): p. 346-52.

329. Wang, H., et al., *Caffeine inhibits homology-directed repair of I-SceI-induced DNA double-strand breaks.* Oncogene, 2004. **23**(3): p. 824-34.

330. Xue, L., et al., *Regulation of ATM in DNA double strand break repair accounts for the radiosensitivity in human cells exposed to high linear energy transfer ionizing radiation.* Mutat Res, 2009. **670**(1-2): p. 15-23.

331. Zha, S., C. Boboila, and F.W. Alt, *Mre11: roles in DNA repair beyond homologous recombination.* Nat Struct Mol Biol, 2009. **16**(8): p. 798-800.

332. Allen, C., J. Halbrook, and J.A. Nickoloff, *Interactive competition between homologous recombination and non-homologous end joining.* Mol Cancer Res, 2003. **1**(12): p. 913-20.

333. Rothkamm, K. and S. Horn, *gamma-H2AX as protein biomarker for radiation exposure.* Ann Ist Super Sanita, 2009. **45**(3): p. 265-71.

334. Clingen, P.H., et al., *Histone H2AX phosphorylation as a molecular pharmacological marker for DNA interstrand crosslink cancer chemotherapy.* Biochem Pharmacol, 2008. **76**(1): p. 19-27.

335. Marti, T.M., et al., *H2AX phosphorylation within the G1 phase after UV irradiation depends on nucleotide excision repair and not DNA double-strand breaks.* Proc Natl Acad Sci U S A, 2006. **103**(26): p. 9891-6.

336. Baure, J., et al., *Histone H2AX phosphorylation in response to changes in chromatin structure induced by altered osmolarity.* Mutagenesis, 2009. **24**(2): p. 161-7.

337. Noel, G., et al., *Radiosensitization by the poly(ADP-ribose) polymerase inhibitor 4-amino-1,8-naphthalimide is specific of the S phase of the cell cycle and involves arrest of DNA synthesis.* Mol Cancer Ther, 2006. **5**(3): p. 564-74.

338. Vodenicharov, M.D., et al., *Base excision repair is efficient in cells lacking poly(ADP-ribose) polymerase 1.* Nucleic Acids Res, 2000. **28**(20): p. 3887-96.

339. Fisher, A.E., et al., *Poly(ADP-ribose) polymerase 1 accelerates single-strand break repair in concert with poly(ADP-ribose) glycohydrolase.* Mol Cell Biol, 2007. **27**(15): p. 5597-605.

340. Cortes, F. and N. Pastor, *Ionizing radiation damage repair: a role for topoisomerases?* Mutagenesis, 2001. **16**(4): p. 365-8.

341. Salceda, J., X. Fernandez, and J. Roca, *Topoisomerase II, not topoisomerase I, is the proficient relaxase of nucleosomal DNA.* EMBO J, 2006. **25**(11): p. 2575-83.

342. Pastor, N. and F. Cortes, *Bufalin influences the repair of X-ray-induced DNA breaks in Chinese hamster cells.* DNA Repair (Amst), 2003. **2**(12): p. 1353-60.

343. Mateos, S., et al., *Modulation of radiation response by inhibiting topoisomerase II catalytic activity.* Mutat Res, 2006. **599**(1-2): p. 105-15.

344. Wyman, C., D.O. Warmerdam, and R. Kanaar, *From DNA end chemistry to cell-cycle response: the importance of structure, even when it's broken.* Mol Cell, 2008. **30**(1): p. 5-6.

345. Niimi, N., et al., *Genetic interaction between DNA polymerase beta and DNA-PKcs in embryogenesis and neurogenesis.* Cell Death Differ, 2005. **12**(2): p. 184-91.

346. van Rensburg, E.J., et al., *Aphidicolin inhibition of gamma-radiation-induced DNA repair in human lymphocyte subpopulations.* Gen Pharmacol, 1989. **20**(4): p. 433-6.

347. Roots, R., G. Kraft, and E. Gosschalk, *The formation of radiation-induced DNA breaks: the ratio of double-strand breaks to single-strand breaks.* Int J Radiat Oncol Biol Phys, 1985. **11**(2): p. 259-65.

348. Taucher-Scholz, G., et al., *Induction of DNA breaks in SV40 by heavy ions.* Adv Space Res, 1992. **12**(2-3): p. 73-80.

349. Calini, V., C. Urani, and M. Camatini, *Comet assay evaluation of DNA single- and double-strand breaks induction and repair in C3H10T1/2 cells.* Cell Biol Toxicol, 2002. **18**(6): p. 369-79.

350. Lobrich, M., B. Rydberg, and P.K. Cooper, *Repair of x-ray-induced DNA double-strand breaks in specific Not I restriction fragments in human fibroblasts: joining of correct and incorrect ends.* Proc Natl Acad Sci U S A, 1995. **92**(26): p. 12050-4.